Response to Review #1

Thank you for the helpful comments and suggestions. We appreciate your time for reviewing our paper. We have addressed all of your comments as detailed below:

Major comment:

As the authors indicate on multiple occasions, it is imperative to model atmospheric ozone better for the right reasons. This is a high standard to achieve in atmospheric modeling because numerous processes (both chemical and physical) may affect the concentration of a singular important species in the atmosphere. The first justification that the updated chemistry in TS2 improved the simulations of ozone for the right reasons was that its output in box modeling simulations closely matched that of more explicit mechanisms like the MCM as shown in Figures 3-6. This was summarized in the second paragraph of the Conclusions. However, in that same paragraph the authors highlighted important differences between TS2 and MCM seemingly contradicting their previous statement. Inter-model comparisons are not extremely useful in justifying updates to a model because both models may contain quite a few simplifications and/or uncertainties.

We revise the text in the conclusions to explain in more detail why in general MCM does compare well with MOZART-TS2, but due to some inaccurate assumptions in MCM there are differences between the two mechanisms that impact ozone formation. Although we agree that field campaign comparisons are very useful for evaluating new chemical mechanisms, we also believe inter-comparisons between different chemical mechanisms are valuable. Without such comparisons, it would be difficult for future studies to accurately pick the best chemical mechanism to use to answer their specific science question. Also we want to highlight the inaccurate assumption in MCM here, so that future studies that use MCM for terpene oxidation update this chemistry.

"The box modeling results (Section 4.1 and 4.2) demonstrate that TS2 simulates 1st- and later-generation isoprene and terpene oxidation products better than TS1 in comparison to more explicit schemes like the Caltech mechanism and MCM. Verification that the isoprene and terpene oxidation chemistry is correctly represented in TS2 enhances confidence that ozone is accurately simulated for the right reasons. The box-modeling results also uncovered a simplification in MCM where terpene unsaturated hydroxy nitrate oxidation is not accurately represented, leading to large impacts on NO_x recycling and ozone formation (Section 4.2). Future studies using MCM v3.3.1 to simulate the oxidation of terpenes, especially those that contain more than one double bond, should update this simplification."

A better justification was made when comparing the model outputs with experimental data. While Figure 7 illustrates that TS2 does reduce the bias of modeled surface ozone concentrations across the US when compared with US EPA CASTNET data, Figure 9 (1st panel) shows that the model vertical profile is still inaccurate with overpredictions below the planetary boundary layer and underpredictions above it when compared with SEAC4Rs flight tracks. While the changes involving predominantly the organic nitrate chemistry have reduced surface level biases in ozone predictions, challenges remain

including: "PBL height, mixing schemes, clouds, vertical resolution, or ozone dry deposition schemes" (bottom of pg. 25). This should be echoed in the abstract and conclusions with further discussion in the section from which the quote was extracted (Section 4.4 after pg. 25). While the discussion of Figure 9 is extensive, model biases for different observables should be tied back to the ozone profile since this is the focus of the paper. For example, can corrections to jNO2 or the concentrations of biogenic VOCs be enough to predict the correct shape of the ozone vertical profile?

Good points. We revise the text to further highlight how biases in various products like jNO2 and biogenic VOCs will influence ozone:

"The vertical profile shape for ozone is quite different between the model and observations. There are also clear differences between the model and observations for NO_2 photolysis and ozone precursors like NO_x and VOCs. Possible explanations for the remaining biases are further described below and will be explored more completely in future work."

"A cloud-induced reduction in j_{NO2} below 1 km and an increase between 2-4 km would improve the ozone and j_{NO2} profile shapes."

"Future work will evaluate whether using finer horizontal resolution (14 km) removes these biases in biogenic VOCs in CAM-chem. If isoprene and monoterpenes are still under-predicted, increasing these biogenic emissions will enhance the overall bias in ozone."

We also add the following to the conclusions to highlight what the next steps will be in improving the ozone bias in CAM-chem in the future:
"This bias could be caused by remaining uncertainties in the chemistry (Section 5.2) or by processes other than chemistry, which will be evaluated in future work. Considering the analysis against the SEAC^{4}RS field campaign results, the first step toward reducing the remaining ozone bias will be to evaluate how finer horizontal resolution (14 km) impacts the results. Because biogenic and anthropogenic emissions in the southeast U.S. are spatially segregated, improvements in simulated ozone and biogenic VOCs are expected with finer horizontal resolution. Future work will also include evaluating different anthropogenic emission inventories and a more thorough investigation into whether biogenic emissions are accurately represented by MEGAN in CAM-chem. Additionally, cloud biases in CAM-chem will be investigated more in the future given their likelihood for improving the vertical profile shape of ozone, ozone precursors, and j_{NO2}. Considering that biases in the ozone profile shape are enhanced with stronger nudging to meteorological data (Figure S6), a more thorough analysis on the impact of nudging on CAM-chem dynamics and cloud parameterizations should be conducted. Future work will also evaluate whether enhanced vertical resolution is needed to improve PBL height and mixing schemes. Further evaluation of different chemical solvers (Sun et al., 2017) is also needed. Additionally, ozone dry deposition has a large impact on simulated surface ozone (val Martin et al., 2014; Clifton et al., 2019) and a thorough evaluation and update to the ozone dry deposition scheme used in CAM-chem should be performed. Ozone is a complicated pollutant to accurately simulate in models. This work demonstrates that updating isoprene and terpene gas-phase chemistry clearly improves simulated surface ozone in CAM-chem and that additional studies evaluating and updating other processes are needed to further reduce the ozone bias."

And we added in the abstract:
"Although the updates to isoprene and terpene chemistry greatly reduce the ozone bias in CAM-chem, a large bias remains. Evaluation against SEAC^{4}RS field campaign results suggests future improvements to horizontal resolution and cloud parameterizations in CAM-chem may be particularly important for further reducing this bias."

Minor comments:

1. Reference to CMAQ isoprene updates should be added to the Introduction on page 2 line 29 (see Pye et al. Environ. Sci. Technol. 2013, 47, 19, 11056-11064)

Yes, thanks for pointing this out. We have added this reference.

2. It was unusual not to see some of the organic nitrates in Figures 1 and 2 in blue when they are isomers of other species that undergo aerosol uptake. It isn't until 2.2.1 (pg. 7 line 7) that the author's mention tertiary nitrates are more likely to experience reactive aerosol uptake. This could also be specified in the captions to avoid confusion.

Yes, we have added:
"As shown, only certain isomers of organic nitrates undergo aerosol uptake as explained in Section 2.4.

3. Are there gray boxes that can be added to Figure 2 like in Figure 1 to denote new chemistry?

Yes, we have added gray boxes as done in Figure 1 for clarity.

4. dH/R should precede "6014 K" on line 16, page 5 of the manuscript for clarity of where the value comes from.

Yes, we update this sentence to:
"If the Henry's law temperature dependence **(dH/R)** was unavailable in the literature, 6014 K was assumed consistent with GECKO-A."

5. The yield of IEPOX from ISOPOOH + OH should be stated in the text on page 6 in order to understand its contribution to recycling HOx and aerosol formation. Other products of ISOPOOH + OH include the formation of isoprene dihydroperoxides (ISOPOOHOOH) that consume HOx (and therefore may give rise to less ozone) as in Liu et al. Environ. Sci. Technol. 2016, 50, 9872-9880 and Piletic et al. J. Phys. Chem. A, 2019, 123, 4, 906-919. Why were such products that potentially affect HOx, ozone and aerosol yields not included in an updated isoprene mechanism?

The MOZART-TS2 mechanism does not treat ISOPOOHOOH as a separate species in order to reduce cost because it is a minor product. However, ISOPOOHOOH is included in the surrogate compound ISOPHFP, which represents all isoprene highly functionalized hydroperoxides and

there is a yield of ISOPHFP from ISOPOOH + OH reaction. Considering the yield of ISOPOOHOOH and other low-volatility products formed from 1,5-H-shifts from ISOPOOH + OH reaction is uncertain including a lumped tracer ISOPHFP for these processes is reasonable. ISOPHFP and other low-volatility products do have a loss to aerosol in CAM-chem, so that HO_x and O_3 are more accurately represented, but they do not form SOA directly. In CAM-chem, SOA is formed via a VBS scheme, which was not updated in this work. Future work will link products like ISOPHFP to form SOA directly in CAM-chem, but such updates are beyond the scope of this work.

We update the title to "Comprehensive isoprene and terpene **gas-phase** chemistry improves simulated surface ozone in the southeastern U.S." to emphasize the scope of this work is to update the gas-phase mechanism.

We recognize that the description did not include enough detail for the isoprene low-NO_x chemistry and so have added the following to the MOZART-TS2 mechanism description in Section 2.2.1 and cited the papers above:

"OH addition to ISOPOOH forms a 0.85 yield of isoprene epoxydiol (IEPOX) & OH; a 0.07 yield of glycolaldehyde, hydroxyacetone, & OH; and a 0.08 yield of ISOPHFP, which is a surrogate compound for all isoprene highly functionalized hydroperoxides (Krechmer et al. 2015; Riva et al., 2016; St. Clair et al., 2016; Liu et al., 2016; Piletic et al., 2019). ISOPHFP undergoes aerosol uptake in TS2 to more accurately represent loss processes of HO_x, but like organic nitrates does not explicitly form SOA. SOA is formed by a volatility basis set (VBS) scheme in CAM-chem, which was not updated in this work. Directly forming SOA from low-volatility products like ISOPHFP in CAM-chem is a goal for future work."

6. Many papers regarding Criegee intermediates have the 'C' capitalized. Please correct this in the manuscript.

Thanks, we have updated this.

7. On page 17, line 8, it states that "TS2 was altered to use RCIM assumptions for formation and loss of PAN and: : :" What specifically was altered in this sensitivity test?

We remove "which are explicitly listed in Table S7" and add in a more complete sentence stating: "The revised reactions for each of these sensitivity tests are listed explicitly in Table S7." And added:
"Unlike TS2, RCIM does not include PAN photolysis or the $CH_3CO_3 + CH_3CO_3$ reaction and RCIM uses different reaction rate constants than TS2 for PAN formation, thermal decomposition, and reaction with OH (Table S7)."

8. On page 19, line 18, it states "Commonly, in MCM, unsaturated hydroxy nitrates will react with OH via H-abstraction : : :". Please add "derived from terpenes" after nitrates to specify that this does not involve hydroxy nitrates derived from isoprene.

Very good clarification, thanks this has been added in this location and a couple others for clarity.

9. Figure 9 should have same color scheme for TS1 and TS2 with its predecessors (Figs 3-6) for consistency.

This has been updated TS1 is red and TS2 is purple in all figures now.

10. The equation used to derive the organic nitrate yields using alpha and n in the Supporting Information (pgs. 49-51) should be stated with the reference included for clarity.

We updated the description in the Table S6 to "see notes [a]" with a link, so that it is clear that more information is in the table notes. Then we also update the note to include the formula used along with the reference.

Response to Review #2

Thank you for the helpful comments and suggestions. We appreciate your time for reviewing our paper. We have addressed all of your comments as detailed below:

Overall

The mechanism is expected to be included in future versions of the CESM model and is offered to any interested party if they'd like to access the updates prior to the new release. If for whatever reason the TS2 mechanism does not make it into a future CESM release the authors should guarantee an alternative location for the code to be made available.

We have updated the code data availability section to include more details. The TS2 chemistry will very likely be released as a new compset in CESM 2.2. We include reference to the CAM-chem wiki, which will always have the updated status of the new and old chemical mechanisms available in CAM-chem. If for some very unlikely reason, TS2 is not implemented into CESM 2.2, we will provide directions for how to implement the changes on this referenced wiki-page. We do not want to upload the code now as the updates include both a new chemical mechanism and source code modifications, and we do not want users to inaccurately implement the code. We also upload ozone hourly and SEAC^{4}Rs flight track data used in this work to a repository and describe this here:

"The code updates described in this work will be made available as a new compset in a future release of CESM likely CESM 2.2. Chemical mechanisms used in CAM-chem are listed on the CAM-chem wiki page at https://wiki.ucar.edu/display/camchem/Gas-Phase+Chemistry, which includes a brief description, a citation reference, and information on their current status. Please contact Rebecca Schwantes (rschwant@ucar.edu) if you would like the TS2 updates prior to their future release in CESM. CESM/CAM-chem output for 2013 August hourly ozone, 2013 August monthly average default output, and SEAC^{4}RS flight tracks used in this work are provided on NCAR's Digital Asset Services Hub (DASH) here: https://dashrepo.ucar.edu/dataset/68_rschwant.html (Schwantes and Emmons 2020)."

Comments

Figures 1 and 2 should point to Table S2.

The following has been added to the caption for Figure 1 and 2:
"All species names used in TS2 are described in Table S2."

Figures 1 and 2 are schematics of OH oxidation and Figures S1 and S2 are schematics of NO3 oxidation. Why were no schematics of O3 oxidation included (and only described in Sections 2.2.2 and 2.3.2). For completeness, I feel that O3 oxidation schematics could be included in the supplement.

For clarity we have added a schematic for O_3 oxidation of isoprene and terpenes to the Supplement in Figure S3. We add reference to Figure S3 in Section 2, 2.2.2, 2.3.2.

"and for O_3-initiated oxidation in Figures S3."
"O_3-initiated oxidation of isoprene is simply described in Figure S3"
"O_3-initiated oxidation of the terpene surrogate compounds in TS2 is described in a simplified schematic in Figure S3."

Page 7, Line 1: The authors mention that "multiple isomers were only incorporated into TS2 if grouping them together would bias HOx or NOx budgets." How was this determined? Were there sensitivity or testing runs conducted and that are not described? Please describe.

We have reworded this and added more detail. We did not run sensitivity tests for this. Instead this was determined based on the chemistry.
"To save computational cost, multiple isomers were only incorporated into TS2 if grouping them together would bias the HO_x or NO_x budgets. For example, the two dominant isomers of ISOPOOH react with OH to produce similar yields of OH and a similar distribution of IEPOX isomers (Wennberg et al. 2018), so grouping isomers of ISOPOOH and IEPOX together to reduce computational cost is warranted. In contrast, TS2 includes multiple isomers of HPALDs and hydroxy nitrates because different isomers react with OH to produce varying levels of OH and NO_2, so combining these isomers together would inaccurately influence the HO_x and NO_x budgets."

Page 7, Line 9: The authors mention that the "number of organic nitrates in TS2 was optimized to accurately represent" varying reaction rates. What sort of optimization was done? What were the optimization criteria? This needs more detail.

Good point, we updated this sentence below. Specifically, we changed "optimized" to "selected" here because there was not an optimization program run. The selection was instead based on reaction rates, products, and atmospheric fate of each isomer.
"The organic nitrates in TS2 were carefully selected to account for these varying fates, but also when possible to combine isomers with similar reaction rates, oxidation products, and overall atmospheric fate together to reduce computational cost."

The supplemental Figures S1 and S2 should be referenced more thoroughly in the manuscript, esp. within the captions of Figures 1 and 2 and in the accompanying sections (Section 2.2.3 and 2.3.3).

We add additional references to Figures S1 and S2 in Section 2.2.3 and 2.3.3.
"Isoprene NO_3-initiated oxidation in TS2 is described in a simplified schematic in Figure S1 and …"
"Where structurally similar, organic nitrates from OH and NO_3 oxidation are shared to reduce computational cost (Figure 1 and S1).
"as summarized in a simplified schematic in Figure S2."
"… and TERPNPS1 (unsaturated primary/secondary) (Figure S2)"
"… the corresponding saturated nitrooxy hydroperoxide (Figure S2)"

As suggested, we also now reference the NO_3 and O_3 supplemental figures in the caption of Figure 1 and 2 to make certain the reader knows these figures are available.
"Similar schematics for NO_3- and O_3-initiated oxidation of isoprene are provided in Figure S1 and S3 in the supplement."
"Similar schematics for NO_3- and O_3-initiated oxidation of terpenes are provided in Figure S2 and S3 in the supplement."

Page 10, Line 10: Were there any alternative approaches that could be made to represent terpene products here? Were these approaches tested or considered? A description of why this particular choice was made (and what the likely impact on computational cost and resulting chemistry would be) should be included.

We did not test many different versions of the TS2 mechanisms, but agree that in the future creating reduced chemical mechanisms more systematically from explicit chemical mechanisms would be useful. We add the following to describe in more detail why the oxidation products selected here were used.

"The terpene products described above were selected, so that compounds that are chemically similar (i.e. contain the same functional groups and react with OH, O_3, and NO_3 at similar rates) are grouped together. The complexity of the chemistry is largely determined by the current knowledge of the system. There may be advantages to adding more complexity into TS2 in the future as more knowledge about terpene oxidation especially later-generation chemistry becomes available. Given terpene-later-generation chemistry is not well understood and that chemistry of many terpene products is largely estimated based on similar more well-studied compounds, adding separate products for each of the terpene surrogate compounds would increase cost without adding a lot of additional information into the system."

Section 2.4: I feel that a more thorough descriptions of the impacts of the TS2 mechanism on aerosol formation can be included. The existing section is sparse compared to the other sections, and although the authors make not of the large uncertainties that remain, I feel that more can be added. Perhaps the manuscript title can include the word "gas-phase" after the word "Comprehensive" in order to highlight that this manuscript is largely focused on the gas-phase chemistry of isoprene and terpene and that future development of the aerosol scheme is slated for future work.

Yes, good point we add "gas-phase" to the title. This work is more focused on the gas-phase chemistry. The Volatility Basis Set scheme that forms SOA in CAM-chem was not changed in this work. We update Section 2.4:

"In TS2, aerosol uptake of organic nitrates is only a gas-phase sink for organic nitrates and does not form SOA directly. SOA in TS2 only forms from a VBS scheme (Tilmes et al., 2020), which was not updated in this work. Better connecting gas-phase chemistry and SOA formation is a goal for future work as uptake of organic nitrates to form SOA is important for accurately representing gas-phase ozone as well as the overall magnitude of SOA. Aerosol uptake of organic nitrates is quite uncertain (Section 5.2) and further studies investigating the processes of

organic nitrate uptake and hydrolysis as well as more complex implementation of these processes in models is warranted and a goal for future work."

The results and discussion section (Section 4) is very long (21 pages) and I feel can be split into separate sections. Perhaps the evaluation of the explicit schemes (Sections 4.1 and 4.2) and the global modeling evaluation against surface observations and field campaign data (Sections 4.3 and 4.4) can remain in Section 4, while the discussion of the organic nitrate fate (Section 4.5) and the overall discussion of uncertainties (Section 4.6) can be moved to a Discussion Section (Section 5). The existing Conclusion section (Section 5) can then me moved to Section 6.

We have split the results and discussion section and agree this adds clarity. Thanks for the suggestion.

In Figures 3, 4, 5, and 6, I find it somewhat difficult to differentiate between the blue colors used to label TS1 and TS2. Changing one of them to a more distinct color (green, perhaps?) would aid in clarity. [NOTE: This appears to be the case only when I print the manuscript out, and the colors are clearly distinguishable when I look at a digital copy]

The colors have been updated such that blue and cyan are no longer included together in any of the plots, so we have updated Figures 3, 4, 5, 6, S4, S5, 9, 10, S6, S7. We have also increased the width of the lines and all Test cases for the box-model analysis are in dashed lines to make it easier to differentiate the different lines on the plot.

The sensitivity tests in the Figures are labelled as "Test 1, Test 2", while in the captions are labelled "test 1, test 2" and in the manuscript as "first sensitivity test, second sensitivity test." I suggest sticking with the "Test 1, Test 2" format and making this consistent throughout the sections.

Yes, we have adjusted this to refer to the sensitivity tests as a whole as "sensitivity tests" and individually as Test 1, Test 2, etc.

Page 19, Line 26: The authors state that "These unrealistically fast cycles are commonly used in MCM to reduce the number of species...". Is there a citation for this claim? How do the authors know this is the case?

We have seen this for other systems too (e.g., cresol oxidation pathway - Schwantes et al. 2017, ACP), but because we have not done a thorough examination and it is possible these are the only 2 instances, we remove:
"are commonly used in MCM to reduce the number of species and"

Page 31 Line 7-8: Could you expand (speculate) on some of the possible sources of uncertainties that are less-well known?

Yes, we have added an example:

"For example, our understanding of reaction rates and products from peroxy radical isomerization reactions that lead to auto-oxidation is rudimentary and under-constrained (Wennberg et al. 2018). Because much is unknown about peroxy radical isomerization reactions, there is not a clear understanding of how important these reactions are in the ambient atmosphere."

Page 34, Line 2 – Page 35, Line 1: This point has also been made by Mao et al. (2018) (www.atmos-chem-phys.net/18/2615/2018/) (see page 2622), and should be referenced.

This reference has been added.

Page 37, Line 28: I suggest including the Sun et al. (2017) reference in which they were able to reduce Eastern US ozone bias via the utilization of a new solver scheme (https://agupubs.onlinelibrary.wiley.com/doi/full/10.1002/2016MS000863). Additionally, I believe a slightly expanded discussion of the remaining sources of uncertainty would significantly enhance this final paragraph.

Great point. This reference has been added to the introduction and chemical solver is added as an additional uncertainty in the conclusions. Additional discussion of the remaining sources of uncertainty also has been added to the conclusion:

"This bias could be caused by remaining uncertainties in the chemistry (Section 5.2) or by processes other than chemistry, which will be evaluated in future work. Considering the analysis against the SEAC^{4}RS field campaign results, the first step toward reducing the remaining ozone bias will be to evaluate how finer horizontal resolution (14 km) impacts the results. Because biogenic and anthropogenic emissions in the southeast U.S. are spatially segregated, improvements in simulated ozone and biogenic VOCs are expected with finer horizontal resolution. Future work will also include evaluating different anthropogenic emission inventories and a more thorough investigation into whether biogenic emissions are accurately represented by MEGAN in CAM-chem. Additionally, cloud biases in CAM-chem will be investigated more in the future given their likelihood for improving the vertical profile shape of ozone, ozone precursors, and j_{NO2}. Considering that biases in the ozone profile shape are enhanced with stronger nudging to meteorological data (Figure S6), a more thorough analysis on the impact of nudging on CAM-chem dynamics and cloud parameterizations should be conducted. Future work will also evaluate whether enhanced vertical resolution is needed to improve PBL height and mixing schemes. Further evaluation of different chemical solvers (Sun et al., 2017) is also needed. Additionally, ozone dry deposition has a large impact on simulated surface ozone (val Martin et al., 2014; Clifton et al., 2019) and a thorough evaluation and update to the ozone dry deposition scheme used in CAM-chem should be performed. Ozone is a complicated pollutant to accurately simulate in models. This work demonstrates that updating isoprene and terpene gas-phase chemistry clearly improves simulated surface ozone in CAM-chem and that additional studies evaluating and updating other processes are needed to further reduce the ozone bias."

Response to Review #3

Thank you for the helpful comments and suggestions. We appreciate your time for reviewing our paper. We have addressed all of your comments as detailed below:

1) The box model simulations, comparing TS2 with TS1 and explicit mechanisms, currently only uses one set of chemical and meteorological conditions (August in Mississippi). It would have been helpful for box model simulations to have been conducted separately for high-NOx and low-NOx conditions. Given the very different oxidation pathways under these conditions, this would have provided a more stringent set of tests for the new mechanism. (I realize that new simulations would impose a significant analysis burden on the authors, so may not be practical.)

We do agree this would be useful. A more thorough box-modeling study comparing MOZART-TS2 against additional reduced and explicit mechanisms at varying NO_x levels, VOC levels, temperatures, aerosol concentrations, photolysis levels, etc. would be extremely useful and a goal for a future study.

2) It might be helpful to split Results (4.1-4.4) and Discussions (4.5-4.6) into separate sections.

Great point, we have done this.

Specific comments

1. Introduction
page 3, lines 11-12 – Rephrase for clarity. For instance, "to determine the extent to which [improvements to] the chemical mechanism can explain ...."

Yes we update to the following:
"will be updated to determine the extent to which improvements to the gas-phase chemical mechanism for biogenic VOCs can explain the simulated surface ozone bias over the southeastern U.S."

2.1 Updates to Henry's Law Constants
p.5, l.15-16 – Clarify the definition of Henry's law temperature dependence (given here as 6014 K).

As suggested by reviewer 1 we add:
"If the Henry's law temperature dependence **(dH/R)** was unavailable in the literature, 6014 K was assumed consistent with GECKO-A."

p.5, l. 16 – Add "used for dry deposition" after "reactivity factor (F0)."

As suggested we update to:

"The reactivity factor (F_0) **used for dry deposition and ranging** from 0 to 1 with 1 being as reactive as ozone is also listed in Table S4."

3.1 Box modeling
p.13, l.24 – Planetary boundary layer *height*?

Yes, thanks we have added "height" here.

p.13, l.24 – Clarify here that only "general" photolysis rate constants are taken from CESM/CAM-chem-TS1 (as explained later).

Yes we add "general" here.

p.13, l. 27-28 – Explain how deposition from CESM/CAM-chem is implemented in box model. For instance, dry deposition velocities? wet deposition loss frequencies? No ventilation/dilution of the box with background air is included, correct?

Yes, thanks we have revised this to be more descriptive.
"Aerosol uptake of the following inorganic compounds: HO_2, N_2O_5, NO_2, NO_3 were included based on the reaction rate constants output from the CESM/CAM-chem base simulation. Dry deposition of the following inorganic compounds: O_3, CO, NO, NO_2, HNO_3, N_2O_5, HO_2NO_2, H_2O_2, and SO_2 were included using the dry deposition velocities from the CESM/CAM-chem base simulation. The box is mixed based on the planetary boundary layer height with background air, which has fixed concentrations of isoprene, terpenes, H_2O, CH_4, H_2, CO, O_3, NO, NO_2, SO_2, and N_2O from the CESM/CAM-chem TS1 base simulation."

p.14, l.13-14 – "These are ideal scenarios designed" to "These idealized scenarios are designed ...."

Yes, we updated this.

3.2 Global modeling
p.14, l.18-21 – Which meteorological fields are nudged to reanalysis?

We update this to a more complete list:
"The meteorology (air and surface temperature, horizontal winds, surface pressure, sensible and latent heat flux, and wind stress)"

p.15, l.4-5 – Which years were used for spinup?

We added the following for clarity:
"separately spun-up for 2.5 years **(i.e., Jan 1, 2011 to July 31, 2013)"**

4. Results and Discussions
Figures 3-6 – Difficult to distinguish some of the individual lines in these plots. Try to modify colors, or make lines thicker.

Yes, the colors have been updated, the line width increased, and the sensitivity tests are now in dashed lines for easier viewing.

p.17, l.8-9 – Explain the differences between the representations of PAN formation and loss (TS2 versus RCIM).

We added the following:
"Unlike TS2, RCIM does not include PAN photolysis or the CH_3CO_3 + CH_3CO_3 reaction and RCIM uses different reaction rate constants than TS2 for PAN formation, thermal decomposition, and reaction with OH (Table S7)."

p.17, l.11 – Add "from RCIM" after "The PAN assumptions."

Added "from RCIM"

p.17, l.13 – Are the RCIM photolysis rates faster or slower? By how much?

This is explained in the next paragraph. We rearrange these paragraphs, so that this is clearer.

4.2 Terpene Evaluation Against Explicit Species
p.19, l.5 – Clarify what is meant here by "total products produced."

We revise this sentence to the following:
In general, the types of compounds formed are their concentrations are reasonably consistent between MCM and TS2.

p.20, l.3 – Add "oxidation of" before "the alpha-pinene."

Yes, added this.

4.4 Evaluation Against Field Campaign Data
Figure 7 – Add mean bias for Eastern US / Western US to figure panels.

The mean bias has been added here.

p.28, l.1-3 – How do the dry deposition velocities of OVOCs compare in GEOS-Chem versus CESM/CAM-chem?

I do not have data for the dry deposition velocities of OVOCs in the standard version of GEOS-Chem to compare to my data with CAM-chem, so I cannot make this comparison at this time. However, more comparisons between GEOS-Chem and CAM-chem in the future would be really useful and hopefully can be performed in the near future. We are in the process of evaluating a new version of CESM/CAM-chem with finer horizontal resolution down to 14 km. This future study will include a comparison for OVOC dry deposition velocities measured during SOAS with CAM-chem results.

4.6.2 Uncertainties in Loss of Organic Nitrates
p.35, l.24 and l.26 – Clarify the meaning of "largely" here, e.g., do you mean "primary and secondary organic nitrates *largely* will not" and "... are *largely* lost ...."

Yes, good point this "largely" should be next to the verb for clarity. I move this and change the first instance to "generally".

Technical corrections
1. Introduction
p.3, l.3 – Hyphenate "terpene-derived" (and "isoprene-derived" throughout manuscript).

Yes, we updated this.

2. Development of MOZART-TS2
p.3, l.11 – Capitalize "Model."

Yes, updated.

3.1 Box modeling
p.14, l.6 – Include units for lat/lon (deg N, deg E).

Yes, added these units.

3.2 Global modeling
p.14, l.22 – Run-on sentence. Break into two, starting with "Using a weak ...."

Yes, this sentence was revised:
"This study uses 32 vertical levels and a weak relaxation time (50 h) for nudging in order to reduce variability while also limiting the impact of nudging on model parameterizations."

p.14, l.34 – Change to "(Table S3), using ...."

We realized that the description for vertical levels may not be clear enough. We have added more detail here and in the paragraph above:

"First, the ``TS1" case uses the default CESM2.1.0/CAM-chem code and the default TS1 chemical mechanism **with the two changes described above: 32 vertical levels and** an expansion of the biogenic volatile organic compounds emitted from the land model (Table S3)"

And in the paragraph above:
"Using 32 vertical levels, the vertical resolution to which CAM physics, dynamics, and cloud parameterizations are tuned, slightly improves the model bias for ozone near the surface compared to using 56 vertical levels, the native resolution of the MERRA2 meteorological files (Figure S6)."

4. Results and Discussions
p.15, l.15 – "suggests" –> "suggest"

Yes, this is fixed.

p.17, l.1 – Hyphenate "NO3-initiated."

Yes, this is fixed.

4.2 Terpene Evaluation Against Explicit Species
p.20, l.1 – "Terpene-rich"

Yes, this is fixed.

4.4 Evaluation Against Field Campaign Data
p.27, l.3 – Change to "above 2km; when clouds ...."

Yes, this is fixed.

4.5 Organic Nitrate Formation and Fate
p.28, l.34 – "isoprene- and terpene-derived."

Yes this is fixed throughout.

p.29, l.6 – Delete comma.

Yes, this is fixed.

4.6.1 Uncertainties in Formation of Organic Nitrates
p.33, l.6 – Delete comma.

Yes, this is fixed.

4.6.2 Uncertainties in Loss of Organic Nitrates
p.35, l.13 – Delete comma after "(Figure 1)."

I removed comma and put description in parenthesis instead to avoid confusion.

p.35, l.16 – "under-constrained, leading to ...."

Yes, this is fixed

5. Conclusions
p.36, lines 15, 18, 31 – Missing commas.

Yes, this is fixed

p.37, line 9 – Missing comma.

Yes, this is fixed

Comprehensive isoprene and terpene gas-phase chemistry improves simulated surface ozone in the southeastern U.S.

Rebecca H. Schwantes[1], Louisa K. Emmons[1], John J. Orlando[1], Mary C. Barth[1], Geoffrey S. Tyndall[1], Samuel R. Hall[1], Kirk Ullmann[1], Jason M. St. Clair[2,3], Donald R. Blake[4], Armin Wisthaler[5,6], and ThaoPaul V. Bui[7]

[1]Atmospheric Chemistry Observations and Modeling Laboratory, National Center for Atmospheric Research, Boulder, CO 80301, U.S.A.
[2]Atmospheric Chemistry and Dynamics Laboratory, NASA Goddard Space Flight Center, Greenbelt, MD, 20771, USA
[3]Joint Center for Earth Systems Technology, University of Maryland Baltimore County, Baltimore, MD, 21228, USA
[4]Department of Chemistry, University of California-Irvine, 570 Rowland Hall, Irvine, CA 92697-2025, USA
[5]Institute for Ion Physics and Applied Physics, University of Innsbruck, Technikerstrasse 25, 6020 Innsbruck, Austria
[6]Department of Chemistry, University of Oslo, P.O. 1033 - Blindern, 0315 Oslo, Norway
[7]Earth Science Division, NASA Ames Research Center, Moffett Field, CA 94035-1000

Abstract. Ozone is a greenhouse gas and air pollutant that is harmful to human health and plants. During the summer in the southeastern U.S., many regional and global models are biased high for surface ozone compared to observations. Past studies have suggested different solutions including the need for updates to model representation of clouds, chemistry, ozone deposition, and emissions of nitrogen oxides (NO_x) or biogenic hydrocarbons. Here due to the high biogenic emissions in the southeastern U.S., more comprehensive and updated isoprene and terpene chemistry is added into CESM^{TM}/CAM-chem (Community Earth System Model/Community Atmosphere Model with chemistry) to evaluate the impact of chemistry on simulated ozone. Comparisons of the model results with data collected during the Studies of Emissions Atmospheric Composition, Clouds and Climate Coupling by Regional Surveys (SEAC^{4}RS) field campaign and U.S. EPA CASTNET monitoring stations confirm the updated chemistry improves simulated surface ozone, ozone precursors, and NO_x reservoir compounds. The isoprene and terpene chemistry updates reduce the bias in the daily maximum 8-hr average (MDA8) surface ozone by up to 7 ppb. In the past, terpene oxidation in particular has been ignored or heavily reduced in chemical schemes used in many regional and global models, and this study demonstrates comprehensive isoprene and terpene chemistry is needed to reduce surface ozone model biases. Sensitivity tests were performed in order to evaluate the impact of lingering uncertainties in isoprene and terpene oxidation on ozone. Results suggest that even though isoprene emissions are higher than terpene emissions in the southeastern U.S., remaining uncertainties in isoprene and terpene oxidation have similar impacts on ozone due to lower uncertainties in isoprene oxidation. Additionally, this study identifies the need for further constraints on aerosol uptake of organic nitrates derived from isoprene and terpenes in order to reduce uncertainty in simulated ozone. Although the updates to isoprene and terpene chemistry greatly reduce the ozone bias in CAM-chem, a large bias remains. Evaluation against SEAC^{4}RS field campaign results suggests future improvements to horizontal resolution and cloud parameterizations in CAM-chem may be particularly important for further reducing this bias.

1 Introduction

Many regions of the world have poor air quality due to high levels of tropospheric ozone (O_3). Tropospheric ozone is also a greenhouse gas and is an important source of OH radicals, which impacts the lifetime of other greenhouse gases such as methane (Monks et al., 2015; IPCC, 2013). Recent health studies have suggested ozone negatively impacts human health more than previously thought by increasing the risk of both respiratory and circulatory mortality (Turner et al., 2016). Additionally, to protect human health and vegetation in 2015, the U.S. EPA strengthened the ozone standard to not exceed a maximum daily 8 hour average (MDA8) of 70 ppb for more than 3 days a year (U.S.EPA, 2015). Models must accurately simulate ozone for the right reasons to be most effective for predicting future air quality trends (e.g., Val Martin et al., 2015) or to attribute sources of ozone correctly (e.g., Cooper et al., 2015). Because ozone is not directly emitted into the atmosphere and is controlled by large nonlinear sources and losses, ozone is intrinsically difficult to simulate in climate and chemistry models.

Generally, global models capture ozone spatial patterns throughout the troposphere reasonably well, but simulated ozone is typically biased high in the northern hemisphere and low in the southern hemisphere and there are regional and seasonal biases that are not fully understood (Young et al., 2018). During the summer in the southeastern U.S., there is a persistent high bias for surface ozone in many models compared to observations (Fiore et al., 2009; Reidmiller et al., 2009; Brown-Steiner et al., 2015; Tilmes et al., 2015; Canty et al., 2015; Im et al., 2015). Model bias in surface ozone is a good indicator that nitrogen oxides (NO_x) or volatile organic compounds (VOCs) budgets and processing are poorly constrained. Past studies have suggested different solutions including the need for updates to model representation of clouds (Ryu et al., 2018), emissions of NO (Travis et al., 2016; McDonald et al., 2018b) or biogenic hydrocarbons (Kaiser et al., 2018), chemistry (Squire et al., 2015), chemical solver (Sun et al., 2017), and deposition (Val Martin et al., 2014; Clifton et al., 2019).

Tropospheric ozone is produced in the atmosphere when ozone precursors, anthropogenic or biogenic VOCs and NO_x, interact in the presence of sunlight (Monks et al., 2015). The hydroxyl radical (OH) reacts with a VOC to form a peroxy radical (RO_2), which reacts with NO to form an organic nitrate or an alkoxy radical and NO_2. NO_2 will photolyze to form NO and ozone. Organic nitrates are an example of a NO_x reservoir species, a species that has the potential to recycle NO_x back into the system, transport NO_x to a different location, or to permanently remove NO_x from the atmosphere. Correctly representing the production and loss pathways of NO_x reservoir species is critical for accurately representing ozone for the right reasons.

In the southeastern U.S., there are particularly large emissions of biogenic hydrocarbons like isoprene and terpenes, which motivates updating the formation and fate of ~~isoprene and terpene derived~~ isoprene- and terpene-derived organic nitrates in order to assess if more complex and current chemistry reduces model biases in surface ozone. The recent significant improvements in our understanding of isoprene oxidation chemistry (Wennberg et al., 2018, and references therein) have motivated many models to update their isoprene chemistry including GEOS-Chem (Fisher et al., 2016; Bates and Jacob, 2019), GFDL AM3 (Li et al., 2018), MAGRITTEv1.0 (Muller et al., 2018), WRF-Chem (Zare et al., 2018), ~~and~~ CESM2 (Emmons et al., 2020), and CMAQ (Pye et al., 2013).

Most studies so far have focused on updating isoprene oxidation with significantly less attention to terpenes. In general terpene oxidation has been ignored or heavily reduced in chemical schemes in many regional and global models used in the

past despite recent field campaigns suggesting the importance of terpene chemistry (Xu et al., 2015; Zhang et al., 2018). Many mechanisms represent monoterpenes as a single tracer (e.g., Emmons et al., 2020; Li et al., 2018; Muller et al., 2018). Monoterpenes were expanded to include two surrogate compounds first in WRF-Chem (Browne et al., 2014; Zare et al., 2018) and then in GEOS-Chem (Fisher et al., 2016). These models with expanded terpene chemistry demonstrate the importance of ~~terpene derived~~ terpene-derived organic nitrates for the NO_x budget in both the southeastern U.S. (Fisher et al., 2016) and over the boreal forests of Canada (Browne et al., 2014). These past studies motivate adding increased complexity for terpenes. Two surrogate compounds are not sufficient to accurately represent all terpene chemistry given the large variety of chemical structures and reactivities (Guenther et al., 2012). Our understanding of terpene chemistry is more limited than isoprene chemistry, but experimental and theoretical data are still available to generate a chemical scheme (Atkinson and Arey, 2003; Johnson and Marston, 2008; Ng et al., 2017, and references therein).

Here, isoprene and terpene chemistry in MOZART-TS1, the default chemical mechanism used in the Community Earth System Model/ Community Atmosphere ~~model~~ Model with full chemistry (CESM^{TM}/CAM-chem), will be updated ~~in order to determine how much chemistry~~ to determine the extent to which improvements to the gas-phase chemical mechanism for biogenic VOCs can explain the simulated surface ozone bias over the southeastern U.S. A bias in simulated surface ozone over North America in summer compared to observations was present in past releases of CESM/CAM-chem (Tilmes et al., 2015; Brown-Steiner et al., 2015) and continues to exist in the current release (CESM2.1.0) used in this work (see Section 4.3). For isoprene, the chemical mechanism updates are of similar complexity to Muller et al. (2018) and Bates and Jacob (2019) and more complex than Travis et al. (2016) and Li et al. (2018). For terpenes, the chemistry updates are significantly more complex than any other reduced scheme currently available (Browne et al., 2014; Fisher et al., 2016; Zare et al., 2018).

The updated isoprene and terpene chemistry will be evaluated against more explicit chemical mechanisms using a box model and against observations using CESM2/CAM-chem. In particular, the formation and fate of the organic nitrates between the new and old schemes will be described and evaluated. There are a number of lingering uncertainties for both isoprene and terpene chemistry related to the formation and fate of organic nitrates (e.g., differences in measured organic nitrate yields between studies or disagreement among researchers on how to estimate organic nitrate yields for unstudied compounds). These uncertainties will be assessed to determine which uncertainties have the largest impact on simulated surface ozone.

2 Development of MOZART-TS2

In this study a new version ("T2") of the MOZART (Model of OZone And Related chemical Tracers) tropospheric chemical mechanism has been developed for use in CESM/CAM-chem and other models. In CAM-chem the T2 mechanism is combined with the current stratospheric mechanism in CESM2 (Emmons et al., 2020), with the result called MOZART-TS2 or "TS2" hereafter. The TS2 mechanism includes a more complex representation of isoprene and terpene oxidation based on recent experimental data than in MOZART-TS1 (Emmons et al., 2020; Knote et al., 2014) or "TS1" hereafter. The updates for isoprene chemistry include an additional 21 transported species, 18 non-transported species, and 139 reactions, which increases the simulation time by ~18%. The updates for terpene chemistry include an additional 25 transported species, 22 non-transported

species, and 219 reactions, which increases the simulation time by ~26%. Thus, together these isoprene and terpene updates increase the simulation time by ~50%. As described in Section 4.1 and 4.2, this additional cost is necessary in order to correctly simulate HO_x and NO_x recycling and O_3 production.

A list of all TS2 species, photolysis reactions, and kinetic reactions is provided in the Supplement (Tables S2, S5, and S6). A simplified version of TS2 for isoprene and terpene OH-initiated oxidation is shown in Figures 1 and 2~~and~~ , for NO_3-initiated oxidation in Figures S1 and S2, and for O_3-initiated oxidation in Figure S3. These figures do not contain all of the detail in TS2, but illustrate the complexity to facilitate comparisons with other reduced schemes and define many of the surrogate species used throughout the text. Explicit chemical mechanisms including MCMv3.3.1 (Jenkin et al., 2015) and the Caltech isoprene mechanism (Wennberg et al., 2018) and several review papers (Atkinson and Arey, 2003; Johnson and Marston, 2008; Ng et al., 2017) strongly guided the creation of the reduced TS2 mechanism. Surrogate compounds are shared from NO_3, O_3, and OH-initiated oxidation to ensure accurate representation of the chemistry while reducing the number of surrogate compounds and the computational cost.

~~Simplified schematic of the TS2 mechanism for isoprene OH-initiated oxidation. Gray boxes indicates new chemistry added or updated in TS2. Blue compounds undergo aerosol uptake.~~ When available, all reaction rate constants were updated to those recommended in either JPL (Burkholder et al., 2015) or IUPAC (Atkinson et al., 2004, 2006). For those reaction rates not in IUPAC or JPL, typically the Caltech isoprene mechanism (Wennberg et al., 2018) or MCM v3.3.1 (Jenkin et al., 1997; Saunders et al., 2003; Jenkin et al., 2012, 2015) was used. For isoprene and terpene reactions, the peroxy (RO_2) and peroxyacyl (RCO_3) reaction rates were consistently assigned throughout the mechanism using the assumptions specified in Table S1. ~~Simplified schematic of the TS2 chemical mechanism for terpene OH-initiated oxidation. Blue compounds undergo aerosol uptake.~~

2.1 Updates to Henry's Law Constants

Currently, in TS1, only certain species undergo wet and dry deposition (Emmons et al., 2020). For TS2, all compounds undergo wet and dry deposition except for radicals and compounds constrained with lower-boundary conditions. As listed in Table S4, Henry's law constants were updated to the most recent literature recommendations (Burkholder et al., 2015; Sander, 2015; Schwartz and White, 1981; Leu and Zhang, 1999; Goldstein and Czapski, 1997; Fried et al., 1994; Chameides, 1984; Reichl, 1995; Kames and Schurath, 1995; Leng et al., 2013; Chan et al., 2010; Staudinger and Roberts, 2001; Dohnal and Fenclova, 1995; Hiatt, 2013; Guo and Brimblecombe, 2007; McNeill et al., 2012; Allou et al., 2011; Sieg et al., 2009; Iraci et al., 1999; Smith and Martell, 1976; Copolovici and Niinemets, 2005; van Roon et al., 2005). The effective Henry's law ~~calculations~~ equations used in CAM-chem are described in the notes at the end of Table S4. Henry's law constants for halogens important mainly for stratospheric chemistry were not changed from previous versions (Emmons et al., 2020). For all oxygenated organic gases that condense to form SOA, Henry's law coefficients were based on values from GECKO-A as in Hodzic et al. (2014, 2016) with no changes from previous versions (Emmons et al., 2020). When Henry's law constants were unavailable in the literature, the value was approximated based on a close surrogate or by GROMHE (Raventos-Duran et al., 2010). GROMHE is the theoretical structure activity relationship method used to estimate Henry's law constants by the Generator of Explicit Chemistry and Kinetics for Organics in the Atmosphere (GECKO-A) (Aumont et al., 2005). If the Henry's law temperature

dependence (dH/R) was unavailable in the literature, 6014 K was assumed consistent with GECKO-A. The reactivity factor (F_0) , which ranges used for dry deposition and ranging from 0 to 1 with 1 being as reactive as ozone ,is also listed in Table S4. The F_0 for oxygenated volatile organic compounds is assumed to be 1 consistent with recent observational studies (Karl et al., 2010; Nguyen et al., 2015).

2.2 Updates to Isoprene Chemistry

Isoprene oxidation by OH (Section 2.2.1), O_3 (Section 2.2.2), and NO_3 (Section 2.2.3) were all updated in TS2 from TS1. All new photolysis reactions were mapped with an optional scaling factor to photolysis rate constants already incorporated into CESM2. Scaling to known photolysis rates is common in reduced chemical mechanisms and even explicit mechanisms like MCM as photolysis rates for many surrogate compounds have not been measured. In general, products and photolysis rate constants were guided by explicit schemes: MCM v3.3.1 (Jenkin et al., 2015) and the Caltech isoprene mechanism (Wennberg et al., 2018). δ-hydroperoxy aldehydes (HPALD1 and HPALD2) were assumed to photolyze with the cross sections of methacrolein (Wennberg et al., 2018) and the quantum yield estimated by Liu et al. (2017). Carbonyl nitrates were assumed to photolyze with the fast photolysis rate constants reported in Muller et al. (2014). Like MCM v3.3.1 (Jenkin et al., 2015), the various carbonyl nitrate photolysis rates are scaled to that of propanone nitrate (NOA). The photolysis rate constant for isoprene carbonyl nitrate from isoprene NO_3-initiated oxidation (NC4CHO) is based on the measurement from Xiong et al. (2016).

2.2.1 OH-Initiated Oxidation

Isoprene reacts with OH and then O_2 to form 6 distinct isoprene hydroxy peroxy radicals (Figure 1), which are represented explicitly in TS2 based on reaction rate constants reported by Teng et al. (2017). The Caltech isoprene mechanism recommends a possible reduction to represent this 1^{st}-generation peroxy radical chemistry, but this reduction scheme does not perform as well in urban regions with high NO and short RO_2 lifetimes (Wennberg et al., 2018). Here this chemistry is represented explicitly (i.e. 4 isoprene hydroxy alkyl radical isomers and 6 isoprene hydroxy peroxy radical isomers) because radical species are not transported in CESM/CAM-chem and so do not considerably contribute to the computational cost. This more explicit chemistry allows TS2 to be used at finer horizontal resolutions that better resolve urban regions with high NO levels, which is a goal for future studies. The δ-Z-isoprene hydroxy peroxy radicals will isomerize in TS2 to form four isomers (2-β and 2-δ) of hydroperoxy aldehydes (HPALDs) among other products based on recommendations from Wennberg et al. (2018), but more reduced. There are still large uncertainties in the rates, product yields, and HO_x recycling from photolysis and OH oxidation of HPALDs. Once more is known, greater detail may be added to TS2.

While TS1 assumes a unity yield of isoprene hydroxy hydroperoxide (ISOPOOH) from the isoprene RO_2 + HO_2 reaction, TS2 adds a small yield of methyl vinyl ketone and methacrolein from this pathway (Liu et al., 2013; Wennberg et al., 2018). The ISOPOOH + OH reaction rate and products have been updated to be consistent with St. Clair et al. (2016). Chemistry for OH addition to ISOPOOH forms a 0.85 yield of isoprene epoxydiol (IEPOX) , & OH; a 0.07 yield of glycolaldehyde, hydroxyacetone, & OH; and a 0.08 yield of ISOPHFP, which is a surrogate compound for all isoprene highly functionalized

hydroperoxides (Krechmer et al., 2015; Riva et al., 2016; St. Clair et al., 2016; Liu et al., 2016; Piletic et al., 2019). ISOPHFP undergoes aerosol uptake in TS2 to more accurately represent loss processes of HO_x, but like organic nitrates does not explicitly form SOA. SOA is formed by a volatility basis set (VBS) scheme in CAM-chem, which was not updated in this work. Directly forming SOA from low-volatility products like ISOPHFP in CAM-chem is a goal for future work. Chemistry for IEPOX, the dominant product from ISOPOOH + OH reaction, has also been updated in TS2 (Bates et al., 2014, 2016; Jacobs et al., 2013; Wennberg et al., 2018). TS2 only has one isomer of ISOPOOH and IEPOX, which is more reduced than the Caltech mechanism (Wennberg et al., 2018), but this simplification has minimal impact on the total ISOPOOH or IEPOX concentration (Section 4.1). To save computational cost, multiple isomers were only incorporated into TS2 if grouping them together would bias the HO_x or NO_x budgets~~(e. g. ,~~. For example, the two dominant isomers of ISOPOOH react with OH to produce similar yields of OH and a similar distribution of IEPOX isomers (Wennberg et al., 2018), so grouping isomers of ISOPOOH and IEPOX together to reduce computational cost is warranted. In contrast, TS2 includes multiple isomers of HPALDs and hydroxy nitrates ~~)~~because different isomers react with OH to produce varying levels of OH and NO_2, so combining these isomers together would inaccurately influence the HO_x and NO_x budgets.

In TS2, additional organic nitrates are added to better represent NO_x recycling in the mechanism. Four (ISOPN4D, ISOPN1D, ISOPN2B, ISOPN3B) instead of two 1st-generation hydroxy nitrate isomers are included using the temperature and pressure dependent yields recommended by Wennberg et al. (2018) and Teng et al. (2017) ($\sim$0.13 at 297K). Often different isomers of the same compound will have very different fates in the atmosphere. For example, β and δ-hydroxy nitrates have different reaction rates with OH and O_3 and form different products (Lee et al., 2014). Additionally, tertiary organic nitrates will be more likely to undergo aerosol uptake due to their rapid hydrolysis in the particle phase compared to secondary or primary organic nitrates (Section 2.4). The ~~number of~~ organic nitrates in TS2 ~~was optimized to accurately represent~~ were carefully selected to account for these varying fates, but also when possible to combine isomers with similar reaction rates, oxidation products, and overall atmospheric fate together to reduce computational cost. The differences in organic nitrate formation and fate between TS1 and TS2 are described in more detail in Section 5.1.

In TS1, OH oxidation of the 1st-generation hydroxy nitrates immediately forms stable products from the RO_2 + NO channel rather than going through a peroxy radical intermediate. Conversely, in TS2, when an isoprene hydroxy nitrate is oxidized by OH, a peroxy radical forms, which can either isomerize or react with NO or HO_2 (Jacobs et al., 2014; Lee et al., 2014; Wennberg et al., 2018). Because NO_x emissions are generally decreasing or expected to decrease in the United States (Kharol et al., 2015; EPA, 2018; Jiang et al., 2018) and mixed regimes are becoming more prevalent, chemical mechanisms that do not fix the fate of the peroxy radical to the 1st-generation fate will become increasingly important. For example, in TS2, peroxy radicals from OH oxidation of unsaturated organic nitrates produced from the RO_2 + NO channel and IEPOX produced from the RO_2 + HO_2 channel can react either with NO or HO_2 in the later-generation step. A wide variety of later-generation organic nitrates are added to TS2 including those from decomposition (C_2-C_4) and functionalization (ISOPFNP and ISOPFDN in Figure 1). Including additional surrogate compounds for highly functionalized nitrates, whose fates are likely to remove NO_x through aerosol uptake/hydrolysis or wet/dry deposition, is important for accurately representing the NO_x budget.

Methacrolein and methyl vinyl ketone, which are 1st-generation products from isoprene, react with OH to form separate peroxy radicals in TS2 (Figure 1), so that the methacrolein hydroxy peroxy radical can undergo an isomerization reaction (Crounse et al., 2012). In TS2, methacrolein and methyl vinyl ketone peroxy radicals react with HO_2 to form not only hydroxy hydroperoxides (MACROOH and MVKOOH) like in TS1, but also OH and decomposition products (Praske et al., 2015; Wennberg et al., 2018). The organic nitrate yields from the methacrolein and methyl vinyl ketone RO_2 + NO reactions have been updated and form distinct organic nitrates (MACRN and MVKN) (Crounse et al., 2012; Praske et al., 2015). Products from the reaction of HO_2 with all acyl peroxy radicals including the one derived from methacrolein were updated to IUPAC recommendations (Atkinson et al., 2006) based on the following studies (Hasson et al., 2004; Jenkin et al., 2007; Dillon and Crowley, 2008; Niki et al., 1985; Horie and Moortgat, 1992) and averaging in results from a more recent study (Grob et al., 2014).

2.2.2 O_3-Initiated Oxidation

O_3-initiated oxidation of isoprene is simply described in Figure S3 and largely based on Grosjean et al. (1993a), Aschmann and Atkinson (1994), Nguyen et al. (2016), and IUPAC (Atkinson et al., 2006). Given isoprene is typically emitted in regions with high RH, the stabilized ~~criegees~~ Criegees are not represented explicitly in the mechanism and instead are assumed to react immediately with H_2O and $(H_2O)_2$ in equal amounts, which is approximately the case for RH > 60%, to form hydroxymethyl hydroperoxide (HMHP), formaldehyde and H_2O_2, or formic acid (Nguyen et al., 2016). HMHP, a new product in TS2, photolyzes and reacts with OH based on Roehl et al. (2007), Allen et al. (2018), and Wennberg et al. (2018). The reaction of $HOCH_2OO$ + HO_2, which includes HMHP as a product, was updated to IUPAC recommendations (Atkinson et al., 2006).

2.2.3 NO_3-Initiated Oxidation

Isoprene NO_3-initiated oxidation ~~is~~ in TS2 is described in a simplified schematic in Figure S1 and is largely based on the following studies: Schwantes et al. (2015) and Wennberg et al. (2018) for 1st-generation and Schwantes et al. (2015), Lee et al. (2014), Xiong et al. (2016), and Jacobs et al. (2014) for 2nd-generation products. Both TS1 and TS2 only have one surrogate compound for the nitrooxy peroxy radical formed when isoprene reacts with NO_3. Based on the products formed, TS1 assumes all the nitrooxy peroxy radicals are δ-isomers while TS2 uses the yields in Schwantes et al. (2015), which estimated approximately equal amounts of β- and δ-nitrooxy peroxy radicals. Additionally, TS2 assumes a non-unity yield of nitrooxy hydroperoxide from the RO_2 + HO_2 channel consistent with recent work (Schwantes et al., 2015; Wennberg et al., 2018; Rollins et al., 2009; Kwan et al., 2012). Where structurally similar, organic nitrates from ~~the~~ OH and NO_3 ~~system~~ oxidation are shared to reduce computational cost (Figure 1 and S1). Two isomers (β and a δ) of isoprene nitrooxy hydroxy epoxide formed from OH oxidation of nitrooxy hydroperoxide are added to TS2 (Schwantes et al., 2015; Wennberg et al., 2018). Similar to OH-initiated oxidation, the organic nitrates derived from NO_3-initiated oxidation react with OH to form a peroxy radical that can isomerize or react with NO or HO_2 (Lee et al., 2014; Jacobs et al., 2014; Schwantes et al., 2015; Wennberg et al., 2018; Xiong et al., 2016).

2.3 Updates to Terpene Chemistry

In TS1, all monoterpenes are grouped into one surrogate (MTERP) and all sesquiterpenes are grouped into one surrogate (BCARY). The OH, O_3, and NO_3 reaction rate constants are different between MTERP and BCARY, but the oxidation chemistry is identical. An expanded version of the TS1 terpene chemistry used primarily in WRF-Chem, called T1 (Emmons et al., 2020; Knote et al., 2015a), replaced MTERP with four monoterpene surrogates: α-pinene (APIN), β-pinene (BPIN), limonene (LIMON) and myrcene (MYRC). In T1, the five terpene surrogates have different reaction rates with OH, O_3, and NO_3, but their oxidation chemistry is identical. Here in TS2, we start from the T1 mechanism and group all rather than a subset of the terpenes in MEGAN v2.1 (online in CESM) according to their chemical structure and reactivity into the 5 terpene surrogate compounds: APIN, BPIN, LIMON, MYRC, and BCARY (Table S3). Unlike T1, in TS2 each terpene surrogate has unique chemistry. Even though the chemistry is different for each terpene surrogate in TS2, the 1st- and later-generation products are often shared to save computational cost. For example, the terpene hydroxy nitrate surrogate compounds are split according to their chemical structure (saturated versus unsaturated and primary/secondary versus tertiary) instead of based on their VOC precursor (i.e. there are not unique APIN hydroxy nitrates and BPIN hydroxy nitrates). Terpene oxidation chemistry by OH (Section 2.3.1), O_3 (Section 2.3.2), and NO_3 (Section 2.3.3) were all updated in TS2 from TS1. Like isoprene, rates for all photolysis reactions were mapped to photolysis rate constants already incorporated into CESM2 (Table S5). In general, photolysis reactions and rate constants were guided by MCM v3.3.1 (Jenkin et al., 2015).

2.3.1 OH-Initiated Oxidation

The terpene surrogate compounds react with OH to form hydroxy peroxy radicals that react with NO, NO_3, RO_2, or HO_2. For APIN, BPIN, LIMON, MYRC, and BCARY, the products from RO_2 + NO reaction, which have been reasonably well studied, were used to extrapolate the products from the RO_2 + NO_3 and $RO_2 + RO_2$ reactions. The hydroxy hydroperoxide yield from the RO_2 + HO_2 channel has only been measured for α-pinene (Noziere et al., 1999; Eddingsaas et al., 2012). For the rest, the hydroxy hydroperoxide yield is estimated based on the parameterization recommended by Wennberg et al. (2018) assuming the same RO_2 distribution used in the RO_2 + NO reaction. Below we explain briefly the experimental and theoretical studies used to determine the product distribution from the RO_2 + NO reaction for each terpene surrogate compound. Organic nitrate yields from the RO_2 + NO pathway for many later-generation terpene oxidation products (e.g., pinonaldehyde, nopinone, and limonaldehyde) have not been measured; in this case, the organic nitrate yield is approximated from the parameterization by Wennberg et al. (2018) up to a maximum of 0.3. Experimental work on the alkane system suggests that the organic nitrate yield plateaus at 0.3 (Arey et al., 2001; Yeh and Ziemann, 2014). No past literature studies have evaluated whether this plateau is different for oxygenated VOCs, which could have important consequences on ozone. Future experimental studies constraining organic nitrate yields from oxygenated VOCs is highly recommended for further improvement of the TS2 mechanism. Due to the large uncertainties in the organic nitrate yields from terpene oxidation, no temperature or pressure dependency was included.

The APIN RO_2 will react with NO to form hydroxy nitrates (yield = 0.23) (Noziere et al., 1999; Ruppert et al., 1999; Rindelaub et al., 2015), acetone (Aschmann et al., 1998; Noziere et al., 1999; Orlando et al., 2000; Wisthaler et al., 2001), formaldehyde (Noziere et al., 1999; Orlando et al., 2000), pinonaldehyde (TERPA) (Arey et al., 1990; Hakola et al., 1994; Wisthaler et al., 2001; Aschmann et al., 2002a), and the remaining products are based on theoretical work (Vereecken et al., 2007). The hydroxy nitrate isomer distribution is based on one experimental study (Berndt et al., 2016) and theoretical work (Vereecken et al., 2007). The products from the RO_2 + HO_2 channel (TERPOOH, TERP1OOH, TERPA) are based on experimental (Noziere et al., 1999; Eddingsaas et al., 2012) and theoretical (Vereecken et al., 2007) studies. Fewer studies have been conducted on β-pinene than α-pinene, but still enough information is available to develop a scheme. The BPIN RO_2 will react with NO to form nopinone (TERPK) (Arey et al., 1990; Hakola et al., 1994; Wisthaler et al., 2001; Lee et al., 2006b; Jaoui and Kamens, 2003), formaldehyde (Hatakeyama et al., 1991; Orlando et al., 2000; Lee et al., 2006b), acetone (Aschmann et al., 1998; Orlando et al., 2000; Wisthaler et al., 2001; Lee et al., 2006b), hydroxy nitrates (yield = 0.25) (Ruppert et al., 1999), and the remaining products are based on theory (Vereecken and Peeters, 2012). The RO_2 isomer distribution is based on the measured product yields defined above for hydroxy nitrates and nopinone and theoretical work from Vereecken and Peeters (2012).

The LIMON RO_2 isomer distribution is approximated using the SAR developed by Peeters et al. (2007). These RO_2 will react with NO to form hydroxy nitrates (yield = 0.23) (Ruppert et al., 1999), formaldehyde (Lee et al., 2006b), and a terpene oxidation product containing one double bond (TERPF1), which represents both limonaldehyde and limaketone. MYRC RO_2 isomer distribution is also approximated by the SAR developed by Peeters et al. (2007) and reacts with NO to form hydroxy nitrates (yield = 0.29) (Ruppert et al., 1999), acetone (Reissell et al., 1999; Orlando et al., 2000; Lee et al., 2006b), formaldehyde (Orlando et al., 2000), and the main product is assumed to be TERPF2, which is a functionalized terpene oxidation product with two double bonds. OH-initiated oxidation is quite uncertain for β-caryophyllene, the surrogate for all sesquiterpenes. From the BCARY RO_2 reaction with NO we form a sesquiterpene nitrate called SQTN (yield = 0.3) and TERPF2. The sesquiterpenes have 2-4 double bonds (Guenther et al., 2012), so we assume TERPF2 forms as the primary 1st-generation product. Because SQTN has at least one double bond and is low in volatility, it or its oxidation products, which will retain the nitrate group, will likely deposit or undergo aerosol uptake. Thus, we do not include further reaction of SQTN with OH or photolysis.

In order to save computational cost and still represent the chemistry as accurately as possible, the 1st- and later-generation products for all the terpene surrogate compounds are shared. There are a number of aldehyde surrogate compounds including: TERPA, which represents pinonaldehyde type products; TERPA2, which represents norpinaldehyde type products; and TERPA3, which represent aldehydes largely produced from limonaldehyde and limaketone oxidation. These aldehyde products react with OH, O_3, and NO_3 based on pinonaldehyde from MCM v3.3.1 (Saunders et al., 2003). Each of these will form corresponding carboxylic/peroxy acids (TERPACID,TERPACID2, TERPACID3) and ~~PANs~~ peroxy acyl nitrates (TERPAPAN, TERPA2PAN, TERPA3PAN). One ketone is included: TERPK, which represents nopinone type products and reacts with OH using the rate from Calogirou et al. (1999). There are two unsaturated compounds, which represent functionalized terpene oxidation products with one (TERPF1) or two (TERPF2) double bonds. TERPF1 reacts with OH, O_3, and NO_3 like limonaldehyde (Calogirou et al., 1999) and TERPF2 reacts with OH and NO_3 like isoprene (Atkinson et al., 2006) and O_3 like

1st-generation products from β-caryophyllene (Winterhalter et al., 2009). There are three hydroperoxides: TERPOOH, which represents saturated hydroxy hydroperoxides with a ring (e.g., from α-pinene); TERPOOHL, which represents saturated hydroxy hydroperoxides without a ring (e.g., from limonene); TERP1OOH, which represent hydroxy hydroperoxides with one double bond; and TERP2AOOH, which represent hydroxy hydroperoxides with two double bonds. In order to represent terpenes with multiple double bonds accurately, the later-generation products must continue to contain a double bond that undergoes OH-addition. There are four 1st-generation hydroxy nitrates: TERPNS (primary and secondary saturated), TERPNS1 (primary and secondary unsaturated), TERPNT (tertiary saturated), and TERPNT1 (tertiary unsaturated). Saturated and unsaturated hydroxy nitrates are separated because they have different reaction rates and products from oxidation by OH. Tertiary hydroxy nitrates are separated from primary/secondary hydroxy nitrates because tertiary nitrates will undergo aerosol uptake due to their rapid hydrolysis (Section 2.4). There are also a number of low-volatility highly functionalized compounds such as TERPFDN, which represents highly functionalized terpene dinitrates; TERPHFN, which represents highly functionalized terpene nitrates; and TERPDHDP, which represents terpene dihydroxy dihydroperoxides.

The terpene products described above were selected, so that compounds that are chemically similar (i.e. contain the same functional groups and react with OH, O_3, and NO_3 at similar rates) are grouped together. The complexity of the chemistry is largely determined by the current knowledge of the system. There may be advantages to adding more complexity into TS2 in the future as more knowledge about terpene oxidation especially later-generation chemistry becomes available. Given terpene-later-generation chemistry is not well understood and that chemistry of many terpene products is largely estimated based on similar more well-studied compounds, adding separate products for each of the terpene surrogate compounds would increase cost without adding a lot of additional information into the system.

2.3.2 O_3-Initiated Oxidation

O_3-initiated oxidation of the terpene surrogate compounds in TS2 is described in a simplified schematic in Figure S3. O_3-initiated oxidation of APIN is based on MCM (Saunders et al., 2003), IUPAC (Atkinson et al., 2006), theoretical calculations (Zhang and Zhang, 2005; Kurten et al., 2015), and experimental results (Ma et al., 2008). The OH yield (0.77) is quite high (Chew and Atkinson, 1996; Paulson et al., 1998; Rickard et al., 1999; Siese et al., 2001; Berndt et al., 2003; Forester and Wells, 2011). The stabilized ~~criegees~~ Criegees are not represented explicitly in the mechanism and instead are assumed to react immediately with H_2O to form either H_2O_2 and pinonaldehyde (TERPA) or pinonic acid (TERPACID). O_3-initiated oxidation of BPIN is based on MCM (Saunders et al., 2003), IUPAC (Atkinson et al., 2006), experimental results (Hakola et al., 1994; Grosjean et al., 1993b; Yu et al., 1999; Ma and Marston, 2008; Winterhalter et al., 2000; Hasson et al., 2001), and theory (Nguyen et al., 2009). The OH yield (0.3) from β-pinene ozonolysis is much lower than that from α-pinene due to differences in their molecular structures (Atkinson et al., 1992; Rickard et al., 1999). Again the stabilized ~~criegee~~ Criegee intermediates are not explicitly represented and instead assumed to react directly with H_2O to form H_2O_2 and nopinone (TERPK).

Only a few products with low yields have been detected from limonene ozonolysis (Atkinson and Arey, 2003). The chemical mechanism for O_3-initiated LIMON oxidation is based on MCM (Saunders et al., 2003) and IUPAC (Atkinson et al., 2006). The OH yield is 0.66 (Aschmann et al., 2002a; Forester and Wells, 2011; Herrmann et al., 2010). The majority of products are

grouped into one surrogate species, TERPF1, which is a terpene functionalized oxidation product with one double bond. Again stabilized ~~criegee~~ Criegee intermediates were not included explicitly and instead assumed to react with H_2O to form H_2O_2 and TERPF1 or TERPACID in similar yields to that in the α-pinene system. O_3-initiated oxidation of MYRC is based on Ruppert et al. (1999), Boge et al. (2013) and Lee et al. (2006a) with an OH yield of 0.63 from Aschmann et al. (2002a). The dominant products are hydroxy acetone (HYAC), acetone, and 4-vinyl-4-pentenal (TERPF2). O_3-initiated oxidation of BCARY is based on Winterhalter et al. (2009) and Jaoui et al. (2003) with an OH yield of 0.08 (Shu and Atkinson, 1994; Winterhalter et al., 2009) to form TERPACID and TERPF2.

2.3.3 NO_3-Initiated Oxidation

For NO_3-initiated oxidation, α-pinene has been studied the most completely. Based on the few studies investigating the other monoterpenes, α-pinene oxidation by NO_3 is unique (Hallquist et al., 1999; Fry et al., 2014; Kurten et al., 2017), so α-pinene is handled separately in TS2 as APIN. In TS2, monoterpenes react with NO_3 to form a nitrooxy peroxy radical, which then reacts with HO_2, NO, NO_3, CH_3CO_3, CH_3O_2, and itself to form different yields of organic nitrates as summarized in a simplified schematic in Figure S2. There are few experimental studies that explicitly state the RO_2 fate, when reporting a nitrate yield. In all future experiments, reporting the RO_2 fate is recommended, so that laboratory results can be directly used in the development of condensed and explicit chemical mechanisms.

In TS1, when the nitrooxy peroxy radical reacts with HO_2, one nitrooxy hydroperoxide isomer forms with unity yield. In contrast, TS2 forms four nitrooxy hydroperoxide isomers: TERPNPT (saturated tertiary), TERPNPS (saturated secondary/primary), TERPNPT1 (unsaturated tertiary), and TERPNPS1 (unsaturated primary/secondary) (Figure S2). Recent work suggests that the α-pinene nitrooxy peroxy radical reacts with HO_2 to form nitrooxy hydroperoxide (0.3) and pinonaldehyde (0.7) (Kurten et al., 2017). The yield of nitrooxy hydroperoxides for all other surrogate terpene compounds is estimated from the parameterization in Wennberg et al. (2018). Berndt and Boge (1997) measured a 0.14 nitrate or 0.07 dinitrate yield from α-pinene nitrooxy peroxy + NO reaction. Because the α-pinene nitrooxy alkoxy radical is unlikely to decompose to form organic nitrates (Fry et al., 2014; Kurten et al., 2017), this signal is assumed to be from dinitrates. Thus, in TS2, all terpene surrogate nitrooxy peroxy radicals react with NO to form a yield of 0.07 dinitrates. Most NO_3-initiated oxidation laboratory experiments have focused on RO_2 + RO_2 chemistry. The fate of the alkoxy radical can be inferred from these product distributions and used to estimate the oxidation products from the other pathways (i.e., RO_2 + HO_2, RO_2 + NO_3, and RO_2 + NO).

APIN nitrooxy peroxy radical + RO_2 reactions form organic nitrates and pinonaldehyde (TERPA) (Wangberg et al., 1997; Hallquist et al., 1999; Spittler et al., 2006). The nitrooxy peroxy radical isomer distribution is based on MCM v3.3.1 (Saunders et al., 2003). The APIN nitrooxy alkoxy radical is assumed not to form any organic nitrates. For BPIN, the tertiary peroxy radical (yield of 0.9) is dominant (Boyd et al., 2015), so the RO_2 + RO_2 reactions are presumed to mostly form alkoxy radicals rather than carbonyl or hydroxy nitrates. Nopinone is produced in a low yield (0.02) (Hallquist et al., 1999), and the remaining products are quite uncertain. The alkoxy radical from δ-3-carene, which is grouped with β-pinene, breaks preferentially at the $C-C(H_2)$ bond to retain the nitrate group rather than the $C-C(ONO_2)$ bond to release NO_2 (Kurten et al., 2017). For RO_2 + RO_2 reactions from BPIN, the organic nitrate yield is based on Hallquist et al. (1999) and Fry et al. (2009). The BPIN alkoxy

radical is assumed to decompose to form organic nitrates based on the average between β-pinene and δ-3-carene, which are grouped into one surrogate compound (Fry et al., 2014).

LIMON NO_3-initiated oxidation is more complicated because of the 2 double bonds. Spittler et al. (2006) determined that NO_3 addition is more selective than OH, and so NO_3 dominantly reacts with the endocylic double bond of limonene. LIMON NO_3-initiated oxidation was assumed to form a similar initial nitrooxy peroxy radical distribution as α-pinene. The organic nitrate yield for RO_2 + RO_2 reactions is based on Hallquist et al. (1999), Spittler et al. (2006) and Fry et al. (2014). MYRC NO_3-initiated oxidation has not been constrained by any studies. MYRC nitrooxy peroxy radical distribution was calculated based on SARs (Pfrang et al., 2006) and the following assumptions. For conjugated double bonds, NO_3 adds to the less substituted position and equal amounts of δ- and β-peroxy radicals form consistent with isoprene oxidation (Teng et al., 2017; Schwantes et al., 2015). For the non-conjugated double bond, NO_3 adds in the same ratio as that for α-pinene. For organic nitrate yields, all secondary/tertiary alkoxy radicals were assumed to release NO_2 and all primary alkoxy radicals were assumed to produce carbonyl nitrates. The RO_2 + RO_2 reaction was assumed to form the same organic nitrate yield as α-pinene. All of these assumptions are quite speculative. Better understanding of less studied monoterpenes like myrcene is necessary.

There are also few constraints on NO_3-initiated oxidation of β-caryophyllene. All ~~sesquiterpene derived~~ sesquiterpene-derived organic nitrates are grouped together as SQTN consistent with OH-initiated oxidation. Fry et al. (2014) detected all of the organic nitrates from β-caryophyllene in the particle phase. Thus, the main loss of SQTN in the atmosphere and in TS2 is aerosol uptake and wet/dry deposition to permanently remove NO_x in the atmosphere. The BCARY peroxy radical distribution and organic nitrate yields were assumed to be similar to that of α-pinene. Sesquiterpene NO_3-initiated oxidation is quite uncertain and difficult to constrain given current literature data. However, ~~sesquiterpene derived~~ sesquiterpene-derived nitrates, which quickly partition to the particle-phase or deposit on surfaces, may be important missing removal pathways for NO_x and so deserve further study.

The four nitrooxy hydroperoxides derived from NO_3-initiated oxidation react with OH and photolyze largely based on MCM v3.3.1 (Saunders et al., 2003). However, in MCM v3.3.1, unsaturated nitrooxy hydroperoxides react with OH via hydrogen abstraction rather than addition to the double bond. This over-simplification ~~is common in later-generation oxidation pathways~~ ~~in~~ in MCM v3.3.1 ~~, and~~ leads to inaccurate NO_x recycling (Section 4.2). Instead of using MCM v3.3.1 recommendations, OH is assumed to react with the unsaturated nitrooxy hydroperoxides at the same rate as limonaldehyde (Calogirou et al., 1999) and to largely form the corresponding saturated nitrooxy hydroperoxide ~~.~~(Figure S2).

2.4 Aerosol Uptake of Isoprene and Terpene Organic Nitrates

In CESM/CAM-chem, uptake of gas-phase organic nitrates to aerosols is represented simply by converting an organic nitrate to nitric acid thereby neglecting the entire particle-phase hydrolysis reaction. TS1 uses aerosol uptake parameters based on Fisher et al. (2016) for organic nitrates derived from isoprene (γ = 0.005) and ~~terpene~~ terpenes (γ = 0.01)~~derived organic nitrates~~. Fisher et al. (2016) recommends a bulk aerosol uptake coefficient for all isoprene hydroxy nitrate isomers, even though only tertiary and δ-allylic-hydroxy nitrates will undergo fast enough hydrolysis for aerosol uptake to be relevant in the atmosphere (Jacobs et al., 2014). In TS2, only tertiary isoprene and terpene organic nitrates and isoprene δ-allylic-hydroxy nitrates undergo

aerosol uptake (Jacobs et al., 2014), but with a larger aerosol uptake coefficient ($\gamma = 0.02$) recommended by Wolfe et al. (2015). The newly added ~~multifunctional~~ multi-functional isoprene and terpene low-volatility organic nitrates in TS2 undergo rapid aerosol uptake ($\gamma = 0.1$) based on Marais et al. (2016). In TS2, aerosol uptake of organic nitrates is only a gas-phase sink for organic nitrates and does not form SOA directly. SOA in TS2 only forms from a VBS scheme (Tilmes et al., 2020), which was not updated in this work. Better connecting gas-phase chemistry and SOA formation is a goal for future work as uptake of organic nitrates to form SOA is important for accurately representing gas-phase ozone as well as the overall magnitude of SOA. Aerosol uptake of organic nitrates is quite uncertain (Section 5.2) and ~~deserves further study.~~

further studies investigating the processes of organic nitrate uptake and hydrolysis as well as more complex implementation of these processes in models is warranted and a goal for future work.

3 Methods

The newly developed TS2 mechanism was evaluated against explicit mechanisms using a box model (Section 3.1) and against field observations using CESM/CAM-chem (Section 3.2).

3.1 Box Modeling

MOZART-TS2 was compared with MOZART-TS1, MCM v3.3.1 (Jenkin et al., 2015), and the Caltech isoprene mechanism (Wennberg et al., 2018) using BOXMOX v1.7 (Knote et al., 2015b), a box model wrapper for the Kinetic Preprocessor (KPP) (Sandu and Sander, 2006). The Master Chemical Mechanism, MCM v3.3.1, was downloaded via the website: http://mcm.leeds.ac.uk/MCM, last access: 7 September 2018 (Jenkin et al., 1997; Saunders et al., 2003; Jenkin et al., 2012, 2015). The Caltech mechanism (RCIM), isoprene reduced plus v4.1, was downloaded from http://doi.org/10.22002/D1.247, last access: 23 March 2018 (Bates and Wennberg, 2017). The inorganic reactions from MCM v3.3.1 were used for all mechanisms in order to focus on differences caused by isoprene and terpene chemistry. To capture differences in OH, O_3, and NO_3 oxidation, an ideal diurnal cycle was simulated in the box model with the planetary boundary layer height, temperature, general photolysis rate constants, emissions of NO, CO, isoprene, formaldehyde, formic acid, methanol, glycolaldehyde, sulfur dioxide, sesquiterpenes, and monoterpenes from the CESM/CAM-chem base TS1 simulation. Aerosol uptake of the following inorganic compounds: HO_2, N_2O_5, NO_2, NO_3 ~~and~~ were included based on the reaction rate constants output from the CESM/CAM-chem base simulation. Dry deposition of the following inorganic compounds: O_3, CO, NO, NO_2, HNO_3, N_2O_5, HO_2NO_2, H_2O_2, and SO_2 were ~~also~~ included using the dry deposition velocities from the CESM/CAM-chem base simulation. The box is mixed based on the planetary boundary layer height with background air, which has fixed concentrations of isoprene, terpenes, H_2O, CH_4, H_2, CO, O_3, NO, NO_2, SO_2, and N_2O from the CESM/CAM-chem TS1 base simulation. Each mechanism (Caltech, MCM, and TS1/TS2) calculates photolysis rates differently. In CESM/CAM-chem, general photolysis rates are calculated using a lookup table (Lamarque et al., 2012) and all other photolysis rates are mapped to these general photolysis rates with an optional scaling factor. In the box model setup, general photolysis rates from CESM/CAM-chem are used for all mechanisms and the scaling factors are mechanism specific. This approach ensures consistency in the general

photolysis reactions across mechanisms, but still evaluates mechanism specific scaling factors for photolysis of isoprene and terpene oxidation products.

CESM/CAM-chem TS1 base case model output was used to initialize BOXMOX. In order to pick a location with high biogenic emissions, the grid box containing the Coffeeville U.S. EPA CASTNET monitoring site located in Mississippi (~~lat = 34.002747, lon = -89.799183°~~ N, 89.799183° W) was selected because it has a forest land use type as classified by the U.S. EPA. Aug 3, 2013 was selected to represent this ideal day due to high biogenic emissions (i.e., highest noon isoprene and monoterpene emissions in August) and minimal cloud cover (i.e. within top five highest noon j_{NO2} values in August). To reduce complexity and increase traceability, each box model simulation was initialized with only one non-oxygenated VOC at a time (e.g., only isoprene or α-pinene). To ensure reasonable oxidant concentrations, isoprene, monoterpene, and sesquiterpene emissions were scaled by 1.6, 13, and 88, respectively, such that their molar total was equal to the molar total emissions of the major non-oxygenated VOCs (alkanes, alkenes, aromatics, isoprene, and terpenes). This method was selected instead of holding the oxidants (i.e. OH, O_3, and NO_3) constant in order to evaluate differences in O_3, HO_x, and NO_x between the mechanisms. These ~~are ideal scenarios~~ idealized scenarios are designed to examine and clearly present the impact variations in the chemistry of a single VOC have on oxidants and oxidation products and not to accurately represent the chemistry of a specific location.

3.2 Global Modeling

The Community Earth System Model/Community Atmosphere Model with chemistry (CESM^{TM}/CAM-chem) released version 2.1.0 was used with a horizontal resolution of 0.9° x 1.25° (Emmons et al., 2020; Tilmes et al., 2020). The meteorology (~~temperature and winds~~air and surface temperature, horizontal winds, surface pressure, sensible and latent heat flux, and wind stress) was nudged with a 50 h relaxation time as described in Lamarque et al. (2012) to the Modern-Era Retrospective analysis for Research and Applications, Version 2 (MERRA2) (Gelaro et al., 2017) meteorological fields interpolated to the native CAM model resolution of 32 levels. ~~CAM physics, dynamics, and cloud parameterizations are tuned at this 32 level vertical resolution and using a weak relaxation time (50 h) for nudging reduces variability while also limiting the impact of nudging on model parameterizations. In Figures S5 and~~ In Figures S6 and S7, the impact of using different vertical resolutions and nudging relaxation times are shown for ozone, ozone precursors, and isoprene oxidation products. Using a stronger nudging relaxation time (i.e ~~6~~ 5 h rather than the 50 h used in this study) increases model bias in the vertical profile shape of ozone (Figure ~~S5).~~ S6). Using 32 vertical levels, the vertical resolution to which CAM physics, dynamics, and cloud parameterizations are tuned, slightly improves the model bias for ozone near the surface compared to using 56 vertical levels, the native resolution of the MERRA2 meteorological files (Figure S6). This study uses 32 vertical levels and a weak relaxation time (50 h) for nudging in order to reduce variability while also limiting the impact of nudging on model parameterizations. Biogenic emissions were calculated online in the community land model (CLM) based on Model of Emissions of Gases and Aerosols from Nature (MEGAN) v2.1 (Guenther et al., 2012). Satellite derived plant functional type (PFT) and leaf area index (LAI) from AVHRR and MODIS data are used in the CLM model (Lawrence and Chase, 2007). The default biogenic emissions used in CESM/CAM-chem v2.1.0 were expanded to include more volatile organic compounds as listed in Table S3 for all simulations.

Global anthropogenic emissions are from the Community Emissions Data System (CEDS) (Hoesly et al., 2018) and global biomass burning emissions are from van Marle et al. (2017).

Four main model simulations were conducted. First, the "TS1" case uses the default CESM2.1.0/CAM-chem code and the default TS1 chemical mechanism with the two changes described above: 32 vertical levels and an expansion of the biogenic volatile organic compounds emitted from the land model (Table S3)~~and using 32 vertical levels as described above~~. Second, the "Henry's Law" case uses the Henry's law constant updates as described in Section 2.1 in the wet and dry deposition schemes. Third, the "ISOP" case uses the Henry's law updates and the isoprene oxidation chemistry described in Section 2.2. Fourth, the "TS2" case includes all of the TS2 chemistry updates: Henry's law, isoprene, and terpene updates (described in Section 2.3). Each case is progressively more complicated. Because new surrogates incorporated into the chemical mechanism of CESM are initialized to 0, these four cases were separately spun-up for 2.5 years ~~to~~ (i.e., Jan 1, 2011 to July 31, 2013) to ensure that all new species were equilibrated and all simulations were performed consistently. Sensitivity tests were also conducted to evaluate the impact of uncertainties remaining in the chemical mechanism on simulated surface ozone. All sensitivity tests were identical to the TS2 case with small variations in the chemistry as described in Section 5.2. These sensitivity tests were spun-up from exact restarts from the TS2 case for 3 months, which is sufficient because no new species were added.

4 Results~~and Discussion~~

Evaluation against more explicit schemes like the Caltech mechanism and MCM verifies that TS2 more accurately simulates isoprene (Section 4.1) and terpene (Section 4.2) chemistry compared to TS1. These comparisons verify that the current number of tracers and reactions in TS2 are sufficient to reasonably capture the isoprene and terpene chemistry represented by more explicit schemes. Comparisons with CASTNET monitoring observations (Section 4.3) and SEAC^4~~Rs~~ RS field campaign data (Section 4.4) ~~suggests~~ suggest that ozone, ozone precursors, and NO_x reservoir species are generally better represented in TS2 than TS1. ~~The differences in simulated ozone between the two mechanisms are largely caused by differences in formation and fate of organic nitrates, which is explained in Section 5.1. Although much is known about isoprene and terpene chemistry, lingering uncertainties remain. These uncertainties are evaluated in Section 5.2 demonstrating that further studies on terpene oxidation and isoprene and terpene derived organic nitrate loss processes, in particular aerosol uptake, are needed in order to reduce uncertainties in simulated surface ozone.~~

4.1 Isoprene Evaluation Against Explicit Schemes

As described in detail in Section 3.1, CESM/CAM-chem TS1 base case model output from the grid box containing the Coffeeville U.S. EPA CASTNET monitoring site was used to initialize BOXMOX so that TS2 can be compared to explicit chemical mechanisms like RCIM (the Caltech mechanism) and MCM in an idealized diurnal cycle. As shown in Figure 3, in general TS1, TS2, MCM, and RCIM agree fairly well for major oxidants and isoprene oxidation products. TS1 already included a good general structure for isoprene oxidation (Section 2.2), which is likely why ozone changes from TS1 to TS2 are moderate (Figure 3) at least under the single NO regime tested by the box model. There are large differences in some of the low-NO_x

oxidation products (ISOPOOH and IEPOX) and the isomer distribution of the 1st-generation hydroxy nitrates (ISOPN). TS1 produces a fixed yield of δ- and β-hydroxy nitrates while TS2 similar to MCM and RCIM allows for the δ- and β-hydroxy nitrate distribution to vary based on the isoprene RO_2 lifetime (Section 2.2.1).

~~BOXMOX results for isoprene oxidation using TS1 (blue), MCM (gray), RCIM (black), TS2 (cyan), TS2 with RCIM assumptions for PAN and dihydroperoxy carbonyls - test 1 (red), and TS2 with RCIM assumptions for PAN, dihydroperoxy carbonyls, and carbonyl nitrates - test 2 (gold). The model configuration is explained in Section 3.1. The following acronyms are used: ISOP (isoprene), ISOPOOH (isoprene hydroxy hydroperoxide), IEPOX (isoprene dihydroxy epoxide), ISOPN (isoprene hydroxy nitrate), ISOPNOOH (isoprene nitrooxy hydroperoxide), HPALD (isoprene hydroperoxy aldehyde), O3 (ozone), OH (hydroxyl radical), HO2 (hydroperoxy radical), NO (nitrogen monoxide), PAN (peroxy acyl nitrate), MACR (methacrolein), MVK (methyl vinyl ketone), NOA (propanone nitrate), MACRN (methacrolein hydroxy nitrate), MVKN (methyl vinyl ketone hydroxy nitrate), NO3CH2CHO (ethanal nitrate), and MPAN (methacryloyl peroxynitrate).~~ The overall isoprene RO_2 distribution impacts the distribution of 1st- (ISOPN) and later-generation organic nitrates (e.g., NOA, NO3CH2CHO, MACRN, and MVKN). As shown in Figure 3, these organic nitrates are more similar to the explicit schemes in TS2 than TS1. Simulated organic nitrates from NO_3 ~~initiated~~ initiated oxidation are also improved. For example, in TS2 isoprene nitrooxy hydroperoxide (ISOPNOOH), which forms from isoprene + NO_3 oxidation, is consistent with the recently updated RCIM and not MCM or TS1 (Figure 3), because ISOPNOOH is no longer formed in unity yield in TS2 and RCIM (Section 2.2.3). In general, MCM over-estimates hydroperoxides because it consistently assumes unity yields when multi-functional peroxy radicals react with HO_2 contrary to the most recent experimental evidence (Orlando and Tyndall, 2012; Wennberg et al., 2018).

As shown in Figure 3, RCIM simulates less ozone than TS2. Several sensitivity tests ~~, which are explicitly listed in Table S7,~~ were performed in order to understand this difference. ~~In the first sensitivity test~~The revised reactions for each of these sensitivity tests are listed explicitly in Table S7. In Test 1, TS2 was altered to use RCIM assumptions for PAN formation and loss ~~of PAN~~ and for photolysis of C_4 dihydroperoxy carbonyls (DHPMPAL, Figure 1). Unlike TS2, RCIM does not include PAN photolysis or the CH_3CO_3 + CH_3CO_3 reaction and RCIM uses different reaction rate constants than TS2 for PAN formation, thermal decomposition, and reaction with OH (Table S7). In TS2, DHPMPAL is added as a surrogate compound with fast, but not instantaneous photolysis rates. In RCIM, DHPMPAL is assumed to photolyze so fast that only its photolysis products are included in the mechanism. The PAN assumptions from RCIM decrease O_3 and the DHPMPAL assumptions from RCIM increase OH. ~~Then for the second sensitivity test,~~ TS2 was ~~adjusted to include the assumptions in the first sensitivity test and the photolysis rates used in RCIM for carbonyl nitrates. This further reduces nearly to the level produced by RCIM itself (Figure 3). TS2 was~~ not updated based on ~~these sensitivity tests~~Test 1 results. In TS2, reliable rate recommendations from JPL for PAN formation/thermal decomposition and OH oxidation are used (Burkholder et al., 2015). The photolysis of the C_4 dihydroperoxy carbonyls is unknown and expected to be fast, but possibly not instantaneous. Future studies measuring the photolysis rate of C_4 dihydroperoxy carbonyls are warranted given the impact on OH using different assumptions.

~~The~~

Then for Test 2, TS2 was adjusted to include the assumptions in Test 1 and the photolysis rates for ~~the~~ carbonyl nitrates used in RCIM. This further reduces O_3 nearly to the level produced by RCIM itself (Figure 3). TS2 was also not adjusted

based on Test 2 results because the photolysis rates for the carbonyl nitrates in RCIM are lower than that suggested by recent experimental studies (Muller et al., 2014) and were recently updated to values similar to that used in TS2 when RCIM was incorporated into the GEOS-Chem chemical transport model (Bates and Jacob, 2019).

In general, the box modeling results (Figure 3) demonstrate that TS2 simulates 1st- and later-generation isoprene oxidation products better than TS1 compared to explicit schemes. Confidence that simulated ozone is right for the right reasons is enhanced in TS2 because the chemistry is more accurately represented. These results confirm that although TS1 may have too few tracers to fully capture isoprene chemistry, adding only 39 more species significantly increases the chemical accuracy without needing the immense cost that a nearly fully explicit chemical mechanism like MCM would require.

4.2 Terpene Evaluation Against Explicit Schemes

More significant changes were made to the terpene chemistry than the isoprene chemistry when developing TS2 (Section 2.3). TS2 is compared to TS1 and the more explicit MCM mechanism in Figures 4-6 and ~~S3-S4~~S4-S5, for all five surrogate compounds: APIN, BPIN, LIMON, MYRC, and BCARY. TS2 separates hydroxy nitrates and hydroxy hydroperoxides based on their chemical structure (i.e. primary/secondary versus tertiary, saturated or unsaturated, and presence of multi-functional groups) instead of their generation. Thus, MCM C_4 and greater organic hydroperoxides, nitrates, and peroxy acyl nitrates are summed in Figure 4 as a fairer comparison with the surrogate compounds in TS2. Nitrooxy hydroperoxides (NTERPOOH) are not included as total nitrates or total hydroperoxides because TS2 considers these separately.

~~BOXMOX results for α-pinene (APIN) oxidation using TS1 (blue), MCM (gray), TS2 (cyan), TS2 with MCM pinonaldehyde nitrate yield - Test 1 (red), TS2 with MCM pinonaldehyde and limonaldehyde nitrate yield - Test 2 (gold), and TS2 with MCM pinonaldehyde and limonaldehyde nitrate yield and assumptions for oxidation of unsaturated hydroxy nitrates - Test 3 (purple). The model configuration is explained in Section 3.1. APIN (α-pinene surrogate), TERPOOH (terpene hydroxy hydroperoxide), Total ROOH (all terpene hydroperoxides C_4 and up), TERPNIT (terpene hydroxy nitrate), Total RNO3 (all terpene nitrates C_4 and up), NTERPOOH (terpene nitrooxy hydroperoxide), CH3COCH3 (acetone), TERPROD1 + TERPROD2 (all terpene 1st + 2nd generation products except hydroperoxides, nitrates, and PANs), TERPA (terpene aldehyde like pinonaldehyde), TERPA3 (terpene aldehyde like limonaldehyde), TERPK (terpene ketone), TERPF1 (terpene product - one double bond), TERPACID (terpene acid), PAN (peroxy acyl nitrate), and Total RPAN (all terpene PANs C_4 and up).~~ TERPROD1 and TERPROD2 are terpene oxidation products from 1st- and 2nd-generation chemistry respectively in TS1. In TS2, these have been separated based not on their generation, but on their chemical structure: terpene aldehydes (TERPA, TERPA2, TERPA3), terpene ketones (TERPK), terpene unsaturated products (TERPF1, TERPF2), and terpene acids (TERPACID, TERPACID2, TERPACID3) (Section 2.3.1). MCM 1st and 2nd-generation species are combined into the same categories for comparison with the TS2 mechanism. In general, the ~~total products produced are similar and the~~ types of compounds formed are their concentrations are reasonably consistent between MCM and TS2.

Although MCM is one of the most explicit chemical mechanisms available, after careful examination of the chemistry, there are a number of general assumptions in MCM that are outdated or overly simplified for terpene oxidation. Even though TS2 is

more condensed compared to MCM, TS2 may be more accurate because it has been updated more recently and simplifications used in TS2 were carefully selected to limit their impact on NO_x and HO_x recycling.

To justify this, several sensitivity tests were performed as summarized in Table S7. These sensitivity tests confirm that much of the disagreement between MCM and TS2 is due to several differences in assumptions and not due to the simplification process. ~~The first sensitivity test reduced~~ In Test 1, the nitrate yields from pinonaldehyde oxidation were reduced to those recommended by MCM. TS2 uses the nitrate yield estimation procedure in Wennberg et al. (2018) with an upper limit of 0.3 as more explicitly described in Section 2.3.1. ~~The second sensitivity test~~ Test 2 included adjustments from ~~the first sensitivity test~~ Test 1 and reduced the nitrate yields from limonaldehyde oxidation to those recommended by MCM. ~~The third sensitivity test~~ Test 3 included all the adjustments in ~~the second sensitivity test~~ Test 2 as well as adjustments in the MCM assumptions for the oxidation of unsaturated hydroxy nitrates. ~~Commonly, in~~ In MCM, unsaturated hydroxy nitrates derived from terpenes often will react with OH via H-abstraction to produce only NO_2 and an unsaturated aldehyde or ketone rather than via addition to the double bond to produce a multi-functional organic nitrate. Because OH addition to a double bond consistently occurs at a faster rate than H-abstraction, this simplification inaccurately increases NO_2 recycling and ozone formation.

Similarly, in MCM unsaturated hydroxy hydroperoxides will react with OH via H-abstraction to produce OH and an unsaturated aldehyde or ketone or via H-abstraction of the hydrogen on the hydroperoxide group to form a hydroxy peroxy radical. In particular, when OH reacts with an unsaturated hydroperoxide with a fast rate, given the presence of a double bond, to H-abstract the hydrogen on the hydroperoxide moiety, an unrealistically fast cycle is created (i.e., $RO_2 \underset{OH}{\overset{HO2}{\rightleftharpoons}} ROOH$; each cycle removes 2 HO_x radicals). These unrealistically fast cycles ~~are commonly used in MCM to reduce the number of species and can lead to~~ lead to an over-estimation of the removal of HO_x depending on the number of cycles that occur, ~~overestimation~~ an over-estimation of the 1st-generation hydroperoxides, and an under-estimation of later-generation low-volatility hydroperoxides, which will impact predicted SOA if SOA formation is coupled directly to the gas-phase chemistry.

Unlike MCM, TS2 does not contain these unrealistically fast cycles and is designed to accurately account for low-volatility compounds, so that in the future terpene SOA formation can be accurately coupled directly to gas-phase chemistry like recent studies have done for isoprene (Marais et al., 2016; Bates and Jacob, 2019; Stadtler et al., 2018) and monoterpenes (Zare et al., 2019). In MCM, unsaturated aldehydes and ketones typically react with OH via addition to the double bond as well as H-abstraction, so this simplification only impacts unsaturated hydroxy nitrate and hydroxy hydroperoxide oxidation. Future studies that use MCM for prediction of ozone or SOA in ~~terpene rich~~ terpene-rich regimes should update these simplifications, so that ozone, SOA, and the HO_x and NO_x budgets are accurately simulated.

In Figure 4, oxidation of the α-pinene (APIN) surrogate compound is compared with TS1 and MCM. Terpene oxidation is largely based on α-pinene in TS1, so as expected APIN in TS2 compares reasonably well with MTERP in TS1 (Figure 4). When accounting for total hydroperoxides, MCM and TS2 agree well. Total organic nitrates are higher and ozone is lower in TS2 than MCM mostly due to the use of different nitrate yields from pinonaldehyde oxidation (~~sensitivity test~~ Test 1). Unfortunately, there are few studies measuring the organic nitrate yields from later-generation products, making it difficult to determine whether the organic nitrate yield parameterizations from MCM are better than those from Wennberg et al. (2018) used in TS2. These sensitivity tests demonstrate that more measurements of organic nitrate yields from multi-functional later-

generation products are needed. NTERPOOH is larger in MCM than TS1 because MCM in general assumes a unity yield of hydroperoxides from all multi-functional peroxy radicals reaction with HO_2 contrary to recent studies (e.g., Kurten et al., 2017).

Because the β-pinene (BPIN) surrogate compound is less reactive with O_3 and NO_3 than α-pinene, TS1 greatly underestimates the β-pinene concentration at night and does not simulate β-pinene oxidation products well either (Figure 5). In TS1, organic nitrates are under-predicted and ozone is over-predicted compared to MCM. There are some differences in MCM compared to TS2. The organic nitrates are larger in ~~the~~ TS2, but most of this bias is caused by inaccurate oxidation of the unsaturated hydroxy nitrates derived from terpenes in MCM (~~sensitivity test~~ Test 3). The nopinone yield (TERPK) for OH- and NO_3-initiated oxidation of β-pinene in TS2, which is based on recent experimental and theoretical studies (Section 2.3.1 and 2.3.3), is much lower than the yield assumed by MCM. The TS2 mechanism assumes the formation of aldehyde type products based largely on theoretical studies (Vereecken and Peeters, 2012; Kurten et al., 2017) and consistent with a recent experimental study as well (Xu et al., 2019). Most reduced chemical schemes do not separate α-pinene and β-pinene, but the results from these box model comparisons demonstrate the need for such separation (Figure 4 and 5). TS1, which largely assumes all monoterpenes react like α-pinene, simulates very different oxidant and terpene oxidation product concentrations than TS2.

~~BOXMOX results for β-pinene (BPIN) oxidation using TS1 (blue), MCM (gray), TS2 (cyan), TS2 with MCM pinonaldehyde nitrate yield - Test 1 (red), TS2 with MCM pinonaldehyde and limonaldehyde nitrate yield - Test 2 (gold), and TS2 with MCM pinonaldehyde and limonaldehyde nitrate yield and assumptions for oxidation of unsaturated hydroxy nitrates - Test 3 (purple). The model configuration is explained in Section 3.1. All species names are identical to Figure 4.~~ All limonene (LIMON) surrogate compounds contain two double bonds and so are more reactive than α-pinene. Because TS1 does not account for this extra double bond, limonene oxidation is not well represented compared to MCM (Figure 6). As explained above, contrary to experimental knowledge, MCM assumes that OH reacts with an unsaturated hydroxy nitrate to hydrogen abstract rather than react with a double bond (~~sensitivity test~~ Test 3), which causes a large underprediction of organic nitrates and an overprediction of ozone. This especially impacts limonene oxidation, which due to the presence of two double bonds, produces unsaturated first-generation products. Consistent with MCM, limonene oxidation in TS2 produces mostly terpene unsaturated products like limonaldehyde and limaketone (TERPF1). In MCM, the nitrate yields from these terpene unsaturated products are lower than that assumed in TS2, which has a moderate impact on the total organic nitrates and ozone (~~sensitivity test~~ Test 2). TS2 simplifies limonene chemistry by not explicitly tracking aldehydes on hydroperoxides, nitrates, or unsaturated terpene products and by not adding separate tracers for unsaturated and saturated terpene acids and terpene PANs. These simplification cause some disagreement between TS2 TERPF1, TERPA3, TERPACID, and total terpene PANs compared to MCM. Even with these simplifications, TS2 terpene PANs, which will impact the NO_x budget, are consistent with MCM. At this time, later-generation chemistry from limonene oxidation is not understood well enough to motivate increasing the computational cost by adding in many additional tracers to directly track the presence of aldehydes along with the other functional groups (e.g., nitrates, hydroperoxides, unsaturated products).

~~BOXMOX results for limonene (LIMON) oxidation using TS1 (blue), MCM (gray), TS2 (cyan), TS2 with MCM pinonaldehyde nitrate yield - Test 1 (red), TS2 with MCM pinonaldehyde and limonaldehyde nitrate yield - Test 2 (gold), and TS2 with MCM pinonaldehyde and limonaldehyde nitrate yield and assumptions for oxidation of unsaturated hydroxy nitrates - Test 3 (purple). The model configuration is explained in Section 3.1. All species names are identical to Figure 4.~~ The box model comparisons for myrcene (MYRC) and β-caryophyllene (BCARY) ~~and myrcene (MYRC)~~ surrogate compounds are shown in Figure ~~S3 and~~ S4 and S5. Because these surrogate compounds contain more than one double bond, the differences between TS2, TS1, and MCM are similar to those shown for limonene in Figure 6. Comparisons against MCM for myrcene are not available because no equivalent tracer exists in MCM. The TS2 surrogate compound for β-caryophyllene is assumed to have three double bonds since sesquiterpenes have between 2 and 4 double bonds (Guenther et al., 2012), so differences are expected when comparing directly with MCM's β-caryophyllene, which only has two double bonds.

From all of the box model comparisons (Figures 4-6 and ~~S3-S4~~S4-S5), some general trends for terpene oxidation can be deduced. As explained above, MCM v3.3.1 has some limitations that influence O_3 formation. Especially for reactive terpenes with more than one double bond, MCM does not accurately represent NO_x recycling because of inaccurate simplifications for unsaturated hydroxy nitrate oxidation. Because this is an erroneous representation of the chemistry, this sensitivity test is not evaluated in the global model in Section 5.2. The pinonaldehyde and limonaldehyde nitrate yields assumed in MCM are lower than those used in the TS2 mechanism (~~Sensitivity test~~ Test 1 and 2). The nitrate yields from these later-generation products have not been experimentally measured and are highly uncertain. The impact of assuming lower nitrate yields from these 1st-generation terpene oxidation products are tested in the global model in Section 5.2. Using a more complex terpene oxidation scheme like TS2 seems to be important for accurately simulating later-generation products in addition to oxidants and 1st-generation products. For example, TS1 consistently over-estimates the formation of acetone for all of the terpene surrogate compounds compared to MCM and TS2.

4.3 Surface Ozone Impact in CESM/CAM-chem

Comparing models with surface ozone measurements from the U.S. EPA CASTNET monitoring network is particularly useful compared to air quality monitoring data because typically stations in the CASTNET network are in rural locations and carefully selected to be representative of a specific region (U.S.EPA). As discussed in the introduction, CESM/CAM-chem using TS1 chemistry substantially overestimates surface ozone during the summer in the eastern U.S. compared to data from the CASTNET monitoring network (Figure 7a). Consistent with the box model results shown in Sections 4.1 and 4.2, the ozone bias is greatly improved with the updated TS2 mechanism, but a large bias remains (Figure 7b). In all cases, the surface ozone is the value in the lowest model layer with a midpoint of $\sim$ 66 m above the ground. Brown-Steiner et al. (2015) determined correcting CESM/CAM-chem data to 10 m where CASTNET data are measured reduced MDA8 surface ozone by $\sim$2%. For now no correction was applied, but future work with more comprehensive comparisons to CASTNET monitoring data will evaluate this correction.

~~Surface Ozone Daily Max 8-hr Average (MDA8) CESM/CAM-chem results over CONUS using the default TS1 mechanism (panel a) and the updated TS2 mechanism (panel b) compared to U.S. EPA CASTNET data (filled circles) averaged over August~~

2013. The same data are presented in a scatter plot for TS1 (panel c) and TS2 (panel d) with Eastern U.S. (longitude > -96°) in blue and Western U.S. (longitude < -96°) in red. The chemistry updates were added in sequential order so that the effect of each update on ozone could be diagnosed. As shown in Figure 8a, updates to the Henry's law constants had only moderate effects on MD8A surface ozone, but in certain locations reduced MDA8 ozone by a couple ppb. Updates to Henry's law constants and isoprene reduced MDA8 ozone more consistently throughout the U.S. by a couple ppb and up to 6 ppb (Figure 8b). All TS2 updates (Henry's law, isoprene, and terpene updates) reduced MDA8 ozone generally in the eastern U.S. by around 4-5 3-4 ppb and up to 7 ppb (Figure 8c). In particular, the terpene updates reduced the MDA8 ozone bias most substantially in the southeast U.S. where the model ozone bias is largest (Figure 7). Terpene chemistry greatly impacts simulated surface ozone even though it has received much less attention in model and experimental studies in the past. Changes in surface ozone daily max 8-hr average (MDA8) between the TS2 updated case and the TS1 case averaged over August 2013. The minimum and maximum over the domain pictured is displayed on the bottom right for each case.

4.4 Evaluation Against Field Campaign Data

The CASTNET monitoring data is useful for evaluating surface ozone itself. However, to verify that the model is accurately simulating ozone for the right reasons, evaluation against ozone precursors (e.g., NO_x and VOCs) and NO_x reservoir species (e.g., PANs and organic nitrates) is necessary. Field campaigns like Studies of Emissions and Atmospheric Composition, Clouds and Climate Coupling by Regional Surveys (SEAC^{4}RS), whose goals included investigating oxidation chemistry of biogenic VOCs and measuring ozone, ozone precursors, and NO_x reservoir species, are critical for evaluating whether models are accurately representing ozone. The SEAC^{4}RS field campaign was conducted during August through September of 2013 (Toon et al., 2016) with many of the flights centered over the southeastern U.S. In SEAC^{4}RS and in many other past field campaigns, terpene oxidation products were not quantitatively measured. More measurements in the future of terpene oxidation products will be beneficial for further evaluation of TS2.

Median vertical profile plots over the SEAC^{4}Rs flight tracks for observations (Obs - black), TS1 (red), TS2 with only Henry's Law updates (HL - gold), TS2 with Henry's Law and isoprene updates (ISOP - blue), and TS2 with Henry's Law, isoprene and terpene updates (TS2 - cyan). Acronyms are defined in Figure 3. Data are grouped into 0.5 km bins and exclude urban plumes (> 4 ppb), fire plumes (acetonitrile > 0.2 ppb), and stratospheric air (/> 1.25) as done in previous work (Travis et al., 2016). Domain includes the southeast U.S. (29.5-40°N, 75-94.5°W), and local sun time 9 am to 5 pm. Observational uncertainty is shown in gray bars.

Median vertical profiles are displayed in Figure 9 where data are grouped into 0.5 km bins and urban plumes (NO_2> 4 ppb), fire plumes (acetonitrile > 0.2 ppb), and stratospheric air (O_3/CO > 1.25) are excluded as done in previous work (Travis et al., 2016). Only the southeastern U.S. was selected for local sun times between 9 am to 5 pm. Version 7 of the SEAC^{4}4RS 60 s merge was used and data flagged as missing or as an upper limit of detection were not used and data flagged as a lower limit of detection were set to 0. For each compound, data unavailable in the observational dataset were also removed from the model dataset. This ensures that the observational and modeling data for each compound are directly comparable, but in some cases also prohibits direct comparison between different species since the sampling data may be different. For example, the model

vertical profiles for NO_2 are different for the chemilumenescence instrument from NOAA Earth System Research Laboratory (ESRL) and the thermal dissociation-laser induced fluorescence (TD-LIF) instrument because each instrument has different unavailable data (Figure 9). As shown in Figure 9, even though CESM/CAM-chem was only nudged to meteorological data with a 50 h relaxation time, temperature (T), winds (zonal - U and meridional -V), and clouds (as evaluated by NO_2 photolysis) were all consistent between the simulations ensuring that this light nudging sufficiently reduced model variability.

Consistent with the surface ozone analysis in Section 4.3, CESM/CAM-chem over-predicts ozone throughout the planetary boundary layer (PBL). The Henry's law and isoprene updates do not change ozone much above the surface while the terpene updates do reduce ozone in the PBL. The vertical profile ~~shapes for ozone , NO, isoprene, and monoterpenes are~~ shape for ozone is quite different between the model and observations~~suggesting that updates to the PBL height, mixing schemes, clouds (Ryu et al., 2018), vertical resolution, or ozone dry deposition schemes (Clifton et al., 2019) may be needed to further reduce ozone biases in CESM/CAM-chem~~. There are also clear differences between the model and observations for NO_2 photolysis and ozone precursors like NO_x and VOCs. Possible explanations for the remaining biases are further described below and will be explored more completely in future work.

Although the simulated NO_2 photolysis (j_{NO2} - Figure 9) is within the uncertainty of the observations, biases within the NO_2 photolysis vertical profile shape suggest biases in simulated clouds. Sampling biases could also impact agreement between the model and observations for NO_2 photolysis because field campaigns typically avoid sampling clouds on a scale not resolved by the model (Hall et al., 2018). In Ryu et al. (2018), WRF-chem similar to CAM-chem under-predicts NO_2 photolysis above 2 km~~and ~~; when clouds derived from satellites are incorporated into WRF-chem the NO_2 photolysis bias is removed and MDA8 surface ozone decreases by 1 to 5 ppb. Additionally, studies using large eddy simulations have determined that shallow cumulus clouds enhance vertical transport of passive (i.e., no aqueous-phase processing) chemical compounds as compared to clear sky conditions (Vila-Guerau de Arellano et al., 2005; Li et al., 2017). The vertical biases in NO_2 photolysis combined with the biogenic VOCs (isoprene and monoterpenes) not adequately lofting above the surface in the model compared to the observations (Figure 9) possibly suggest that CAM-chem is not accurately simulating the dynamics and/or location of shallow cumulus clouds. A cloud-induced reduction in j_{NO2} below 1 km and an increase between 2-4 km would improve the ozone and j_{NO2} profile shapes. Cloud biases in CAM-chem will be further evaluated in future work due to their potential to improve simulated NO_2 photolysis, biogenic VOCs, and ozone in and above the PBL.

NO and NO_2, as measured by ESRL using chemilumenescence, are over-predicted near the surface in CESM/CAM-chem for all model simulations. However, NO_2 is reduced with the updates to the terpene chemistry. This demonstrates that disagreement between simulated and observed NO_2 is not necessarily due to emissions, but can also be caused by an inaccurate representation of the losses of NO_x or NO_x reservoir compounds. Interestingly, the model bias compared to measurements for NO_2 from the TD-LIF instrument is lower than that from ESRL, which will be explored more in future simulations at finer horizontal resolution where NO_x emissions are better resolved.

In general, biogenic VOCs (isoprene and monoterpenes) are under-predicted by CESM/CAM-chem compared to the SEAC^4~~Rs~~RS observations (Figure 9). Even though the total monoterpenes measured using a proton transfer reaction - mass spectrometer (PTR-MS) are under-predicted, interestingly α-pinene and β-pinene measured by the whole air sampler are over-predicted by

CESM/CAM-chem near the surface when compared to the APIN and BPIN surrogate compounds, respectively. The APIN surrogate compound largely only includes α-pinene while the BPIN surrogate compound includes β-pinene and many other monoterpenes with a single double bond (Table S3). At least for β-pinene, possibly the unmeasured other monoterpenes included in the BPIN surrogate compound contribute to this bias. Further analysis at higher horizontal resolution where BVOC emissions are better resolved will be done in the future to explore the differences between CESM/CAM-chem and the observations and also the differences between the two monoterpene measurement techniques.

The slight under-prediction in the biogenic VOCs by CESM/CAM-chem could be caused by a number of possibilities. The 0.9°x1.25° resolution with a 30 minute time step may not be sufficient to capture the varied landscape in the southeast U.S., which has a number of large urban regions surrounded by forests. Additionally, Kim et al. (2016) used large eddy simulations to demonstrate that isoprene chemical reactivity is impacted by turbulent mixing in the boundary layer because these two processes occur at similar rates. Considering the model bias in isoprene and monoterpenes is particularly high in the middle of the PBL, this effect may explain part of the low bias for isoprene and monoterpenes with similar reactivities to isoprene (e.g., limonene). However, the isoprene 1st-generation oxidation products, which are less reactive than isoprene and so less impacted by turbulent mixing, are also low compared to the SEAC^4~~Rs~~ RS observations. This then suggests that emissions may be simply biased low for isoprene and monoterpenes. Interestingly, GEOS-Chem using the same MEGAN v2.1 algorithm as used in CESM/CAM-chem, recently concluded that isoprene emissions are too high by 40% in the southeast U.S. (Kaiser et al., 2018). Although the emissions factors are likely the same in the two models, the surface temperatures are different and CESM/CAM-chem uses LAI and plant functional types from the community land model (CLM). ~~All of the discussed possibilities may play some role in the bias warranting a more complete study evaluating biogenic emissions in CESM/~~Future work will evaluate whether using finer horizontal resolution (14 km) removes these biases in biogenic VOCs in CAM-chem~~in the future~~. If isoprene and monoterpenes are still under-predicted, increasing these biogenic emissions will enhance the overall bias in ozone.

TS2 updated isoprene chemistry generally improves the description of isoprene 1st- and later-generation oxidation products (Figure 9). Because isoprene is under-predicted in CESM/CAM-chem, as expected the isoprene 1st-generation products are also under-predicted. The high bias in isoprene hydroxy hydroperoxide (ISOPOOH), which forms under low-NO conditions, is corrected in TS2 relative to TS1. HPALD, which includes all four isomers of isoprene hydroperoxy aldehydes as well as the isoprene carbonyl hydroxy epoxide, is closer to the observations in TS2 than TS1, but still under-predicted. HPALD yields and photolysis/oxidation are rather uncertain. Additionally, HPALD formation, which occurs under very low-NO levels from peroxy radical H-shifts (Figure 1), may be quite sensitive to horizontal resolution. For example, large grid boxes with averaged medium levels of NO_x will produce different HPALD production rates than smaller grid boxes with separated high and low levels of NO_x. HPALD formation will be further evaluated in future work at finer horizontal resolution. In TS2, the formation and loss processes of isoprene hydroxy nitrates (ISOPN) are both increased resulting in very little overall difference in ISOPN concentration even though there are clear differences in the chemistry. TS1 groups all later-generation organic nitrates as propanone nitrate (NOA). The addition of more tracers in TS2 improves the description of these later-generation organic nitrates (NOA, MACRN+MVKN, and NO3CH2CHO) when compared to observations. Grouping all later-generation isoprene

organic nitrates as NOA produces too many later-generation organic nitrates as the fate of NOA is different from the fate of the newly added tracers (MACRN+MVKN, and NO3CH2CHO). More measurements of terpene oxidation products in future field campaigns would be useful for a similar evaluation of reduced terpene mechanisms.

Total organic nitrates are under-predicted in all simulations compared to observations, while ~~peroxy nitrates~~ total PANs are slightly over-predicted. If the ultimate fate of these missing organic nitrates is to remove NO_x, this could explain part of the remaining ozone bias. The low model bias of total organic nitrates is concerning as this implies that the NO_x budget is not completely understood. Part of this bias is caused by not including organic nitrates from small chain (C_3 and under) alkanes and alkenes as demonstrated by Fisher et al. (2016). Although the organic nitrate yields are lower for smaller chain alkanes and alkenes (Arey et al., 2001; Butkovskaya et al., 2010, 2012; Teng et al., 2015), these alkyl nitrates are still important in the atmosphere (Teng et al., 2015). Alkane and alkene nitrates and resulting chemistry will be added to the model in the future, but will only explain a small part of this model bias (Fisher et al., 2016). The overall low model bias for total organic nitrates is consistent with past work using other models (Fisher et al., 2016; Li et al., 2018). CESM/CAM-chem with the TS2 scheme produces less of a bias for total organic nitrates than GEOS-Chem (Fisher et al., 2016) likely due to the improved terpene chemistry as further explained in Section 5.1.

5 Discussion

The differences in simulated ozone between TS1 and TS2 mechanisms are largely caused by differences in formation and fate of organic nitrates, which is explained in Section 5.1. Although much is known about isoprene and terpene chemistry, lingering uncertainties remain. These uncertainties are evaluated in Section 5.2 demonstrating that further studies on terpene oxidation and isoprene- and terpene-derived organic nitrate loss processes, in particular aerosol uptake, are needed in order to reduce uncertainties in simulated surface ozone.

5.1 Organic Nitrate Formation and Fate

Because the total organic nitrates for all simulations are under-predicted compared to the SEAC^{4}RS observations (Figure 9), the speciation of organic nitrates in TS1 versus TS2 over the SEAC^{4}RS flight tracks are compared demonstrating that large differences in ~~isoprene and terpene derived~~ isoprene- and terpene-derived organic nitrates exist between the two mechanisms (Figure 10). For ~~isoprene derived~~ isoprene-derived organic nitrates, TS2 clearly has more β- than δ-isoprene hydroxy nitrates consistent with recent experimental and theoretical studies (Teng et al., 2017; Peeters et al., 2014) (Figure 10a and b). The total ~~isoprene derived~~ isoprene-derived organic nitrates are lower in TS2 than TS1 largely due to the more explicit treatment of later-generation organic nitrates in TS2. In TS1, all later-generation organic nitrates are grouped as NOA. Additional surrogate compounds are added in TS2 including MACRN, MVKN, and NO3CH2CHO, which have higher photolysis rates than NOA. The faster loss processes lead to a lower total organic nitrate level and faster NO_x recycling in TS2 versus TS1. The model comparisons against SEAC^{4}RS observations (Figure 9) confirm ~~,~~that the representation of later-generation isoprene organic nitrates in TS2 is more accurate than TS1.

~~Median vertical profile plots over the SEAC^{4}Rs flight tracks for all isoprene, terpene, and other nitrates formed in the TS1 and TS2 mechanisms binned as specified in Figure 9. For isoprene, ISOPN includes all isoprene hydroxy nitrates, derived includes all nitrates derived only from -initiated oxidation (i.e. ISOPNOOH, INHE, and NC4CHO - Figure S1), 2nd Gen includes all 2nd generation nitrates, and multi-functional includes all multi-functional later-generation nitrates. For terpenes, tertiary includes all tertiary hydroxy nitrates, secondary/primary includes all secondary/primary hydroxy nitrates, NTERPOOH includes all tertiary hydroperoxy nitrates, and 2nd Gen includes all 2nd generation nitrates, which for TS2 includes only the multi-functional low-volatility organic nitrates (Section 4.2). All dinitrates are doubled.~~ In contrast, ~~terpene derived~~ terpene-derived organic nitrates are higher in TS2 than TS1 (Figure 10c and d), which is largely due to the separation of tertiary and primary/secondary organic nitrates in TS2. Tertiary organic nitrates will undergo aerosol uptake and rapid hydrolysis to nitric acid while primary/secondary organic nitrates will not (Jacobs et al., 2014; Hu et al., 2011; Darer et al., 2011). In TS1, ~~terpene derived~~ terpene-derived hydroxy nitrates undergo aerosol uptake slower than TS2, but all hydroxy nitrates undergo aerosol uptake (Section 2.4). In comparison, TS2 has a higher uptake rate, but only tertiary hydroxy nitrates undergo aerosol uptake. Thus, in TS2, primary/secondary organic nitrates remain in the gas phase to be lost by other processes such as reaction with OH and photolysis. Consistent with other recent studies (Muller et al., 2018; Bates and Jacob, 2019; Zare et al., 2018), separating terpene tertiary organic nitrates from primary/secondary organic nitrates is clearly important for accurately representing organic nitrate concentrations and fate in the atmosphere (Figure 10).

Most of the organic nitrates in TS2 are from isoprene and terpene chemistry. The other organic nitrates (Figure 10e and f) are derived from alkanes and alkenes. Some ~~isoprene derived~~ isoprene-derived nitrates are grouped with alkene nitrates in TS1. By adding in additional tracers into TS2 (MACRN and MVKN), the alkene nitrates are largely separated in TS2 and so can be evaluated independently. Even though isoprene and terpene emissions dominate, alkane and alkene nitrates are fairly important over the southeast U.S. in their contribution to the total organic nitrates (Figure 10) likely due to their relatively long atmospheric lifetime.

In order to accurately simulate ozone for the right reasons in any model, the fate of the organic nitrates must be accurately described. As NO_x levels decrease, mixed regimes are becoming more prevalent. For example, during the Southern Oxidant and Aerosol Study (SOAS), isoprene dihydroxy hydroperoxide nitrates were measured, which are likely derived from 1st-generation isoprene hydroxy nitrates reacting with OH to form a peroxy radical that reacts with HO_2 (Lee et al., 2016; Xiong et al., 2015). TS1 fails to capture this mixed regime chemistry because when 1st-generation unsaturated organic nitrates react with OH the resulting peroxy radical is assumed to immediately react with NO to form stable products. In contrast, TS2 assumes 1st-generation unsaturated isoprene and terpene organic nitrates react with OH to form peroxy radicals that then react with NO or HO_2 or in the case of isoprene to isomerize. As an example in Figure 11, the dominant fate of the peroxy radicals ($ISOPNO_2$) formed from isoprene hydroxy nitrates reaction with OH in TS2 is to isomerize. For peroxy radicals ($TERPNO_2$) formed from terpene unsaturated hydroxy nitrates + OH the dominant fate is reaction with NO, but HO_2 is still relevant across the U.S. Not constraining the fate of the peroxy radicals to the first generation fate as done in TS2 will be increasingly important as NO_x levels decrease in the future.

2013 August average peroxy radical fate (fraction) below 2 km using TS2 for isoprene dihydroxy nitrate peroxy radical () formed from isoprene 1st-generation hydroxy nitrate + OH (left) and terpene dihydroxy nitrate peroxy radical () produced from terpene unsaturated hydroxy nitrate + OH (right). The possible fates for organic nitrates in the atmosphere include reaction with OH or O_3, photolysis, wet/dry deposition, or aerosol uptake. Typically photolysis and reaction with OH or O_3 release NO_2 back into the atmosphere while wet/dry deposition and aerosol uptake permanently remove NO_x from the atmosphere. In TS2 aerosol uptake is the dominant fate of the organic nitrates consistent with previous studies (Fisher et al., 2016; Romer et al., 2016; Wolfe et al., 2015; Muller et al., 2018; Bates and Jacob, 2019) (Figure 12). Overall, TS2 has a greater proportion of organic nitrates undergoing aerosol uptake than TS1, which is largely driven by an increase in aerosol uptake of isoprene derived isoprene-derived organic nitrates (Figure 12 and S7S8). There are also differences in the fraction of organic nitrates depositing. TS2 has more terpene derived terpene-derived organic nitrates depositing and less isoprene derived isoprene-derived organic nitrates depositing than TS1 (Figure 12 and S7). 2013 August average organic nitrate fate below 2 km using TS2 for all organic nitrates (left), isoprene organic nitrates (middle), and terpene organic nitrates (right). To avoid double counting, only the final fate is included, so reaction with OH/to form another organic nitrate is omitted from this calculation. S8).

5.2 Chemical Mechanism Uncertainties Impact on Surface Ozone

Although our understanding of isoprene and terpene chemistry has substantially improved over the last decade, many uncertainties remain generally from disagreement between measurements for 1st-generation chemistry and a lack of experimental data for later-generation chemistry. A number of sensitivity tests were performed in order to evaluate how these uncertainties impact simulated surface ozone. Each sensitivity test is briefly described in Table 1 and more completely described in Table S8. We note that the uncertainties evaluated here are only the known uncertainties and we prioritize sensitivity tests related to organic nitrate formation and fate. The bias in simulated surface ozone is still large in CESM/CAM-chem (Figure 7), so contributions from unknown chemistry are also possible.

Sensitivity tests to determine the impact of uncertainties in TS2 on simulated surface ozone. **Name Description** I_TEST1 Isoprene 1st-gen organic nitrate yield updated to 0.09 from ~ 0.13 I_TEST2 Isoprene 2nd-gen organic nitrate yield updated to 0.3 from 0.02-0.2I_TEST3 Isoprene 2nd-gen no isomerization T_TEST1 Terpene 1st-gen organic nitrate yield updated to 0.3 T_TEST2 Terpene 1st-gen organic nitrate yield updated to 0.15 T_TEST3 APIN and BPIN 1st-generation chemistry based on Xu et al. (2019) T_TEST4 Terpene 2nd-gen MCM v3.3.1 organic nitrate yields for pinonaldehyde and limonaldehyde/limaketone oxidation. A_TEST1 Aerosol uptake of all organic nitrates turned off A_TEST2 γ-values similar to GEOS-chem (Fisher et al., 2016)A_TES γ-values similar to Wolfe et al. (2015) Difference in surface ozone daily max 8-hr average (MDA8) averaged over August 2013 between each sensitivity test described in Table 1 and the TS2 case. For each case, the minimum and maximum over the domain pictured is displayed on the bottom right. For example, our understanding of reaction rates and products from peroxy radical isomerization reactions that lead to auto-oxidation is rudimentary and under-constrained (Wennberg et al., 2018). Because much is unknown about peroxy radical isomerization reactions, there is not a clear understanding of how important these reactions are in the ambient atmosphere.

5.2.1 Uncertainties in Formation of Organic Nitrates

The measured 1st-generation isoprene nitrate yield has been converging in recent experimental studies (Jenkin et al., 2015), but a moderately sized uncertainty still remains (0.09-0.13) (Xiong et al., 2015; Teng et al., 2017). This study uses $\sim$ 0.13 consistent with Teng et al. (2017). The CIMS technique in Teng et al. (2017) is potentially more reliable for measuring isoprene hydroxy nitrates than that used by Xiong et al. (2015) because the CIMS in Teng et al. (2017) has nearly equal sensitivities for all isoprene hydroxy nitrate isomers while the CIMS in Xiong et al. (2015) varies in sensitivity depending on the isomer. As shown in Figure 13a, this uncertainty is still important. Using the 0.09 yield from Xiong et al. (2015) increases the MDA8 surface ozone up to 2.6 ppb. Consistent with other systems, the 1st-generation isoprene chemistry is significantly better resolved than the 2nd-generation. In TS2 the later-generation organic nitrate yields are largely based on a parameterization developed by Wennberg et al. (2018). If the 2nd-generation nitrate yield is increased to an upper level limit of 0.3, modest changes in the MDA8 surface ozone occur with a decrease of up to 2.3 ppb (Figure 13b). When isoprene 1st-generation hydroxy nitrates react with OH, the peroxy radicals that form possibly undergo isomerization reactions (Wennberg et al., 2018), but this pathway is quite uncertain and not well studied. Removing this isomerization pathway also has modest impacts on MDA8 ozone (Figure 13c).

For terpenes, even the 1st-generation nitrate yields are not well constrained (Section 2.3.1). For α-pinene, β-pinene, and limonene generally past experimental studies found that the organic nitrate yields varied from 0.15-0.26 (Noziere et al., 1999; Ruppert et al., 1999; Capouet et al., 2004; Rindelaub et al., 2015; Ruppert et al., 1999) with one study measuring a very low organic nitrate yield (0.01) from α-pinene (Aschmann et al., 2002b). A more recent study (Xu et al., 2019) measured substantially lower hydroxy nitrate yields from α-pinene (0.033) and β-pinene (0.064) with slightly higher total organic nitrate yields - α-pinene (0.09) and β-pinene (0.11). As Xu et al. (2019) acknowledge, their instrument is not sensitive to organic nitrates from the H-abstraction pathway bringing their totals close but not quite to the lower end of the previous studies. Understanding why low organic nitrate yields from α and β-pinene have been measured in some cases is quite important. Additionally, greater understanding of how structure impacts the organic nitrate yield is especially valuable for terpenes given their large variety of chemical structures and reactivities (Guenther et al., 2012).

As shown in Figure 13d and e, increasing the 1st-generation organic nitrate yield to 0.3 or decreasing the organic nitrate yield to 0.15 for all terpenes impacts simulated MDA8 surface ozone by up to a couple ppb in either direction. Decreasing the 1st-generation organic nitrate yield from terpenes to 0.15 has a similar impact on simulated surface ozone as decreasing the isoprene 1st-generation organic nitrate to 0.09. Using the assumptions from Xu et al. (2019) (Figure 13f) ~~,~~also has modest impacts on simulated surface ozone increasing the MDA8 by up to 1.8 ppb. The changes from Xu et al. (2019) are likely moderate because only α and β-pinene oxidation was updated and although the organic nitrate yield is lower, the chemistry is quite similar to the theoretical studies that were used to develop TS2 (Vereecken et al., 2007; Vereecken and Peeters, 2012). Uncertainties in the later-generation organic nitrate yields has a large impact on ozone. When nitrate yields from MCM were used for pinonaldehyde and limonaldehyde oxidation rather than the parameterization in Wennberg et al. (2018) used throughout TS2, MDA8 ozone increased by up to 2.8 ppb (Figure 13g).

In general, the uncertainties in isoprene and terpene oxidation evaluated here lead to similar impacts on simulated surface ozone even though terpene emissions are lower than isoprene in the southeast U.S. ~~Uncertainties~~ Consistent with past work (Mao et al., 2018), uncertainties in isoprene chemistry have been significantly reduced over the last decade (Wennberg et al., 2018), such that uncertainties in terpene chemistry contribute equally to uncertainties in ozone. These results suggest more experimental constraints on terpene chemistry would be beneficial to further reduce biases in simulated surface ozone. Based on the results from these terpene sensitivity tests, there is a clear need for more organic nitrate yield measurements from a variety of terpenes and terpene oxidation products with different chemical structures.

5.2.2 Uncertainties in Loss of Organic Nitrates

The uncertainties in aerosol uptake of organic nitrates causes the largest impact on simulated MDA8 (Figures 13h-j). Aerosol uptake was only recently identified as an important loss process for organic nitrates (Fisher et al., 2016; Romer et al., 2016; Li et al., 2018; Muller et al., 2018; Bates and Jacob, 2019). If no aerosol uptake is included in TS2, this increases the MDA8 ozone by up to 5.1 ppb (Figure 13h). Interestingly, in contrast Li et al. (2018) concluded aerosol uptake had little impact on simulated ozone using GFDL AM3, which is likely caused by differences in the representation of the organic nitrate fate. For example, in Li et al. (2018) when aerosol uptake is removed, the β-isoprene hydroxy nitrate surrogate will react with OH to dominantly form other organic nitrates, so there is little expected impact on ozone. Conversely, in TS2 when aerosol uptake is removed, ISOPN2B ~~,~~ (the β-isoprene hydroxy nitrate isomer that undergoes aerosol uptake ~~(~~ Figure 1) ~~,~~ will instead react with OH to predominantly release NO_2 (Wennberg et al., 2018) and ozone will increase.

Most models like CESM/CAM-chem represent aerosol uptake of organic nitrates fairly simply (Section 2.4). Past studies indicate that aerosol uptake of organic nitrates is highly uncertain and under-constrained, leading to quite a few different model implementations. For example, Fisher et al. (2016) determined bulk aerosol uptake coefficients for all isoprene ($\gamma = 0.005$) and terpene ($\gamma = 0.01$) hydroxy nitrates were needed when comparing GEOS-Chem model results with SEAC^4~~Rs~~ RS observations. Wolfe et al. (2015) used SEAC^4~~Rs~~ RS observations over the Ozark Mountains to estimate an aerosol uptake coefficient for isoprene hydroxy nitrates ($\gamma = 0.02$). More recently, Bates and Jacob (2019) increased the tertiary organic nitrate aerosol uptake rate in GEOS-Chem by a factor of 10 compared to previous versions and Muller et al. (2018) used an aerosol uptake coefficient of 0.1 for all isoprene tertiary organic nitrates and 0.01 for all terpene organic nitrates.

From numerous laboratory studies (Jacobs et al., 2014; Hu et al., 2011; Darer et al., 2011), it is now clear that tertiary organic nitrates will undergo aerosol uptake and rapid hydrolysis while ~~largely~~ primary and secondary organic nitrates generally will not. Thus, in TS2 all tertiary organic nitrates undergo aerosol uptake with the aerosol uptake coefficient measured by Wolfe et al. (2015), and ~~largely~~ primary and secondary organic nitrates are largely lost by other processes such as oxidation, photolysis, or deposition. To evaluate the range of possibilities, when all isoprene and ~~terpene derived~~ terpene-derived organic nitrates (tertiary, primary, and secondary) underwent aerosol uptake, but with the lower aerosol uptake used by Fisher et al. (2016), the MDA8 ozone increased by up to 2.1 ppb (Figure 13i). On the other hand, when aerosol uptake of all isoprene and ~~terpene derived~~ terpene-derived organic nitrates occurred with the higher aerosol uptake from Wolfe et al. (2015), the MDA8 ozone decreased by up to 3 ppb (Figure 13j).

Considering the large impact aerosol uptake of organic nitrates has on simulated surface ozone (Figure 13) and the varied interpretations of past model studies explained above, more constraints are clearly needed. There have been noticeably more studies evaluating the formation of organic nitrates than their losses, but uncertainties in loss processes like aerosol uptake have substantial impacts on simulated ozone (Figure 13), and thus deserve equal attention.

6 Conclusions

The overall objective of this study is to add more observationally-based constraints to models (e.g., results from laboratory kinetic and product studies), in order to more realistically describe the chemistry and reduce uncertainty introduced by lumped species. To do this, more complex and updated isoprene and terpene chemistry was added into the default MOZART-TS1 mechanism in CESM2/CAM-Chem creating a new mechanism called MOZART-TS2. TS2 has isoprene chemistry with similar complexity as other recent work (Bates and Jacob, 2019; Muller et al., 2018) and terpene chemistry significantly more complex than past work (Browne et al., 2014; Fisher et al., 2016). The TS2 scheme could be easily adapted for use by other models. Although the focus of this work was to evaluate the impact of biogenic VOCs on simulated ozone, the TS2 mechanism will also be useful for other emission sources. For example, the use of volatile chemical products (McDonald et al., 2018a) and also biomass burning (Koss et al., 2018) lead to the emission of a variety of terpenes into the atmosphere. TS2 with more speciated terpenes and more complex chemistry will be useful for accurately simulating ozone from these systems as well.

The box modeling results (Section 4.1 and 4.2) demonstrate that TS2 simulates 1st- and later-generation isoprene and terpene oxidation products better than TS1 in comparison to more explicit schemes like the Caltech mechanism and MCM~~, which~~. Verification that the isoprene and terpene oxidation chemistry is correctly represented in TS2 enhances confidence that ozone is accurately simulated for the right reasons. ~~Comparisons between TS2 and MCM terpene chemistry demonstrate that MCM is inaccurately representing the oxidation chemistry for terpene unsaturated hydroxy nitrates~~ The box-modeling results also uncovered a simplification in MCM where terpene unsaturated hydroxy nitrate oxidation is not accurately represented, leading to large impacts on NO_x recycling and ozone formation ~~.~~ (Section 4.2). Future studies using MCM v3.3.1 to simulate the oxidation of terpenes, especially those that contain more than one double bond, should update this simplification.

Global model simulations using CESM/CAM-chem demonstrate enhanced capability of TS2 versus TS1 in simulating MDA8 surface ozone compared to CASTNET monitoring data, with a reduction of biases up to 7 ppb in the eastern U.S. (Section 4.3). TS2 more accurately represents ozone, ozone precursors, and NO_x reservoir species than TS1, when compared to the SEAC^{4}RS field campaign data (Section 4.4). Considering TS2 greatly increases the accuracy of isoprene and terpene chemistry, the $\sim$ 50% increase in computational cost caused by adding 86 new species is reasonable. In particular, results from this study demonstrate the importance of terpene chemistry, which has been heavily reduced or ignored in models in the past. Future work is needed to improve terpene schemes used in other models, to measure more terpene oxidation products in the field, and to conduct more laboratory studies to better understand terpene oxidation.

Comparisons of TS2 with the SEAC^{4}RS field campaign data also demonstrate remaining biases. Although substantial changes were made to organic nitrate formation and fate in TS2 compared to TS1 (Section 5.1), there remain large biases

in modeled and observed total organic nitrates, which are not unique to CESM/CAM-chem (e.g., Fisher et al., 2016). If these missing organic nitrates have large losses, they could help to explain the remaining bias in simulated surface ozone.

Although our understanding of isoprene and terpene chemistry has increased significantly over the last several decades, many lingering uncertainties in the chemistry remain. A number of sensitivity tests were performed in order to evaluate how uncertainties in isoprene and terpene chemistry, with a focus on organic nitrate formation and fate, translate to uncertainties in simulated MDA8 ozone (Section 5.2). Even though isoprene emissions are much larger than terpene emissions, because isoprene chemistry is better understood, uncertainties in isoprene and terpene chemistry have similarly modest impacts on MDA8 surface ozone. An increased understanding of terpene oxidation including later-generation chemistry will provide important further constraints to CESM/CAM-chem. Considering the diversity of terpenes and their oxidation products, measurements of organic nitrate yields from all compounds is not practical. Perhaps, measurements from a small subset of terpene and terpene oxidation products with wide structural differences may be particularly useful for identifying patterns and creating parameterizations that will reasonably extrapolate to the rest.

Past work has largely focused on formation processes of organic nitrates, but the sensitivity tests performed here (Section 5.2) suggest loss processes are equally important and quite under-constrained. In particular, future work to better understand aerosol uptake of organic nitrates and to incorporate more complex parameterizations in models is needed. In the future organic nitrate aerosol uptake will be updated to a more complex scheme in CESM/CAM-chem. Organic nitrates will undergo aerosol uptake based on their volatility like the volatility basis set scheme for SOA formation ~~combined with the addition of hydrolysis reactions in the particle-phase to form~~ and hydrolysis reactions will be added to the mechanism to convert the particulate organic nitrate to nitric acid. Hydrolysis rates of many organic nitrates have already been measured in the laboratory (e.g., Liu et al., 2012; Jacobs et al., 2014; Rindelaub et al., 2015) or inferred from field campaign observations (Lee et al., 2016; Romer et al., 2016). Additional processes to represent aqueous-phase chemistry of organic nitrates loss in clouds through a similar process as that which occurs on aerosols ~~should~~ would also be considered and included. Currently in CAM-chem, organic nitrates are lost to clouds via wet deposition, but do not undergo hydrolysis in the cloud to form HNO_3. Because tertiary nitrates have very different loss processes than secondary/primary nitrates, a greater understanding of the isomer distribution is also needed. Recent studies investigating the isomer distribution of various compounds have been conducted using both experimental (Teng et al., 2017; Boyd et al., 2015; Xu et al., 2019) and theoretical (Vereecken et al., 2007; Vereecken and Peeters, 2012) approaches, but more future studies are needed to ensure the fate of organic nitrates is accurately represented in models.

Additionally, TS2 has been designed to include surrogates for isoprene and terpene SOA precursors, which is the beginning framework for coupling SOA formation directly to gas-phase chemistry in CESM/CAM-chem as recent studies have done with other models (Marais et al., 2016; Bates and Jacob, 2019; Stadtler et al., 2018; Zare et al., 2019). Considering the sensitivity of simulated ozone on aerosol uptake of organic nitrates (Figure 13), accurately representing SOA and ozone seems to be a more connected problem than previously recognized. Better coupling SOA formation to gas-phase chemistry in models is likely important for accurately simulating both ozone and SOA.

As shown in Figure 7, TS2 greatly reduces the surface ozone bias in CESM/CAM-chem, but a relatively large bias remains. This bias could be caused by remaining uncertainties in the chemistry ~~either by those described in Section 5.2or by unknown uncertainties. Other factors~~(Section 5.2) or by processes other than chemistry, which will be evaluated in future ~~studies, are likely also important including horizontal~~ work. Considering the analysis against the SEAC^{4}RS field campaign results, the first step toward reducing the remaining ozone bias will be to evaluate how finer horizontal resolution (14 km) impacts the results. Because biogenic and anthropogenic emissions in the southeast U.S. are spatially segregated, improvements in simulated ozone and biogenic VOCs are expected with finer horizontal resolution. Future work will also include evaluating different anthropogenic emission inventories and a more thorough investigation into whether biogenic emissions are accurately represented by MEGAN in CAM-chem. Additionally, cloud biases in CAM-chem will be investigated more in the future given their likelihood for improving the vertical profile shape of ozone, ozone precursors, and ~~vertical resolution, clouds, vertical transport in and above the planetary boundary layer, ozone deposition, anthropogenic emissions, and biogenic emissions.~~ j_{NO2}. Considering that biases in the ozone profile shape are enhanced with stronger nudging to meteorological data (Figure S6), a more thorough analysis on the impact of nudging on CAM-chem dynamics and cloud parameterizations should be conducted. Future work will also evaluate whether enhanced vertical resolution is needed to improve PBL height and mixing schemes. Further evaluation of different chemical solvers (Sun et al., 2017) is also needed. Additionally, ozone dry deposition has a large impact on simulated surface ozone (Val Martin et al., 2014; Clifton et al., 2019) and a thorough evaluation and update to the ozone dry deposition scheme used in CAM-chem should be performed. Ozone is a complicated pollutant to accurately simulate in models. This work demonstrates that updating isoprene and terpene gas-phase chemistry clearly improves simulated surface ozone in CAM-chem and that additional studies evaluating and updating other processes are needed to further reduce the ozone bias.

Code and data availability.

CESM2.1.0 is a publicly released version of the Community Earth System Model available from http://www.cesm.ucar.edu/. The code updates described in this work will be made available as a new compset in a future release of CESM likely CESM 2.2. Chemical mechanisms used in CAM-chem are listed on the CAM-chem wiki page https://wiki.ucar.edu/display/camchem/Gas-Phase+Chemistry, which includes a brief description, a citation reference, and information on their current status. Please contact Rebecca Schwantes (rschwant@ucar.edu) if you would like the TS2 updates prior to their future release in CESM. CESM/CAM-chem output for 2013 August hourly ozone, 2013 August monthly average default output, and SEAC^{4}RS flight tracks used in this work are provided on NCAR's Digital Asset Services Hub (DASH) here: https://dashrepo.ucar.edu/dataset/68_rschwant.html (Schwantes and Emmons, 2020) . BOXMOX is also publicly available (https://boxmodeling.meteo.physik.uni-muenchen.de/). The MCM v3.3.1 mechanism, which was added into BOXMOX for this work, will be added to a future release of BOXMOX. Please contact Rebecca Schwantes (rschwant@ucar.edu) if you would like the BOXMOX mechanisms, initialization files, or output used in this work.

Author contributions. RHS designed the study. RHS updated the isoprene and terpene chemistry with assistance from JJO, GST, and LKE. MCB determined all updates to Henry's Law constants for the MOZART-TS1 mechanism. RHS expanded this for the MOZART-TS2 mechanism and incorporated all values into CESM/CAM-chem. RHS performed all model simulations with help from LKE. SRH and KU collected actinic flux spectroradiometer measurements and calculated photolysis rate constants during the SEAC^{4}RS field campaign. JMSC measured isoprene oxidation products with the Caltech CF_3O^- CIMS. DRB measured carbon monoxide, isoprene, and α- & β-pinene using the whole air sampler during SEAC^{4}RS. AW measured acetonitrile and monoterpenes using proton transfer reaction - mass spectrometry (PTR-MS) during SEAC^{4}RS. TVB measured wind and temperature during SEAC^{4}RS.

Competing interests. The authors declare that they have no conflict of interest.

Acknowledgements. This material is based upon work supported by the National Center for Atmospheric Research, which is a major facility sponsored by the National Science Foundation (NSF) under Cooperative Agreement No. 1852977. RHS acknowledges the NCAR Advanced Study Program postdoctoral fellowship for support of this work. The CESM project is supported primarily by the NSF. Computing and data storage resources, including the Cheyenne supercomputer (doi:10.5065/D6RX99HX), were provided by the Computational and Information Systems Laboratory (CISL) at NCAR (CISL, 2017). We thank Simone Tilmes for assistance with CESM simulations. We thank the following for collecting SEAC^{4}RS field campaign data: Paul O. Wennberg and John D. Crounse for measuring isoprene oxidation products with the Caltech CF_3O^- CIMS; Ronald C. Cohen for measuring NO_2, organic nitrates, and total peroxy acyl nitrates with the thermal dissociation-lacer induced fluorescence (TD-LIF) instrument; and Thomas B. Ryerson and the NOAA NOyO3 team for measuring NO, NO_2, and O_3. PTR-MS VOC measurements aboard the NASA DC-8 during SEAC^{4}RS were supported by the Austrian Federal Ministry for Transport, Innovation and Technology (bmvit) through the Austrian Space Applications Programme (ASAP) of the Austrian Research Promotion Agency (FFG). Tomas Mikoviny is acknowledged for his support during SEAC^{4}RS with the PTR-MS. We thank Alma Hodzic and Siyuan Wang for helpful discussions.

References

Allen, H. M., Crounse, J. D., Bates, K. H., Teng, A. P., Krawiec-Thayer, M. P., Rivera-Rios, J. C., Keutsch, F. N., St. Clair, J. M., Hanisco, T. F., Moller, K. H., Kjaergaard, H. G., and Wennberg, P. O.: Kinetics and product yields of the OH initiated oxidation of hydroxymethyl hydroperoxide, J. Phys. Chem. A., 122, 6292–6302, https://doi.org/10.1021/acs.jpca.8b04577, 2018.

Allou, L., Maimouni, L. E., and Le Calve, S.: Henry's law constant measurements for formaldehyde and benzaldehyde as a function of temperature and water composition, Atmos. Environ., 45, 2991–2998, https://doi.org/10.1016/j.atmosenv.2010.05.044, 2011.

Arey, J., Atkinson, R., and Aschmann, S. M.: Product study of the gas-phase reactions of monoterpenes with the OH radical in the presence of NO_x, J. Geophys. Res. Atmos., 95, 18 539–18 546, https://doi.org/10.1029/JD095iD11p18539, 1990.

Arey, J., Aschmann, S. M., Kwok, E. S. C., and Atkinson, R.: Alkyl nitrate, hydroxyalkyl nitrate, and hydroxycarbonyl formation from the NO_x-air photooxidations of C_5-C_8 n-alkanes, J. Phys. Chem. A., 105, 1020–1027, https://doi.org/10.1021/jp003292z, 2001.

Aschmann, S. M. and Atkinson, R.: Formation yields of methyl vinyl ketone and methacrolein from the gas-phase reaction of O_3 with isoprene, Environ. Sci. Technol., 28, 1539–1542, https://doi.org/10.1021/es00057a025, 1994.

Aschmann, S. M., Reisseil, A., Atkinson, R., and Arey, J.: Products of the gas phase reactions of the OH radical with α- and β-pinene in the presence of NO, J. Geophys. Res. Atmos., 103, 25 553–25 561, https://doi.org/10.1029/98JD01676, 1998.

Aschmann, S. M., Arey, J., and Atkinson, R.: OH radical formation from the gas-phase reactions of O_3 with a series of terpenes, Atmos. Environ., 36, 4347–4355, https://doi.org/10.1016/S1352-2310(02)00355-2, 2002a.

Aschmann, S. M., Atkinson, R., and Arey, J.: Products of reaction of OH radicals with α-pinene, J. Geophys. Res. Atmos., 107, https://doi.org/10.1029/2001JD001098, 2002b.

Atkinson, R. and Arey, J.: Gas-phase tropospheric chemistry of biogenic volatile organic compounds: a review, Atmos. Envrion., 37 Supplement No. 2, S197–S219, https://doi.org/10.1016/S1352-2310(03)00391-1, 2003.

Atkinson, R., Aschmann, S. M., Arey, J., and Shores, B.: Formation of OH radicals in the gas phase reactions of O_3 with a series of terpenes, J. Geophys. Res. Atmos., 97, 6065–6073, https://doi.org/10.1029/92JD00062, 1992.

Atkinson, R., Baulch, D. L., Cox, R. A., Crowley, J. N., Hampson, R. F., Hynes, R. G., Jenkin, M. E., Rossi, M. J., and Troe, J.: Evaluated kinetic and photochemical data for atmospheric chemistry: Volume I - gas phase reactions of O_x, HO_x, NO_x and SO_x species, Atmos. Chem. Phys., 4, 1461–1738, https://doi.org/10.5194/acp-4-1461-2004, 2004.

Atkinson, R., Baulch, D. L., Cox, R. A., Crowley, J. N., Hampson, R. F., Hynes, R. G., Jenkin, M. E., Rossi, M. J., Troe, J., and Subcommittee, I.: Evaluated kinetic and photochemical data for atmospheric chemistry: Volume II – gas phase reactions of organic species, Atmos. Chem. Phys., 6, 3625–4055, https://doi.org/10.5194/acp-6-3625-2006, 2006.

Aumont, B., Szopa, S., and Madronich, S.: Modelling the evolution of organic carbon during its gas-phase tropospheric oxidation: development of an explicit model based on a self generating approach, Atmos. Chem. Phys., 5, 2497–2517, https://doi.org/10.5194/acp-5-2497-2005, 2005.

Bates, K. and Wennberg, P.: Isoprene Oxidation Model, https://doi.org/10.1021/es980530j, version 4.1, 2017.

Bates, K. H. and Jacob, D. J.: A new model mechanism for atmospheric oxidation of isoprene: global effects on oxidants, nitrogen oxides, organic products, and secondary organic aerosol, Atmos. Chem. Phys. Discuss., In Review, https://doi.org/10.1021/acs.jpca.5b10335, 2019.

Bates, K. H., Crounse, J. D., St. Clair, J. M., Bennett, N. B., Nguyen, T. B., Seinfeld, J. H., Stoltz, B. M., and Wennberg, P. O.: Gas phase production and loss of isoprene epoxydiols, J. Phys. Chem. A., 118, 1237–1246, https://doi.org/10.1021/jp4107958, 2014.

Bates, K. H., Nguyen, T. B., Teng, A. P., Crounse, J. D., Kjaergaard, H. G., Stoltz, B. M. Seinfeld, J. H., and Wennberg, P. O.: Production and fate of C_4 dihydroxycarbonyl compounds from isoprene oxidation, J. Phys. Chem. A., 120, 106–117, https://doi.org/10.1021/acs.jpca.5b10335, 2016.

Berndt, T. and Boge, O.: Products and mechanism of the gas-phase reaction of NO_3 radicals with α-pinene, J. Chem. Soc. Faraday Trans., 93, 3021–3027, https://doi.org/10.1039/A702364B, 1997.

Berndt, T., Boge, O., and Stratmann, F.: Gas-phase ozonolysis of α-pinene:gaseous products and particle formation, Atmos. Environ., 37, 3933–3945, https://doi.org/10.1016/S1352-2310(03)00501-6, 2003.

Berndt, T., Richters, S., Jokinen, T., Hyttinen, N., Kurten, T., Otkjaer, R. V., Kjaergaard, H. G., Stratmann, F., Herrmann, H., Sipila, M., Kulmala, M., and Ehn, M.: Hydroxyl radical-induced formation of highly oxidized organic compounds, Nat. Commun., 7, 13 677, https://doi.org/10.1038/ncomms13677, 2016.

Boge, O., Mutzel, A., Iinuma, Y., Yli-Pirila, P., Kahnt, A., Joutsensaari, J., and Herrmann, H.: Gas-phase products and secondary organic aerosol formation from the ozonolysis and photooxidation of myrcene, Atmos. Environ., 79, 553–560, https://doi.org/10.1016/j.atmosenv.2013.07.034, 2013.

Boyd, C. M., Sanchez, J., Xu, L., Eugene, A. J., Nah, T., Tuet, W. Y., Guzman, M. I., and Ng, N. L.: Secondary organic aerosol formation from the β-pinene + NO_3 system: effect of humidity and peroxy radical fate, Atmos. Chem. Phys., 15, 7497–7522, https://doi.org/10.5194/acp-15-7497-2015, 2015.

Brown-Steiner, B., Hess, P. G., and Lin, M. Y.: On the capabilities and limitations of GCCM simulations of summertime regional air quality: A diagnostic analysis of ozone and temperature simulations in the US using CESM CAM-Chem, Atmos. Environ., 101, 134–148, https://doi.org/10.1016/j.atmosenv.2014.11.001, 2015.

Browne, E. C., Wooldridge, P. J., Min, K.-E., and Cohen, R. C.: On the role of monoterpene chemistry in the remote continental boundary layer, Atmos. Chem. Phys., 14, 1225–1238, https://doi.org/10.5194/acp-14-1225-2014, 2014.

Burkholder, J. B., Sander, S. P., Abbatt, J., Barker, J. R., Huie, R. E., Kolb, C. E., Kurylo, M. J., Orkin, V. L., Wilmouth, D. M., and Wine, P. H.: Chemical Kinetics and Photochemical Data for Use in Atmospheric Studies, Evaluation No. 18, Tech. Rep. JPL Publication 15-10, Jet Propulsion Laboratory, Pasadena, CA, http://jpldataeval.jpl.nasa.gov, 2015.

Butkovskaya, N., Kukui, A., and Le Bras, G.: Pressure and temperature dependence of ethyl nitrate formation in the $C_2H_5O_2$ + NO reaction, J. Phys. Chem. A., 114, 956–964, https://doi.org/10.1021/jp910003a, 2010.

Butkovskaya, N., Kukui, A., and Le Bras, G.: Pressure and temperature dependence of methyl nitrate formation in the CH_3O_2 + NO reaction, J. Phys. Chem. A., 116, 5972–5980, https://doi.org/10.1021/jp210710d, 2012.

Calogirou, A., Jensen, N. R., Nielsen, C. J., Kotzias, D., and Hjorth, J.: Gas-phase reactions of nopinone, 3-isopropenyl-6-oxo-heptanal, and 5-methyl-5-vinyltetrahydrofuran-2-ol with OH, NO_3, and ozone, Environ. Sci. Technol., 33, 453–460, https://doi.org/10.1021/es980530j, 1999.

Canty, T. P., Hembeck, L., Vinciguerra, T. P., Anderson, D. C., Goldberg, D. L., Carpenter, S. F., Allen, D. J., Loughner, C. P., Salawitch, R. J., and Dickerson, R. R.: Ozone and NO_x chemistry in the eastern US: evaluation of CMAQ/CB05 with satellite (OMI) data, Atmos. Chem. Phys., 15, 10 965–10 982, https://doi.org/10.5194/acp-15-10965-2015, 2015.

Capouet, M., Peeters, J., Noziere, B., and Muller, J.-F.: Alpha-pinene oxidation by OH: simulations of laboratory experiments, Atmos. Chem. Phys., 4, 2285–2311, https://doi.org/10.5194/acp-4-2285-2004, 2004.

Chameides, W. L.: The Photochemistry of a Remote Marine Stratiform Cloud, J. Geophys. Res. Atmos., 89, 4739–4755, https://doi.org/10.1029/JD089iD03p04739, 1984.

Chan, M. N., Surratt, J. D., Claeys, M., Edgerton, E. S., Tanner, R. L., Shaw, S. L., Zheng, M., Knipping, E. M., Eddingsaas, N. C., Wennberg, P. O., and Seinfeld, J. H.: Characterization and quantification of isoprene-derived epoxydiols in ambient aerosol in the Southeastern United States, Environ. Sci. Technol., 44, 4590–4596, https://doi.org/10.1021/es100596b, 2010.

Chew, A. A. and Atkinson, R.: OH radical formation yields from the gas-phase reactions of O_3 with alkenes and monoterpenes, J. Geophys. Res., 101, 28 649–28 653, https://doi.org/10.1029/96JD02722, 1996.

CISL: Cheyenne: HPE/SGI ICE XA System (NCAR Community Computing), Computational and Information Systems Laboratory, National Center for Atmospheric Research, Boulder, CO, doi:10.5065/D6RX99HX, 2017.

Clifton, O. E., Fiore, A. M., Munger, J. W., and Wehr, R.: Spatiotemporal Controls on Observed Daytime Ozone Deposition Velocity Over Northeastern U.S. Forests During Summer, J. Geophys. Res. Atmos., 124, 5612–5628, https://doi.org/10.1029/2018JD029073, 2019.

Cooper, O. R., Langford, A. O., Parrish, D. D., and Fahey, D. W.: Challenges of a lowered U.S. ozone standard: Source attribution science can help areas of the U.S. west, Science, 348, 1096–1097, https://doi.org/10.1126/science.aaa5748, 2015.

Copolovici, L. O. and Niinemets, U.: Temperature dependencies of Henry's law constants and octanol/water partition coefficients for key plant volatile monoterpenoids, Chemosphere, 61, 1390–1400, https://doi.org/10.1016/j.chemosphere.2005.05.003, 2005.

Crounse, J. D., Knap, H. C., Ornso, K. B., Jorgensen, S., Paulot, F., Kjaergaard, H. G., and Wennberg, P. O.: Atmospheric fate of methacrolein. 1. peroxy radical isomerization following addition of OH and O_2., J. Phys. Chem. A, 116, 5756–5762, https://doi.org/10.1021/jp211560u, 2012.

Darer, A. I., Cole-Filipiak, N., O'Connor, A. E., and Elrod, M. J.: Formation and stability of atmospherically relevant isoprene-derived organosulfates and organonitrates, Environ. Sci. Technol., 45, 1895–1902, https://doi.org/10.1021/es103797z, 2011.

Dillon, T. J. and Crowley, J. N.: Direct detection of OH formation in the reactions of HO_2 with $CH_3C(O)O_2$ and other substituted peroxy radicals, Atmos. Chem. Phys., 8, 4877–4889, https://doi.org/10.5194/acp-8-4877-2008, 2008.

Dohnal, V. and Fenclova, D.: Air-water partitioning and aqueous solubility of phenols, J. Chem. Eng. Data, 40, 478–483, https://doi.org/10.1021/je00018a027, 1995.

Eddingsaas, N. C., Loza, C. L., Yee, L. D., Seinfeld, J. H., and Wennberg, P. O.: α-pinene photooxidation under controlled chemical conditions – Part 1: Gas-phase composition in low- and high-NO_x environments, Atmos. Chem. Phys., 12, 6489–6504, https://doi.org/10.5194/acp-12-6489-2012, 2012.

Emmons, L. K., Orlando, J. J., Tyndall, G., Schwantes, R. H., Kinnison, D., Lamarque, J.-F., Marsh, D., Mills, M., Tilmes, S., Buchholz, R., Gettelman, A., Garcia, R., Simpson, I., Blake, D., and Petron, G.: The chemistry mechanism in the Community Earth System Model version 2 (CESM2) [In Review], JAMES, http://www.cesm.ucar.edu/publications/, 2020.

EPA: Our Nation's Air: Status and Trends Through 2018, https://gispub.epa.gov/air/trendsreport/2019/#home, 2018.

Fiore, A. M., Dentener, F. J., Wild, O., Cuvelier, C., Schultz, M. G., Hess, P., Textor, C., Schulz, M., Doherty, R. M., Horowitz, L. W., MacKenzie, I. A., Sanderson, M. G., Shindell, D. T., Stevenson, D. S., Szopa, S., Van Dingenen, R., Zeng, G., Atherton, C., Bergmann, D., Bey, I., Carmichael, G., Collins, W. J., Duncan, B. N., Faluvegi, G., Folberth, G., Gauss, M., Gong, S., Hauglustaine, D., Holloway, T., Isaksen, I. S. A., Jacob, D. J., Jonson, J. E., Kaminski, J. W., Keating, T. J., Lupu, A., Marmer, E., Montanaro, V., Park, R. J., Pitari, G., Pringle, K. J., Pyle, J. A., Schroeder, S., Vivanco, M. G., Wind, P., Wojcik, G., Wu, S., and Zuber, A.: Multimodel estimates of intercontinental source-receptor relationships for ozone pollution, J. Geophys. Res. Atmos., 114, D04 301, https://doi.org/10.1029/2008JD010816, 2009.

Fisher, J. A., Jacob, D. J., Travis, K. R., Kim, P. S., Marais, E. A., Miller, C. C., Yu, K., Zhu, L., Yantosca, R. M., Sulprizio, M. P., Mao, J., Wennberg, P. O., Crounse, J. D., Teng, A. P., Nguyen, T. B., St. Clair, J. M., Cohen, R. C., Romer, P., Nault, B. A., Wooldridge, P. J.,

Jimenez, J. L., Campuzano-Jost, P., Day, D. A., Hu, W., Shepson, P. B., Xiong, F., Blake, D. R., Goldstein, A. H., Misztal, P. K., Hanisco, T. F., Wolfe, G. M., Ryerson, T. B., Wisthaler, A., and Mikoviny, T.: Organic nitrate chemistry and its implications for nitrogen budgets in an isoprene- and monoterpene-rich atmosphere: constraints from aircraft (SEAC^{4}RS) and ground-based (SOAS) observations in the Southeast US, Atmos. Chem. Phys., 16, 5969–5991, https://doi.org/10.5194/acp-16-5969-2016, 2016.

Forester, C. D. and Wells, J. R.: Hydroxyl radical yields from reactions of terpene mixtures with ozone, Indoor Air, 21, 400–409, https://doi.org/10.1111/j.1600-0668.2011.00718.x, 2011.

Fried, A., Henry, B. E., Calvert, J. G., and Mozurkewich, M.: The reaction probability of N_2O_5 with sulfuric acid aerosols at stratospheric temperatures and compositions, J. Geophys. Res. Atmos., 99, 3517–3532, https://doi.org/10.1029/93JD01907, 1994.

Fry, J. L., Kiendler-Scharr, A., Rollins, A. W., Wooldridge, P. J., Brown, S. S., Fuchs, H., Dube, W., Mensah, A., dal Maso, M., Tillmann, R., Dorn, H.-P., Brauers, T., and Cohen, R. C.: Organic nitrate and secondary organic aerosol yield from NO_3 oxidation of β-pinene evaluated using a gas-phase kinetics/aerosol partitioning model, Atmos. Chem. Phys., 9, 1431–1449, https://doi.org/10.5194/acp-9-1431-2009, 2009.

Fry, J. L., Draper, D. C., Barsanti, K. C., Smith, J. N., Ortega, J., Winkler, P. M., Lawler, M. J., Brown, S. S., Edwards, P. M., Cohen, R. C., and Lee, L.: Secondary organic aerosol formation and organic nitrate yield from NO_3 oxidation of biogenic hydrocarbons, Environ. Sci. Technol., 48, 11 944–11 953, https://doi.org/10.1021/es502204x, 2014.

Gelaro, R., McCarty, W., Suarez, M. J., Todling, R., Molod, A., Takacs, L., Randles, C. A., Darmenov, A., Bosilovich, M. G., Reichle, R., Wargan, K., Coy, L., Cullather, R., Draper, C., Akella, S., Buchard, V., Conaty, A., da Silva, A. M., Gu, W., Kim, G. K., Koster, R., Lucchesi, R., Merkova, D., Nielsen, J. E., Partyka, G., Pawson, S., Putman, W., Rienecker, M., Schubert, S. D., Sienkiewicz, M., and Zhao, B.: The Modern-Era Retrospective Analysis for Research and Applications, Version 2 (MERRA-2), J. of Climate, 30, 5419–5454, https://doi.org/10.1175/JCLI-D-16-0758.1, 2017.

Goldstein, S. and Czapski, G.: Reactivity of peroxynitric acid (O_2NOOH): A pulse radiolysis study, Inorg. Chem., 36, 4156–4162, https://doi.org/10.1021/ic961186z, 1997.

Grob, C. B. M., Dillon, T. J., Schuster, G., Lelieveld, J., and Crowley, J. N.: Direct kinetic study of OH and O_3 formation in the reaction of $CH_3C(O)O_2$ with HO_2, J. Phys. Chem. A., 118, 974–985, https://doi.org/10.1021/jp412380z, 2014.

Grosjean, D., Williams, E. L., and Grosjean, E.: Atmospheric chemistry of isoprene and of its carbonyl products, Environ. Sci. Technol., 27, 830–840, https://doi.org/10.1021/es00042a004, 1993a.

Grosjean, D., Williams, E. L., Grosjean, E., Andino, J. M., and Seinfeld, J. H.: Atmospheric oxidation of biogenic hydrocarbons: reaction of ozone with β-pinene, *D*-limonene and *trans*-caryophyllene, Environ. Sci. Technol., 27, 2754–5758, https://doi.org/10.1021/es00049a014, 1993b.

Guenther, A. B., Jiang, X., Heald, C. L., Sakulyanontvittaya, T., Duhl, T., Emmons, L. K., and Wang, X.: The model of emissions of gases and aerosols from nature version 2.1 (MEGAN2.1): an extended and updated framework for modeling biogenic emissions, Geosci. Model Dev., 5, 1471–1492, https://doi.org/10.5194/gmd-5-1471-2012, 2012.

Guo, X. X. and Brimblecombe, P.: Henry's law constants of phenol and mononitrophenols in water and aqueous sulfuric acid, Chemosphere, 68, 436–444, https://doi.org/10.1016/j.chemosphere.2007.01.011, 2007.

Hakola, H., Arey, J., Ashmann, S. M., and Atkinson, R.: Product formation from the gas-phase reactions of OH radicals and 0_3 with a series of monoterpenes, J. Atmos. Chem., 18, 75–102, https://doi.org/10.1007/BF00694375, 1994.

Hall, S. R., Ullmann, K., Prather, M. J., Flynn, C. M., Murray, L. T., Fiore, A. M., Correa, G., Strode, S. A., Steenrod, S. D., Lamarque, J.-F., Guth, J., Josse, B., Flemming, J., Huijnen, V., Abraham, N. L., , and Archibald, A. T.: Cloud impacts on photochemistry: building a

climatology of photolysis rates from the Atmospheric Tomography mission, Atmos. Chem. Phys., 18, 16 809–16 828, https://doi.org/10.5194/acp-18-16809-2018, 2018.

Hallquist, M., Wangberg, I., Ljungstrom, E., Barnes, I., and Becker, K.-H.: Aerosol and product yields from NO_3 radical-initiated oxidation of selected monoterpenes, Environ. Sci. Technol., 33, 553–559, https://doi.org/10.1021/es980292s, 1999.

Hasson, A. S., Ho, A. W., Kuwata, K. T., and Paulson, S. E.: Production of stabilized Criegee intermediates and peroxides in the gas phase ozonolysis of alkenes 2. Asymmetric and biogenic alkenes, J. Geophys. Res. Atmos., 106, 34 143–34 153, https://doi.org/10.1029/2001JD000598, 2001.

Hasson, A. S., Tyndall, G. S., and Orlando, J. J.: A product yield study of the reaction of HO_2 radicals with ethyl peroxy ($C_2H_5O_2$), acetyl peroxy ($CH_3C(O)O_2$), and acetonyl peroxy ($CH_3C(O)CH_2O_2$) radicals, J. Phys. Chem. A., 108, 5979–5989, https://doi.org/10.1021/jp048873t, 2004.

Hatakeyama, S., Izumi, K., Fukuyama, T., Akimoto, H., and Washida, N.: Reactions of OH with α-pinene and β-pinene in air: Estimate of global CO production from the atmospheric oxidation of teprenes, J. Geophys. Res. Atmos., 96, 947–958, https://doi.org/10.1029/90JD02341, 1991.

Herrmann, F., Winterhalter, R., Moortgat, G. K., and Williams, J.: Hydroxyl radical (OH) yields from the ozonolysis of both double bonds for five monoterpenes, Atmos. Envrion., 44, 3458–3464, https://doi.org/10.1016/j.atmosenv.2010.05.011, 2010.

Hiatt, M. H.: Determination of Henry's law constants using internal standards with benchmark values, J. Chem. Eng. Data, 58, 902–908, https://doi.org/10.1021/je3010535, 2013.

Hodzic, A., Aumont, B., Knote, C., Lee-Taylor, J., Madronich, S., and Tyndall, G.: Volatility dependence of Henry's law constants of condensable organics: Application to estimate depositional loss of secondary organic aerosols, Geophys. Res. Lett., 41, 4795–4804, https://doi.org/10.1002/2014GL060649, 2014.

Hodzic, A., Kasibhatla, P. S., Jo, D. S., Cappa, C. D., Jimenez, J. L., Madronich, S., and Park, R. J.: Rethinking the global secondary organic aerosol (SOA) budget: stronger production, faster removal, shorter lifetime, Atmos. Chem. Phys., 16, 7917–7941, https://doi.org/10.5194/acp-16-7917-2016, 2016.

Hoesly, R. M., Smith, S. J., Feng, L., Klimont, Z., Janssens-Maenhout, G., Pitkanen, T., Seibert, J. J., Vu, L., Andres, R. J., Bolt, R. M., Bond, T. C., Dawidowski, L., Kholod, N., Kurokawa, J., Li, M., Liu, L., Lu, Z., Moura, M. C. P., O'Rourke, P. R., and Zhang, Q.: Historical (1750–2014) anthropogenic emissions of reactive gases and aerosols from the Community Emissions Data System (CEDS), Geosci. Model Dev., 11, 369–408, https://doi.org/10.5194/gmd-11-369-2018, 2018.

Horie, O. and Moortgat, G. K.: Reactions of $CH_3C(O)O_2$ radicals with CH_3O_2 and HO_2 between 263 and 333 K. A product study, J. Chem. Soc. Faraday Trans., 88, 3305–3312, https://doi.org/10.1039/FT9928803305, 1992.

Hu, K. S., Darer, A. I., and Elrod, M. J.: Thermodynamics and kinetics of the hydrolysis of atmospherically relevant organonitrates and organosulfates, Atmos. Chem. Phys., 11, 8307–8320, https://doi.org/10.5194/acp-11-8307-2011, 2011.

Im, U., Bianconi, R., Solazzo, E., Kioutsioukis, I., Badia, A., Balzarini, A., Baro, R., Bellasio, R., Brunner, D., Chemel, C., Curci, G., Flemming, J., Forkel, R., Giordano, L., Jimenez-Guerrero, P., Hirtl, M., Hodzic, A., Honzak, L., Jorba, O., Knote, C., Kuenen, J. J. P., Makar, P. A., Manders-Groot, A., Neal, L., Perez, J. L., Pirovano, G., Pouliot, G., San Jose, R., Savage, N., Tuccella, P., Werhahn, J., Wolke, R., Yahya, K., Zabkar, R., Zhang, Y., Zhang, J., Hogrefe, C., and Galmarini, S.: Evaluation of operational on-line-coupled regional air quality models over Europe and North America in the context of AQMEII phase 2. Part I: Ozone, Atmos. Environ., 115, 404–420, http://doi.org/10.1016/j.atmosenv.2014.09.042, 2015.

IPCC: Climate Change 2013: The Physical Science Basis. Contribution of Working Group I to the Fifth Assessment Report of the Intergovernmental Panel on Climate Change [Stocker, T.F., D. Qin, G.-K. Plattner, M. Tignor, S.K. Allen, J. Boschung, A. Nauels, Y. Xia, V. Bex and P.M. Midgley (eds.)], Cambridge University Press, Cambridge, United Kingdom and New York, NY, USA, 2013.

Iraci, L. T., Baker, B. M., Tyndall, G. S., and Orlando, J. J.: Measurements of the Henry's law coefficients of 2-methyl-3-buten-2-ol, methacrolein, and methylvinyl ketone, J. Atmos. Chem., 33, 321–330, https://doi.org/10.1023/A:1006169029230, 1999.

Jacobs, M. I., Darer, A. I., and Elrod, M. J.: Rate constants and products of the OH reaction with isoprene-derived epoxides, Environ. Sci. Technol., 47, 12 868–12 876, https://doi.org/10.1021/es403340g, 2013.

Jacobs, M. I., Burke, W. J., and Elrod, M. J.: Kinetics of the reactions of isoprene-derived hydroxynitrates: gas phase epoxide formation and solution phase hydrolysis, Atmos. Chem. Phys., 14, 8933–8946, https://doi.org/10.5194/acp-14-8933-2014, 2014.

Jaoui, M. and Kamens, R. M.: Mass balance of gaseous and particulate products from β-pinene/O_3/air in the absence of light and β-pinene/NO_x/air in the presence of natural sunlight, J. Atmos. Chem., 45, 101–141, https://doi.org/10.1023/A:1024093710794, 2003.

Jaoui, M., Leungsakul, S., and Kamens, R. M.: Gas and particle products distribution from the reaction of β-caryophyllene with ozone, J. Atmos. Chem., 45, 261–287, https://doi.org/10.1023/A:1024263430285, 2003.

Jenkin, M. E., Saunders, S. M., and Pilling, M. J.: The tropospheric degradation of volatile organic compounds: A protocol for mechanism development, Atmos. Environ., 31, 81–104, https://doi.org/10.1016/S1352-2310(96)00105-7, 1997.

Jenkin, M. E., Hurley, M. D., and Wallington, T. J.: Investigation of the radical product channel of the $CH_3C(O)O_2$ + HO_2 reaction in the gas phase, Phys. Chem. Chem. Phys., 9, 3149–3162, https://doi.org/10.1039/B702757E, 2007.

Jenkin, M. E., Wyche, K. P., Evans, C. J., Carr, T., Monks, P. S., Alfarra, M. R., Barley, M. H., McFiggans, G. B., Young, J. C., and Rickard, A. R.: Development and chamber evaluation of the MCM v3.2 degradation scheme for β-caryophyllene, Atmos. Chem. Phys., 12, 5275–5308, https://doi.org/10.5194/acp-12-5275-2012, 2012.

Jenkin, M. E., Young, J. C., and Rickard, A. R.: The MCM v3.3.1 degradation scheme for isoprene, Atmos. Chem. Phys., 15, 11 433–11 459, https://doi.org/10.5194/acp-15-11433-2015, 2015.

Jiang, Z., McDonald, B. C., Worden, H., Worden, J. R., Miyazaki, K., Qu, Z., Henze, D. K., Jones, D. B. A., Arellano, A. F., Fischer, E. V., Zhu, L., and Boersma, K. F.: Unexpected slowdown of US pollutant emission reduction in the past decade, PNAS, 115, 5099–5104, https://doi.org/10.1073/pnas.1801191115, 2018.

Johnson, D. and Marston, G.: The gas-phase ozonolysis of unsaturated volatile organic compounds in the troposphere, Chem. Soc. Rev., 37, 699–716, https://doi.org/10.1039/B704260B, 2008.

Kaiser, J., Jacob, D. J., Zhu, L., Travis, K. R., Fisher, J. A., Gonzalez Abad, G., Zhang, L., Zhang, X., Fried, A., Crounse, J. D., St. Clair, J. M., and Wisthaler, A.: High-resolution inversion of OMI formaldehyde columns to quantify isoprene emission on ecosystem-relevant scales: application to the southeast US, Atmos. Chem. Phys., 18, 5483–5497, https://doi.org/10.5194/acp-18-5483-2018, 2018.

Kames, J. and Schurath, U.: Henry's law and hydrolysis-rate constants for peroxyacyl nitrates (PANs) using a homogeneous gas-phase source, J. Atmos. Chem., 21, 151–164, https://doi.org/10.1007/BF00696578, 1995.

Karl, T., Harley, P., Emmons, L., Thornton, B., Guenther, A., Basu, C., Turnipseed, A., and Jardine, K.: Efficient atmospheric cleansing of oxidized organic trace gases by vegetation, Science, 330, 816–819, https://doi.org/10.1126/science.1192534, 2010.

Kharol, S. K., Martin, R. V., Philip, S., Boys, B., Lamsal, L. N., Jerrett, M., Brauer, M., Crouse, D. L., McLinden, C., and Burnett, R. T.: Assessment of the magnitude and recent trends in satellite-derived ground-level nitrogen dioxide over North America, Atmos. Environ., 118, 236–245, https://doi.org/10.1016/j.atmosenv.2015.08.011, 2015.

Kim, S.-W., Barth, M. C., and Trainer, M.: Impact of turbulent mixing on isoprene chemistry, Geophys. Res. Lett., 43, 7701–7708, https://doi.org/10.1002/2016GL069752, 2016.

Knote, C., Hodzic, A., Jimenez, J. L., Volkamer, R., Orlando, J. J., Baidar, S., Brioude, J., Fast, K., Gentner, D. R., Goldstein, A. H., Hayes, P. L., Knighton, W. B., Oetjen, H., Setyan, A., Stark, H., Thalman, R., Tyndall, G., Washenfelder, R., Waxman, E., and Zhang, Q.: Simulation of semi-explicit mechanisms of SOA formation from glyoxal in aerosol in a 3-D model, Atmos. Chem. Phys., 14, 6213–6239, https://doi.org/10.5194/acp-14-6213-2014, 2014.

Knote, C., Hodzic, A., and Jimenez, J. L.: The effect of dry and wet deposition of condensable vapors on secondary organic aerosols concentrations over the continental US, Atmos. Chem. Phys., 15, 1–18, https://doi.org/10.5194/acp-15-1-2015, 2015a.

Knote, C., Tuccella, P., Curci, G., Emmons, L., Orlando, J. J., Madronich, S., Baro, R., Jimenez-Guerrero, P., Luecken, D., Hogrefe, C., Forkel, R., Werhahn, J., Hirtl, M., Perez, J. L., San Jose, R., Giordano, L., Brunner, D., Yahya, K., and Zhang, Y.: Influence of the choice of gas-phase mechanism on predictions of key gaseous pollutants during the AQMEII phase-2 intercomparison, Atmos. Environ., 115, 553–568, https://doi.org/10.1016/j.atmosenv.2014.11.066, 2015b.

Koss, A. R., Sekimoto, K., Gilman, J. B., Selimovic, V., Coggon, M. M., Zarzana, K. J., Yuan, B., Lerner, B. M., Brown, S. S., Jimenez, J. L., Krechmer, J., Roberts, J. M., Warneke, C., Yokelson, R. J., and de Gouw, J.: Non-methane organic gas emissions from biomass burning: identification, quantification, and emission factors from PTR-ToF during the FIREX 2016 laboratory experiment, Atmos. Chem. Phys., 18, 3299–3319, https://doi.org/10.5194/acp-18-3299-2018, 2018.

Krechmer, J. E., Coggon, M. M., Massoli, P., Nguyen, T. B., Crounse, J. D., Hu, W., Day, D. A., Tyndall, G. S., Henze, D. K., Rivera-Rios, J. C., Nowak, J. B., Kimmel, J. R., Mauldin, R. L., Stark, H., Jayne, J. T., Sipila, M., Junninen, H., St. Clair, J. M., Zhang, X., Feiner, P. A., Zhang, L., Miller, D. O., Brune, W. H., Keutsch, F. N., Wennberg, P. O., Seinfeld, J. H., Worsnop, D. R., Jimenez, J. L., and Canagaratna, M. R.: Formation of low volatility organic compounds and secondary organic aerosol from isoprene hydroxyhydroperoxide low-NO oxidation, Environ. Sci. Technol., 49, 10 330–10 339, https://doi.org/10.1021/acs.est.5b02031, 2015.

Kurten, T., Rissanen, M. P., Mackeprang, K., Thronton, J. A., Hyttinen, N., Jorgensen, S., Ehn, M., and Kjaergaard, H. G.: Computational study of hydrogen shifts and ring-opening mechanisms in α-pinene ozonolysis products, J. Phys. Chem. A., 119, 11 366–11 375, https://doi.org/10.1021/acs.jpca.5b08948, 2015.

Kurten, T., Moller, K. H., Nguyen, T. B., Schwantes, R. H., Misztal, P. K., Su, L., Wennberg, P. O., Fry, J. L., and Kjaergaard, H. G.: Alkoxy radical bond scissions explain the anomalously low secondary organic aerosol and organonitrate yields from α-pinene + NO_3, J. Phys. Chem. Lett., 8, 2826–2834, https://doi.org/10.1021/acs.jpclett.7b01038, 2017.

Kwan, A. J., Chan, A. W. H., Ng, N. L., Kjaergaard, H. G., Seinfeld, J. H., and Wennberg, P. O.: Peroxy radical chemistry and OH radical production during the NO_3-initiated oxidation of isoprene, Atmos. Chem. Phys., 12, 7499–7515, https://doi.org/10.5194/acp-12-7499-2012, 2012.

Lamarque, J.-F., Emmons, L. K., Hess, P. G., Kinnison, D. E., Tilmes, S., Vitt, F., Heald, C. L., Holland, E. A., Lauritzen, P. H., Neu, J., Orlando, J. J., Rasch, P. J., and Tyndall, G. K.: CAM-chem: description and evaluation of interactive atmospheric chemistry in the Community Earth System Model, Geosci. Model Dev., 5, 369–411, https://doi.org/10.5194/gmd-5-369-2012, 2012.

Lawrence, P. J. and Chase, T. N.: Representing a new MODIS consistent land surface in the CommunityLand Model (CLM 3.0), J. Geophys. Res. Biogeosci., 112, G01 023, https://doi.org/10.1029/2006JG000168, 2007.

Lee, A., Goldstein, A. H., Keywood, M. D., Gao, S., Varutbangkul, V., Bahreini, R., Ng, N. L., Flagan, R. C., and Seinfeld, J. H.: Gas-phase products and secondary aerosol yields from the ozonolysis of ten different terpenes, J. Geophys. Res. Atmos., 111, D07 302, https://doi.org/10.1029/2005JD006437, 2006a.

Lee, A., Goldstein, A. H., Kroll, J. H., Ng, N. L., Varutbangkul, V., Flagan, R. C., and Seinfeld, J. H.: Gas-phase products and secondary aerosol yields from the photooxidation of 16 different terpenes, J. Geophys. Res. Atmos., 111, D17 305, https://doi.org/10.1029/2006JD007050, 2006b.

Lee, B. H., Mohr, C., Lopez-Hilfiker, F. D., Lutz, A., Hallquist, M., Lee, L., Romer, P., Cohen, R. C., Iyer, S., Kurten, T., Hu, W., Day, D. A., Campuzano-Jost, P., Jimenez, J. L., Xu, L., Ng, N. L., Guo, H., Weber, R. J., Wild, R. J., Brown, S. S., Koss, A., de Gouw, J., Olson, K., Goldstein, A. H., Seco, R., Kim, S., McAvey, K., Shepson, P. B., Starn, T., Baumann, K., Edgerton, E. S., Liu, J., Shilling, J. E., Miller, D. O., Brune, W., Schobesberger, S., D'Ambro, E. L., and Thornton, J. A.: Highly functionalized organic nitrates in the southeast United States: Contribution to secondary organic aerosol and reactive nitrogen budgets, Proc. Natl. Acad. Sci., 113, 1516–1521, https://doi.org/10.1073/pnas.1508108113, 2016.

Lee, L., Teng, A. P., Wennberg, P. O., Crounse, J. D., and Cohen, R. C.: On rates and mechanisms of OH and O_3 reactions with isoprene-derived hydroxy nitrates, J. Phys. Chem. A, 118, 1622–1637, https://doi.org/10.1021/jp4107603, 2014.

Leng, C., Kish, J. D., Kelley, J., Mach, M., Hiltner, J., Zhang, Y., and Liu, Y.: Temperature-dependent henry's law constants of atmospheric organics of biogenic origin, J. Phys. Chem. A, 117, 10 359–10 367, https://doi.org/10.1021/jp403603z, 2013.

Leu, M.-T. and Zhang, R.: Solubilities of $CH_3C(O)O_2NO_2$ and HO_2NO_2 in water and liquid H_2SO_4, Geophys. Res. Lett., 26, 1129–1132, https://doi.org/10.1029/1999GL900158, 1999.

Li, J., Mao, J., Fiore, A. M., Cohen, R. C., Crounse, J. D., Teng, A. P., Wennberg, P. O., Lee, B. H., Lopez-Hilfiker, F. D., Thornton, J. A., Peischl, J., Pollack, I. B., Ryerson, T. B., Veres, P., Roberts, J. M., Neuman, J. A., Nowak, J. B., Wolfe, G. M., Hanisco, T. F., Fried, A., Singh, H. B., Dibb, J., Paulot, F., and Horowitz, L. W.: Decadal changes in summertime reactive oxidized nitrogen and surface ozone over the Southeast United States, Atmos. Chem. Phys., 18, 2341–2361, https://doi.org/10.5194/acp-18-2341-2018, 2018.

Li, Y., Barth, M. C., Patton, E. G., and Steiner, A. L.: Impact of In-Cloud Aqueous Processes on the Chemistry and Transport of Biogenic Volatile Organic Compounds, J. Geophys. Res. Atmos., 122, 11 131–11 153, https://doi.org/10.1002/2017JD026688, 2017.

Liu, J., D'Ambro, E. L., Lee, B. H., Lopez-Hilfiker, F. D., Zaveri, R. A., Rivera-Rios, J. C., Keutsch, F. N., Iyer, S., Kurten, T., Zhang, Z., Gold, A., Surratt, J. D., Shilling, J. E., and Thornton, J. A.: Efficient isoprene secondary organic aerosol formation from a non-IEPOX pathway, Environ. Sci. Technol., 50, 9872–9880, https://doi.org/10.1021/acs.est.6b01872, 2016.

Liu, S., Shilling, J. E., Song, C., Hiranuma, N., Zaveri, R. A., and Russell, L. M.: Hydrolysis of organonitrate functional groups in aerosol particles, Aerosol Sci. Technol., 46:12, 1359–1369, https://doi.org/10.1080/02786826.2012.716175, 2012.

Liu, Y. J., Herdlinger-Blatt, I., McKinney, K. A., and Martin, S. T.: Production of methyl vinyl ketone and methacrolein via the hydroperoxyl pathway of isoprene oxidation, Atmos. Chem. Phys., 13, 5715–5730, https://doi.org/10.5194/acp-13-5715-2013, 2013.

Liu, Z., Nguyen, V. S., Harvey, J., Muller, J. F., and Peeters, J.: Theoretically derived mechanisms of HPALD photolysis in isoprene oxidation, Phys. Chem. Chem. Phys., 19, 9096–9106, https://doi.org/10.1039/c7cp00288b, 2017.

Ma, Y. and Marston, G.: Multifunctional acid formation from the gas-phase ozonolysis of β-pinene, Phys. Chem. Chem. Phys., 10, 6115–6126, https://doi.org/10.1039/b807863g, 2008.

Ma, Y., Russell, A. T., and Marston, G.: Mechanisms for the formation of secondary organic aerosol components from the gas-phase ozonolysis of α-pinene, Phys. Chem. Chem. Phys., 10, 4294–4312, https://doi.org/10.1039/B803283A, 2008.

Mao, J., Carlton, A., Cohen, R. C., Brune, W. H., Brown, S. S., Wolfe, G. M., Jimenez, J. L., Pye, H. O. T., Ng, N. L., Xu, L., McNeil, V. F., Tsigaridis, K., McDonald, B. C., Warneke, C., Guenther, A., Alvarado, M. J., de Gouw, J., Mickley, L. J., Leibensperger, E. M., Mathur, R., Nolte, C. G., Portmann, R. W., Unger, N., Tosca, M., and Horowitz, L. W.: Southeast Atmosphere Studies: learning from model-observation syntheses, Atmos. Chem. Phys., 18, 2615–2651, https://doi.org/10.5194/acp-18-2615-2018, 2018.

Marais, E. A., Jacob, D. J., Jimenez, J. L., Campuzano-Jost, P., Day, D. A., Hu, W., Krechmer, J., Zhu, L., Kim, P. S., Miller, C. C., Fisher, J. A., Travis, K., Yu, K., Hanisco, T. F., Wolfe, G. M., Arkinson, H. L., Pye, H. O. T., Froyd, K. D., Liao, J., and McNeill, V. F.: Aqueous-phase mechanism for secondary organic aerosol formation from isoprene: application to the southeast United States and co-benefit of SO_2 emission controls, Atmos. Chem. Phys., 16, 1603–1618, https://doi.org/10.5194/acp-16-1603-2016, 2016.

McDonald, B. C., de Gouw, J. A., Gilman, J. B., Jathar, S. H., Akherati, A., Cappa, C. D., Jimenez, J. L., Lee-Taylor, J., Hayes, P. L., McKeen, S. A., Cui, Y. Y., Kim, S.-W., Gentner, D. R., Isaacman-VanWertz, G., Goldstein, A. H., Harley, R. A., Frost, G. J., Roberts, J. M., Ryerson, T. B., and Trainer, M.: Volatile chemical products emerging as largest petrochemical source of urban organic emissions, Science, 359, 760–764, https://doi.org/10.1126/science.aaq0524, 2018a.

McDonald, B. C., McKeen, S. A., Cui, Y. Y., Ahmadov, R., Kim, S.-W., Frost, G. J., Pollack, I. B., Peischl, J., Ryerson, T. B., Holloway, J. S., Graus, M., Warneke, C., Gilman, J. B., de Gouw, J. A., Kaiser, J., Keutsch, F. N., Hanisco, T. F., Wolfe, G. M., and Trainer, M.: Modeling ozone in the Eastern U.S. using a fuel-based mobile source emissions inventory, Environ. Sci. Technol., 52, 7360–7370, https://doi.org/10.1021/acs.est.8b00778, 2018b.

McNeill, V. F., Woo, J. L., Kim, D. D., Schwier, A. N., Wannell, N. J., Sumner, A. J., and Barakat, J. M.: Aqueous-phase secondary organic aerosol and organosulfate formation in atmospheric aerosols: A modeling study, Environ. Sci. Technol., 46, 8075–8081, https://doi.org/10.1021/es3002986, 2012.

Monks, P. S., Archibald, A. T., Colette, A., Cooper, O., Coyle, M., Derwent, R., Fowler, D., Granier, C., Law, K. S., Mills, G. E., Stevenson, D. S., Tarasova, O., Thouret, V., Schneidemesser, E. v., Sommariva, R., Wild, O., and Williams, M. L.: Tropospheric ozone and its precursors from the urban to the global scale from air quality to short-lived climate forcer, Atmos. Chem. Phys., 15, 8889–8973, https://doi.org/10.5194/acp-15-8889-2015, 2015.

Muller, J. F., Peeters, J., and Stavrakou, T.: Fast photolysis of carbonyl nitrates from isoprene, Atmos. Chem. Phys., 14, 2497–2508, https://doi.org/10.5194/acp-14-2497-2014, 2014.

Muller, J. F., Stavrakou, T., and Peeters, J.: Chemistry and deposition in the Model of Atmospheric composition at Global and Regional scales using Inversion Techniques for Trace gas Emissions (MAGRITTEv1.0). Part A. Chemical mechanism, Geosci. Model Dev. Discuss., https://doi.org/10.5194/gmd-2018-316, 2018.

Ng, N. L., Brown, S. S., Archibald, A. T., Atlas, E., Cohen, R. C., Crowley, J. N., Day, D. A., Donahue, N. M., Fry, J. L., Fuchs, H., Griffin, R. J., Guzman, M. I., Herrmann, H., Hodzic, A., Iinuma, Y., Jimenez, J. L., Kiendler-Scharr, A., Lee, B. H., Luecken, D. J., Mao, J., McLaren, R., Mutzel, A., Osthoff, H. D., Ouyang, B., Picquet-Varrault, B., Platt, U., Pye, H. O. T., Rudich, Y., Schwantes, R. H., Shiraiwa, M., Stutz, J., Thornton, J. A., Tilgner, A., Williams, B. J., and Zaveri, R. A.: Nitrate radicals and biogenic volatile organic compounds: oxidation, mechanisms, and organic aerosol, Atmos. Chem. Phys., 17, 2103–2162, https://doi.org/10.5194/acp-17-2103-2017, 2017.

Nguyen, T. B., Crounse, J. D., Teng, A. P., St. Clair, J. M., Paulot, F., Wolfe, G. M., and Wennberg, P. O.: Rapid deposition of oxidized biogenic compounds to a temperate forest, PNAS, 112, E392–E401, https://doi.org/10.1073/pnas.1418702112, 2015.

Nguyen, T. B., Tyndall, G. S., Crounse, J. D., Teng, A. P., Bates, K. H., Schwantes, R. H., Coggon, M. M., Zhang, L., Feiner, P., Milller, D. O., Skog, K. M., Rivera-Rios, J. C., Dorris, M., Olson, K. F., Koss, A., Wild, R. J., Brown, S. S., Goldstein, A. H., de Gouw, J. A., Brune, W. H., Keutsch, F. N., Seinfeld, J. H., and Wennberg, P. O.: Atmospheric fates of Criegee intermediates in the ozonolysis of isoprene, Phys. Chem. Chem. Phys., 18, 10 241–10 254, https://doi.org/10.1039/C6CP00053C, 2016.

Nguyen, T. L., Winterhalter, R., Moortgat, G., Kanawati, B., Peeters, J., and Vereecken, L.: The gas-phase ozonolysis of β-caryophyllene ($C_{15}H_{24}$). Part II: A theoretical study, Phys. Chem. Chem. Phys., 11, 4173–4183, https://doi.org/10.1039/B817913A, 2009.

Niki, H., Maker, P. D., Savage, C. M., and Breitenbach, L. P.: FTIR study of the kinetics and mechanism for chlorine-atom-initiated reactions of acetaldehyde, J. Phys. Chem., 89, 588–591, https://doi.org/10.1021/j100250a008, 1985.

Noziere, B., Barnes, I., and Becker, K. H.: Product study and mechanisms of the reactions of α-pinene and of pinonaldehyde with OH radicals, J. Geophys. Res. Atmos., 104, 23 645–23 656, https://doi.org/10.1029/1999JD900778, 1999.

Orlando, J. J. and Tyndall, G. S.: Laboratory studies of organic peroxy radical chemistry: an overview with emphasis on recent issues of atmospheric significance, Chem. Soc. Rev., 41, 6294–6317, https://doi.org/10.1039/C2CS35166H, 2012.

Orlando, J. J., Noziere, B., Tyndall, G. S., Orzechowska, G. E., Paulson, S. E., and Rudich, Y.: Product studies of the OH- and ozone-initiated oxidation of some monoterpenes, J. Geophys. Res. Atmos., 105, 11 561–11 572, https://doi.org/10.1029/2000JD900005, 2000.

Paulson, S. E., Chung, M., Sen, A. D., and Orzechowska, G.: Measurement of OH radical formation from the reaction of ozone with several biogenic alkenes, J. Geophys. Res. Atmos., 103, 25 533–25 539, https://doi.org/10.1029/98JD01951, 1998.

Peeters, J., Boullart, W., Pultau, V., Vandenberk, S., and Vereecken, L.: Structure-activity relationship for the addition of OH to (poly)alkenes: Site-specific and total rate constants, J. Phys. Chem. A., 111, 1618–1631, https://doi.org/10.1021/jp066973o, 2007.

Peeters, J., Muller, J.-F., Stavrakou, T., and Nguyen, V.: Hydroxyl radical recycling in isoprene oxidation driven by hydrogen bonding and hydrogen tunneling: The upgraded LIM1 mechanism, J. Phys. Chem. A., 118, 8625–8643, https://doi.org/10.1021/jp5033146, 2014.

Pfrang, C., King, M. D., Canosa-Mas, C. E., and Wayne, R. P.: Structure–activity relations (SARs) for gas-phase reactions of NO_3, OH and O_3 with alkenes: An update, Atmos. Environ., 40, 1180–1186, https://doi.org/10.1016/j.atmosenv.2005.09.080, 2006.

Piletic, I. R., Howell, R., Bartolotti, L. J., Kleindienst, T. E., Kaushik, S. M., and Edney, E. O.: Multigenerational theoretical study of isoprene peroxy radical 1-5-hydrogen shift reactions that regenerate HO_x radicals and produce highly oxidized molecules, J. Phys. Chem. A., 123, 906–919, https://doi.org/10.1021/acs.jpca.8b09738, 2019.

Praske, E., Crounse, J. D., Bates, K. H., Kurten, T., Kjaergard, H. G., and Wennberg, P. O.: Atmospheric fate of methyl vinyl ketone: Peroxy radical reactions with NO and HO_2, J. Phys. Chem. A., 119, 4562–4572, https://doi.org/10.1021/jp5107058, 2015.

Pye, H. O. T., Pinder, R. W., Piletic, I. R., Xie, Y., Capps, S. L., Lin, Y.-H., Surratt, J. D., Zhang, Z., Gold, A., Leucken, D. J., Hutzell, W. T., Jaoui, M., Offenberg, J. H., Kleindienst, T. E., Lewandowski, M., and Edney, E. O.: Epoxide pathways improve model predictions of isoprene markers and reveal key role of acidity in aerosol formation, Environ. Sci. Technol., 47, 11 056–11 064, https://doi.org/10.1021/es402106h, 2013.

Raventos-Duran, T., Camredon, M., Valorso, R., Mouchel-Vallon, C., and Aumont, B.: Structure-activity relationships to estimate the effective Henry's law constants of organics of atmospheric interest, Atmos. Chem. Phys., 10, 7643–7654, https://doi.org/10.5194/acp-10-7643-2010, 2010.

Reichl, A.: Messung und Korrelierung von Gaslöslichkeiten halogenierter Kohlenwasserstoffe, Ph.D. thesis, Technische Universitat Berlin, Germany, 1995.

Reidmiller, D. R., Fiore, A. M., Jaffe, D. A., Bergmann, D., Cuvelier, C., Dentener, F. J., Duncan, B. N., Folberth, G., Gauss, M., Gong, S., Hess, P., Jonson, J. E., Keating, T., Lupu, A., Marmer, E., Park, R., Schultz, M. G., Shindell, D. T., Szopa, S., Vivanco, M. G., Wild, O., and Zuber, A.: The influence of foreign vs. North American emissions on surface ozone in the US, Atmos. Chem. Phys., 9, 5027–5042, https://doi.org/10.5194/acp-9-5027-2009, 2009.

Reissell, A., Harry, C., Aschmann, S., Atkinson, R., and Arey, J.: Formation of acetone from the OH radical- and O_3-initiated reactions of a series of monoterpenes, J. Geophys. Res. Atmos., 104, 13 869–13 879, https://doi.org/10.1029/1999JD900198, 1999.

Rickard, A. R., Johnson, D., McGill, C. D., and Marston, G.: OH yields in the gas-phase reactions of ozone with alkenes, J. Phys. Chem. A, 103, 7656–7664, https://doi.org/10.1021/jp9916992, 1999.

Rindelaub, J. D., McAvey, K. M., and Shepson, P. B.: The photochemical production of organic nitrates from α-pinene and loss via acid-dependent particle phase hydrolysis, Atmos. Environ., 100, 193–201, https://doi.org/10.1016/j.atmosenv.2014.11.010, 2015.

Riva, M., Budisulistiorini, S. H., Chen, Y., Zhang, Z., D'Ambro, E. L., Zhang, X., Gold, A., Turpin, B. J., Thornton, J. A., Canagaratna, M. R., and Surratt, J. D.: Chemical characterization of secondary organic aerosol from oxidation of isoprene hydroxyhydroperoxides, Environ. Sci. Technol., 50, 9889–9899, https://doi.org/10.1021/acs.est.6b02511, 2016.

Roehl, C. M., Marka, Z., Fry, J. L., and Wennberg, P. O.: Near-UV photolysis cross sections of CH_3OOH and $HOCH_2OOH$ determined via action spectroscopy, Atmos. Chem. Phys., 7, 713–720, https://doi.org/10.5194/acp-7-713-2007, 2007.

Rollins, A. W., Kiendler-Scharr, A., Fry, J. L., Brauers, T., Brown, S. S., Dorn, H.-P., Dube, W. P., Fuchs, H., Mensah, A., Mentel, T. F., Rohrer, F., Tillmann, R., Wegener, R., Wooldridge, P. J., and Cohen, R. C.: Isoprene oxidation by nitrate radical: alkyl nitrate and secondary organic aerosol yields, Atmos. Chem. Phys., 9, 6685–6703, https://doi.org/10.5194/acp-9-6685-2009, 2009.

Romer, P. S., Duffey, K. C., Wooldridge, P. J., Allen, H. M., Ayres, B. R., Brown, S. S., Brune, W. H., Crounse, J. D., de Gouw, J., Draper, D. C., Feiner, P. A., Fry, J. L., Goldstein, A. H., Koss, A., Misztal, P. K., Nguyen, T. B., Olson, K., Teng, A. P., Wennberg, P. O., Wild, R. J., Zhang, L., and Cohen, R. C.: The lifetime of nitrogen oxides in an isoprene-dominated forest, Atmos. Chem. Phys., 16, 7623–7637, https://doi.org/10.5194/acp-16-7623-2016, 2016.

Ruppert, L., Becker, K. H., Noziere, B., and Spittler, M.: Development of monoterpene oxidation mechanisms: Results from laboratory and smog chamber studies, WIT Transactions on Ecology and the Environment, 28, 63–68, 1999.

Ryu, Y.-H., Hodzic, A., Barre, J., Descombes, G., and Minnis, P.: Quantifying errors in surface ozone predictions associated with clouds over the CONUS: a WRF-Chem modeling study using satellite cloud retrievals, Atmos. Chem. Phys, 18, 7509–7525, https://doi.org/10.5194/acp-18-7509-2018, 2018.

Sander, R.: Compilation of Henry's law constants (version 4.0) for water as solvent, Atmos. Chem. Phys., 15, 4399–4981, https://doi.org/10.5194/acp-15-4399-2015, 2015.

Sandu, A. and Sander, R.: Technical note: Simulating chemical systems in Fortran90 and Matlab with the Kinetic PreProcessor KPP-2.1, Atmos. Chem. Phys., 6, 187–195, https://doi.org/10.5194/acp-6-187-2006, 2006.

Saunders, S. M., Jenkin, M. E., Derwent, R. G., and Pilling, M. J.: Protocol for the development of the Master Chemical Mechanism, MCM v3 (Part A): tropospheric degradation of non-aromatic volatile organic compounds, Atmos. Chem. Phys., 3, 161–180, https://doi.org/10.5194/acp-3-161-2003, 2003.

Schwantes, R. H. and Emmons, L. K.: CESM/CAM-chem Data for Evaluation of MOZART-TS2., UCAR/NCAR - DASH Repository, doi:10.5065/70zg-0t17, https://dashrepo.ucar.edu/dataset/68_rschwant.html, 2020.

Schwantes, R. H., Teng, A. P., Nguyen, T. B., Coggon, M. M., Crounse, J. D., St. Clair, J. M., Zhang, X., Schilling, K. A., Seinfeld, J. H., and Wennberg, P. O.: Isoprene NO_3 oxidation products from the RO_2 + HO_2 pathway, J. Phys. Chem. A., 119, 10 158–10 171, https://doi.org/10.1021/acs.jpca.5b06355, 2015.

Schwartz, S. E. and White, W. H.: Solubility equilibria of the nitrogen oxides and oxyacids in dilute aqueous solution, in: Advances in Environmental Science and Engineering, edited by Pfafflin, J. R. and Ziegler, E. N., vol. 4, p. 1–45, Gordon and Breach Science Publisher, NY, 1981.

Shu, Y. and Atkinson, R.: Rate constants for the gas-phase reactions of O_3 with a series of terpenes and OH radical formation from the O_3 reactions with sesquiterpenes at 296 $\pm$ 2 K, Int. J. Chem. Kinet., 26, 1193–1205, https://doi.org/10.1002/kin.550261207, 1994.

Sieg, K., Starokozhev, E., Schmidt, M. U., and Puttmann, W.: Inverse temperature dependence of Henry's law coefficients for volatile organic compounds in supercooled water, Chemosphere, 77, 8–14, https://doi.org/10.1016/j.chemosphere.2009.06.028, 2009.

Siese, M., Becker, K. H., Brockmann, K. J., Geiger, H., Hofzumahaus, A., Holland, F., Mihelcic, D., and Wirtz, K.: Direct measurement of OH radicals from ozonolysis of selected alkenes: A EUPHORE simulation chamber study, Envrion. Sci. Technol., 35, 4660–4667, https://doi.org/10.1021/es010150p, 2001.

Smith, R. M. and Martell, A. E.: Critical stability constants, Vol 4: Inorganic complexes, Plenum Press, New York, 1976.

Spittler, M., Barnes, I., Bejan, I., Brockmann, K. J., Benter, T., and Wirtz, K.: Reactions of NO_3 radicals with limonene and α-pinene: Product and SOA formation, Atmos. Environ., 40, S116–S127, https://doi.org/10.1016/j.atmosenv.2005.09.093, 2006.

Squire, O. J., Archibald, A. T., Griffiths, P. T., Jenkin, M. E., Smith, D., and Pye, J. A.: Influence of isoprene chemical mechanism on modelled changes in tropospheric ozone due to climate and land use over the 21st century, Atmos. Chem. Phys., 15, 5123–5143, https://doi.org/10.5194/acp-15-5123-2015, 2015.

St. Clair, J. M., Rivera, J. C., Crounse, J. D., Knap, H. C., Bates, K. H., Teng, A. P., Jorgensen, S., Kjaergaard, H. G., Keutsch, F. N., and Wennberg, P. O.: Kinetics and products of the reaction of the first-generation isoprene hydroxy hydroperoxide (ISOPOOH) with OH, J. Phys. Chem. A., 120, 1441–1451, https://doi.org/10.1021/acs.jpca.5b06532, 2016.

Stadtler, S., Kühn, T., Schröder, S., Taraborrelli, D., Schultz, M. G., and Kokkola, H.: Isoprene-derived secondary organic aerosol in the global aerosol–chemistry–climate model ECHAM6.3.0–HAM2.3–MOZ1.0, Geosci. Model Dev., 11, 3235–3260, https://doi.org/10.5194/gmd-11-3235-2018, 2018.

Staudinger, J. and Roberts, P. V.: A critical compilation of Henry's law constant temperature dependence relations for organic compounds in dilute aqueous solutions, Chemosphere, 44, 561–576, https://doi.org/10.1016/S0045-6535(00)00505-1, 2001.

Sun, J., Fu, J. S., Drake, J., Lamarque, J.-F., Tilmes, S., and Vitt, F.: Improvement of the prediction of surface ozone concentration over conterminous U.S. by a computationally efficient second-order Rosenbrock solver in CAM4-Chem, J. Adv. Model. Earth Syst., 9, 482–500, https://doi.org/10.1002/2016MS000863, 2017.

Teng, A. P., Crounse, J. D., Lee, L., St. Clair, J. M., Cohen, R. C., and Wennberg, P. O.: Hydroxy nitrate production in the OH-initiated oxidation of alkenes, Atmos. Chem. Phys., 15, 4297–4316, https://doi.org/10.5194/acp-15-4297-2015, 2015.

Teng, A. P., Crounse, J. D., and Wennberg, P. O.: Isoprene peroxy radical dynamics, J. Am. Chem. Soc., 139, 5367–5377, https://doi.org/10.1021/jacs.6b12838, 2017.

Tilmes, S., Lamarque, J.-F., Emmons, L. K., Kinnison, D. E., Ma, P.-L., Liu, X., Ghan, S., Bardeen, C., Arnold, S., Deeter, M., Vitt, F., Ryerson, T., Elkins, J. W., Moore, F., Spackman, J. R., and Val Martin, M.: Description and evaluation of tropospheric chemistry and aerosols in the Community Earth System Model (CESM1.2), Geosci. Model Dev., 8, 1395–1426, https://doi.org/10.5194/gmd-8-1395-2015, 2015.

Tilmes, S., Hodzic, A., Emmons, L. K., Mills, M. J., Gettelman, A., Kinnison, D. E., M., P., Lamarque, J.-F., Vitt, F., Shrivastava, M., Campuzano-Jost, P., Jimenez, J. L., and Liu, X.: Climate forcing and trends of organic aerosols in the Community Earth System Model (CESM2), J. Adv. Model. Earth Syst., https://doi.org/10.1029/2019MS001827, 2020.

Toon, O. B., Maring, H., Dibb, J., Ferrare, R., Jacob, D. J., Jensen, E. J., Luo, Z. J., Mace, G. G., Pan, L. L., Pfister, L., Rosenlof, K. H., Redemann, J., Reid, J. S., Singh, H. B., Thompson, A. M., Yokelson, R., Minnis, P., Chen, G., Jucks, K. W., and Pszenny, A.: Planning, implementation, and scientific goals of the Studies of Emissions and Atmospheric Composition, Clouds and Climate Coupling by Regional Surveys (SEAC^{4}RS) field mission, J. Geophys. Res. Atmos., 121, 4967–5009, https://doi.org/10.1002/2015JD024297, 2016.

Travis, K. R., Jacob, D. J., Fisher, J. A., Kim, P. S., Marais, E. A., Zhu, L., Yu, K., Miller, C. C., Yantosca, R. M., Sulprizio, M. P., Thompson, A. M., Wennberg, P. O., Crounse, J. D., St. Clair, J. M., Cohen, R. C., Laughner, J. L., Dibb, J. E., Hall, S. R., Ullmann, K., Wolfe, G. M., Pollack, I. B., Peischl, J., Neuman, J. A., and Zhou, X.: Why do models overestimate surface ozone in the Southeast United States?, Atmos. Chem. Phys., 16, 13 561–13 577, https://doi.org/10.5194/acp-16-13561-2016, 2016.

Turner, M. C., Jerrett, M., Pope, C. A., Krewski, D., Gapstur, S. M., Diver, W. R., Beckerman, B. S., Marshall, J. D., Su, J., Crouse, D. L., and Burnett, R. T.: Long-term ozone exposure and mortality in a large prospective study, Am. J Respir. Crit. Care. Med., 193, 1134–1142, https://doi.org/10.1164/rccm.201508-1633OC, 2016.

U.S.EPA: U.S. Environmental Protection Agency Clean Air Markets Division. Clean Air Status and Trends Network (CASTNET): Ozone 8-Hour Daily Max [Date accessed: December 6, 2017], www.epa.gov/castnet.

U.S.EPA: The National Ambient Air Quality Standards: Overview of EPA's updates to the air quality standards for ground-level ozone, https://www.epa.gov/sites/production/files/2015-10/documents/overview_of_2015_rule.pdf, 2015.

Val Martin, M., Heald, C. L., and Arnold, S. R.: Coupling dry deposition to vegetation phenology in the Community Earth SystemModel: Implications for the simulation of surface O_3, Geophys. Res. Lett., 41, 2988–2996, https://doi.org/10.1002/2014GL059651, 2014.

Val Martin, M., Heald, C. L., Lamarque, J.-F., Tilmes, S., Emmons, L. K., and Schichtel, B. A.: How emissions, climate, and land use change will impact mid-century air quality over the United States: a focus on effects at national parks, Atmos. Chem. Phys., 15, 2805–2823, https://doi.org/10.5194/acp-15-2805-2015, 2015.

van Marle, M. J. E., Kloster, S., Magi, B. I., Marlon, J. R., Daniau, A.-L., Field, R. D., Arneth, A., Forrest, M., Hantson, S., Kehrwald, N. M., Knorr, W., Lasslop, G., Li, F., Mangeon, S., Yue, C., Kaiser, J. W., and van der Werf, G. R.: Historic global biomass burning emissions for CMIP6 (BB4CMIP) based on merging satellite observations with proxies and fire models (1750–2015), Geosci. Model Dev., 10, 3329–3357, https://doi.org/10.5194/gmd-10-3329-2017, 2017.

van Roon, A., Parsons, J. R., Kloeze, A.-M. T., and Govers, H. A. J.: Fate and transport of monoterpenes through soils. Part I. Prediction of temperature dependent soil fate model input-parameters, Chemosphere, 61, 599–609, https://doi.org/10.1016/j.chemosphere.2005.02.081, 2005.

Vereecken, L. and Peeters, J.: A theoretical study of the OH-initiated gas-phase oxidation mechanism of β-pinene ($C_{10}H_{16}$): first generation products, Phys. Chem. Chem. Phys., 14, 3802–3815, https://doi.org/10.1039/c2cp23711c, 2012.

Vereecken, L., Muller, J. F., and Peeters, J.: Low-volatility poly-oxygenates in the OH-initiated atmospheric oxidation of a-pinene: impact of non-traditional peroxyl radical chemistry, Phys. Chem. Chem. Phys., 9, 5241–5248, https://doi.org/10.1039/b708023a, 2007.

Vila-Guerau de Arellano, J., Kim, S.-W., Barth, M. C., and Patton, E. G.: Transport and chemical transformations influenced by shallow cumulus over land, Atmos. Chem. Phys., 5, 3219–3231, https://doi.org/10.5194/acp-5-3219-2005, 2005.

Wangberg, I., Barnes, I., and Becker, K. H.: Product and mechanistic study of the reaction of NO_3 radicals with α-pinene, Environ. Sci. Technol., 31, 2130–2135, https://doi.org/10.1021/es960958n, 1997.

Wennberg, P., Bates, K. H., Crounse, J. D., Dodson, L. G., McVay, R. C., Mertens, L. A., Nguyen, T. B., Praske, E., Schwantes, R. H., Smarte, M. D., St Clair, J. M., Teng, A. P., Zhang, X., and Seinfeld, J. H.: Gas-Phase Reactions of Isoprene and Its Major Oxidation Products, Chem. Rev., 118, 3337–3390, https://doi.org/10.1021/acs.chemrev.7b00439, 2018.

Winterhalter, R., Neeb, P., Grossmann, D., Kolloff, A., Horie, O., and Moortgat, G.: Products and mechanism of the gas phase reaction of ozone with β-pinene, J. Atmos. Chem., 35, 165–197, https://doi.org/10.1023/A:1006257800929, 2000.

Winterhalter, R., Herrmann, F., Kanawati, B., Nguyen, T. L., Peeters, J., Vereecken, L., and Moortgat, G. K.: The gas-phase ozonolysis of β-caryophyllene ($C_{15}H_{24}$). Part I: an experimental study, Phys. Chem. Chem. Phys., 11, 4152–4172, https://doi.org/10.1039/b817824k, 2009.

Wisthaler, A., Jensen, N. R., Winterhalter, R., Lindinger, W., and Hjorth, J.: Measurements of acetone and other gas phase product yields from the OH-initiated oxidation of terpenes by proton-transfer-reaction mass spectrometry(PTR-MS), Atmos. Environ., 35, 6181–6191, https://doi.org/10.1016/S1352-2310(01)00385-5, 2001.

Wolfe, G. M., Hanisco, T. F., Arkinson, H. L., Bui, T. P., Crounse, J., Dean-Day, J., Goldstein, A., Guenther, A., Hall, S. R., Huey, G., Jacob, D. J., Karl, T., Kim, P. S., Liu, X., Marvin, M. R., Mikoviny, T., Misztal, P. K., Nguyen, T. B., Peischl, J., Pollack, I., Ryerson, T., St. Clair, J. M., Teng, A., Travis, K. R., Ullmann, K., Wennberg, P. O., and Wisthaler, A.: Quantifying sources and sinks of reactive gases in the lower atmosphere using airborne flux observations, Geophys. Res. Lett., 42, 8231–8240, https://doi.org/10.1002/2015GL065839, 2015.

Xiong, F., McAvey, K. M., Pratt, K. A., Groff, C. J., Hostetler, M. A., Lipton, M. A., Starn, T. K., Seeley, J. V., Bertman, S. B., Teng, A. P., Crounse, J. D., Nguyen, T. B., Wennberg, P. O., Misztal, P. K., Goldstein, A. H., Guenther, A. B., Koss, A. R., Olson, K. F., de Gouw, J. A., Baumann, K., Edgerton, E. S., Feiner, P. A., Zhang, L., Miller, D. O., Brune, W. H., and Shepson, P. B.: Observation of isoprene hydroxynitrates in the southeastern United States and implications for the fate of $\mathrm{NO_x}$, Atmos. Chem. Phys., 15, 11 257–11 272, https://doi.org/10.5194/acp-15-11257-2015, 2015.

Xiong, F., Borca, C. H., Slipchenko, L. V., and Shepson, P. B.: Photochemical degradation of isoprene-derived 4,1-nitrooxy enal, Atmos. Chem. Phys., 16, 5595–5610, https://doi.org/10.5194/acp-16-5595-2016, 2016.

Xu, L., Guo, H., Boyd, C. M., Klein, M., Bougiatioti, A., Cerully, K. M., Hite, J. R., Isaacman-VanWertz, G., Kreisberg, N. M., Knote, C., Olson, K., Koss, A., Goldstein, A. H., Hering, S. V., de Gouw, J., Baumann, K., Lee, S.-H., Nenes, A., Weber, R. J., and Ng, N. L.: Effects of anthropogenic emissions on aerosol formation from isoprene and monoterpenes in the southeastern United States, PNAS, 112, 37–42, https://doi.org/10.1073/pnas.1417609112, 2015.

Xu, L., Moller, K. H., Crounse, J. D., Otkjaer, R. V., Kjaergaard, H. G., and Wennberg, P. O.: Unimolecular reactions of peroxy radicals formed in the oxidation of α-pinene and β-pinene by hydroxyl radicals, J. Phys. Chem. A., XX, XX, https://doi.org/10.1021/acs.jpca.8b11726, 2019.

Yeh, G. K. and Ziemann, P. J.: Alkyl nitrate formation from the reactions of $\mathrm{C_8-C_{14}}$ n-alkanes with OH radicals in the presence of $\mathrm{NO_x}$: Measured yields with essential corrections for gas-wall partitioning, J. Phys. Chem. A., 118, 8147–8157, https://doi.org/10.1021/jp500631v, 2014.

Young, P. J., Naik, V., Fiore, A. M., Gaudel, A., Guo, J., Lin, M. Y., Neu, J. L., Parrish, D. D., Rieder, H. E., Schnell, J. L., Tilmes, S., Wild, O., Zhang, L., Ziemke, J. R., Brandt, J., Delcloo, A., Doherty, R. M., Geels, C., Hegglin, M. I., Hu, L., Im, U., Kumar, R., Luhar, A., Murray, L., Plummer, D., Rodriguez, J., Saiz-Lopez, A., Schultz, M. G., Woodhouse, M. T., and Zeng, G.: Tropospheric ozone assessment report: Assessment of global-scale model performance for global and regional ozone distributions, variability, and trends, Elem. Sci. Anth., 6, https://doi.org/10.1525/elementa.265, 2018.

Yu, J., Cocker, D. R., Griffin, R. J., Flagan, R. C., and Seinfeld, J. H.: Gas-phase ozone oxidation of monoterpenes: Gaseous and particulate products, J. Atmos. Chem., 34, 207–258, https://doi.org/10.1023/A:1006254930583, 1999.

Zare, A., Romer, P. S., Nguyen, T., Keutsch, F. N., Skog, K., and Cohen, R. C.: A comprehensive organic nitrate chemistry: insights into the lifetime of atmospheric organic nitrates, Atmos. Chem. Phys., 18, 15 419–15 436, https://doi.org/10.5194/acp-18-15419-2018, 2018.

Zare, A., Fahey, K. M., Sarwar, G., Cohen, R. C., and Pye, H. O. T.: Vapor-pressure pathways initiate but hydrolysis products dominate the aerosol estimated from organic mitrates, ACS Earth Space Chem., 3, 1426–1437, https://doi.org/10.1021/acsearthspacechem.9b00067, 2019.

Zhang, D. and Zhang, R.: Ozonolysis of α-pinene and β-pinene: Kinetics and mechanism, J. Chem. Phys., 122, 114 308, https://doi.org/10.1063/1.1862616, 2005.

Zhang, H., Yee, L. D., Lee, B. H., Curtis, M. P., Worton, D. R., Isaacman-VanWertz, G., Offenberg, J. H., Lewandowski, M., Kleindienst, T. E., Beaver, M. R., Holder, A. L., Lonneman, W. A., Docherty, K. S., Jaoui, M., Pye, H. O. T., Hu, W., Day, D. A., Campuzano-Jost, P., Jimenez, J. L., Guo, H., Weber, R. J., de Gouw, J., Koss, A. R., Edgerton, E. S., Brune, W., Mohr, C., Lopez-Hilfiker, F. D., Lutz, A.,

Kreisberg, N. M., Spielman, S. R., Hering, S. V., Wilson, K. R., Thornton, J. A., and Goldstein, A. H.: Monoterpenes are the largest source of summertime organic aerosol in the southeastern United States, PNAS, 115, 2038–2043, https://doi.org/10.1073/pnas.1717513115, 2018.

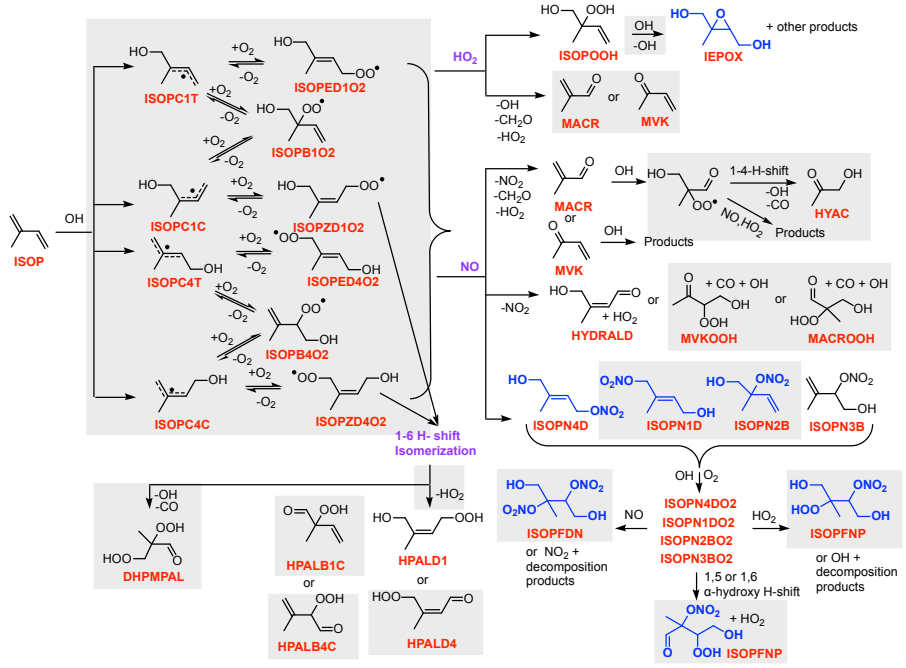

Figure 1. Simplified schematic of the TS2 mechanism for isoprene OH-initiated oxidation. Gray boxes indicates new chemistry added or updated in TS2. Blue compounds undergo aerosol uptake. As shown, only certain isomers of organic nitrates undergo aerosol uptake as explained in Section 2.4. All species names used in TS2 are described in Table S2. Similar schematics for NO_3- and O_3-initiated oxidation of isoprene are provided in Figure S1 and S3 in the supplement.

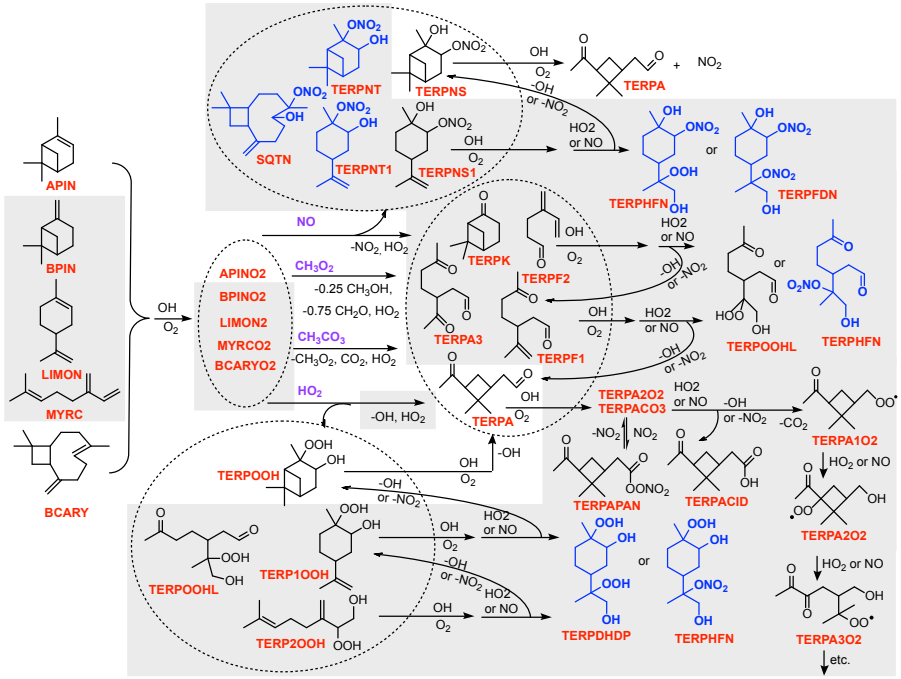

Figure 2. Simplified schematic of the TS2 chemical mechanism for terpene OH-initiated oxidation. Gray boxes indicates new chemistry added or updated in TS2. Blue compounds undergo aerosol uptake. All species names used in TS2 are described in Table S2. Similar schematics for NO_3- and O_3-initiated oxidation of terpenes are provided in Figure S2 and S3 in the supplement.

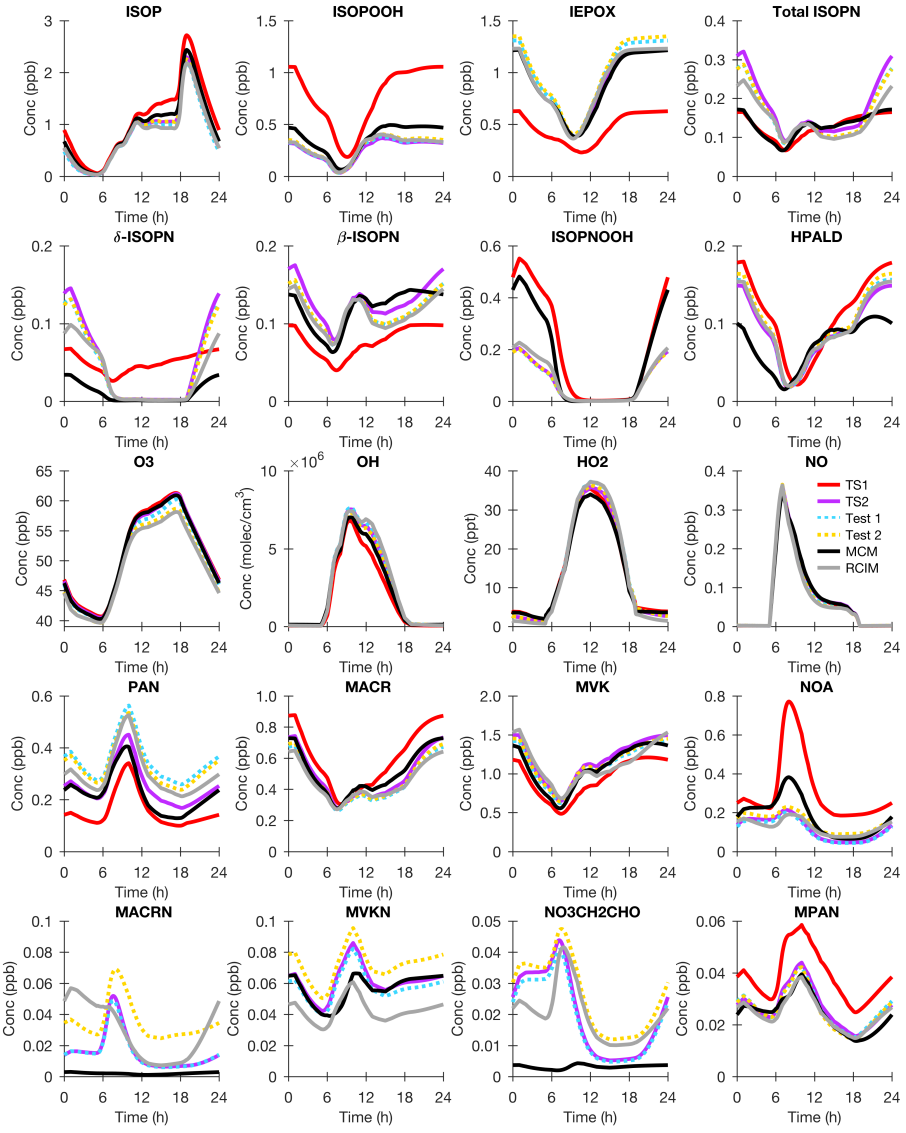

Figure 3. BOXMOX results for isoprene oxidation using TS1 (red), MCM (black), RCIM (gray), TS2 (purple), TS2 with RCIM assumptions for peroxy acyl nitrate (PAN) and C_4 dihydroperoxy carbonyls - Test 1 (blue), and TS2 with RCIM assumptions for PAN, C_4 dihydroperoxy carbonyls, and carbonyl nitrates - Test 2 (gold). The model configuration is explained in Section 3.1. The following acronyms are used: ISOP (isoprene), ISOPOOH (isoprene hydroxy hydroperoxide), IEPOX (isoprene dihydroxy epoxide), ISOPN (isoprene hydroxy nitrate), ISOPNOOH (isoprene nitrooxy hydroperoxide), HPALD (isoprene hydroperoxy aldehyde), O3 (ozone), OH (hydroxyl radical), HO2 (hydroperoxy radical), NO (nitrogen monoxide), PAN (peroxy acyl nitrate), MACR (methacrolein), MVK (methyl vinyl ketone), NOA (propanone nitrate), MACRN (methacrolein hydroxy nitrate), MVKN (methyl vinyl ketone hydroxy nitrate), NO3CH2CHO (ethanal nitrate), and MPAN (methacryloyl peroxynitrate).

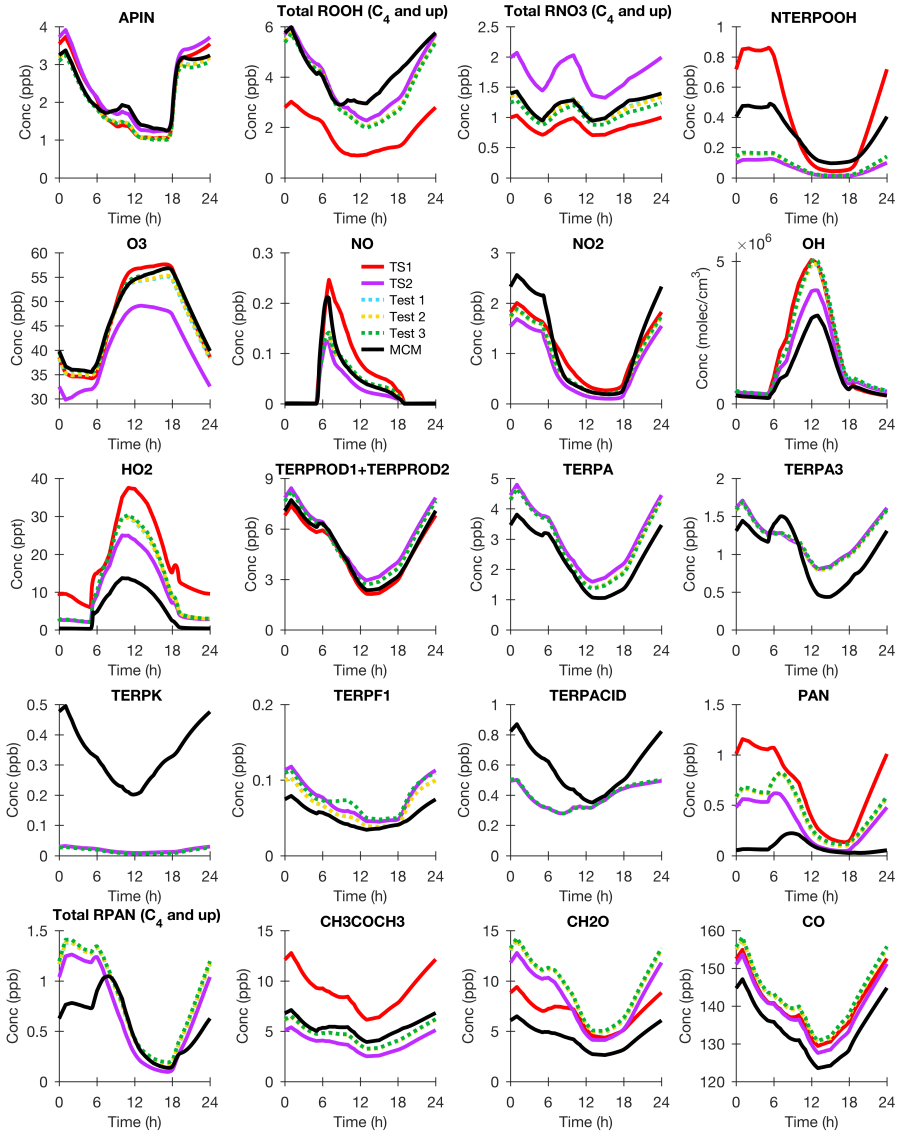

Figure 4. BOXMOX results for α-pinene (APIN) oxidation using TS1 (red), MCM (black), TS2 (purple), TS2 with MCM pinonaldehyde nitrate yield - Test 1 (blue), TS2 with MCM pinonaldehyde and limonaldehyde nitrate yield - Test 2 (gold), and TS2 with MCM pinonaldehyde and limonaldehyde nitrate yield and assumptions for oxidation of unsaturated hydroxy nitrates - Test 3 (green). The model configuration is explained in Section 3.1. APIN (α-pinene surrogate), TERPOOH (terpene hydroxy hydroperoxide), Total ROOH (all terpene hydroperoxides C_4 and up), TERPNIT (terpene hydroxy nitrate), Total RNO3 (all terpene nitrates C_4 and up), NTERPOOH (terpene nitrooxy hydroperoxide), CH3COCH3 (acetone), TERPROD1 + TERPROD2 (all terpene 1st + 2nd generation products except hydroperoxides, nitrates, and PANs), TERPA (terpene aldehyde like pinonaldehyde), TERPA3 (terpene aldehyde like limonaldehyde), TERPK (terpene ketone), TERPF1 (terpene product - one double bond), TERPACID (terpene acid), PAN (peroxy acyl nitrate), and Total RPAN (all terpene PANs C_4 and up).

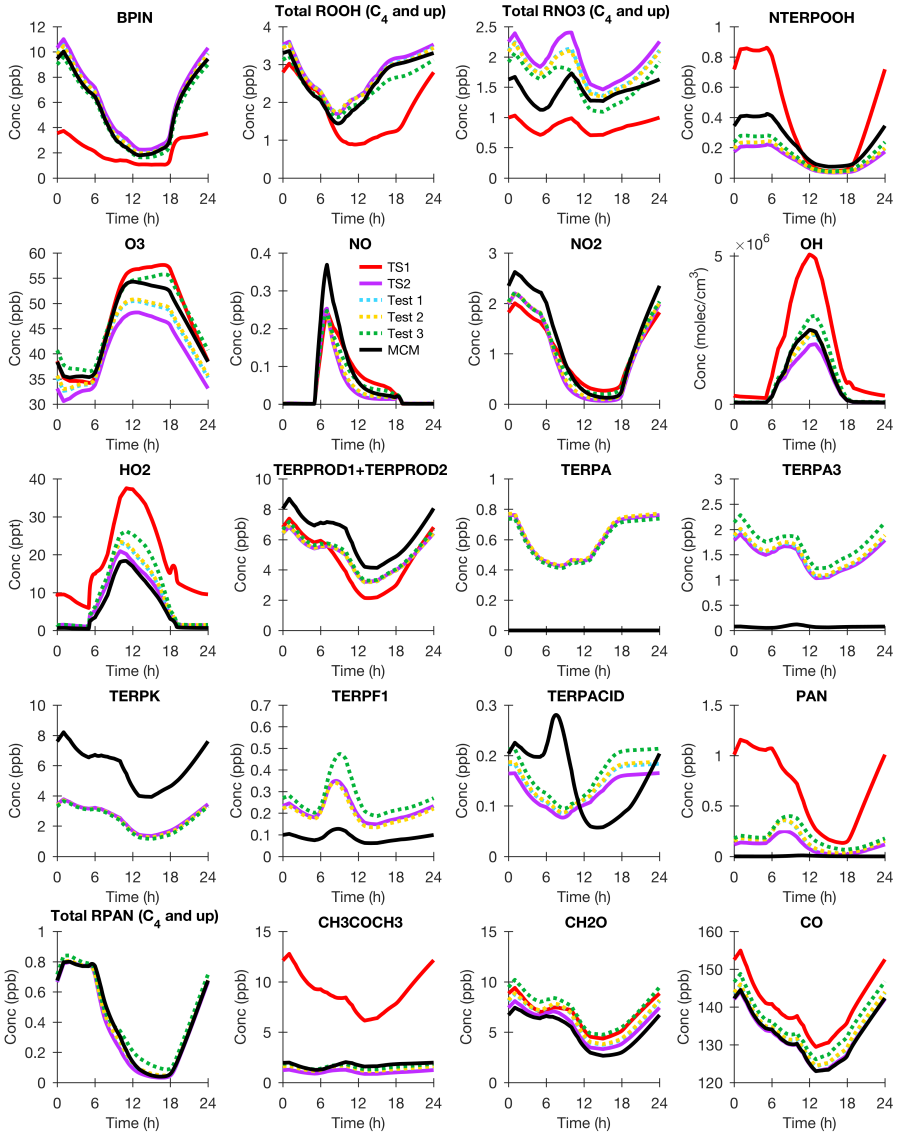

Figure 5. BOXMOX results for β-pinene (BPIN) oxidation using TS1 (red), MCM (black), TS2 (purple), TS2 with MCM pinonaldehyde nitrate yield - Test 1 (blue), TS2 with MCM pinonaldehyde and limonaldehyde nitrate yield - Test 2 (gold), and TS2 with MCM pinonaldehyde and limonaldehyde nitrate yield and assumptions for oxidation of unsaturated hydroxy nitrates - Test 3 (green). The model configuration is explained in Section 3.1. All species names are identical to Figure 4.

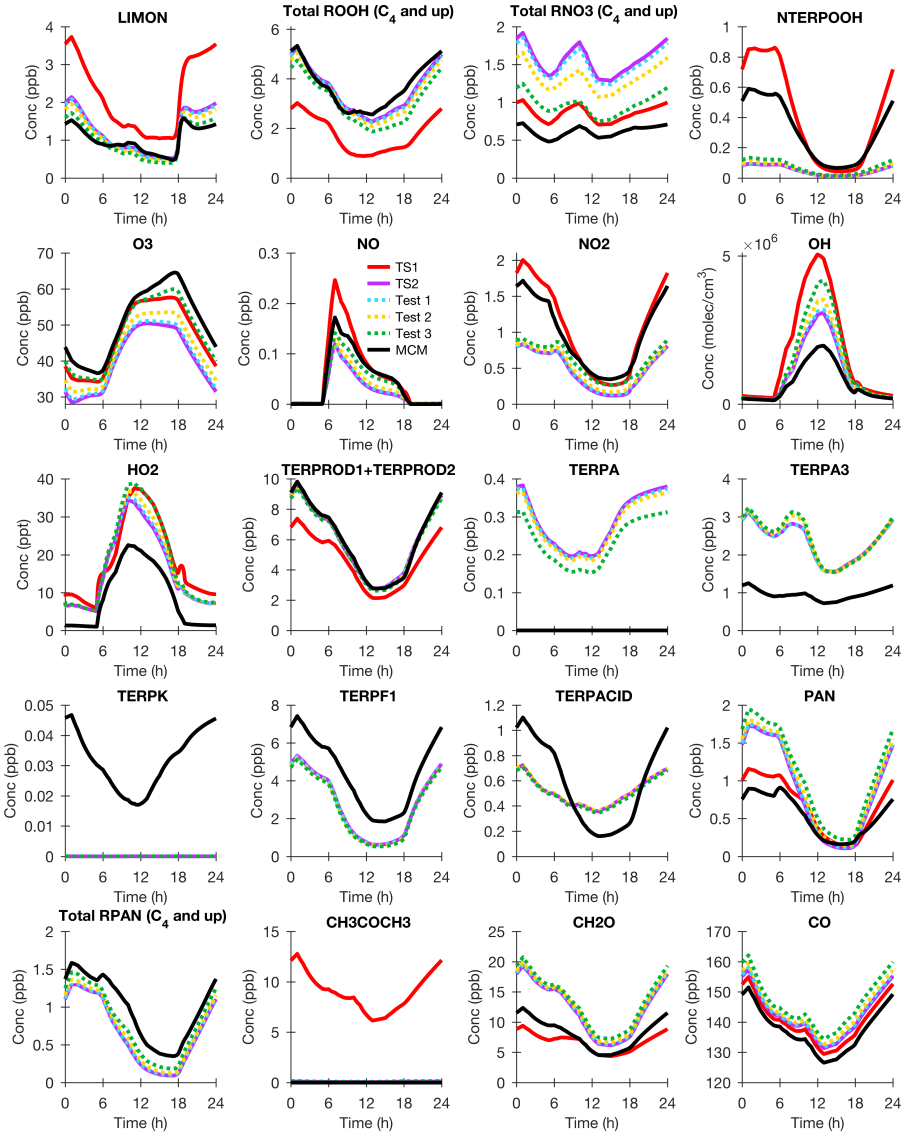

Figure 6. BOXMOX results for limonene (LIMON) oxidation using TS1 (red), MCM (black), TS2 (purple), TS2 with MCM pinonaldehyde nitrate yield - Test 1 (blue), TS2 with MCM pinonaldehyde and limonaldehyde nitrate yield - Test 2 (gold), and TS2 with MCM pinonaldehyde and limonaldehyde nitrate yield and assumptions for oxidation of unsaturated hydroxy nitrates - Test 3 (green). The model configuration is explained in Section 3.1. All species names are identical to Figure 4.

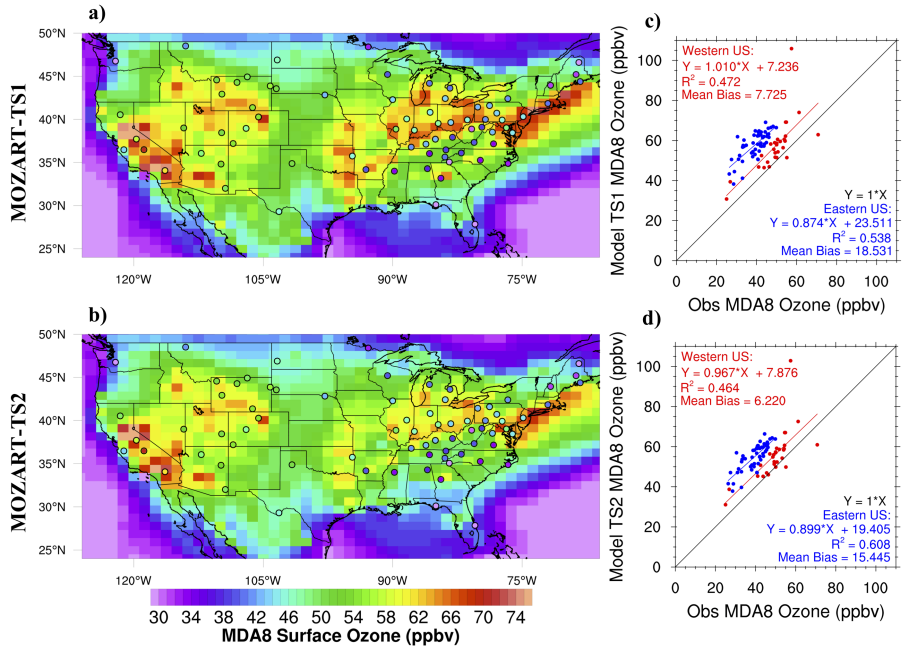

Figure 7. Surface Ozone Daily Max 8-hr Average (MDA8) CESM/CAM-chem results over CONUS using the default TS1 mechanism (panel a) and the updated TS2 mechanism (panel b) compared to U.S. EPA CASTNET data (filled circles) averaged over August 2013. The same data are presented in a scatter plot for TS1 (panel c) and TS2 (panel d) with Eastern U.S. (longitude > -96°) in blue and Western U.S. (longitude < -96°) in red.

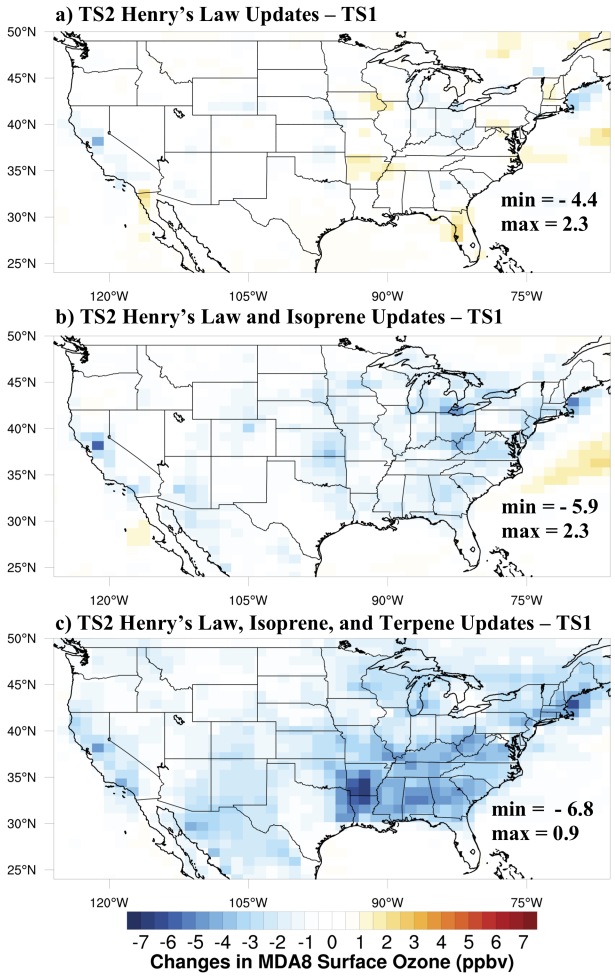

Figure 8. Changes in surface ozone daily max 8-hr average (MDA8) between the TS2 updated case and the TS1 case averaged over August 2013. The minimum and maximum over the domain pictured is displayed on the bottom right for each case.

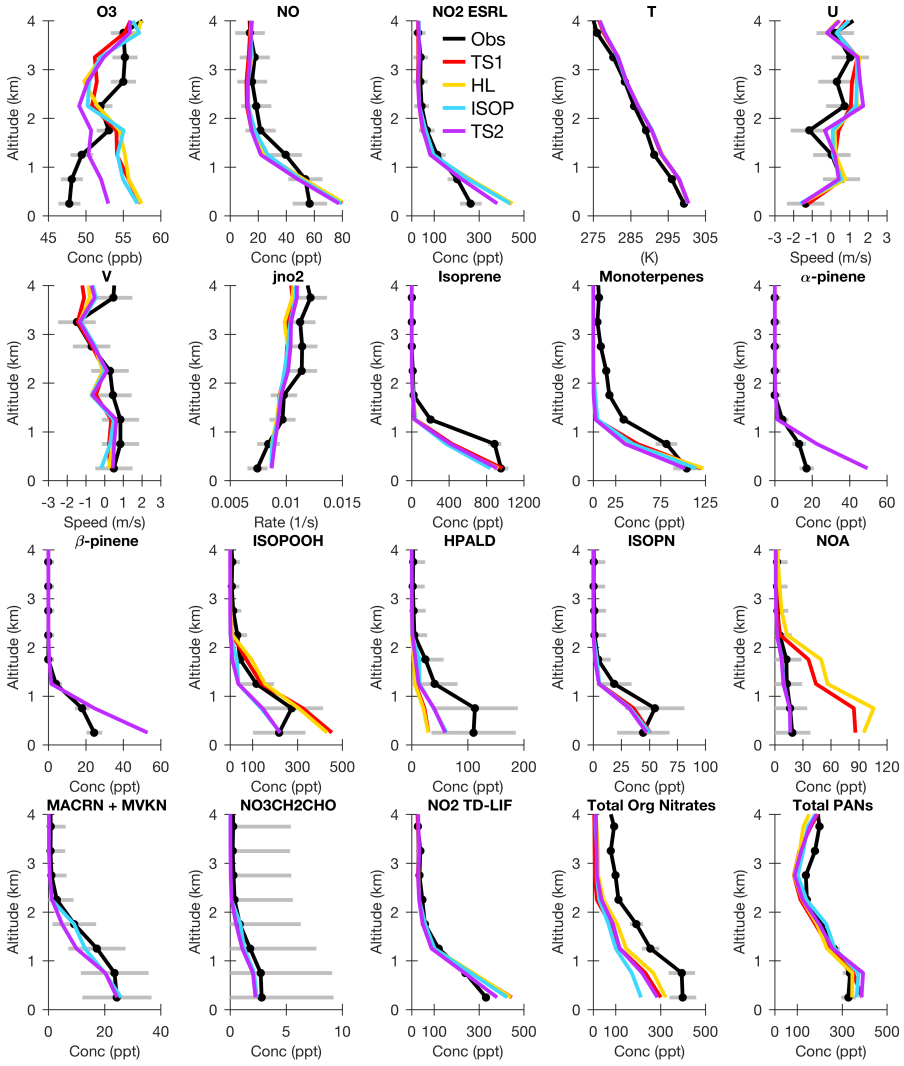

Figure 9. Median vertical profile plots over the SEAC[4]RS flight tracks for observations (Obs - black), TS1 (red), TS2 with only Henry's Law updates (HL - gold), TS2 with Henry's Law and isoprene updates (ISOP - blue), and TS2 with Henry's Law, isoprene and terpene updates (TS2 - purple). Acronyms are defined in Figure 3. Data are grouped into 0.5 km bins and exclude urban plumes (NO_2> 4 ppb), fire plumes (acetonitrile > 0.2 ppb), and stratospheric air (O_3/CO > 1.25) as done in previous work (Travis et al., 2016). Domain includes the southeast U.S. (29.5-40°N, 75-94.5°W), and local sun time 9 am to 5 pm. Observational uncertainty is shown in gray bars.

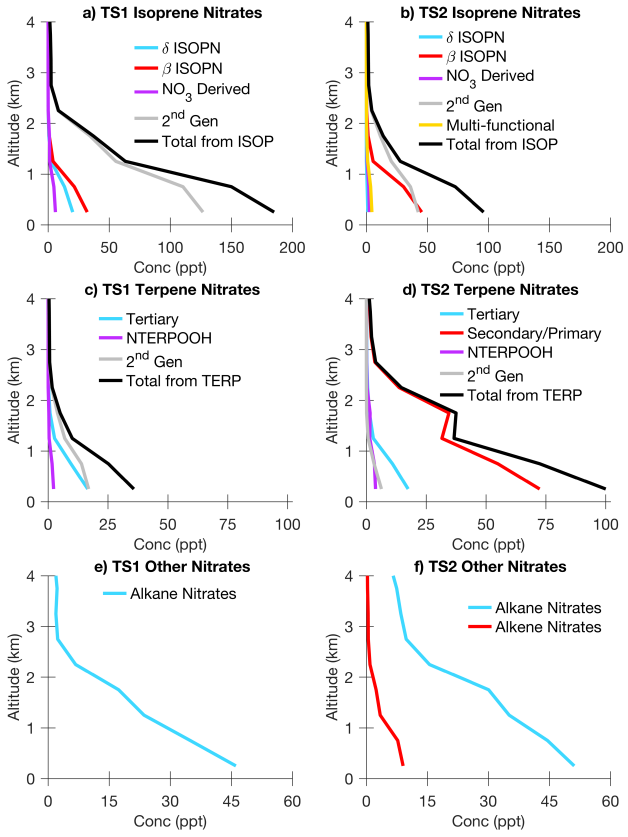

Figure 10. Median vertical profile plots over the SEAC[4]RS flight tracks for all isoprene, terpene, and other nitrates formed in the TS1 and TS2 mechanisms binned as specified in Figure 9. For isoprene, ISOPN includes all isoprene hydroxy nitrates, NO_3 derived includes all nitrates derived only from NO_3-initiated oxidation (i.e. ISOPNOOH, INHE, and NC4CHO - Figure S1), 2nd Gen includes all 2nd generation nitrates, and multi-functional includes all multi-functional later-generation nitrates. For terpenes, tertiary includes all tertiary hydroxy nitrates, secondary/primary includes all secondary/primary hydroxy nitrates, NTERPOOH includes all tertiary hydroperoxy nitrates, and 2nd Gen includes all 2nd generation nitrates, which for TS2 includes only the multi-functional low-volatility organic nitrates (Section 4.2). All dinitrates are doubled.

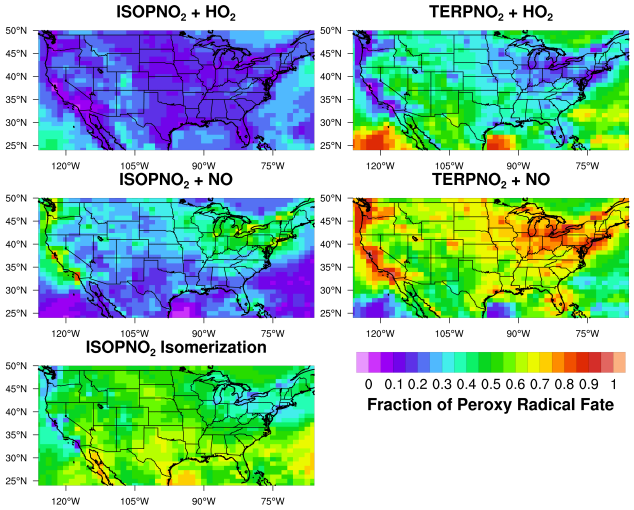

Figure 11. 2013 August average peroxy radical fate (fraction) below 2 km using TS2 for isoprene dihydroxy nitrate peroxy radical ($ISOPNO_2$) formed from isoprene 1st-generation hydroxy nitrate + OH (left) and terpene dihydroxy nitrate peroxy radical ($TERPNO_2$) produced from terpene unsaturated hydroxy nitrate + OH (right).

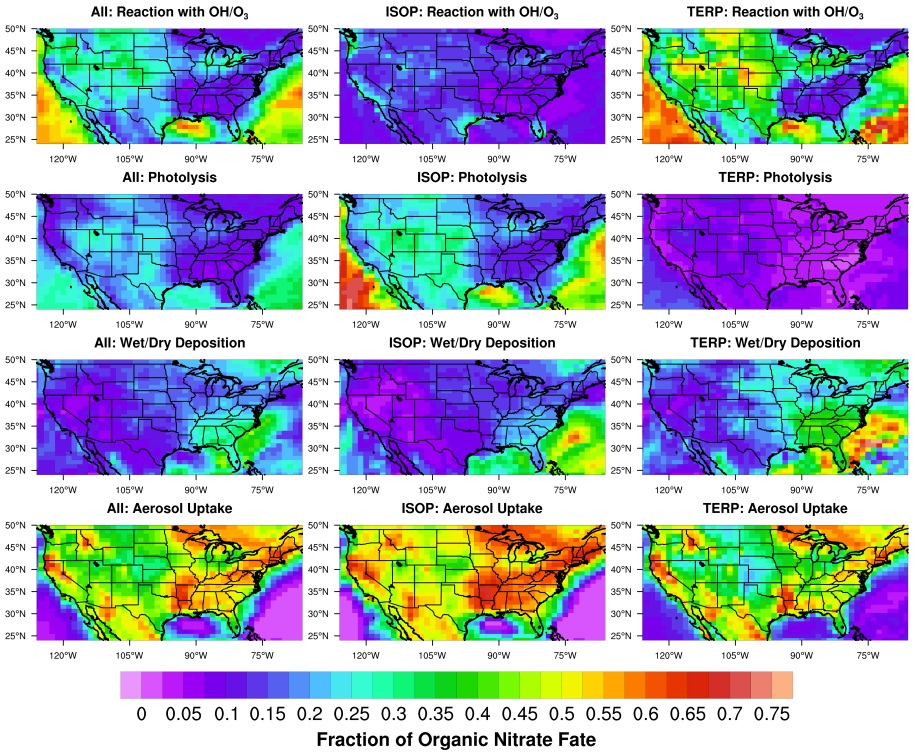

Figure 12. 2013 August average organic nitrate fate below 2 km using TS2 for all organic nitrates (left), isoprene organic nitrates (middle), and terpene organic nitrates (right). To avoid double counting, only the final fate is included, so reaction with OH/O_3 to form another organic nitrate is omitted from this calculation.

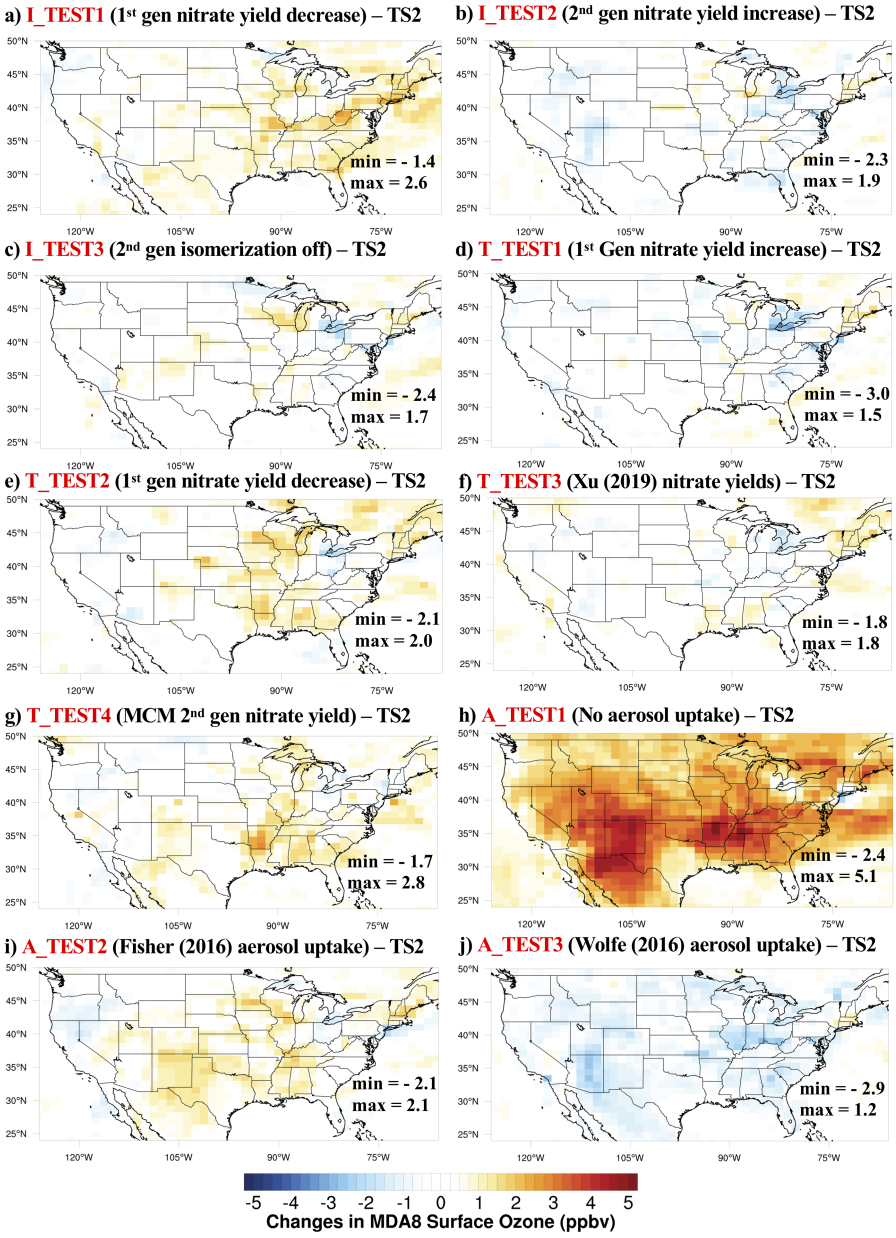

Figure 13. Difference in surface ozone daily max 8-hr average (MDA8) averaged over August 2013 between each sensitivity test described in Table 1 and the TS2 case. For each case, the minimum and maximum over the domain pictured is displayed on the bottom right.

Table 1. Sensitivity tests to determine the impact of uncertainties in TS2 on simulated surface ozone.

Name	Description
Uncertainties in Isoprene Chemistry	
I_TEST1	Isoprene 1st-gen organic nitrate yield updated to 0.09 from $\sim$ 0.13
I_TEST2	Isoprene 2nd-gen organic nitrate yield updated to 0.3 from 0.02-0.2
I_TEST3	Isoprene 2nd-gen no isomerization
Uncertainties in Terpene Chemistry	
T_TEST1	Terpene 1st-gen organic nitrate yield updated to 0.3
T_TEST2	Terpene 1st-gen organic nitrate yield updated to 0.15
T_TEST3	APIN and BPIN 1st-generation chemistry based on Xu et al. (2019)
T_TEST4	Terpene 2nd-gen MCM v3.3.1 organic nitrate yields for pinonaldehyde and limonaldehyde/limaketone oxidation.
Uncertainties in Aerosol Uptake of Organic Nitrates	
A_TEST1	Aerosol uptake of all organic nitrates turned off
A_TEST2	γ-values similar to GEOS-chem (Fisher et al., 2016)
A_TEST3	γ-values similar to Wolfe et al. (2015)

Supplement to Comprehensive isoprene and terpene gas-phase chemistry improves simulated surface ozone in the southeastern U.S.

Rebecca H. Schwantes[1], Louisa K. Emmons[1], John J. Orlando[1], Mary C. Barth[1], Geoffrey S. Tyndall[1], Samuel R. Hall[1], Kirk Ullmann[1], Jason M. St. Clair[2,3], Donald R. Blake[4], Armin Wisthaler[5,6], and ThaoPaul V. Bui[7]

[1]Atmospheric Chemistry Observations and Modeling Laboratory, National Center for Atmospheric Research, Boulder, CO 80301, U.S.A.
[2]Atmospheric Chemistry and Dynamics Laboratory, NASA Goddard Space Flight Center, Greenbelt, MD, 20771, USA
[3]Joint Center for Earth Systems Technology, University of Maryland Baltimore County, Baltimore, MD, 21228, USA
[4]Department of Chemistry, University of California-Irvine, 570 Rowland Hall, Irvine, CA 92697-2025, USA
[5]Institute for Ion Physics and Applied Physics, University of Innsbruck, Technikerstrasse 25, 6020 Innsbruck, Austria
[6]Department of Chemistry, University of Oslo, P.O. 1033 - Blindern, 0315 Oslo, Norway
[7]Earth Science Division, NASA Ames Research Center, Moffett Field, CA 94035-1000

Correspondence to: Rebecca H. Schwantes (rschwant@ucar.edu)

Contents

List of Figures

List of Tables

S1 Schematics of NO_3 oxidation

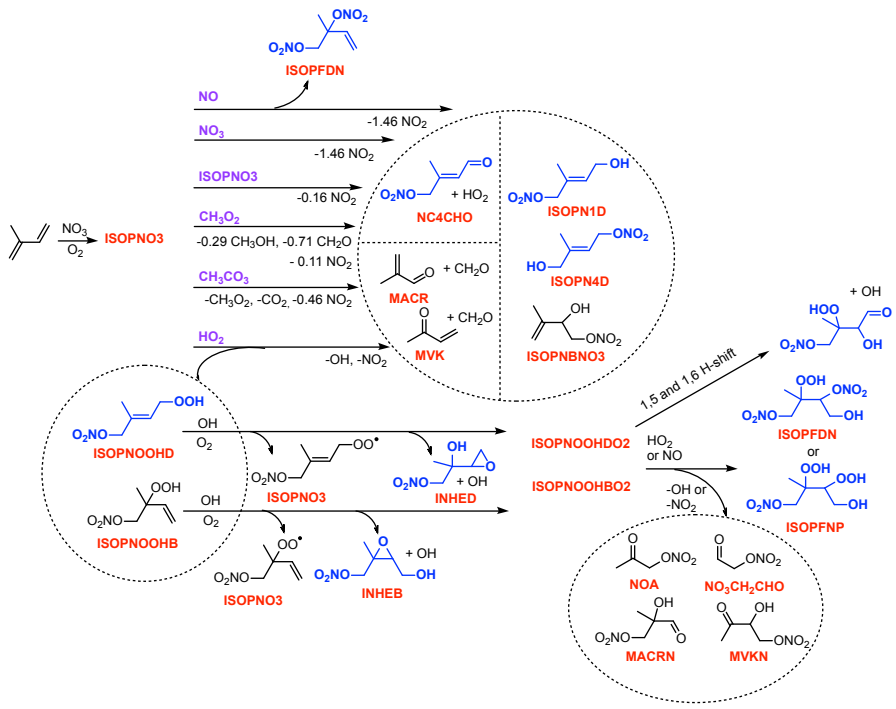

Figure S1. Simplified schematic of the MOZART-TS2 chemical mechanism for isoprene NO_3-initiated oxidation. Blue compounds undergo aerosol uptake.

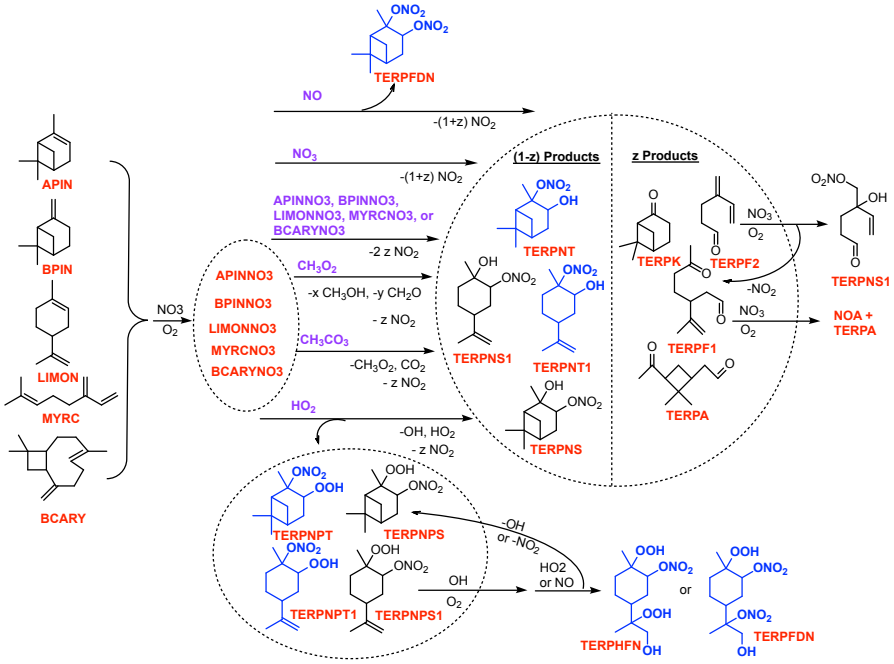

Figure S2. Simplified schematic of the MOZART-TS2 chemical mechanism for terpene NO_3-initiated oxidation. Blue compounds undergo aerosol uptake.

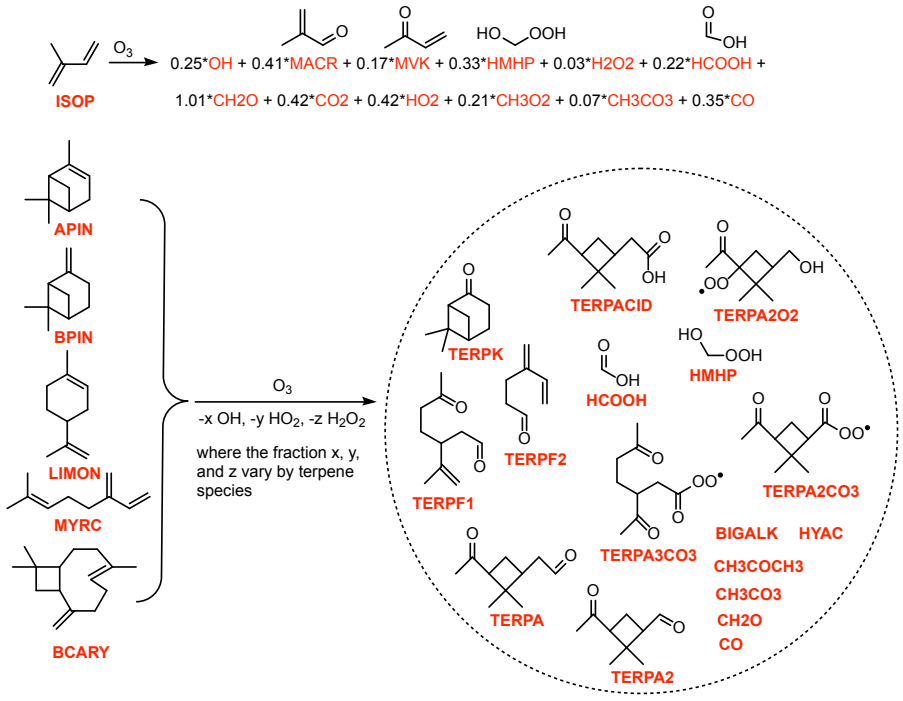

Figure S3. Simplified schematic of the MOZART-TS2 chemical mechanism for isoprene and terpene O_3-initiated oxidation.

S2 Evaluation Against More Explicit Chemical Schemes for Myrcene and β-caryophyllene

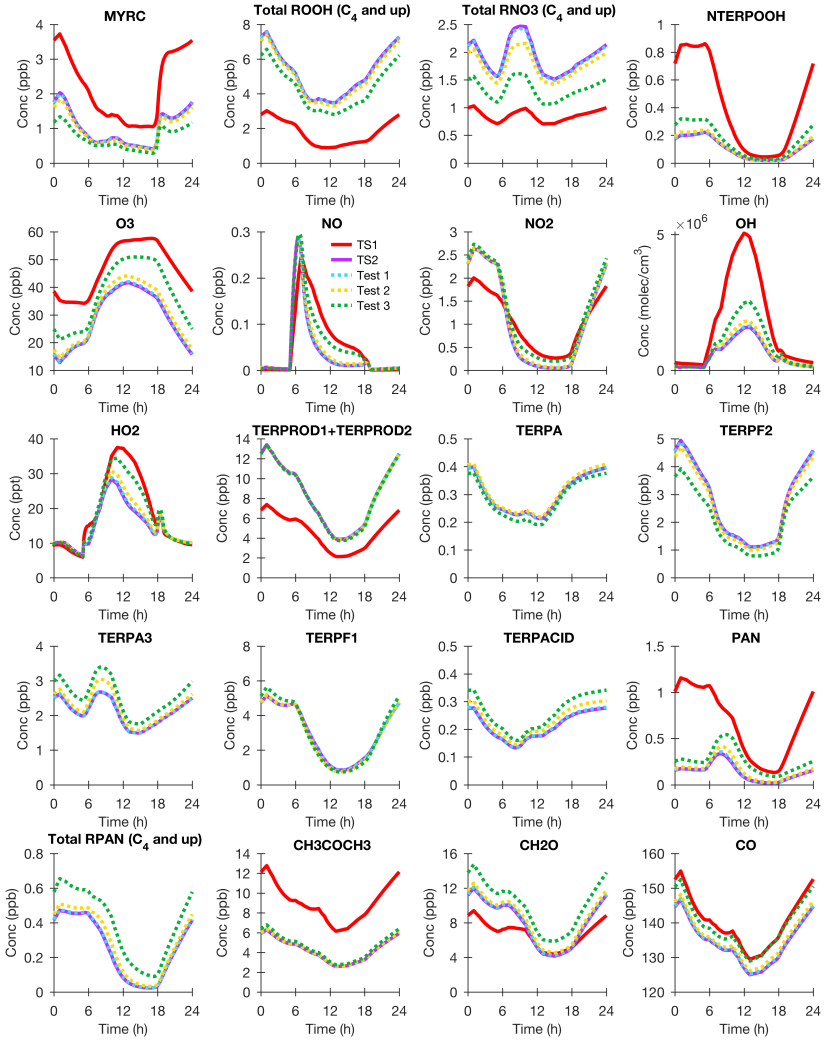

Figure S4. BOXMOX results for myrcene (MYRC) oxidation using TS1 (~~blue~~red), TS2 (~~cyan~~purple), TS2 with MCM pinonaldehyde nitrate yield - Test 1 (~~red~~blue), TS2 with MCM pinonaldehyde and limonaldehyde/limaketone nitrate yield - Test 2 (gold), and TS2 with MCM pinonaldehyde and limonaldehyde/limaketone nitrate yield and assumptions for oxidation of unsaturated hydroxy nitrates - Test 3 (~~purple~~green). MYRC (myrcene surrogate), TERPOOH (terpene hydroxy hydroperoxide), Total ROOH (all terpene hydroperoxides C_4 and up), TERPNIT (terpene hydroxy nitrate), Total RNO3 (all terpene derived nitrates C_4 and up), O3 (ozone), NO (nitrogen oxide), NO2 (nitrogen dioxide), OH (hydroxyl radical), HO2 (hydroperoxy radical), CH3COCH3 (acetone), TERPROD1 + TERPROD2 (all terpene 1st- and 2nd-gen products except hydroperoxides, nitrates and PANs), TERPA (terpene aldehyde like pinonaldehyde), TERPF2 (terpene product - 2 double bonds), TERPA3 (terpene aldehyde like limonaldehyde), TERPF1 (terpene product - 1 double bond), TERPACID (terpene acid), PAN (peroxy acyl nitrate), and Total RPAN (all terpene PANs C_4 and up), and CO (carbon monoxide).

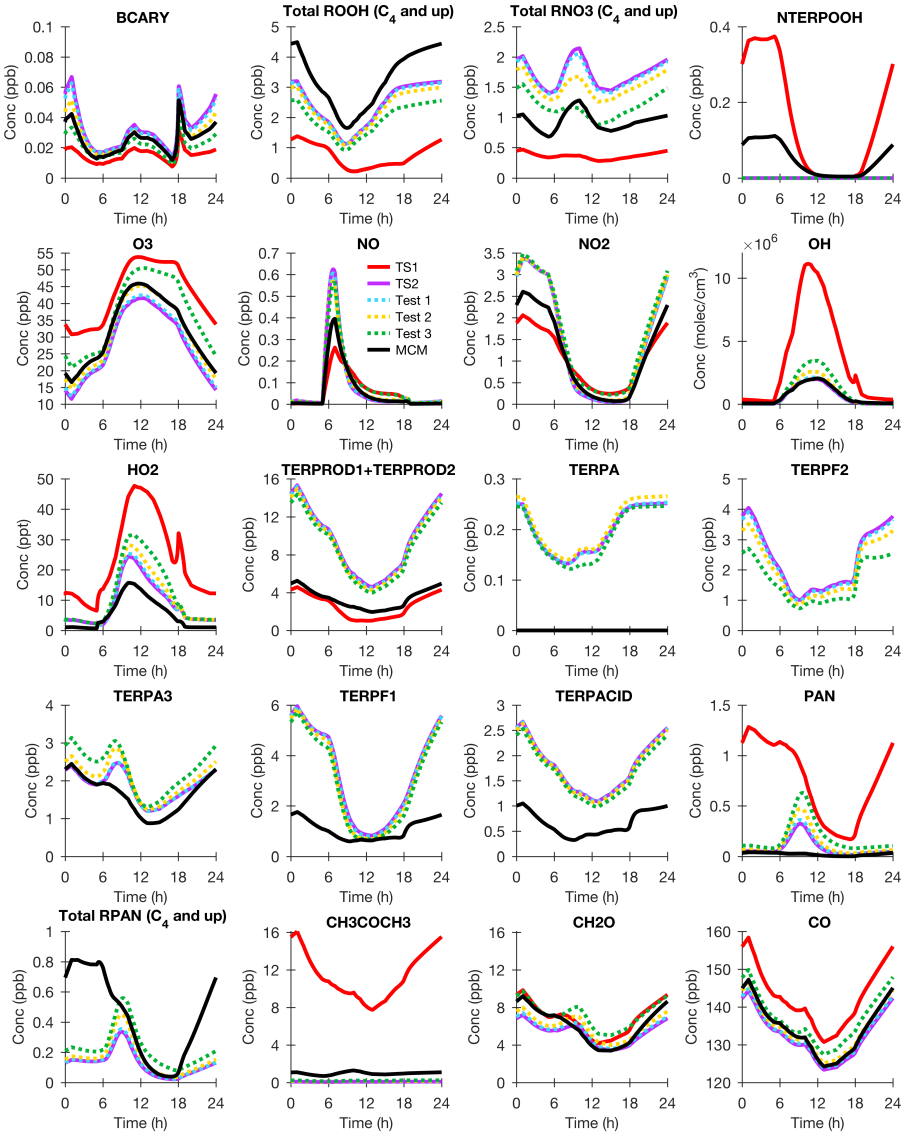

Figure S5. BOXMOX results for β-caryophyllene (BCARY) oxidation using TS1 (~~blue~~red), TS2 (~~cyan~~purple), MCM (~~gray~~black), TS2 with MCM pinonaldehyde nitrate yield - Test 1 (~~red~~blue), TS2 with MCM pinonaldehyde and limonaldehyde/limaketone nitrate yield - Test 2 (gold), and TS2 with MCM pinonaldehyde and limonaldehyde/limaketone nitrate yield and assumptions for oxidation of unsaturated hydroxy nitrates - Test 3 (~~purple~~green). All species are identical to Figure S4.

S3 Nudging and Vertical Level Resolution in CESM/CAM-Chem

As shown in Figure ~~S5 and~~ S6 and S7, nudging at 50 h versus 5 h relaxation times increases the biogenic emissions likely because of increased surface temperatures, improves the representation of winds compared to observations, but also increases

biases in the ozone vertical profile. There are some small differences in ozone and other compounds when using 32 levels versus 56 levels. Given that CESM/CAM-Chem is tuned using 32 levels and nudging with a 50 h relaxation time appears to add less biases into the ozone vertical profile, 32 levels with a 50 h nudging relaxation time were used in all simulations for this work. The model results do appear to be quite sensitive to the choice of the nudging relaxation time, which will be explored more completely in future work.

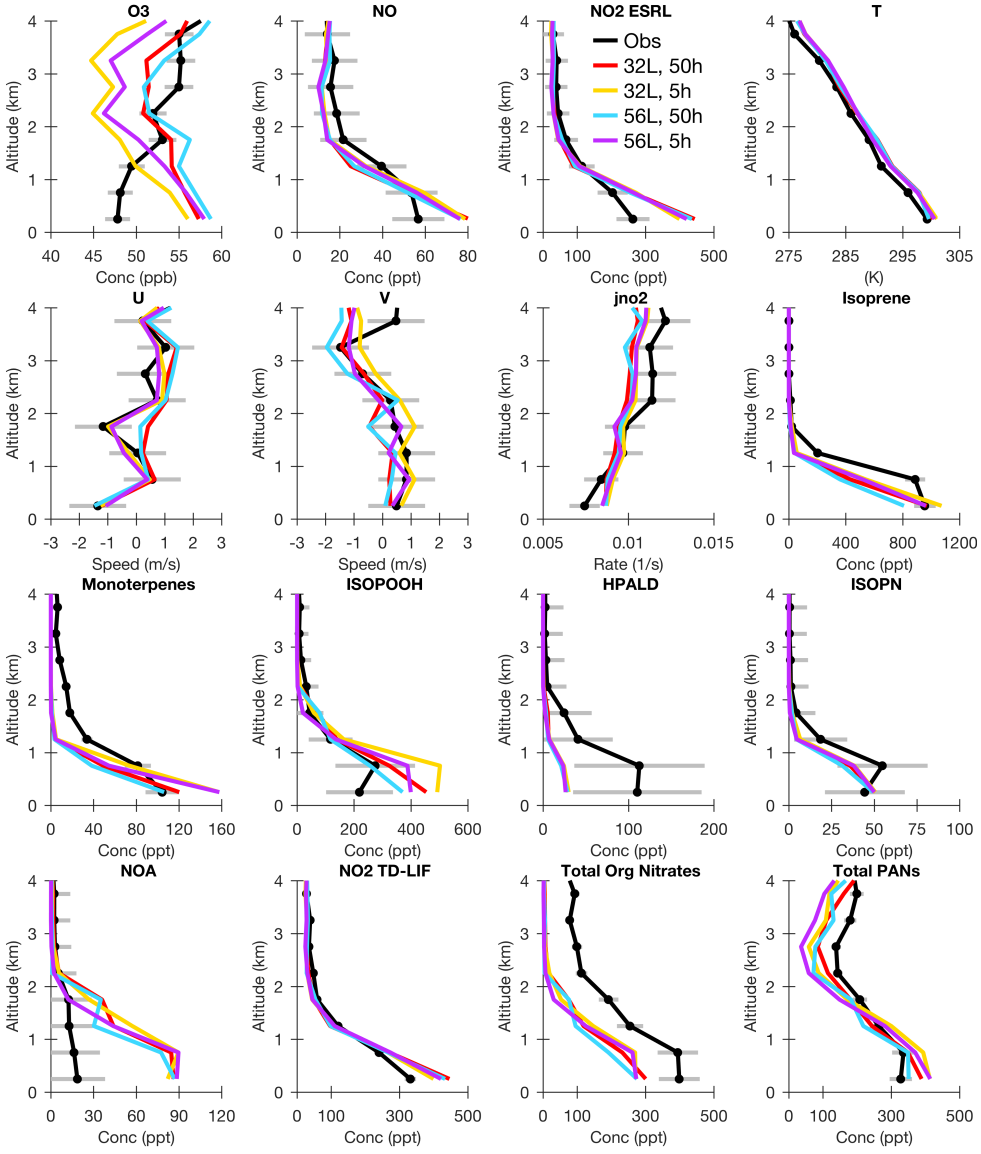

Figure S6. Median vertical profile plots up to 4 km over the SEAC^{4}Rs flight tracks for observations (black), MOZART-TS1 with 32 vertical levels and 50 h relaxation time (red), MOZART-TS1 with 32 vertical levels and 5 h relaxation time (gold), MOZART-TS1 with 56 vertical levels and 50 h relaxation time (blue), and MOZART-TS1 with 56 vertical levels and 5 h relaxation time (~~cyan~~purple). Acronyms are defined in Figure S4. Data are grouped into 0.5 km bins and exclude urban plumes (NO_2> 4 ppb), fire plumes (acetonitrile > 0.2 ppb), and stratospheric air (O_3/CO > 1.25) as done in previous work (Travis et al., 2016). Domain includes the Southeast U.S. (29.5-40°N, 75-94.5°W), and local sun time 9 am to 5 pm. Observational uncertainty is shown in gray bars.

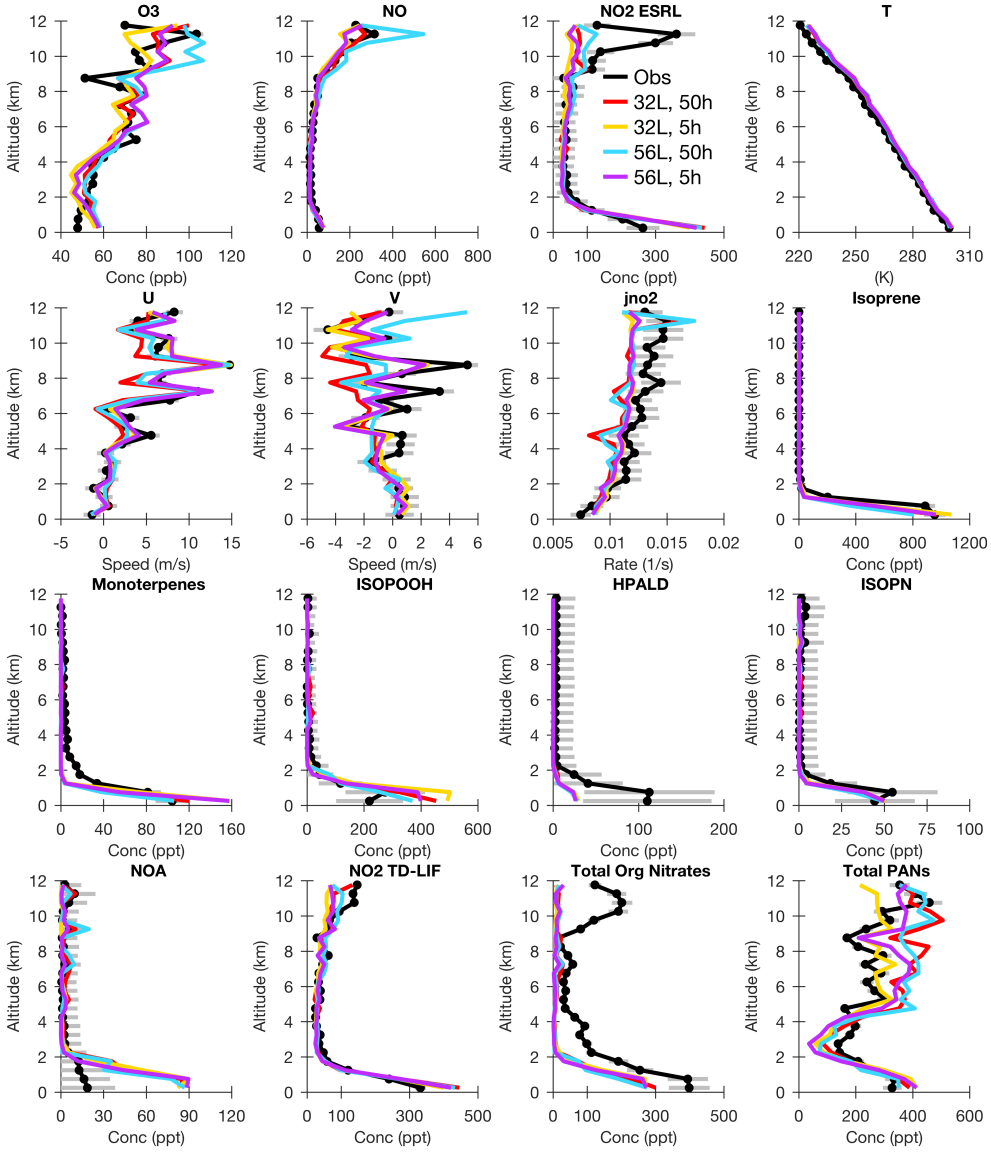

Figure S7. Median vertical profile plots over the SEAC[4]Rs flight tracks identical to Figure ~~S5~~ S6 except up to 12 km altitude instead of 4 km.

S4 Organic Nitrate Fate in MOZART-TS1

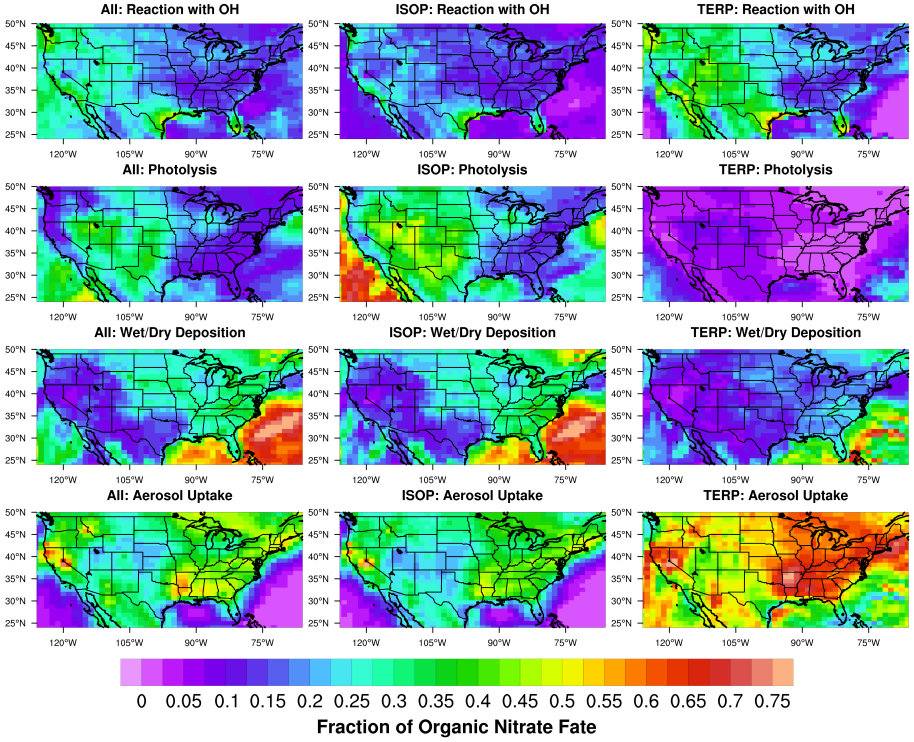

Figure S8. 2013 August average organic nitrate fate below 2 km using MOZART-TS1 for all organic nitrates (left), isoprene organic nitrates (middle), and terpene organic nitrates (right). To avoid double counting, only the final fate is included, so reaction with OH/O_3 to form another organic nitrate is omitted from this calculation.

S5 Tables Defining Chemical Compounds and Reactions in MOZART-TS2

Table S1: General peroxy (RO_2) and peroxyacyl (RCO_3) reaction rate constant sources used in MOZART-TS2 for isoprene and terpene chemistry

Reaction	**Source of rate constant**
RO_2 + CH_3O_2	Either isoprene general rate (Jenkin et al., 1998) or geometric mean of RO_2 + RO_2 and CH_3O_2 + CH_3O_2 from IUPAC (Atkinson et al., 2006)
RO_2 + CH_3CO_3	JPL (CH_3O_2 + CH_3CO_3), Burkholder et al. (2015)
RO_2 + RCO_3	JPL (CH_3O_2 + CH_3CO_3), Burkholder et al. (2015)
RO_2 + HO_2	Wennberg et al. (2018) parameterization based on n (# of C + O + N - 2 atoms in the peroxy radical)
RO_2 + NO	MCM v3.3.1, Jenkin et al. (2015)
RO_2 + NO_3	MCM v3.3.1, Jenkin et al. (2015)
RCO_3 + CH_3CO_3	JPL (CH_3CO_3 + CH_3CO_3), Burkholder et al. (2015)
RCO_3 + RCO_3	JPL (CH_3CO_3 + CH_3CO_3), Burkholder et al. (2015)
RCO_3 + CH_3O_2	JPL (CH_3O_2 + CH_3CO_3), Burkholder et al. (2015)
RCO_3 + HO_2	JPL (CH_3CO_3 + HO_2), Burkholder et al. (2015)
RCO_3 + NO	JPL (CH_3CO_3 + NO), Burkholder et al. (2015)
RCO_3 + NO_3	IUPAC (CH_3CO_3 + NO_3), Atkinson et al. (2006)
RCO_3 + NO_2	JPL (CH_3CO_3 + NO_2), Burkholder et al. (2015)
RPAN + M	JPL (PAN + M), Burkholder et al. (2015)

Table S2: MOZART-TS2 chemical species

Species name	Chemical Formula	Description
ACBZO2	$C_7H_5O_3$	acylperoxy radical from benzaldehyde
ALKNIT	$C_5H_{11}ONO_2$	standard alkyl nitrate from BIGALK+OH
ALKO2	$C_5H_{11}O_2$	lumped alkane peroxy radical from BIGALK
ALKOOH	$C_5H_{12}O_2$	lumped alkane hydroperoxide
AOA_NH	CO	age of air tracer
APIN	$C_{10}H_{16}$	α-pinene surrogate monoterpene
APINNO3	$C_{10}H_{16}NO_5$	peroxy radical from NO_3 + α-pinene
APINO2	$C_{10}H_{17}O_3$	peroxy radical from OH + α-pinene reaction
BCARY	$C_{15}H_{24}$	β-caryophyllene surrogate sesquiterpene
BCARYNO3	$C_{15}H_{24}NO_5$	peroxy radical from NO_3 + sesquiterpenes
BCARYO2	$C_{15}H_{25}O_3$	peroxy radical from OH + sesquiterpenes
BENZENE	C_6H_6	benzene
BENZO2	$C_6H_7O_5$	bicyclic peroxy radical from OH + benzene
BENZOOH	$C_6H_8O_5$	bicyclic hydroperoxide from OH + benzene
BEPOMUC	$C_6H_6O_3$	unsaturated dialdehydic epoxide from OH + benzene
BIGALD1	$C_4H_4O_2$	butenedial, a product of aromatic oxidation
BIGALD2	$C_5H_6O_2$	4-oxy-2-pentenal, a product of aromatic oxidation
BIGALD3	$C_5H_6O_2$	2-methyl butenedial, a product of aromatic oxidation
BIGALD4	$C_6H_8O_2$	2-methyl-4-oxo-2-pentenal, a product of aromatic oxidation
BIGALD	$C_5H_6O_2$	lumped aldehyde from terpene ozonolysis
BIGALK	C_5H_{12}	lumped alkanes C>3
BIGENE	C_4H_8	lumped alkenes C>3
BPIN	$C_{10}H_{16}$	β-pinene
BPINNO3	$C_{10}H_{16}NO_5$	peroxy radical from NO_3 + β-pinene
BPINO2	$C_{10}H_{17}O_3$	peroxy radical from OH + $beta$-pinene
BR	Br	bromine radical
BRCL	BrCl	bromine monochloride
BRO	BrO	bromine monooxide radical
BRONO2	$BrONO_2$	bromine nitrate
BRY	Br_Y	total reactive bromine
BZALD	C_7H_6O	benzaldehyde
BZOO	$C_7H_7O_2$	peroxy radical from toluene oxidation
BZOOH	$C_7H_8O_2$	hydroperoxide from toluene oxidation
C2H2	C_2H_2	ethyne (acetylene)
C2H4	C_2H_4	ethene

Table S2: MOZART-TS2 chemical Species

Species name	Chemical Formula	Description
C2H5O2	$C_2H_5O_2$	ethylperoxy radical
C2H5OH	C_2H_5OH	ethanol
C2H5OOH	C_2H_5OOH	ethyl hydroperoxide
C2H6	C_2H_6	ethane
C3H6	C_3H_6	propene
C3H7O2	$C_3H_7O_2$	propylperoxy radical
C3H7OOH	C_3H_7OOH	propyl hydrogen peroxide
C3H8	C_3H_8	propane
C6H5O2	$C_6H_5O_2$	phenylperoxy radical
C6H5OOH	C_6H_5OOH	phenyl hydroperoxide
CCL4	CCl_4	carbon tetrachloride (LBC)
CF2CLBR	CF_2ClBr	bromochlorodifluoromethane (LBC)
CF3BR	CF_3Br	Bromotrifluoromethane (LBC)
CFC113	CCl_2FCClF_2	1,1,2-trichlorotrifluoroethane (LBC)
CFC114	$CClF_2CClF_2$	1,2-dichlorotetrafluoroethane (LBC)
CFC115	$CClF_2CF_3$	chloropentafluoroethane (LBC)
CFC11	$CFCl_3$	trichlorofluoromethane (LBC)
CFC12	CF_2Cl_2	difluorodichloromethane (LBC)
CH2BR2	CH_2Br_2	dibromomethane (LBC)
CH2O	CH_2O	formaldehyde
CH3BR	CH_3Br	bromomethane (methyl bromide) (LBC)
CH3CCL3	CH_3CCl_3	1,1,1-trichloroethane (methylchloroform) (LBC)
CH3CHO	CH_3CHO	acetaldehyde
CH3CL	CH_3Cl	chloromethane (methyl chloride) (LBC)
CH3CN	CH_3CN	acetonitrile
CH3CO3	CH_3CO_3	acetylperoxy radical
CH3COCH3	CH_3COCH_3	acetone
CH3COCHO	CH_3COCHO	methyl glyoxal
CH3COOH	CH_3COOH	acetic acid
CH3COOOH	CH_3COOOH	peracetic acid
CH3O2	CH_3O_2	methylperoxy radical
CH3OH	CH_3OH	methanol
CH3OOH	CH_3OOH	methyl hydroperoxide
CH4	CH_4	methane (LBC)
CHBR3	$CHBr_3$	tribromomethane (bromoform) (LBC)

Table S2: MOZART-TS2 chemical Species

Species name	Chemical Formula	Description
CL2	Cl_2	chlorine
CL2O2	Cl_2O_2	dichlorine dioxide
CL	Cl	chlorine radical
CLO	ClO	chlorine monoxide radical
CLONO2	$ClONO_2$	chlorine nitrate
CLY	Cl_Y	total reactive chlorine
CO2	CO_2	carbon dioxide (LBC)
CO	CO	carbon monoxide
COF2	COF_2	carbonyl fluoride
COFCL	COFCl	carbonyl chloride fluoride
CRESOL	C_7H_8O	lumped cresols (hydroxymethylbenzenes)
DHPMPAL	$C_4H_8O_5$	C4 dihydroperoxy carbonyl derived from isoprene
DICARBO2	$C_5H_5O_4$	acylperoxy radical formed from aromatic oxidation, via unsaturated dicarbonyl chemistry
DMS	CH_3SCH_3	dimethyl sulfide
E90	CO	artificial tracer with 90-day lifetime emitted from surface
ENEO2	$C_4H_9O_3$	lumped hydroxyperoxy radical from OH + large alkenes
EO2	$HOCH_2CH_2O_2$	hydroxyperoxy radical from OH + ethene
EO	$HOCH_2CH_2O$	hydroxyalkoxy radical from OH + ethene
EOOH	$HOCH_2CH_2OOH$	hydroxyhydroperoxide from OH + ethene
F	F	fluorine radical
GLYALD	$HOCH_2CHO$	glycolaldehyde
GLYOXAL	$C_2H_2O_2$	glyoxal
H2402	$CBrF_2CBrF_2$	dibromotetrafluoroethane (LBC)
H2	H_2	hydrogen (LBC)
H2O2	H_2O_2	hydrogen peroxide
H2SO4	H_2SO_4	sulfuric acid
H	H	hydrogen radical
HBR	HBr	hydrogen bromide
HCFC141B	CH_3CCl_2F	1,1-dichoro-1-fluoroethane (LBC)
HCFC142B	CH_3CClF_2	1-choro-1,1-difluoroethane (LBC)
HCFC22	CHF_2Cl	difluorochloromethane (LBC)
HCL	HCl	hydrogen chloride
HCN	HCN	hydrogen cyanide
HCOCH2OOH	$C_2H_4O_3$	hydroperoxy acetaldehyde

Table S2: MOZART-TS2 chemical Species

Species name	Chemical Formula	Description
HCOOH	HCOOH	formic acid
HF	HF	hydrogen fluoride
HMHP	CH_4O_3	hydroxy methyl hydroperoxide
HNO3	HNO_3	nitric acid
HO2	HO_2	hydroperoxyl radical
HO2NO2	HO_2NO_2	pernitric acid
HOBR	HOBr	hypobromous acid
HOCH2OO	$HOCH_2OO$	hydroxy-methyl-peroxy radical
HOCL	HOCl	hypochlorous acid
HONITR	$C_4H_9NO_4$	lumped hydroxynitrates from various compounds
HPALD1	$C_5H_8O_3$	hydroperoxy aldehyde from ISOPZD1O2
HPALD4	$C_5H_8O_3$	hydroperoxy aldehyde from ISOPZD4O2
HPALDB1C	$C_5H_8O_3$	β-2-hydroperoxy-1-aldehyde
HPALDB4C	$C_5H_8O_3$	β-3-hydroperoxy-4-aldehyde
HYAC	CH_3COCH_2OH	hydroxyacetone
HYDRALD	$HOCH_2CCH_3CHCHO$	lumped unsaturated hydroxycarbonyl
HYPERACET	$C_3H_6O_3$	hydroperoxy acetone
ICHE	$C_5H_8O_3$	C5 carbonyl hydroxy epoxide
IEPOX	$C_5H_{10}O_3$	isoprene dihydroxy epoxide
IEPOXOO	$C_5H_9O_5$	peroxy radical from IEPOX + OH
INHEB	$C_5H_9NO_5$	β-isoprene nitrooxy hydroxy epoxide
INHED	$C_5H_9NO_5$	δ-isoprene nitrooxy hydroxy epoxide
ISOP	C_5H_8	isoprene
I**SOPB1O2**	$C_5H_9O_3$	OH-1-O_2-2-β-isoprene hydroxy peroxy radical
ISOPB4O2	$C_5H_9O_3$	OH-4-O_2-3-β-isoprene hydroxy peroxy radical
ISOPC1C	C_5H_9O	OH-1-*cis*-isoprene allylic radical
ISOPC1T	C_5H_9O	OH-1-*trans*-isoprene allylic radical
ISOPC4C	C_5H_9O	OH-4-*cis*-isoprene allylic radical
ISOPC4T	C_5H_9O	OH-4-*trans*-isoprene allylic radical
ISOPED1O2	$C_5H_9O_3$	OH-1-O_2-4-E-δ-isoprene hydroxy peroxy radical
ISOPED4O2	$C_5H_9O_3$	OH-4-O_2-1-E-δ-isoprene hydroxy peroxy radical
ISOPFDN	$C_5H_{10}N_2O_8$	isoprene functionalized dinitrates
ISOPFDNC	$C_5H_8N_2O_8$	C5 carbonyl hydroxy dinitrate
ISOPFNC	$C_5H_9NO_7$	C5 carbonyl hydroxy hydroperoxy nitrate
ISOPFNP	$C_5H_{11}NO_7$	isoprene highly functionalized nitrates

Table S2: MOZART-TS2 chemical Species

Species name	Chemical Formula	Description
ISOPHFP	$C_5H_{10}O_5$	isoprene highly functionalized hydroperoxide
ISOPN1D	$C_5H_9NO_4$	δ-isoprene hydroxy nitrate (nitrooxy in 1 position)
ISOPN1DO2	$C_5H_{10}NO_7$	peroxy radical from ISOPN1D + OH
ISOPN2B	$C_5H_9NO_4$	β-isoprene hydroxy nitrate (nitrooxy in 2 position)
ISOPN2BO2	$C_5H_{10}NO_7$	peroxy radical from ISOPN2B + OH
ISOPN3B	$C_5H_9NO_4$	β-isoprene hydroxy nitrate (nitrooxy in 3 position)
ISOPN3BO2	$C_5H_{10}NO_7$	peroxy radical from ISOPN3B + OH
ISOPN4D	$C_5H_9NO_4$	δ-isoprene hydroxy nitrate (nitrooxy in 4 position)
ISOPN4DO2	$C_5H_{10}NO_7$	peroxy radical from ISOPN4D + OH
ISOPNBNO3	$C_5H_9NO_4$	β-isoprene hydroxy nitrate from isoprene NO_3 oxidation (combined isomers)
ISOPNBNO3O2	$C_5H_{10}NO_7$	peroxy radical from ISOPNBNO3 + OH
ISOPNO3	$CH_2CHCCH_3OOCH_2ONO_2$	peroxy radical from isoprene NO_3 oxidation
ISOPNOOHB	$C_5H_9NO_5$	β-isoprene hydroperoxy nitrate
ISOPNOOHBO2	$C_5H_{10}NO_8$	peroxy radical from ISOPNOOHB + OH
ISOPNOOHD	$C_5H_9NO_5$	δ-isoprene hydroperoxy nitrate
ISOPNOOHDO2	$C_5H_{10}NO_8$	peroxy radical from ISOPNOOHD + OH
ISOPOH	$C_5H_{10}O_2$	isoprene diol from RO_2 + RO_2 reactions
ISOPOOH	$HOCH_2C(OOH)(CH_3)CHCH_2$	unsaturated hydroxyhydroperoxide
ISOPZD1O2	$C_5H_9O_3$	OH-1-O_2-4-Z-δ-isoprene hydroxy peroxy radical
ISOPZD4O2	$C_5H_9O_3$	OH-4-O_2-1-Z-δ-isoprene hydroxy peroxy radical
IVOC	$C_{13}H_{28}$	intermediate volatility organic precursor of VBS SOA
LIMON	$C_{10}H_{16}$	limonene
LIMONNO3	$C_{10}H_{16}NO_5$	peroxy radical from NO_3 + limonene
LIMONO2	$C_{10}H_{17}O_3$	peroxy radical from OH + limonene
MACR	CH_2CCH_3CHO	methacrolein
MACRN	$C_4H_7NO_5$	hydroxy nitrate from MACR
MACRO2	$CH_3COCHO_2CH_2OH$	peroxy radical from methacrolein oxidation
MACROOH	$CH_3COCHOOHCH_2OH$	hydroxyhydroperoxide from methacrolein
MALO2	$C_4H_3O_4$	acylperoxy radical from OH reaction with BIGALD1
MCO3	$CH_2CCH_3CO_3$	peroxy radical from OH abstraction reaction with MACR
MDIALO2	$C_4H_5O_4$	peroxy radical from OH addition to BIGALD1
MEK	C_4H_8O	methyl ethyl ketone
MEKO2	$C_4H_7O_3$	peroxy radical formed from MEK oxidation
MEKOOH	$C_4H_8O_3$	hydroperoxide from MEK oxidation

Table S2: MOZART-TS2 chemical Species

Species name	Chemical Formula	Description
MPAN	$CH_2CCH_3CO_3NO_2$	methacryloyl peroxynitrate
MVK	$CH_2CHCOCH_3$	methyl vinyl ketone
MVKN	$C_4H_7NO_5$	hydroxy nitrate from MVK
MVKO2	$C_4H_7O_4$	MVK hydroxy peroxy radical
MVKOOH	$C_4H_8O_4$	C_4 hydroxy hydroperoxide ketone from MVK
MYRC	$C_{10}H_{16}$	myrcene
MYRCNO3	$C_{10}H_{16}NO_5$	peroxy radical from NO_3 + myrcene
MYRCO2	$C_{10}H_{17}O_3$	peroxy radical from OH + myrcene
N2O5	N_2O_5	dinitrogen pentoxide
N2O	N_2O	nitrous oxide (LBC)
N	N	nitrogen radical
NC4CHO	$C_5H_7NO_4$	nitrooxy-aldehyde from NO_3 + isoprene
NC4CHOO2	$C_5H_8NO_7$	peroxy radical from NC4CHO + OH
NDEP	N	diagnostic of nitrogen deposition
NH3	NH_3	ammonia
NH4	NH_4	ammonium ion aerosol
NHDEP	N	diagnostic of ammonia deposition
NH_50	CO	idealized tracer with 50-day loss rate
NH_5	CO	idealized tracer with 5 day loss rate
NO2	NO_2	nitrogen dioxide
NO3	NO_3	nitrate radical
NO3CH2CHO	$C_2H_3O_4N$	ethanal nitrate
NO	NO	nitric oxide
NOA	$CH_3COCH_2ONO_2$	nitrooxyacetone (propanone nitrate)
O1D	O	excited state atomic oxygen
O3	O_3	ozone
O	O	ground state atomic oxygen
OCLO	OClO	chlorine dioxide
OCS	OCS	carbonyl sulfide (LBC)
OH	OH	hydroxyl radical
ONITR	$C_4H_7NO_4$	lumped hydroxynitrates
PAN	$CH_3CO_3NO_2$	peroxy acetyl nitrate
PBZNIT	$C_7H_5NO_5$	peroxy benzoyl nitrate
PHENO2	$C_6H_7O_6$	bicyclic peroxy radical from phenol
PHENO	C_6H_5O	phenoxy radical

Table S2: MOZART-TS2 chemical Species

Species name	Chemical Formula	Description
PHENOL	C_6H_5OH	phenol, product of benzene chemistry
PHENOOH	$C_6H_8O_6$	bicyclic hydroperoxide from phenol
PO2	$C_3H_6(OH)O_2$	propene-derived peroxy radical
POOH	$C_3H_6(OH)OOH$	propene-derived hydroxy hydroperoxide
RO2	$CH_3COCH_2O_2$	peroxy radical from acetone
ROOH	CH_3COCH_2OOH	acetone hydroperoxide
S	S	sulfur radical
SF6	SF_6	sulfur hexafluoride (LBC)
SO2	SO_2	sulfur dioxide
SO3	SO_3	sulfur trioxide
SO	SO	sulfur monoxide
SOAG0	$C_{15}H_{38}O_2$	SOA gas-phase precursor VBS bin 0
SOAG1	$C_{15}H_{38}O_2$	SOA gas-phase precursor VBS bin 1
SOAG2	$C_{15}H_{38}O_2$	SOA gas-phase precursor VBS bin 2
SOAG3	$C_{15}H_{38}O_2$	SOA gas-phase precursor VBS bin 3
SOAG4	$C_{15}H_{38}O_2$	SOA gas-phase precursor VBS bin 4
SQTN	$C_{15}H_{25}NO_4$	nitrate from sesquiterpene oxidation
ST80_25	CO	stratospheric loss tracer
SVOC	$C_{22}H_{46}$	semi-volatile organic precursor of VBS SOA
TEPOMUC	$C_7H_8O_3$	toluene, xylenes product
TERP1OOH	$C_{10}H_{18}O_3$	terpene-derived hydroxy hydroperoxide with 1 double bond
TERP1OOHO2	$C_{10}H_{19}O_6$	peroxy radical from OH + TERP1OOH
TERP2AOOH	$C_{10}H_{18}O_3$	terpene-derived hydroxy hydroperoxide with 2 double bonds
TERP2OOHO2	$C_{10}H_{19}O_6$	peroxy radical from OH + TERP2AOOH
TERPA1O2	$C_9H_{15}O_3$	TERPA peroxy radical 1st step
TERPA2	$C_9H_{14}O_2$	TERPA oxidation product with no double bonds that contains an aldehydic group
TERPA2CO3	$C_9H_{13}O_4$	acyl peroxy radical from TERPA2
TERPA2O2	$C_9H_{15}O_4$	TERPA peroxy radical 2nd step
TERPA2PAN	$C_9H_{13}NO_6$	PAN from TERPA2
TERPA3	$C_9H_{14}O_3$	aldehyde terpene product with no ring like limonaldehyde
TERPA3CO3	$C_9H_{13}O_5$	acyl peroxy radical from TERPA3
TERPA3O2	$C_9H_{15}O_5$	TERPA peroxy radical 3rd step
TERPA3PAN	$C_9H_{13}NO_7$	PAN from TERPA3
TERPA4O2	$C_6H_9O_5$	TERPA peroxy radical 4th step

Table S2: MOZART-TS2 chemical Species

Species name	Chemical Formula	Description
TERPA	$C_{10}H_{16}O_2$	aldehyde terpene product with no double bonds that contains a ring like pinonaldehyde
TERPACID2	$C_9H_{14}O_4$	carboxylic acid/peracid from TERPA2
TERPACID3	$C_9H_{14}O_5$	carboxylic acid/peracid from TERPA3
TERPACID	$C_{10}H_{16}O_4$	carboxylic acid/peracid from TERPA
TERPACO3	$C_{10}H_{15}O_4$	TERPA acyl peroxy radical
TERPAPAN	$C_{10}H_{15}NO_6$	PAN from TERPA
TERPDHDP	$C_{10}H_{20}O_6$	terpene oxidation product, dihydroxy dihydroperoxy
TERPF1	$C_{10}H_{16}O_2$	functionalized terpene product with 1 double bond typically containing carbonyl groups
TERPF1O2	$C_{10}H_{17}O_5$	peroxy radical from OH + TERPF1
TERPF2	$C_7H_{10}O$	functionalized terpene product with 2 double bonds typically containing carbonyl groups
TERPF2O2	$C_7H_{11}O_4$	peroxy radical from OH + TERPF2
TERPFDN	$C_{10}H_{18}N_2O_8$	terpene highly functionalized organic dinitrate
TERPHFN	$C_{10}H_{19}NO_7$	terpene highly functionalized nitrate
TERPK	$C_9H_{14}O$	terpene product containing a ketone group
TERPNPS1	$C_{10}H_{17}NO_5$	terpene-derived unsaturated secondary or primary hydroperoxy nitrate
TERPNPS1O2	$C_{10}H_{18}NO_8$	peroxy radical from OH + TERPNPS1
TERPNPS	$C_{10}H_{17}NO_5$	terpene-derived saturated secondary or primary hydroperoxy nitrate
TERPNPT1	$C_{10}H_{17}NO_5$	terpene-derived unsaturated tertiary hydroperoxy nitrate
TERPNPT1O2	$C_{10}H_{18}NO_8$	peroxy radical from OH + TERPNPT1
TERPNPT	$C_{10}H_{17}NO_5$	terpene-derived saturated tertiary hydroperoxy nitrate
TERPNS1	$C_{10}H_{17}NO_4$	terpene-derived unsaturated secondary or primary nitrate
TERPNS1O2	$C_{10}H_{18}NO_7$	peroxy radical from OH + TERPNS1
TERPNS	$C_{10}H_{17}NO_4$	terpene-derived saturated secondary or primary nitrate
TERPNT1	$C_{10}H_{17}NO_4$	terpene-derived unsaturated tertiary nitrate
TERPNT1O2	$C_{10}H_{18}NO_7$	peroxy radical from OH + TERPNT1
TERPNT	$C_{10}H_{17}NO_4$	terpene-derived saturated tertiary nitrate
TERPOOH	$C_{10}H_{18}O_3$	terpene-derived saturated hydroperoxide with ring
TERPOOHL	$C_{10}H_{18}O_5$	terpene-derived saturated hydroperoxide with no ring
TOLO2	$C_7H_9O_5$	bicyclic peroxy radical from toluene
TOLOOH	$C_7H_{10}O_5$	bicyclic hydroperoxide from toluene
TOLUENE	C_7H_8	toluene

Table S2: MOZART-TS2 chemical Species

Species name	Chemical Formula	Description
XYLENES	C_8H_{10}	lumped xylenes
XYLENO2	$C_8H_{11}O_5$	bicyclic peroxy radical from OH + XYLENES
XYLENOOH	$C_8H_{12}O_5$	bicyclic hydroperoxide from OH+ XYLENES
XYLOL	$C_8H_{10}O$	dimethyl phenol from xylenes oxidation
XYLOLO2	$C_8H_{11}O_6$	bicyclic peroxy radical from OH + XYLOL
XYLOLOOH	$C_8H_{12}O_6$	bicyclic hydroperoxide from OH+XYLOL
bc_a1	C	black carbon, MAM accumulation mode
bc_a4	C	black carbon, MAM primary carbon mode
dst_a1	$AlSiO_5$	dust, MAM accumulation mode
dst_a2	$AlSiO_5$	dust, MAM Aitken mode
dst_a3	$AlSiO_5$	dust, MAM coarse mode
ncl_a1	NaCl	sea salt, MAM accumulation mode
ncl_a2	NaCl	sea salt, MAM Aitken mode
ncl_a3	NaCl	sea salt, MAM coarse mode
num_a1	H	aerosol number concentration, MAM accumulation mode
num_a2	H	aerosol number concentration, MAM Aitken mode
num_a3	H	aerosol number concentration, MAM coarse mode
num_a4	H	aerosol number concentration, MAM primary carbon mode
pom_a1	C	primary organic matter, MAM accumulation mode
pom_a4	C	primary organic matter, MAM primary carbon mode
so4_a1	NH_4HSO_4	sulfate aerosol, MAM accumulation mode
so4_a2	NH_4HSO_4	sulfate aerosol, MAM Aitken mode
so4_a3	NH_4HSO_4	sulfate aerosol, MAM coarse mode
soa1_a1	$C_{15}H_{38}O_2$	SOA bin 1, MAM accumulation mode
soa1_a2	$C_{15}H_{38}O_2$	SOA bin 1, MAM Aitken mode
soa2_a1	$C_{15}H_{38}O_2$	SOA bin 2, MAM accumulation mode
soa2_a2	$C_{15}H_{38}O_2$	SOA bin 2, MAM Aitken mode
soa3_a1	$C_{15}H_{38}O_2$	SOA bin 3, MAM accumulation mode
soa3_a2	$C_{15}H_{38}O_2$	SOA bin 3, MAM Aitken mode
soa4_a1	$C_{15}H_{38}O_2$	SOA bin 4, MAM accumulation mode
soa4_a2	$C_{15}H_{38}O_2$	SOA bin 4, MAM Aitken mode
soa5_a1	$C_{15}H_{38}O_2$	SOA bin 5, MAM accumulation mode
soa5_a2	$C_{15}H_{38}O_2$	SOA bin 5, MAM Aitken mode

Compounds with the species name in **bold** are new compounds added to the MOZART-TS2 chemical mechanism. Non-bolded compounds are unchanged from the MOZART-TS1 chemical mechanism Emmons et al. (2020))

Table S2: MOZART-TS2 chemical Species

Species name	Chemical Formula	Description

LBC = lower boundary conditions are specified for this species.

Table S3: Biogenic VOCs from MEGAN assignments to MOZART-TS1 and MOZART-TS2 surrogate species

TS1 Surrogate Species	**TS2 Surrogate Species**	**Biogenic VOC**
ISOP	ISOP	isoprene
MTERP	APIN	α-pinene, **myrtenal**
MTERP	BPIN	3-carene, α-thujene, bornene, α-fenchene, β-pinene, sabinene, camphene, **4-terpineol**, **α-terpineol**, **α-terpinyl acetate**
MTERP	LIMON	terpinolene, limonene, α-phellandrene, γ-terpinene, α-terpinene, β-phellandrene, **linalool**, **β-ionone**, **geranyl acetone**, **neryl acetone**, **jasmone**, **verbenene**, **ipsenol**
MTERP	MYRC	allo-ocimene, myrcene, *t*-β-ocimene, *c*-β-ocimene, **dimethyl-nonatriene**
BCARY	BCARY	**α-farnescene**, β-caryophyllene, **acoradiene**, **aromadendrene**, α-bergamotene, **β-bergamotene**, **α-bisabolene**, β-bisabolene, **β-bourbonene**, **δ-cadinene**, **γ-cadinene**, **α-cedrene**, **α-copaene**, **α-cubebene**, **β-cubebene**, **β-elemene**, β-farnescene, **germacrene B**, **germacrene D**, **β-gurjunene**, α-humulene, **γ-humulene**, **isolongifolene**, **longifolene**, **longipinene**, **α-muurolene**, **γ-muurolene**, **β-selinene**, **δ-selinene**, ***c*-nerolidol**, ***t*-nerolidol**
BIGALK	BIGALK	tricyclene, **camphor**, **fenchone**, **α-thujone**, **β-thujone**, **1,8-cineole**, **borneol**, **bornyl acetate**, **cedrol**, **decanal**, **heptanal**, heptane, hexane, **nonanal**, **octanal**, **octanol**, **oxopentanal**, pentane, **hexanal**, **1-hexanol**, **pentanal**, **heptanone**
BIGENE	BIGENE	dimethyl styrene, **estragole**, **piperitone**, ***c*-linalool oxide**, ***t*-linalool oxide**, **1-dodecene**, **methyl heptenone**, **nonenal**, **1,3-octenol**, **1-tetradecene**, butene, **di-allyl disulfide**, **methyl propenyl disulfide**, **methyl jasmonate**, ***c*-3-hexenal**, ***t*-2-hexenal**, ***c*-3-hexenol**, ***c*-3-hexenyl acetate**
TOLUENE	TOLUENE	toluene, **methyl benzoate**, **phenylacetaldehyde**, **methyl salicylate**, **indole**, **anisole**, **benzyl acetate**, **benzyl alcohol**, **napthalene**
N/A	XYLENES	*p*-cymene, *o*-cymene, **homosalate**, ***m*-cymenene**
CH3OH	CH3OH	methanol
CH3COCH3	CH3COCH3	acetone
CH3CHO	CH3CHO	acetaldehyde
C2H5OH	C2H5OH	ethanol
HCOOH	HCOOH	formic acid
CH2O	CH2O	formaldehyde
CH3COOH	CH3COOH	acetic acid
N/A	BZALD	**benzaldehyde**
N/A	MEK	**2-butanone**

Table S3: Biogenic VOCs from MEGAN assignments to MOZART-TS1 and MOZART-TS2 surrogate species

TS1 Surrogate Species	**TS2 Surrogate Species**	**Biogenic VOC**
CO	CO	carbon monoxide
C2H6	C2H6	ethane
C2H4	C2H4	ethene
HCN	HCN	hydrogen cyanide
C3H8	C3H8	propane
C3H6	C3H6	propene

Compounds in **bold** are not included in the default version of CESM 2.1. N/A = not applicable.

Compounds underlined are moved from MTERP (default) to BIGALK or XYLENES

Table S4: Effective Henry's law constants and reactivity factors for all species

Species	KH_{298} ($M\ atm^{-1}$)	dH/R (K)	$K1_{298}$	dH1/R (K)	$K2_{298}$	dH2/R (K)	F_0	Sources
MOZART-TS1 Species								
ALKNIT	1.01	5790	0	0	0	0	1	JPL(2015)
ALKOOH	3.36E+02	5995	0	0	0	0	1	S:C2H5OOH
BCARY	5.57E-03	2800	0	0	0	0	1E-36	S:C3H6
BENZENE	1.8E-01	3800	0	0	0	0	1E-36	Sander(2015), Hiatt(2013)
BENZOOH	2.3E+03	5995	0	0	0	0	1	T
BEPOMUC	3.0E+07	6014	0	0	0	0	1	S:IEPOX
BIGALD	9.6	6220	0	0	0	0	1	JPL(2015)
BIGALD1	1.0E+05	5890	0	0	0	0	1	T
BIGALD2	2.9E+04	5890	0	0	0	0	1	T
BIGALD3	2.2E+04	5890	0	0	0	0	1	T
BIGALD4	2.2E+04	5890	0	0	0	0	1	T
BIGALK	1.24E-03	3010	0	0	0	0	1E-36	JPL(2015)
BIGENE	5.96E-03	2365	0	0	0	0	1E-36	S:C2H4
BZALD	3.24E+01	6300	0	0	0	0	1	Sander(2015), Allou(2011)
BZOOH	3.36E+02	5995	0	0	0	0	1	S:C2H5OOH
C2H2	4.14E-02	1890	0	0	0	0	1E-36	JPL(2015)
C2H4	5.96E-03	2200	0	0	0	0	1E-36	JPL(2015)
C2H5OH	1.90E+02	6500	0	0	0	0	1	JPL(2015)
C2H5OOH	3.36E+02	5995	0	0	0	0	1	JPL(2015)
C2H6	1.88E-03	2750	0	0	0	0	1E-36	JPL(2015)
C3H6	5.57E-03	2800	0	0	0	0	1E-36	Sander(2015), Reichl(1995)
C3H7OOH	3.36E+02	5995	0	0	0	0	1	S:C2H5OOH
C3H8	1.51E-03	3120	0	0	0	0	1E-36	JPL(2015)
C6H5OOH	3.36E+02	5995	0	0	0	0	1	S:C2H5OOH
CH2O	3.23E+03	7100	0	0	0	0	1	JPL(2015)
CH3CHO	1.29E+01	5890	0	0	0	0	1	JPL(2015)
CH3CN	5.28e+01	3970	0	0	0	0	1E-36	JPL(2015)
CH3COCH3	2.78E+01	5530	0	0	0	0	1	JPL(2015)
CH3COCHO	3.50E+03	7545	0	0	0	0	1	JPL(2015)
CH3COOH	4.1E+03	6200	0	0	0	0	1	JPL(2015)

Table S4: Effective Henry's law constants and reactivity factors for all species

Species	**KH_{298}** ($M\ atm^{-1}$)	**dH/R** (K)	**$K1_{298}$**	**dH1/R** (K)	**$K2_{298}$**	**dH2/R** (K)	**F_0**	**Sources**
CH3COOOH	8.37E+02	5310	1.8E-04	-20	0	0	1	JPL(2015), S:HCOOH
CH3OH	2.03E+02	5645	0	0	0	0	1	JPL(2015)
CH3OOH	3.00E+02	5280	0	0	0	0	1	JPL(2015)
CO	9.81E-04	1650	0	0	0	0	1E-36	JPL(2015)
CRESOL	5.67E+02	5800	0	0	0	0	1	Sander(2015), Dohnal(1995)
DMS	5.4E-01	3460	0	0	0	0	1E-36	JPL(2015)
EOOH	1.9E+06	6014	0	0	0	0	1	T
GLYALD	4.00E+04	4630	0	0	0	0	1	JPL(2015)
GLYOXAL	4.19e+05	7480	0	0	0	0	1	JPL(2015)
H2O2	8.70E+04	7320	2.2e-12	-3730	0	0	1	JPL(2015)
H2SO4	1.0E+11	6014	0	0	0	0	1E-36	Note A
HCN	9.02	8258	0	0	0	0	1E-36	JPL(2015)
HCOOH	8.90E+03	6100	1.8E-04	-20	0	0	1	JPL(2015), Chameides(1984)
HNO3	2.10E+05	8700	2.2e+01	0	0	0	1E-36	Schwartz(1981)
HO2NO2	4.00E+01	8400	1.3E-06	0	0	0	0.1	Sander(2015), Leu(1999), Goldstein(1997)
HONITR	2.64E+03	6014	0	0	0	0	1	T
HPALD	2.30E+05	6014	0	0	0	0	1	T
HYAC	1.46E+03	6014	0	0	0	0	1	T
HYDRALD	1.10E+05	6000	0	0	0	0	1	T
IEPOX	3.0E+07	6014	0	0	0	0	1	Sander(2015), Chan(2010)
ISOP	3.45E-02	4400	0	0	0	0	1E-36	Sander(2015), Leng(2013)
ISOPNITA	8.34E+03	6014	0	0	0	0	1	T
ISOPNITB	4.82E+04	6014	0	0	0	0	1	T
ISOPNOOH	8.75E+04	6014	0	0	0	0	1	T
ISOPOOH	3.5E+06	5995	0	0	0	0	1	T
MACR	6.50	6014	0	0	0	0	1	JPL(2015)
MACROOH	4.4E+06	6014	0	0	0	0	1	T

Table S4: Effective Henry's law constants and reactivity factors for all species

Species	**KH_{298}** ($M\ atm^{-1}$)	**dH/R** (K)	**$K1_{298}$**	**dH1/R** (K)	**$K2_{298}$**	**dH2/R** (K)	**F_0**	**Sources**
MEK	1.80E+01	5740	0	0	0	0	1	JPL(2015)
MEKOOH	6.4E+04	6014	0	0	0	0	1	T
MPAN	1.72	5700	0	0	0	0	1	Sander(2015), Kames(1995)
MTERP	2.94E-02	1800	0	0	0	0	1E-36	S: APIN
MVK	4.10E+01	6014	0	0	0	0	1	JPL(2015)
N2O5	2.14	3362	0	0	0	0	0.1	Sander(2015), Fried(1994)
NC4CH2OH	4.02E+04	9500	0	0	0	0	1	T
NC4CHO	1.46E+03	6014	0	0	0	0	1	T
NH3	6.02E+01	4160	1.7E-05	-4325	1.0E-14	-6716	1E-36	JPL(2015), Chameides(1984)
NO	1.92E-03	1762	0	0	0	0	0	JPL(2015)
NO2	1.20E-02	2440	0	0	0	0	0.1	JPL(2015)
NOA	1.0E+03	6014	0	0	0	0	1	JPL(2015)
NTERPOOH	6.67E+04	6014	0	0	0	0	1	T
O3	1.03E-02	2830	0	0	0	0	1	JPL(2015)
ONITR	1.44E+03	6014	0	0	0	0	1	T
PAN	2.80E+00	5730	0	0	0	0	0.1	JPL(2015)
PBZNIT	2.8	5730	0	0	0	0	1	S: PAN
PHENOL	2.84E+03	2700	0	0	0	0	1	Sander(2015), Guo(2007)
PHENOOH	1.5E+06	5995	0	0	0	0	1	T
POOH	1.50E+06	6014	0	0	0	0	1	T
ROOH	3.36E+02	5995	0	0	0	0	1	S: C2H5OOH
SO2	1.36	3100	1.30E-02	1960	6.6E-08	1500	1E-36	JPL(2015), Smith(1976)
TEPOMUC	2.5E+05	6014	0	0	0	0	1	Sander(2015), McNeil(2012)
TERP2OOH	3.36E+02	5995	0	0	0	0	1	S: C2H5OOH
TERPNIT	8.41E+03	6014	0	0	0	0	1	T
TERPOOH	1.9E+06	5995	0	0	0	0	1	Note B
TERPROD1	3.92E+04	6014	0	0	0	0	1	T
TERPROD2	7.20E+04	6014	0	0	0	0	1	T

Table S4: Effective Henry's law constants and reactivity factors for all species

Species	**KH_{298}** ($M\ atm^{-1}$)	**dH/R** (K)	**$K1_{298}$**	**dH1/R** (K)	**$K2_{298}$**	**dH2/R** (K)	**F_0**	**Sources**
TOLOOH	2.30E+04	5995	0	0	0	0	1	T
TOLUENE	1.5E-01	4300	0	0	0	0	1E-36	Sander(2015), Staudinger(2001)
XOOH	1.0E+11	5995	0	0	0	0	1	Note C
XYLENES	2.0E-01	4300	0	0	0	0	1E-36	Sander(2015), Sieg(2009)
XYLENOOH	3.36E+02	5995	0	0	0	0	1	S: C2H5OOH
XYLOL	1.01E+03	6800	0	0	0	0	1	Sander(2015), Dohnal(1995)
XYLOLOOH	1.9E+06	5995	0	0	0	0	1	Note B
New MOZART-TS2 Species								
APIN	2.94E-02	1800	0	0	0	0	1E-36	Sander(2015), Leng(2013)
BPIN	1.52E-02	4500	0	0	0	0	1E-36	Sander(2015), Copolovici(2005)
DHPMPAL	9.37E+07	6014	0	0	0	0	1	T
HCOCH2OOH	2.99E+04	6014	0	0	0	0	1	T
HMHP	1.70E+06	9870	0	0	0	0	1	T
HPALD1	2.30E+05	6014	0	0	0	0	1	T
HPALD4	2.30E+05	6014	0	0	0	0	1	T
HPALDB1C	5.43E+04	6014	0	0	0	0	1	T
HPALDB4C	5.43E+04	6014	0	0	0	0	1	T
HYPERACET	1.16E+04	6014	0	0	0	0	1	T
ICHE	2.09E+06	6014	0	0	0	0	1	T
INHEB	1.05E+05	6014	0	0	0	0	1	T
INHED	1.51E+05	6014	0	0	0	0	1	T
ISOPFDN	5.02E+08	6014	0	0	0	0	1	T
ISOPFDNC	7.16E+09	6014	0	0	0	0	1	T
ISOPFNC	1.41E+11	6014	0	0	0	0	1	T
ISOPFNP	2.97E+11	6014	0	0	0	0	1	T
ISOPHFP	7.60E+09	6014	0	0	0	0	1	T
ISOPN1D	4.82E+04	6014	0	0	0	0	1	T
ISOPN2B	8.34E+03	6014	0	0	0	0	1	T
ISOPN3B	8.34E+03	6014	0	0	0	0	1	T

Table S4: Effective Henry's law constants and reactivity factors for all species

Species	**KH_{298}** ($M\ atm^{-1}$)	**dH/R** (K)	**$K1_{298}$**	**dH1/R** (K)	**$K2_{298}$**	**dH2/R** (K)	**F_0**	**Sources**
ISOPN4D	4.82E+04	6014	0	0	0	0	1	T
ISOPNBNO3	8.34E+03	6014	0	0	0	0	1	T
ISOPNOOHB	6.61E+04	6014	0	0	0	0	1	T
ISOPNOOHD	9.67E+04	6014	0	0	0	0	1	T
ISOPOH	8.77E+06	6014	0	0	0	0	1	T
LIMON	4.86E-02	4600	0	0	0	0	1E-36	Sander(2015), Leng(2013)
MACRN	4.14E+06	6014	0	0	0	0	1	T
MVKN	1.84E+05	6014	0	0	0	0	1	T
MVKOOH	1.24E+06	6014	0	0	0	0	1	T
MYRC	7.30E-02	2800	0	0	0	0	1E-36	Sander(2015), van Roon(2005)
NO3CH2CHO	3.39E+04	6014	0	0	0	0	1	T
SQTN	9.04E+03	6014	0	0	0	0	1	T
TERPOOH	3.6E+06	6014	0	0	0	0	1	T
TERP1OOH	3.64E+06	6014	0	0	0	0	1	T
TERP2AOOH	3.67E+06	6014	0	0	0	0	1	T
TERPA	3.92E+04	6014	0	0	0	0	1	T
TERPA2	7.20E+04	6014	0	0	0	0	1	T
TERPA2PAN	9.59E+03	6014	0	0	0	0	1	T
TERPA3	1.04E+08	6014	0	0	0	0	1	T
TERPA3PAN	1.23E+07	6014	0	0	0	0	1	T
TERPACID	5.63E+06	6014	0	0	0	0	1	T
TERPACID2	2.64E+06	6014	0	0	0	0	1	T
TERPACID3	3.38E+09	6014	0	0	0	0	1	T
TERPAPAN	7.94E+03	6014	0	0	0	0	1	T
TERPDHDP	3.41E+14	6014	0	0	0	0	1	T
TERPF1	4.05E+04	6014	0	0	0	0	1	T
TERPF2	6.54E+01	6014	0	0	0	0	1	T
TERPFDN	1.65E+09	6014	0	0	0	0	1	T
TERPHFN	7.53E+11	6014	0	0	0	0	1	T
TERPK	6.39E+01	6014	0	0	0	0	1	T
TERPNPS	6.67E+04	6014	0	0	0	0	1	T
TERPNPS1	6.78E+04	6014	0	0	0	0	1	T

Table S4: Effective Henry's law constants and reactivity factors for all species

Species	**KH_{298}** (M atm^{-1})	**dH/R** (K)	**$K1_{298}$**	**dH1/R** (K)	**$K2_{298}$**	**dH2/R** (K)	**F_0**	**Sources**
TERPNPT	6.67E+04	6014	0	0	0	0	1	T
TERPNPT1	6.78E+04	6014	0	0	0	0	1	T
TERPNS	8.41E+03	6014	0	0	0	0	1	T
TERPNS1	8.55E+03	6014	0	0	0	0	1	T
TERPNT	8.41E+03	6014	0	0	0	0	1	T
TERPNT1	8.55E+03	6014	0	0	0	0	1	T
TERPOOHL	4.41E+12	6014	0	0	0	0	1	T

For acids: $H_{eff} = K_H \left(1 + \frac{K_1}{[H+]} \left(1 + \frac{K_2}{[H+]} \right) \right)$

For bases: $H_{eff} = K_H \left(1 + \frac{K_1}{K_2} [H+] \right)$

Where: $K_H = KH_{298} \exp\left(dH/R \left(\frac{1}{T} - \frac{1}{298} \right) \right)$, $K_1 = K1_{298} \exp\left(dH1/R \left(\frac{1}{T} - \frac{1}{298} \right) \right)$,

$K_2 = K2_{298} \exp\left(dH2/R \left(\frac{1}{T} - \frac{1}{298} \right) \right)$, and $[H+] = 10^{-pH}$

F_0 is the reactivity factor. S = surrogate. T = Theoretically estimated using GROMHE (Raventos-Duran et al., 2010).

Note A: Henry's law constant set high to ensure all H_2SO_4 is in water.

Note B: KH(C2H5OOH) * (KH(HMHP) / KH(MHP)).

Note C: Henry's law constant set high due to large number of multifunctional groups.

Table S5: MOZART-TS2 Photolysis Reactions

Reactant		Products	Rate
Odd Oxygen			
H2O + hν	$\rightarrow$	H2 + O1D	jh2o_b
H2O + hν	$\rightarrow$	OH + H	jh2o_a
H2O + hν	$\rightarrow$	2*H + O	jh2o_c
H2O2 + hν	$\rightarrow$	2*OH	jh2o2
O2 + hν	$\rightarrow$	O + O1D	jo2_a
O2 + hν	$\rightarrow$	2*O	jo2_b
O3 + hν	$\rightarrow$	O1D + O2	jo3_a
O3 + hν	$\rightarrow$	O + O2	jo3_b
Odd Nitrogen			
HNO3 + hν	$\rightarrow$	NO2 + OH	jhno3
HO2NO2 + hν	$\rightarrow$	OH + NO3	jho2no2_a
HO2NO2 + hν	$\rightarrow$	NO2 + HO2	jho2no2_b
N2O + hν	$\rightarrow$	O1D + N2	jn2o
N2O5 + hν	$\rightarrow$	NO2 + NO3	jn2o5_a
N2O5 + hν	$\rightarrow$	NO + O + NO3	jn2o5_b
NO + hν	$\rightarrow$	N + O	jno
NO2 + hν	$\rightarrow$	NO + O	jno2
NO3 + hν	$\rightarrow$	NO + O2	jno3_b
NO3 + hν	$\rightarrow$	NO2 + O	jno3_a
Organics			
ALKNIT + hν	$\rightarrow$	NO2 + 0.4*CH3CHO + 0.1*CH2O + 0.25*CH3COCH3 + HO2 + 0.8*MEK	jch3ooh
ALKOOH + hν	$\rightarrow$	0.4*CH3CHO + 0.1*CH2O + 0.25*CH3COCH3 + 0.9*HO2 + 0.8*MEK + OH	jch3ooh
BENZOOH + hν	$\rightarrow$	OH + GLYOXAL + 0.5*BIGALD1 + HO2	jch3ooh
BEPOMUC + hν	$\rightarrow$	BIGALD1 + 1.5*HO2 + 1.5*CO	0.10*jno2
BIGALD + hν	$\rightarrow$	0.45*CO + 0.13*GLYOXAL + 0.56*HO2 + 0.13*CH3CO3 + 0.18*CH3COCHO	0.2*jno2
BIGALD1 + hν	$\rightarrow$	0.6*MALO2 + HO2	0.14*jno2
BIGALD2 + hν	$\rightarrow$	0.6*HO2 + 0.6*DICARBO2	0.20*jno2
BIGALD3 + hν	$\rightarrow$	0.6*HO2 + 0.6*CO + 0.6*MDIALO2	0.20*jno2
BIGALD4 + hν	$\rightarrow$	HO2 + CO + CH3COCHO + CH3CO3	0.006*jno2
BZOOH + hν	$\rightarrow$	BZALD + OH + HO2	jch3ooh
C2H5OOH + hν	$\rightarrow$	CH3CHO + HO2 + OH	jch3ooh

Table S5: MOZART-TS2 Photolysis Reactions

Reactant		Products	Rate
C3H7OOH + hν	→	0.82*CH3COCH3 + OH + HO2	jch3ooh
C6H5OOH + hν	→	PHENO + OH	jch3ooh
CH2O + hν	→	CO + 2*H	jch2o_a
CH2O + hν	→	CO + H2	jch2o_b
CH3CHO + hν	→	CH3O2 + CO + HO2	jch3cho
CH3COCH3 + hν	→	CH3CO3 + CH3O2	jacet
CH3COCHO + hν	→	CH3CO3 + CO + HO2	jmgly
CH3COOOH + hν	→	CH3O2 + OH + CO2	0.28*jh2o2
CH3OOH + hν	→	CH2O + H + OH	jch3ooh
CH4 + hν	→	1.44*H2 + 0.18*CH2O + 0.18*O + 0.33*OH + 0.33*H + 0.44*CO2 + 0.38*CO + 0.05*H2O	jch4_b
CH4 + hν	→	H + CH3O2	jch4_a
CO2 + hν	→	CO + O	jco2
DHPMPAL + hν	→	**0.5*CH3COCHO + 1.5*OH + 0.5*CH2O + 0.5*HYPERACET + 0.5*HO2 + 0.5*CO**	**4.62*jch3ooh**
EOOH + hν	→	EO + OH	jch3ooh
GLYALD + hν	→	2*HO2 + CO + CH2O	jglyald
GLYOXAL + hν	→	2*CO + 2*HO2	jmgly
HCOCH2OOH + hν	→	**CH2O + HO2 + CO + OH**	**jch3ooh**
HMHP + hν	→	**2*OH + CH2O**	**0.75*jch3ooh**
HONITR + hν	→	NO2 + 0.67*HO2 + 0.33*CH3CHO + 0.33*CH2O + 0.33*CO + 0.33*GLYALD + 0.33*CH3CO3 + 0.17*HYAC + 0.17*CH3COCH3	jch2o_a
HPALD1 + hν	→	**0.62*HO2 + 1.32*CO + 0.68*CH3COCHO + 0.17*CO2 + 0.04*CH3O2 + 0.05*CH3CO3 + 1.11*OH + 0.23*MVKO2 + 0.41*HCOOH**	**110.0*jmacr_a**
HPALD4 + hν	→	**0.56*HO2 + 1.74*CO + 0.67*CH3COCHO + 0.28*CO2 + 0.07*CH3O2 + 0.07*CH3CO3 + 1.18*OH + 0.19*MACRO2**	**110.0*jmacr_a**
HPALDB1C + hν	→	**OH + MVK + CO + HO2**	**4.62*jch3ooh**
HPALDB4C + hν	→	**OH + HO2 + CO + MACR**	**4.62*jch3ooh**
HYAC + hν	→	CH3CO3 + HO2 + CH2O	jhyac
HYDRALD + hν	→	**3*OH + HO2 + CO + CO2 + CH3COCHO**	**jmacr_a**
HYDRALD + hν	→	**1.5*HO2 + 1.5*CO + 0.5*HYAC + 0.5*CH3CO3 + 0.5*GLYALD**	**jmacr_b**
HYPERACET + hν	→	**CH3CO3 + CH2O + OH**	**jacet**
HYPERACET + hν	→	**CH3CO3 + CH2O + OH**	**jch3ooh**
INHEB + hν	→	**NO2 + ICHE + HO2**	**jch3ooh**

Table S5: MOZART-TS2 Photolysis Reactions

Reactant		Products	Rate
INHED + hν	→	**NO2 + ICHE + HO2**	**jch3ooh**
ISOPFDN + hν	→	**HYAC + 2*NO2 + GLYALD**	**jch3ooh**
ISOPFDNC + hν	→	**2*NO2 + 0.5*CH3COCHO + 0.5*GLYALD + 0.5*HYAC + 0.5*GLYOXAL**	**10.0*jch2o_a**
ISOPFNC + hν	→	**OH + NO2 + 0.5*GLYALD + 0.5*CH3COCHO + 0.5*HYAC + 0.5*GLYOXAL**	**10.0*jch2o_a**
ISOPFNP + hν	→	**OH + NO2 + GLYALD + HYAC**	**jch3ooh**
ISOPHFP + hν	→	**OH + HO2 + 0.72*CH3COCHO + 0.72*GLYALD + 0.28*GLYOXAL + 0.28*HYAC**	**jch3ooh**
ISOPN1D + hν	→	**NO2 + 0.45*HYDRALD + 0.45*HO2 + 0.55*MACROOH + 0.55*CO + 0.55*OH**	**jch3ooh**
ISOPN2B + hν	→	**NO2 + MVK + CH2O + HO2**	**jch3ooh**
ISOPN3B + hν	→	**NO2 + MACR + CH2O + HO2**	**jch3ooh**
ISOPN4D + hν	→	**NO2 + 0.45*HYDRALD + 0.45*HO2 + 0.55*MVKOOH + 0.55*CO + 0.55*OH**	**jch3ooh**
ISOPNBNO3 + hν	→	**NO2 + HO2 + CH2O + 0.5*MVK + 0.5*MACR**	**jch3ooh**
ISOPNOOHB + hν	→	**OH + CH2O + NO2 + 0.88*MVK + 0.12*MACR**	**jch3ooh**
ISOPNOOHD + hν	→	**OH + HO2 + NC4CHO**	**jch3ooh**
ISOPOOH + hν	→	**0.7*MVK + 0.3*MACR + OH + CH2O + HO2**	jch3ooh
MACR + hν	→	**HO2 + CO + CH2O + 0.35*CH3CO3 + 0.65*CH3O2 + 0.65*CO**	jmacr_b
MACR + hν	→	**HO2 + MCO3**	jmacr_a
MACRN + hν	→	**0.75*CO + 0.75*NO2 + 0.5*HYAC + 1.25*HO2 + 0.25*CH3COCHO + 0.25*CH2O + 0.25*NOA**	**5.8*jch2o_a**
MACROOH + hν	→	**OH + HO2 + 0.86*HYAC + 0.86*CO + 0.14*CH2O + 0.14*CH3COCHO**	**jch3ooh**
MEK + hν	→	CH3CO3 + C2H5O2	jacet
MEKOOH + hν	→	OH + CH3CO3 + CH3CHO	jch3ooh
MPAN + hν	→	MCO3 + NO2	jpan
MVK + hν	→	0.7*C3H6 + 0.7*CO + 0.3*CH3O2 + 0.3*CH3CO3	jmvk
MVKN + hν	→	**0.75*NO2 + 0.25*NO3CH2CHO + 0.75*CH3CO3 + 0.5*GLYALD + 0.5*HO2 + 0.25*CH2O + 0.25*CH3COCHO**	**1.26*jch2o_a**
MVKOOH + hν	→	**OH + 0.56*GLYALD + 0.56*CH3CO3 + 0.44*CH2O + 0.44*HO2 + 0.44*CH3COCHO**	**jch3ooh**
NC4CHO + hν	→	**NO2 + HO2 + HYDRALD**	**9.2*jch2o_a**
NO3CH2CHO + hν	→	**NO2 + CH2O + CO + HO2**	**4.3*jch2o_a**

Table S5: MOZART-TS2 Photolysis Reactions

Reactant		Products	Rate
NOA + hν	→	NO2 + CH2O + CH3CO3	jch2o_a
ONITR + hν	→	NO2	jch3cho
PAN + hν	→	0.6*CH3CO3 + 0.6*NO2 + 0.4*CH3O2 + 0.4*NO3 + 0.4*CO2	jpan
PHENOOH + hν	→	OH + HO2 + 0.7*GLYOXAL	jch3ooh
POOH + hν	→	CH3CHO + CH2O + HO2 + OH	jch3ooh
ROOH + hν	→	CH3CO3 + CH2O + OH	jch3ooh
TEPOMUC + hν	→	0.5*CH3CO3 + HO2 + 1.5*CO	0.10*jno2
TERP1OOH + hν	→	**OH + TERPF1 + HO2**	**jch3ooh**
TERP2AOOH + hν	→	**OH + TERPF2 + HO2**	**jch3ooh**
TERPA + hν	→	**CO + HO2 + TERPA1O2**	**jch3cho**
TERPA2 + hν	→	**CO + HO2 + TERPA2O2**	**jch3cho**
TERPA2PAN + hν	→	**TERPA2CO3 + NO2**	**jpan**
TERPA3 + hν	→	**CO + HO2 + TERPA4O2**	**jch3cho**
TERPA3PAN + hν	→	**TERPA3CO3 + NO2**	**jpan**
TERPACID + hν	→	**OH + CO2 + TERPA1O2**	**0.71*jch3ooh**
TERPACID2 + hν	→	**OH + CO2 + TERPA2O2**	**0.71*jch3ooh**
TERPACID3 + hν	→	**OH + CO2 + TERPA4O2**	**0.71*jch3ooh**
TERPAPAN + hν	→	**TERPACO3 + NO2**	**jpan**
TERPDHDP + hν	→	**TERPOOH + OH + HO2**	**2.0*jch3ooh**
TERPFDN + hν	→	**TERPNS + HO2 + NO2**	**jch3ooh**
TERPHFN + hν	→	**TERPNS + OH + HO2**	**jch3ooh**
TERPNPS + hν	→	**OH + 0.5*TERPNS + 0.5*HO2 + 0.5*TERPA + 0.5*NO2**	**jch3ooh**
TERPNPS1 + hν	→	**OH + 0.54*TERPNS1 + 0.54*HO2 + 0.46*TERPF1 + 0.46*NO2**	**jch3ooh**
TERPNPT + hν	→	**TERPA + NO2 + OH**	**jch3ooh**
TERPNPT1 + hν	→	**OH + 0.54*TERPNT1 + 0.54*HO2 + 0.46*TERPF1 + 0.46*NO2**	**jch3ooh**
TERPNS + hν	→	**NO2 + HO2 + TERPA**	**jch3ooh**
TERPNS1 + hν	→	**NO2 + HO2 + TERPF1**	**jch3ooh**
TERPNT + hν	→	**NO2 + HO2 + TERPA**	**jch3ooh**
TERPNT1 + hν	→	**NO2 + HO2 + TERPF1**	**jch3ooh**
TERPOOH + hν	→	**OH + TERPA + HO2**	jch3ooh
TERPOOHL + hν	→	**OH + TERPA3 + HO2**	**jch3ooh**
TOLOOH + hν	→	OH + 0.6*GLYOXAL + 0.4*CH3COCHO + HO2 + 0.2*BIGALD1 + 0.2*BIGALD2 + 0.2*BIGALD3	jch3ooh
XYLENOOH + hν	→	OH + HO2 + 0.34*GLYOXAL + 0.54*CH3COCHO + 0.06*BIGALD1 + 0.2*BIGALD2 + 0.15*BIGALD3 + 0.21*BIGALD4	jch3ooh

Table S5: MOZART-TS2 Photolysis Reactions

Reactant		Products	Rate
XYLOLOOH + hν	$\rightarrow$	OH + 0.17*GLYOXAL + 0.51*CH3COCHO + HO2	jch3ooh
Halogens			
BRCL + hν	$\rightarrow$	BR + CL	jbrcl
BRO + hν	$\rightarrow$	BR + O	jbro
BRONO2 + hν	$\rightarrow$	BRO + NO2	jbrono2_b
BRONO2 + hν	$\rightarrow$	BR + NO3	jbrono2_a
CCL4 + hν	$\rightarrow$	4*CL	jccl4
CF2CLBR + hν	$\rightarrow$	BR + CL + COF2	jcf2clbr
CF3BR + hν	$\rightarrow$	BR + F + COF2	jcf3br
CFC11 + hν	$\rightarrow$	2*CL + COFCL	jcfcl3
CFC113 + hν	$\rightarrow$	2*CL + COFCL + COF2	jcfc113
CFC114 + hν	$\rightarrow$	2*CL + 2*COF2	jcfc114
CFC115 + hν	$\rightarrow$	CL + F + 2*COF2	jcfc115
CFC12 + hν	$\rightarrow$	2*CL + COF2	jcf2cl2
CH2BR2 + hν	$\rightarrow$	2*BR	jch2br2
CH3BR + hν	$\rightarrow$	BR + CH3O2	jch3br
CH3CCL3 + hν	$\rightarrow$	3*CL	jch3ccl3
CH3CL + hν	$\rightarrow$	CL + CH3O2	jch3cl
CHBR3 + hν	$\rightarrow$	3*BR	jchbr3
CL2 + hν	$\rightarrow$	2*CL	jcl2
CL2O2 + hν	$\rightarrow$	2*CL	jcl2o2
CLO + hν	$\rightarrow$	CL + O	jclo
CLONO2 + hν	$\rightarrow$	CL + NO3	jclono2_a
CLONO2 + hν	$\rightarrow$	CLO + NO2	jclono2_b
COF2 + hν	$\rightarrow$	2*F	jcof2
COFCL + hν	$\rightarrow$	F + CL	jcofcl
H2402 + hν	$\rightarrow$	2*BR + 2*COF2	jh2402
HBR + hν	$\rightarrow$	BR + H	jhbr
HCFC141B + hν	$\rightarrow$	CL + COFCL	jhcfc141b
HCFC142B + hν	$\rightarrow$	CL + COF2	jhcfc142b
HCFC22 + hν	$\rightarrow$	CL + COF2	jhcfc22
HCL + hν	$\rightarrow$	H + CL	jhcl
HF + hν	$\rightarrow$	H + F	jhf
HOBR + hν	$\rightarrow$	BR + OH	jhobr
HOCL + hν	$\rightarrow$	OH + CL	jhocl

Table S5: MOZART-TS2 Photolysis Reactions

Reactant		**Products**	**Rate**
OCLO + hν	$\rightarrow$	O + CLO	joclo
SF6 + hν	$\rightarrow$	sink	jsf6
Sulfur compounds			
H2SO4 + hν	$\rightarrow$	SO3 + H2O	jh2so4
OCS + hν	$\rightarrow$	S + CO	jocs
SO + hν	$\rightarrow$	S + O	jso
SO2 + hν	$\rightarrow$	SO + O	jso2
SO3 + hν	$\rightarrow$	SO2 + O	jso3
Secondary organic aerosol tracers			
soa1_a1 + hν	$\rightarrow$		0.0004*jno2
soa1_a2 + hν	$\rightarrow$		0.0004*jno2
soa2_a1 + hν	$\rightarrow$		0.0004*jno2
soa2_a2 + hν	$\rightarrow$		0.0004*jno2
soa3_a1 + hν	$\rightarrow$		0.0004*jno2
soa3_a2 + hν	$\rightarrow$		0.0004*jno2
soa4_a1 + hν	$\rightarrow$		0.0004*jno2
soa4_a2 + hν	$\rightarrow$		0.0004*jno2
soa5_a1 + hν	$\rightarrow$		0.0004*jno2
soa5_a2 + hν	$\rightarrow$		0.0004*jno2

Table S6: MOZART-TS2 Kinetic Reactions

Reactant		Products	Rate
Odd-Oxygen			
O1D + H2	→	H + OH	1.200e-10
O1D + H2O	→	2*OH	1.63e-10 exp(60.00 / t)
O1D + N2	→	O + N2	2.15e-11 exp(110.00 / t)
O1D + O2	→	O + O2	3.30e-11 exp(55.00 / t)
O1D + O3	→	O2 + O2	1.200e-10
O + O3	→	2*O2	8.00e-12 exp(-2060.00 / t)
O + O + M	→	O2 + M	2.76e-34 exp(720 / t)
O + O2 + M	→	O3 + M	6e-34 (300 / t)$^{2.4}$
Odd-Hydrogen			
H2 + O	→	OH + H	1.60e-11 exp(-4570.00 / t)
H2O2 + O	→	OH + HO2	1.40e-12 exp(-2000.00 / t)
H + HO2	→	H2 + O2	6.900e-12
H + HO2	→	2*OH	7.200e-11
H + HO2	→	H2O + O	1.600e-12
H + O2 + M	→	HO2 + M	TROEE(4.40e-32, 1.30, 7.500000e-11, -0.20, 0.60)
HO2 + O	→	OH + O2	3.00e-11 exp(200.00 / t)
HO2 + O3	→	OH + 2*O2	1.00e-14 exp(-490.00 / t)
H + O3	→	OH + O2	1.40e-10 exp(-470.00 / t)
OH + H2	→	H2O + H	2.80e-12 exp(-1800.00 / t)
OH + H2O2	→	H2O + HO2	1.800e-12
OH + HO2	→	H2O + O2	4.80e-11 exp(250.00 / t)
OH + O	→	H + O2	1.80e-11 exp(180.00 / t)
OH + O3	→	HO2 + O2	1.70e-12 exp(-940.00 / t)
OH + OH	→	H2O + O	1.800e-12
OH + OH + M	→	H2O2 + M	TROEE(6.90e-31, 1.00, 2.600000e-11, 0.00, 0.60)
HO2 + HO2	→	H2O2 + O2	(3.0e-13 exp(460 / t) + 2.1e-33 [M] exp(920 / t)) (1+1.4e-21[H2O] exp(2200 / t))
Odd-Nitrogen			
HO2NO2 + OH	→	H2O + NO2 + O2	1.30e-12 exp(380.00 / t)
N + NO	→	N2 + O	2.10e-11 exp(100.00 / t)
N + NO2	→	N2O + O	2.90e-12 exp(220.00 / t)

Table S6: MOZART-TS2 Kinetic Reactions

Reactant		Products	Rate
N + NO2	→	2*NO	1.45e-12 exp(220.00 / t)
N + NO2	→	N2 + O2	1.45e-12 exp(220.00 / t)
N + O2	→	NO + O	1.50e-11 exp(-3600.00 / t)
NO2 + O	→	NO + O2	5.10e-12 exp(210.00 / t)
NO2 + O3	→	NO3 + O2	1.20e-13 exp(-2450.00 / t)
NO2 + O + M	→	NO3 + M	TROEE(2.50e-31, 1.80, 2.200000e-11, 0.70, 0.60)
NO3 + HO2	→	OH + NO2 + O2	3.500e-12
NO3 + NO	→	2*NO2	1.50e-11 exp(170.00 / t)
NO3 + O	→	NO2 + O2	1.000e-11
NO3 + OH	→	HO2 + NO2	2.200e-11
N + OH	→	NO + H	5.000e-11
NO + HO2	→	NO2 + OH	3.30e-12 exp(270.00 / t)
NO + O3	→	NO2 + O2	3.00e-12 exp(-1500.00 / t)
NO + O + M	→	NO2 + M	TROEE(9.00e-32, 1.50, 3.000000e-11, 0.00, 0.60)
O1D + N2O	→	2*NO	7.26e-11 exp(20.00 / t)
O1D + N2O	→	N2 + O2	4.64e-11 exp(20.00 / t)
NO2 + HO2 + M	→	HO2NO2 + M	TROEE(1.90e-31, 3.40, 4.000000e-12, 0.30, 0.60)
NO2 + NO3 + M	→	N2O5 + M	TROEE(2.40e-30, 3.00, 1.600000e-12, -0.10, 0.60)
NO2 + OH + M	→	HNO3 + M	TROEE(1.80e-30, 3.00, 2.800000e-11, 0.00, 0.60)
HNO3 + OH	→	NO3 + H2O	k0 + k3[M] / (1+k3[M]/k2): k0 = 2.4e-14 exp(460 / t), k2 = 2.7e-17 exp(2199 / t), k3 = 6.5e-34 exp(1335 / t)
HO2NO2 + M	→	HO2 + NO2 + M	k(NO2+HO2+M) * exp(- 10900 / t) / 2.1e-27)
N2O5 + M	→	NO2 + NO3 + M	k(NO2+NO3) * 2.724138e26 exp(-10840 / t)
Odd-Chlorine			
CL + CH2O	→	HCL + HO2 + CO	8.10e-11 exp(-30.00 / t)
CL + CH4	→	CH3O2 + HCL	7.10e-12 exp(-1270.00 / t)

Table S6: MOZART-TS2 Kinetic Reactions

Reactant		Products	Rate
CL + H2	→	HCL + H	3.05e-11 exp(-2270.00 / t)
CL + H2O2	→	HCL + HO2	1.10e-11 exp(-980.00 / t)
CL + HO2	→	HCL + O2	1.40e-11 exp(270.00 / t)
CL + HO2	→	OH + CLO	3.60e-11 exp(-375.00 / t)
CL + O3	→	CLO + O2	2.30e-11 exp(-200.00 / t)
CLO + CH3O2	→	CL + HO2 + CH2O	3.30e-12 exp(-115.00 / t)
CLO + CLO	→	2*CL + O2	3.00e-11 exp(-2450.00 / t)
CLO + CLO	→	CL2 + O2	1.00e-12 exp(-1590.00 / t)
CLO + CLO	→	CL + OCLO	3.50e-13 exp(-1370.00 / t)
CLO + HO2	→	O2 + HOCL	2.60e-12 exp(290.00 / t)
CLO + NO	→	NO2 + CL	6.40e-12 exp(290.00 / t)
CLONO2 + CL	→	CL2 + NO3	6.50e-12 exp(135.00 / t)
CLO + NO2 + M	→	CLONO2 + M	TROEE(1.80e-31, 3.40, 1.500000e-11, 1.90, 0.60)
CLONO2 + O	→	CLO + NO3	3.60e-12 exp(-840.00 / t)
CLONO2 + OH	→	HOCL + NO3	1.20e-12 exp(-330.00 / t)
CLO + O	→	CL + O2	2.80e-11 exp(85.00 / t)
CLO + OH	→	CL + HO2	7.40e-12 exp(270.00 / t)
CLO + OH	→	HCL + O2	6.00e-13 exp(230.00 / t)
HCL + O	→	CL + OH	1.00e-11 exp(-3300.00 / t)
HCL + OH	→	H2O + CL	1.80e-12 exp(-250.00 / t)
HOCL + CL	→	HCL + CLO	3.40e-12 exp(-130.00 / t)
HOCL + O	→	CLO + OH	1.700e-13
HOCL + OH	→	H2O + CLO	3.00e-12 exp(-500.00 / t)
O1D + CCL4	→	4*CL	2.607e-10
O1D + CF2CLBR	→	CL + BR + COF2	9.750e-11
O1D + CFC11	→	2*CL + COFCL	2.070e-10
O1D + CFC113	→	2*CL + COFCL + COF2	2.088e-10
O1D + CFC114	→	2*CL + 2*COF2	1.170e-10
O1D + CFC115	→	CL + F + 2*COF2	4.644e-11
O1D + CFC12	→	2*CL + COF2	1.204e-10
O1D + HCL	→	CL + OH	9.900e-11
O1D + HCL	→	CLO + H	3.300e-12
CLO + CLO + M	→	CL2O2 + M	TROEE(1.90e-32, 3.60, 3.700000e-12, 1.60, 0.60)

Table S6: MOZART-TS2 Kinetic Reactions

Reactant		Products	Rate
CL2O2 + M	→	CLO + CLO + M	usr_CL2O2_M
Odd-Bromine			
BR + CH2O	→	HBR + HO2 + CO	1.70e-11 exp(-800.00 / t)
BR + HO2	→	HBR + O2	4.80e-12 exp(-310.00 / t)
BR + O3	→	BRO + O2	1.60e-11 exp(-780.00 / t)
BRO + BRO	→	2*BR + O2	1.50e-12 exp(230.00 / t)
BRO + CLO	→	BR + OCLO	9.50e-13 exp(550.00 / t)
BRO + CLO	→	BR + CL + O2	2.30e-12 exp(260.00 / t)
BRO + CLO	→	BRCL + O2	4.10e-13 exp(290.00 / t)
BRO + HO2	→	HOBR + O2	4.50e-12 exp(460.00 / t)
BRO + NO	→	BR + NO2	8.80e-12 exp(260.00 / t)
BRO + NO2 + M	→	BRONO2 + M	TROEE(5.20e-31, 3.20, 6.900000e-12, 2.90, 0.60)
BRONO2 + O	→	BRO + NO3	1.90e-11 exp(215.00 / t)
BRO + O	→	BR + O2	1.90e-11 exp(230.00 / t)
BRO + OH	→	BR + HO2	1.70e-11 exp(250.00 / t)
HBR + O	→	BR + OH	5.80e-12 exp(-1500.00 / t)
HBR + OH	→	BR + H2O	5.50e-12 exp(200.00 / t)
HOBR + O	→	BRO + OH	1.20e-10 exp(-430.00 / t)
O1D + CF3BR	→	BR + F + COF2	4.500e-11
O1D + CHBR3	→	3*BR	4.620e-10
O1D + H2402	→	2*BR + 2*COF2	1.200e-10
O1D + HBR	→	BR + OH	9.000e-11
O1D + HBR	→	BRO + H	3.000e-11
Odd-Fluorine			
F + CH4	→	HF + CH3O2	1.60e-10 exp(-260.00 / t)
F + H2	→	HF + H	1.40e-10 exp(-500.00 / t)
F + H2O	→	HF + OH	1.40e-11 exp(0.00 / t)
F + HNO3	→	HF + NO3	6.00e-12 exp(400.00 / t)
O1D + COF2	→	2*F	2.140e-11
O1D + COFCL	→	F + CL	1.900e-10
Organic Halogens			
CH2BR2 + CL	→	2*BR + HCL	6.30e-12 exp(-800.00 / t)
CH2BR2 + OH	→	2*BR + H2O	2.00e-12 exp(-840.00 / t)
CH3BR + CL	→	HCL + HO2 + BR	1.46e-11 exp(-1040.00 / t)

Table S6: MOZART-TS2 Kinetic Reactions

Reactant		**Products**	**Rate**
CH3BR + OH	→	BR + H2O + HO2	1.42e-12 exp(-1150.00 / t)
CH3CCL3 + OH	→	H2O + 3*CL	1.64e-12 exp(-1520.00 / t)
CH3CL + CL	→	HO2 + CO + 2*HCL	2.03e-11 exp(-1100.00 / t)
CH3CL + OH	→	CL + H2O + HO2	1.96e-12 exp(-1200.00 / t)
CHBR3 + CL	→	3*BR + HCL	4.85e-12 exp(-850.00 / t)
CHBR3 + OH	→	3*BR	9.00e-13 exp(-360.00 / t)
HCFC141B + OH	→	CL + COFCL	1.25e-12 exp(-1600.00 / t)
HCFC142B + OH	→	CL + COF2	1.30e-12 exp(-1770.00 / t)
HCFC22 + OH	→	H2O + CL + COF2	9.20e-13 exp(-1560.00 / t)
O1D + CH2BR2	→	2*BR	2.570e-10
O1D + CH3BR	→	BR	1.800e-10
O1D + HCFC141B	→	CL + COFCL	1.794e-10
O1D + HCFC142B	→	CL + COF2	1.300e-10
O1D + HCFC22	→	CL + COF2	7.650e-11
C1 Organics			
CH2O + HO2	→	HOCH2OO	9.70e-15 exp(625.00 / t)
CH2O + NO3	→	CO + HO2 + HNO3	6.00e-13 exp(-2058.00 / t)
CH2O + O	→	HO2 + OH + CO	3.40e-11 exp(-1600.00 / t)
CH2O + OH	→	CO + H2O + H	5.50e-12 exp(125.00 / t)
CH3O2 + CH3O2	→	2*CH2O + 2*HO2	5.00e-13 exp(-424.00 / t)
CH3O2 + CH3O2	→	CH2O + CH3OH	1.90e-14 exp(706.00 / t)
CH3O2 + HO2	→	CH3OOH + O2	4.10e-13 exp(750.00 / t)
CH3O2 + NO	→	CH2O + NO2 + HO2	2.80e-12 exp(300.00 / t)
CH3OH + OH	→	HO2 + CH2O	2.90e-12 exp(-345.00 / t)
CH3OOH + OH	→	0.7*CH3O2 + 0.3*OH + 0.3*CH2O + H2O	3.80e-12 exp(200.00 / t)
CH4 + OH	→	CH3O2 + H2O	2.45e-12 exp(-1775.00 / t)
CO + OH + M	→	CO2 + HO2 + M	TROEE(5.90e-33, 1.00, 1.100000e-12, -1.30, 0.60)
HCN + OH + M	→	HO2 + M	TROEE(4.28e-33, 0.00, 9.300000e-15, -4.42, 0.80)
HCOOH + OH	→	HO2 + CO2 + H2O	4.000e-13
HMHP + OH	→	**0.5*CH2O + 0.5*HO2 + 0.5*HCOOH + 0.5*OH + H2O**	**1.30e-12 exp(500.00 / t)**
HOCH2OO + HO2	→	**0.5*HMHP + 0.5*HCOOH + 0.3*H2O + 0.2*HO2 + 0.2*OH**	**5.60e-15 exp(2300.00 / t)**
HOCH2OO	→	CH2O + HO2	2.40e+12 exp(-7000.00 / t)

Table S6: MOZART-TS2 Kinetic Reactions

Reactant		Products	Rate
HOCH2OO + NO	→	HCOOH + NO2 + HO2	2.60e-12 exp(265.00 / t)
O1D + CH4	→	CH3O2 + OH	1.310e-10
O1D + CH4	→	CH2O + H + HO2	3.500e-11
O1D + CH4	→	CH2O + H2	9.000e-12
O1D + HCN	→	OH	1.08e-10 exp(105.00 / t)
CO + OH	→	CO2 + H	k0 = 1.5e-13 , ki = 2.1e9 (t / 300)$^{6.1}$, k = (k0/(1+k0/(ki/M))) * (0.6^(1/(1+(log(k0/(ki/M)))^2)))
C2 Organics			
C2H2 + CL + M	→	CL + M	TROEE(5.20e-30, 2.40, 2.200000e-10, 0.70, 0.60)
C2H2 + OH + M	→	0.65*GLYOXAL + 0.65*OH + 0.35*HCOOH + 0.35*HO2 + 0.35*CO + M	TROEE(5.50e-30, 0.00, 8.300000e-13, -2.00, 0.60)
C2H4 + CL + M	→	CL + M	TROEE(1.60e-29, 3.30, 3.100000e-10, 1.00, 0.60)
C2H4 + O3	→	0.63*CO + 0.13*OH + 0.13*HO2 + 0.37*HCOOH + CH2O	1.20e-14 exp(-2630.00 / t)
C2H5O2 + C2H5O2	→	1.6*CH3CHO + 1.2*HO2 + 0.4*C2H5OH	6.800e-14
C2H5O2 + CH3O2	→	0.7*CH2O + 0.8*CH3CHO + HO2 + 0.3*CH3OH + 0.2*C2H5OH	2.000e-13
C2H5O2 + HO2	→	C2H5OOH + O2	7.50e-13 exp(700.00 / t)
C2H5O2 + NO	→	CH3CHO + HO2 + NO2	2.60e-12 exp(365.00 / t)
C2H5OH + OH	→	HO2 + CH3CHO	6.90e-12 exp(-230.00 / t)
C2H5OOH + OH	→	0.5*C2H5O2 + 0.5*CH3CHO + 0.5*OH	3.80e-12 exp(200.00 / t)
C2H6 + CL	→	HCL + C2H5O2	7.20e-11 exp(-70.00 / t)
C2H6 + OH	→	C2H5O2 + H2O	7.66e-12 exp(-1020.00 / t)
CH3CHO + NO3	→	CH3CO3 + HNO3	1.40e-12 exp(-1900.00 / t)
CH3CHO + OH	→	CH3CO3 + H2O	4.63e-12 exp(350.00 / t)
CH3CN + OH	→	HO2	7.80e-13 exp(-1050.00 / t)
CH3CO3 + CH3CO3	→	2*CH3O2 + 2*CO2	2.90e-12 exp(500.00 / t)
CH3CO3 + CH3O2	→	0.9*CH3O2 + CH2O + 0.9*HO2 + 0.9*CO2 + 0.1*CH3COOH	2.00e-12 exp(500.00 / t)
CH3CO3 + HO2	→	**0.36*CH3COOOH + 0.15*CH3COOH + 0.15*O3 + 0.49*OH + 0.49*CH3O2 + 0.49*CO2**	4.30e-13 exp(1040.00 / t)
CH3CO3 + NO	→	CH3O2 + CO2 + NO2	8.10e-12 exp(270.00 / t)
CH3COOH + OH	→	CH3O2 + CO2 + H2O	7.000e-13

Table S6: MOZART-TS2 Kinetic Reactions

Reactant		Products	Rate
CH3COOOH + OH	→	0.5*CH3CO3 + 0.5*CH2O + 0.5*CO2 + H2O	1.000e-12
EO2 + HO2	→	EOOH	7.50e-13 exp(700.00 / t)
EO2 + NO	→	0.5*CH2O + 0.25*HO2 + 0.75*EO + NO2	4.20e-12 exp(180.00 / t)
EO	→	2*CH2O + HO2	1.60e+11 exp(-4150.00 / t)
EO + O2	→	GLYALD + HO2	1.000e-14
GLYALD + OH	→	HO2 + 0.2*GLYOXAL + 0.8*CH2O + 0.8*CO2	1.000e-11
GLYOXAL + OH	→	HO2 + CO + CO2	1.150e-11
HCOCH2OOH + OH	→	**0.89*GLYOXAL + 0.89*OH + 0.11*CH2O + 0.11*HO2 + 0.11*CO**	**3.300e-11**
NO3CH2CHO + OH	→	**CO2 + CH2O + NO2**	**3.400e-12**
PAN + OH	→	CH2O + NO3	4.000e-14
C2H4 + OH + M	→	EO2 + M	TROEE(8.60e-29, 3.10, 9.000000e-12, 0.85, 0.48)
CH3CO3 + NO2 + M	→	PAN + M	TROEE(9.70e-29, 5.60, 9.300000e-12, 1.50, 0.60)
PAN + M	→	CH3CO3 + NO2 + M	k(CH3CO3+NO2+M) * 1.111e28 exp(-14000 / t)
C3 Organics			
C3H6 + NO3	→	NOA	4.60e-13 exp(-1156.00 / t)
C3H6 + O3	→	0.5*CH2O + 0.12*HCOOH + 0.12*CH3COOH + 0.5*CH3CHO + 0.56*CO + 0.28*CH3O2 + 0.1*CH4 + 0.2*CO2 + 0.28*HO2 + 0.36*OH	6.50e-15 exp(-1900.00 / t)
C3H7O2 + CH3O2	→	CH2O + HO2 + 0.82*CH3COCH3	3.75e-13 exp(-40.00 / t)
C3H7O2 + HO2	→	C3H7OOH + O2	7.50e-13 exp(700.00 / t)
C3H7O2 + NO	→	0.82*CH3COCH3 + NO2 + HO2 + 0.27*CH3CHO	4.20e-12 exp(180.00 / t)
C3H7OOH + OH	→	H2O + C3H7O2	3.80e-12 exp(200.00 / t)
C3H8 + OH	→	C3H7O2 + H2O	8.70e-12 exp(-615.00 / t)
CH3COCHO + NO3	→	HNO3 + CO + CH3CO3	1.40e-12 exp(-1860.00 / t)
CH3COCHO + OH	→	CH3CO3 + CO + H2O	8.40e-13 exp(830.00 / t)
HYAC + OH	→	CH3COCHO + HO2	3.000e-12
HYPERACET + OH	→	**0.3*CH3CO3 + 0.3*CH2O + 0.7*CH3COCHO + 0.7*OH**	**1.200e-11**
NOA + OH	→	NO2 + CH3COCHO	6.700e-13
PO2 + HO2	→	POOH + O2	7.50e-13 exp(700.00 / t)
PO2 + NO	→	CH3CHO + CH2O + HO2 + NO2	4.20e-12 exp(180.00 / t)

Table S6: MOZART-TS2 Kinetic Reactions

Reactant		Products	Rate
POOH + OH	→	0.5*PO2 + 0.5*OH + 0.5*HYAC + H2O	3.80e-12 exp(200.00 / t)
RO2 + CH3O2	→	0.3*CH3CO3 + 0.8*CH2O + 0.3*HO2 + 0.2*HYAC + 0.5*CH3COCHO + 0.5*CH3OH	7.10e-13 exp(500.00 / t)
RO2 + HO2	→	0.85*ROOH + 0.15*OH + 0.15*CH2O + 0.15*CH3CO3	8.60e-13 exp(700.00 / t)
RO2 + NO	→	CH3CO3 + CH2O + NO2	2.90e-12 exp(300.00 / t)
ROOH + OH	→	RO2 + H2O	3.80e-12 exp(200.00 / t)
C3H6 + OH + M	→	PO2 + M	TROEE(8.00e-27, 3.50, 3.000000e-11, 0.00, 0.50)
CH3COCH3 + OH	→	RO2 + H2O	3.82e-11 exp(-2000 / t) + 1.33e-13
C4 Organics			
BIGENE + NO3	→	NO2 + CH3CHO + 0.5*CH2O + 0.5*CH3COCH3	3.500e-13
BIGENE + OH	→	ENEO2	5.400e-11
DHPMPAL + OH	→	**HYPERACET + CO + OH**	**3.770e-11**
ENEO2 + NO	→	CH3CHO + 0.5*CH2O + 0.5*CH3COCH3 + HO2 + NO2	4.80e-12 exp(120.00 / t)
ENEO2 + NO	→	HONITR	5.10e-14 exp(693.00 / t)
HONITR + OH	→	ONITR + HO2	2.000e-12
MACRN + OH	→	**CO + 0.5*HO2 + 0.5*NOA + 0.5*NO2 + 0.5*HYAC**	**1.290e-11**
MACRO2 + CH3CO3	→	**HO2 + 0.86*HYAC + 0.86*CO + 0.14*CH2O + 0.14*CH3COCHO + CO2 + CH3O2**	**2.00e-12 exp(500.00 / t)**
MACRO2 + CH3O2	→	**0.9*HYAC + 0.9*CO + 1.5*HO2 + 0.1*CH3COCH3 + 1.1*CH2O**	**4.500e-14**
MACRO2 + HO2	→	**0.41*MACROOH + 0.59*OH + 0.59*HO2 + 0.51*HYAC + 0.51*CO + 0.08*CH3COCHO + 0.08*CH2O**	**2.11e-13 exp(1300.00 / t)**
MACRO2	→	**HYAC + CO + OH**	**2.90e+7 exp(-5297.00 / t)**
MACR + O3	→	0.12*CH2O + 0.24*OH + 0.65*CO + 0.1*CH3CO3 + 0.88*CH3COCHO + 0.33*HCOOH + 0.14*HO2	1.50e-15 exp(-2100.00 / t)
MACR + OH	→	**0.55*MACRO2 + 0.45*H2O + 0.45*MCO3**	9.60e-12 exp(360.00 / t)
MACROOH + OH	→	**HYAC + CO + OH**	**3.770e-11**
MCO3 + CH3CO3	→	**2*CO2 + 0.35*CH3CO3 + CH2O + 1.65*CH3O2 + 0.65*CO**	**2.90e-12 exp(500.00 / t)**
MCO3 + CH3O2	→	**CO2 + 0.35*CH3CO3 + 2*CH2O + 0.65*CH3O2 + 0.65*CO + HO2**	2.00e-12 exp(500.00 / t)

Table S6: MOZART-TS2 Kinetic Reactions

Reactant		Products	Rate
MCO3 + HO2	→	**0.49*CH2O + 0.49*OH + 0.49*CO2 + 0.17*CH3CO3 + 0.32*CH3O2 + 0.32*CO + 0.15*O3 + 0.15*CH3COOH + 0.36*CH3COOOH**	4.30e-13 exp(1040.00 / t)
MCO3 + MCO3	→	**2*CO2 + 0.7*CH3CO3 + 2*CH2O + 1.3*CH3O2 + 1.3*CO**	**2.90e-12 exp(500.00 / t)**
MCO3 + NO	→	**NO2 + CO2 + 0.35*CH3CO3 + CH2O + 0.65*CH3O2 + 0.65*CO**	**8.10e-12 exp(270.00 / t)**
MCO3 + NO3	→	**NO2 + CO2 + 0.35*CH3CO3 + CH2O + 0.65*CH3O2 + 0.65*CO**	**4.000e-12**
MEKO2 + HO2	→	0.8*MEKOOH + 0.2*OH + 0.2*CH3CHO + 0.2*CH3CO3	7.50e-13 exp(700.00 / t)
MEKO2 + NO	→	CH3CO3 + CH3CHO + NO2	4.20e-12 exp(180.00 / t)
MEK + OH	→	MEKO2	2.30e-12 exp(-170.00 / t)
MEKOOH + OH	→	MEKO2	3.80e-12 exp(200.00 / t)
MPAN + OH + M	→	**0.25*HYAC + NO3 + 0.25*CO + M**	TROEE(8.00e-27, 3.50, 3.000000e-11, 0.00, 0.50)
MVKN + OH	→	**HO2 + 0.5*ONITR + 0.5*CO + 0.5*NOA**	**1.780e-12**
MVKO2 + CH3CO3	→	**CH3O2 + CO2 + 0.75*GLYALD + 0.75*CH3CO3 + 0.25*CH2O + 0.25*HO2 + 0.25*CH3COCHO**	**2.00e-12 exp(500.00 / t)**
MVKO2 + CH3O2	→	**0.25*CH3OH + 1*CO + 0.87*CH2O + 0.62*HO2 + 0.38*GLYALD + 0.88*CH3CO3 + 0.12*CH3COCHO**	**6.100e-13**
MVKO2 + HO2	→	**0.46*MVKOOH + 0.54*OH + 0.36*GLYALD + 0.49*CH3CO3 + 0.26*CO + 0.18*HO2 + 0.05*CH3COCHO + 0.05*CH2O**	**2.11e-13 exp(1300.00 / t)**
MVK + O3	→	0.6*CH2O + 0.56*CO + 0.1*CH3CHO + 0.1*CO2 + 0.28*CH3CO3 + 0.5*CH3COCHO + 0.28*HO2 + 0.36*OH + 0.12*HCOOH	8.50e-16 exp(-1520.00 / t)
MVK + OH	→	**MVKO2**	**2.70e-12 exp(580.00 / t)**
MVKOOH + OH	→	**1.56*CO + 0.44*HO2 + 0.44*CH3COCHO + 0.56*CH3CO3**	**4.800e-11**
MCO3 + NO2 + M	→	MPAN + M	**TROEE(9.70e-29, 5.60, 9.300000e-12, 1.50, 0.60)**
MPAN + M	→	MCO3 + NO2 + M	k(MCO3+NO2+M) * 1.111e28 exp(-14000 / t)
C5 Organics			
ALKNIT + OH	→	0.4*CH2O + 0.8*CH3CHO + 0.8*CH3COCH3 + NO2	1.600e-12
ALKO2 + HO2	→	ALKOOH	7.50e-13 exp(700.00 / t)

Table S6: MOZART-TS2 Kinetic Reactions

Reactant		Products	Rate
ALKO2 + NO	→	0.4*CH3CHO + 0.1*CH2O + 0.25*CH3COCH3 + HO2 + 0.8*MEK + NO2	6.700e-12
ALKO2 + NO	→	ALKNIT	5.40e-14 exp(870.00 / t)
ALKOOH + OH	→	ALKO2	3.80e-12 exp(200.00 / t)
BIGALK + OH	→	ALKO2	3.500e-12
HPALD1 + OH	→	**0.51*HO2 + 1.06*CO + 0.38*CH3COCHO + 0.54*CO2 + 0.06*CH3O2 + 0.06*CH3CO3 + 0.08*ICHE + 0.07*DHPMPAL + 0.43*OH + 0.35*MVK**	**1.17e-11 exp(450.00 / t)**
HPALD4 + OH	→	**0.41*HO2 + 0.76*CO + 0.03*CH3COCHO + 0.54*CO2 + 0.06*CH3O2 + 0.06*CH3CO3 + 0.15*HYPERACET + 0.18*ICHE + 0.17*DHPMPAL + 0.35*MACR + 0.53*OH**	**1.17e-11 exp(450.00 / t)**
HPALDB1C + OH	→	**0.58*ICHE + OH + 0.42*CO + 0.23*MVK + 0.19*MVKOOH**	**2.20e-11 exp(390.00 / t)**
HPALDB4C + OH	→	**0.77*ICHE + OH + 0.23*CO + 0.14*MACR + 0.09*MACROOH**	**3.50e-11 exp(390.00 / t)**
HYDRALD + OH	→	**1.08*OH + CO + 0.36*CO2 + 0.46*CH3COCHO + 0.32*IEPOXOO + 0.22*HYAC + 0.32*HO2**	**6.420e-11**
ICHE + OH	→	**OH + 1.5*CO + 0.5*HYAC + 0.5*CH3COCHO + 0.5*CH2O**	**9.85e-12 exp(410.00 / t)**
IEPOX + OH	→	**0.19*ICHE + 0.19*HO2 + 0.81*IEPOXOO**	**4.43e-11 exp(-400.00 / t)**
IEPOXOO + HO2	→	**0.35*ISOPHFP + 0.65*OH + 0.65*HO2 + 0.26*CO + 0.37*GLYALD + 0.46*CH3COCHO + 0.15*GLYOXAL + 0.19*HYAC**	**2.38e-13 exp(1300.00 / t)**
INHEB + OH	→	**0.2*INHEB + 0.4*NC4CHOO2 + 0.4*CH3COCHO + 0.4*HCOOH + 0.4*CH2O + 0.4*NO2**	**4.43e-11 exp(-400.00 / t)**
INHED + OH	→	**0.35*NOA + 0.35*CO + 0.4*HO2 + 0.59*CH2O + 0.35*NC4CHOO2 + 0.06*INHED + 0.19*HYAC + 0.19*CO2 + 0.19*NO2 + 0.05*MVKN**	**3.22e-11 exp(-400.00 / t)**
ISOPB1O2 + CH3CO3	→	**MVK + CH2O + HO2 + CO2 + CH3O2**	**2.00e-12 exp(500.00 / t)**
ISOPB1O2 + CH3O2	→	**1.75*CH2O + 0.25*ISOPOH + 0.75*MVK + 1.5*HO2**	**1.600e-13**
ISOPB1O2 + HO2	→	**0.06*MVK + 0.06*CH2O + 0.06*OH + 0.06*HO2 + 0.94*ISOPOOH**	**2.12e-13 exp(1300.00 / t)**
ISOPB1O2	→	**MVK + CH2O + OH**	**1.04e+11 exp(-9746.00 / t)**
ISOPB1O2	→	**ISOPC1C + O2**	**2.24e+15 exp(-10865.00 / t)**

Table S6: MOZART-TS2 Kinetic Reactions

Reactant		Products	Rate
ISOPB1O2	→	ISOPC1T + O2	2.22e+15 exp(-10355.00 / t)
ISOPB4O2 + CH3CO3	→	MACR + CH2O + HO2 + CO2 + CH3O2	2.00e-12 exp(500.00 / t)
ISOPB4O2 + CH3O2	→	0.25*CH3OH + 0.25*HYDRALD + 0.25*ISOPOH + 1.25*CH2O + HO2 + 0.5*MACR	1.400e-12
ISOPB4O2 + HO2	→	0.06*MACR + 0.06*CH2O + 0.06*OH + 0.06*HO2 + 0.94*ISOPOOH	2.12e-13 exp(1300.00 / t)
ISOPB4O2	→	MACR + CH2O + OH	1.88e+11 exp(-9752.00 / t)
ISOPB4O2	→	ISOPC4C + O2	2.49e+15 exp(-11112.00 / t)
ISOPB4O2	→	ISOPC4T + O2	2.49e+15 exp(-10890.00 / t)
O2 + ISOPC1C	→	ISOPB1O2	7.500e-13
ISOPC1C + O2	→	ISOPZD1O2	1.400e-13
ISOPC1T + O2	→	ISOPB1O2	7.500e-13
ISOPC1T + O2	→	ISOPED1O2	3.600e-13
ISOPC4C + O2	→	ISOPB4O2	6.500e-13
ISOPC4C + O2	→	ISOPZD4O2	2.100e-13
ISOPC4T + O2	→	ISOPB4O2	6.500e-13
ISOPC4T + O2	→	ISOPED4O2	4.900e-13
ISOPED1O2 + CH3CO3	→	0.45*HO2 + 0.45*HYDRALD + 0.55*CO + 0.55*OH + 0.55*MVKOOH + CO2 + CH3O2	2.00e-12 exp(500.00 / t)
ISOPED1O2 + CH3O2	→	0.25*CH3OH + 0.25*ISOPOH + 0.75*CH2O + 0.72*HO2 + 0.28*CO + 0.28*OH + 0.28*MVKOOH + 0.47*HYDRALD	1.200e-12
ISOPED1O2 + HO2	→	ISOPOOH	2.12e-13 exp(1300.00 / t)
ISOPED1O2	→	ISOPC1T + O2	1.83e+14 exp(-8930.00 / t)
ISOPED4O2 + CH3CO3	→	0.45*HO2 + 0.45*HYDRALD + 0.55*CO + 0.55*OH + 0.55*MACROOH + CO2 + CH3O2	2.00e-12 exp(500.00 / t)
ISOPED4O2 + CH3O2	→	0.25*CH3OH + 0.25*ISOPOH + 0.75*CH2O + 0.72*HO2 + 0.28*CO + 0.28*OH + 0.28*MACROOH + 0.47*HYDRALD	9.800e-13
ISOPED4O2 + HO2	→	ISOPOOH	2.12e-13 exp(1300.00 / t)
ISOPED4O2	→	ISOPC4T + O2	2.08e+14 exp(-9400.00 / t)
ISOPFDNC + OH	→	CO + NO2 + 0.5*MACRN + 0.5*MVKN	1.850e-11
ISOPFDN + OH	→	ISOPFDNC + HO2	1.630e-12

Table S6: MOZART-TS2 Kinetic Reactions

Reactant		Products	Rate
ISOPFNC + OH	→	**CO + 0.5*NO2 + 0.5*OH + 0.25*MACRN + 0.25*MVKN + 0.25*MACROOH + 0.25*MVKOOH**	**2.500e-11**
ISOPFNP + OH	→	**ISOPFNC + HO2**	**1.100e-11**
ISOPHFP + OH	→	**2*CO + OH + 0.72*CH3COCHO + 0.28*HYAC**	**3.300e-11**
ISOPN1DO2 + HO2	→	**0.42*ISOPFNP + 0.58*OH + 0.58*HO2 + 0.55*NOA + 0.55*GLYALD + 0.03*MACRN + 0.03*CH2O**	**2.60e-13 exp(1300.00 / t)**
ISOPN1DO2	→	**ISOPFNP + HO2**	**1.26e+13 exp(-10000.00 / t)**
ISOPN1D + O3	→	**0.66*H2O2 + 0.83*GLYALD + 0.83*NOA + 0.34*OH + 0.17*NO2 + 0.17*CH3COCHO + 0.17*GLYOXAL + 0.17*HO2**	**2.800e-17**
ISOPN1D + OH	→	**0.08*IEPOX + 0.08*NO2 + 0.04*NC4CHO + 0.04*HO2 + 0.06*MACRN + 0.06*OH + 0.06*CO + 0.82*ISOPN1DO2**	**8.000e-11**
ISOPN2BO2 + HO2	→	**0.48*ISOPFNP + 0.52*OH + 0.06*MACRN + 0.06*CH2O + 0.06*HO2 + 0.46*HYAC + 0.46*NO2 + 0.46*GLYALD**	**2.60e-13 exp(1300.00 / t)**
ISOPN2BO2	→	**ISOPFNC + HO2**	**1.88e+13 exp(-10000.00 / t)**
ISOPN2B + OH	→	**0.15*IEPOX + 0.15*NO2 + 0.85*ISOPN2BO2**	**3.000e-11**
ISOPN3BO2 + HO2	→	**0.4*ISOPFNP + 0.6*OH + 0.6*MVKN + 0.6*CH2O + 0.6*HO2**	**2.60e-13 exp(1300.00 / t)**
ISOPN3BO2	→	**ISOPFNC + HO2**	**1.88e+13 exp(-10000.00 / t)**
ISOPN3B + OH	→	**0.13*IEPOX + 0.13*NO2 + 0.87*ISOPN3BO2**	**4.200e-11**
ISOPN4DO2 + HO2	→	**0.5*ISOPFNP + 0.5*OH + 0.5*HO2 + 0.06*MVKN + 0.06*CH2O + 0.44*HYAC + 0.44*NO3CH2CHO**	**2.60e-13 exp(1300.00 / t)**
ISOPN4DO2	→	**ISOPFNP + HO2**	**5.09e+12 exp(-10000.00 / t)**
ISOPN4D + O3	→	**0.66*H2O2 + 0.83*NO3CH2CHO + 0.83*HYAC + 0.34*OH + 0.17*NO2 + 0.17*GLYOXAL + 0.17*CH3COCHO + 0.17*HO2**	**2.800e-17**
ISOPN4D + OH	→	**0.04*IEPOX + 0.04*NO2 + 0.03*NC4CHO + 0.03*HO2 + 0.04*MVKN + 0.04*CO + 0.04*OH + 0.89*ISOPN4DO2**	**1.100e-10**
ISOPNBNO3O2 + HO2	→	**0.6*ISOPFNP + 0.4*OH + 0.4*HO2 + 0.06*MACRN + 0.04*MVKN + 0.1*CH2O + 0.15*NOA + 0.15*GLYALD + 0.15*HYAC + 0.15*NO3CH2CHO**	**2.60e-13 exp(1300.00 / t)**
ISOPNBNO3 + OH	→	**0.03*INHED + 0.03*OH + 0.05*NC4CHO + 0.05*HO2 + 0.92*ISOPNBNO3O2**	**3.900e-11**
ISOP + NO3	→	ISOPNO3	**2.95e-12 exp(-450.00 / t)**

Table S6: MOZART-TS2 Kinetic Reactions

Reactant		Products	Rate
ISOPNO3 + CH3CO3	→	**CH3O2 + CO2 + 0.46*NO2 + 0.46*CH2O + 0.54*NC4CHO + 0.54*HO2 + 0.42*MVK + 0.04*MACR**	**2.00e-12 exp(500.00 / t)**
ISOPNO3 + CH3O2	→	**0.07*ISOPNBNO3 + 0.71*CH2O + 0.05*MVK + 0.07*NO2 + 0.4*HO2 + 0.02*MACR + 0.53*NC4CHO + 0.36*CH3OH + 0.28*ISOPN1D + 0.05*ISOPN4D**	**1.300e-12**
ISOPNO3 + HO2	→	**0.23*ISOPNOOHB + 0.53*ISOPNOOHD + 0.22*MVK + 0.02*MACR + 0.24*CH2O + 0.24*OH + 0.24*NO2**	**2.47e-13 exp(1300.00 / t)**
ISOPNO3 + ISOPNO3	→	**1.07*NC4CHO + 0.4*HO2 + 0.16*MACR + 0.16*CH2O + 0.16*NO2 + 0.53*ISOPN1D + 0.09*ISOPN4D + 0.15*ISOPNBNO3**	**5.000e-12**
ISOPNO3 + NO3	→	**1.46*NO2 + 0.46*CH2O + 0.54*NC4CHO + 0.54*HO2 + 0.42*MVK + 0.04*MACR**	**2.300e-12**
ISOPNOOHBO2 + HO2	→	**0.49*ISOPFNP + 0.85*OH + 0.17*CH2O + 0.17*HO2 + 0.15*MACRN + 0.02*MVKN + 0.28*NOA + 0.28*GLYALD + 0.06*HYAC + 0.06*NO3CH2CHO**	**2.64e-13 exp(1300.00 / t)**
ISOPNOOHBO2	→	**OH + ISOPFNP**	**8.72e+12 exp(-10000.00 / t)**
ISOPNOOHB + OH	→	**0.17*ISOPNO3 + 0.02*NC4CHO + 0.4*INHEB + 0.42*OH + 0.41*ISOPNOOHBO2**	**3.900e-11**
ISOPNOOHDO2 + HO2	→	**0.17*ISOPFNP + 0.86*OH + 0.03*CH2O + 0.02*MACRN + 0.01*MVKN + 0.68*NOA + 0.68*HCOCH2OOH + 0.12*HYPERACET + 0.12*NO3CH2CHO + 0.8*HO2**	**2.64e-13 exp(1300.00 / t)**
ISOPNOOHDO2	→	**OH + ISOPFNP**	**6.55e+12 exp(-10000.00 / t)**
ISOPNOOHD + O3	→	**0.66*H2O2 + 0.7*HCOCH2OOH + 0.13*HYPERACET + 0.7*NOA + 0.13*NO3CH2CHO + 0.51*OH + 0.17*NO2 + 0.17*CH3COCHO + 0.17*GLYOXAL**	**2.800e-17**
ISOPNOOHD + OH	→	**0.07*ISOPNO3 + 0.09*NC4CHO + 0.29*OH + 0.2*INHED + 0.07*IEPOX + 0.07*NO2 + 0.57*ISOPNOOHDO2**	**9.200e-11**
ISOP + O3	→	**0.25*OH + 0.41*MACR + 0.17*MVK + 0.33*HMHP + 0.03*H2O2 + 0.22*HCOOH + 1.01*CH2O + 0.42*CO2 + 0.42*HO2 + 0.21*CH3O2 + 0.07*CH3CO3 + 0.35*CO**	**1.03e-14 exp(-1995.00 / t)**
ISOP + OH	→	**0.315*ISOPC1T + 0.315*ISOPC1C + 0.111*ISOPC4T + 0.259*ISOPC4C**	**2.70e-11 exp(390.00 / t)**
ISOPOH + OH	→	**HYAC + GLYALD + HO2**	**3.850e-11**

Table S6: MOZART-TS2 Kinetic Reactions

Reactant		Products	Rate
ISOPOOH + OH	→	**0.53*ISOPB1O2 + 0.16*ISOPB4O2 + 0.13*HYDRALD + 0.13*OH + 0.09*HPALDB1C + 0.09*HPALDB4C + 0.18*HO2**	**5.53e-12 exp(200.00 / t)**
ISOPOOH + OH	→	**0.85*IEPOX + 0.92*OH + 0.07*GLYALD + 0.07*HYAC + 0.08*ISOPHFP**	**2.08e-11 exp(390.00 / t)**
ISOPZD1O2 + CH3CO3	→	**0.45*HO2 + 0.45*HYDRALD + 0.55*CO + 0.55*OH + 0.55*MVKOOH + CO2 + CH3O2**	**2.00e-12 exp(500.00 / t)**
ISOPZD1O2 + CH3O2	→	**0.25*CH3OH + 0.25*ISOPOH + 0.75*CH2O + 0.72*HO2 + 0.28*CO + 0.28*OH + 0.28*MVKOOH + 0.47*HYDRALD**	**1.200e-12**
ISOPZD1O2 + HO2	→	**ISOPOOH**	**2.12e-13 exp(1300.00 / t)**
ISOPZD1O2	→	**ISOPC1C + O2**	**1.79e+14 exp(-8830.00 / t)**
ISOPZD4O2 + CH3CO3	→	**0.45*HO2 + 0.45*HYDRALD + 0.55*CO + 0.55*OH + 0.55*MACROOH + CO2 + CH3O2**	**2.00e-12 exp(500.00 / t)**
ISOPZD4O2 + CH3O2	→	**0.25*CH3OH + 0.25*ISOPOH + 0.75*CH2O + 0.72*HO2 + 0.28*CO + 0.28*OH + 0.28*MACROOH + 0.47*HYDRALD**	**9.800e-13**
ISOPZD4O2 + HO2	→	**ISOPOOH**	**2.12e-13 exp(1300.00 / t)**
ISOPZD4O2	→	**ISOPC4C + O2**	**1.75e+14 exp(-9054.00 / t)**
NC4CHOO2 + HO2	→	**0.2*ISOPFNP + 0.8*OH + 0.8*HO2 + 0.1*NOA + 0.1*GLYOXAL + 0.1*CH3COCHO + 0.1*NO3CH2CHO + 0.29*MACRN + 0.31*MVKN + 0.6*CO**	**2.60e-13 exp(1300.00 / t)**
NC4CHOO2	→	**0.51*MACRN + 0.49*MVKN + CO + OH**	**1.00e+7 exp(-5000.00 / t)**
NC4CHO + O3	→	**0.66*H2O2 + 0.66*GLYOXAL + 0.34*CH3COCHO + 0.61*NOA + 0.22*NO3CH2CHO + 0.34*OH + 0.17*NO2 + 0.3*CO + 0.13*HO2 + 0.04*CH3CO3**	**4.400e-18**
NC4CHO + OH	→	**0.45*CO2 + 0.1*CH3CO3 + 0.1*NO3CH2CHO + 0.35*NOA + 0.04*NO2 + 0.04*ICHE + 0.24*MACRN + 0.04*MVKN + 0.63*CO + 0.63*HO2 + 0.23*NC4CHOO2**	**3.600e-11**
IEPOXOO + NO	→	**NO2 + HO2 + 0.57*GLYALD + 0.71*CH3COCHO + 0.4*CO + 0.23*GLYOXAL + 0.29*HYAC**	**see notes [a]: α = 0.025, n = 8**
IEPOXOO + NO	→	**ISOPFNC**	**see notes [a]: α = 0.025, n = 8**
ISOPB1O2 + NO	→	**NO2 + MVK + CH2O + HO2**	**see notes [a]: α = 0.14, n = 6**
ISOPB1O2 + NO	→	**ISOPN2B**	**see notes [a]: α = 0.14, n = 6**
ISOPB4O2 + NO	→	**NO2 + MACR + CH2O + HO2**	**see notes [a]: α = 0.13, n = 6**

Table S6: MOZART-TS2 Kinetic Reactions

Reactant		Products	Rate
ISOPB4O2 + NO	→	**ISOPN3B**	**see notes [a]: α = 0.13, n = 6**
ISOPED1O2 + NO	→	**NO2 + 0.45*HYDRALD + 0.45*HO2 + 0.55*MVKOOH + 0.55*CO + 0.55*OH**	**see notes [a]: α = 0.12, n = 6**
ISOPED1O2 + NO	→	**ISOPN4D**	**see notes [a]: α = 0.12, n = 6**
ISOPED4O2 + NO	→	**NO2 + 0.45*HYDRALD + 0.45*HO2 + 0.55*MACROOH + 0.55*CO + 0.55*OH**	**see notes [a]: α = 0.12, n = 6**
ISOPED4O2 + NO	→	**ISOPN1D**	**see notes [a]: α = 0.12, n = 6**
ISOPN1DO2 + NO	→	**NO2 + HO2 + 0.94*NOA + 0.94*GLYALD + 0.06*MACRN + 0.06*CH2O**	**see notes [a]: α = 0.084, n = 11**
ISOPN1DO2 + NO	→	**ISOPFDN**	**see notes [a]: α = 0.084, n = 11**
ISOPN2BO2 + NO	→	**1.73*NO2 + 0.27*MACRN + 0.27*CH2O + 0.27*HO2 + 0.73*HYAC + 0.73*GLYALD**	**see notes [a]: α = 0.065, n = 11**
ISOPN2BO2 + NO	→	**ISOPFDN**	**see notes [a]: α = 0.065, n = 11**
ISOPN3BO2 + NO	→	**NO2 + MVKN + CH2O + HO2**	**see notes [a]: α = 0.053, n = 11**
ISOPN3BO2 + NO	→	**ISOPFDN**	**see notes [a]: α = 0.053, n = 11**
ISOPN4DO2 + NO	→	**NO2 + HO2 + 0.13*MVKN + 0.13*CH2O + 0.87*HYAC + 0.87*NO3CH2CHO**	**see notes [a]: α = 0.165, n = 11**
ISOPN4DO2 + NO	→	**ISOPFDN**	**see notes [a]: α = 0.165, n = 11**
ISOPNBNO3O2 + NO	→	**NO2 + HO2 + 0.21*MACRN + 0.12*MVKN + 0.33*CH2O + 0.34*NOA + 0.34*GLYALD + 0.33*HYAC + 0.33*NO3CH2CHO**	**see notes [a]: α = 0.203, n = 11**
ISOPNBNO3O2 + NO	→	**ISOPFDN**	**see notes [a]: α = 0.203, n = 11**
ISOPNO3 + NO	→	**1.46*NO2 + 0.46*CH2O + 0.54*NC4CHO + 0.54*HO2 + 0.42*MVK + 0.04*MACR**	**see notes [a]: α = 0.135, n = 9**
ISOPNO3 + NO	→	**ISOPFDN**	**see notes [a]: α = 0.135, n = 9**
ISOPNOOHBO2 + NO	→	**NO2 + 0.53*CH2O + 0.53*HO2 + 0.49*MACRN + 0.04*MVKN + 0.4*NOA + 0.4*GLYALD + 0.07*HYAC + 0.07*NO3CH2CHO + 0.47*OH**	**see notes [a]: α = 0.141, n = 12**
ISOPNOOHBO2 + NO	→	**ISOPFDN**	**see notes [a]: α = 0.141, n = 12**
ISOPNOOHDO2 + NO	→	**NO2 + 0.04*CH2O + 0.04*OH + 0.02*MACRN + 0.02*MVKN + 0.81*NOA + 0.81*HCOCH2OOH + 0.15*HYPERACET + 0.15*NO3CH2CHO + 0.96*HO2**	**see notes [a]: α = 0.045, n = 12**
ISOPNOOHDO2 + NO	→	**ISOPFDN**	**see notes [a]: α = 0.045, n = 12**

Table S6: MOZART-TS2 Kinetic Reactions

Reactant		Products	Rate
ISOPZD1O2	→	**0.15*HPALDB1C + 0.25*HPALD1 + 0.4*HO2 + 0.6*OH + 0.6*DHPMPAL + 0.6*CO**	**5.05e15 exp(-12200.00 / t) exp(1e8 / t^3)**
ISOPZD1O2 + NO	→	**NO2 + 0.45*HYDRALD + 0.45*HO2 + 0.55*MVKOOH + 0.55*CO + 0.55*OH**	**see notes [a]: α = 0.12, n = 6**
ISOPZD1O2 + NO	→	**ISOPN4D**	**see notes [a]: α = 0.12, n = 6**
ISOPZD4O2	→	**0.15*HPALDB4C + 0.25*HPALD4 + 0.4*HO2 + 0.6*OH + 0.6*DHPMPAL + 0.6*CO**	**2.22e9 exp(-7160.00 / t) exp(1e8 / t^3)**
ISOPZD4O2 + NO	→	**NO2 + 0.45*HYDRALD + 0.45*HO2 + 0.55*MACROOH + 0.55*CO + 0.55*OH**	**see notes [a]: α = 0.12, n = 6**
ISOPZD4O2 + NO	→	**ISOPN1D**	**see notes [a]: α = 0.12, n = 6**
MACRO2 + NO	→	**NO2 + HO2 + 0.86*HYAC + 0.86*CO + 0.14*CH2O + 0.14*CH3COCHO**	**see notes [a]: α = 0.06, n = 6**
MACRO2 + NO	→	**MACRN**	**see notes [a]: α = 0.06, n = 6**
MVKO2 + NO	→	**NO2 + 0.24*HO2 + 0.24*CH2O + 0.76*CH3CO3 + 0.76*GLYALD + 0.24*CH3COCHO**	**see notes [a]: α = 0.04, n = 6**
MVKO2 + NO	→	**MVKN**	**see notes [a]: α = 0.04, n = 6**
NC4CHOO2 + NO	→	**NO2 + HO2 + 0.13*NOA + 0.13*GLYOXAL + 0.12*CH3COCHO + 0.12*NO3CH2CHO + 0.39*MACRN + 0.36*MVKN + 0.75*CO**	**see notes [a]: α = 0.021, n = 11**
NC4CHOO2 + NO	→	**ISOPFDNC**	**see notes [a]: α = 0.021, n = 11**
C7 Organics			
ACBZO2 + HO2	→	0.4*C6H5O2 + 0.4*OH	4.30e-13 exp(1040.00 / t)
ACBZO2 + NO	→	C6H5O2 + NO2	7.50e-12 exp(290.00 / t)
BENZENE + OH	→	0.53*PHENOL + 0.12*BEPOMUC + 0.65*HO2 + 0.35*BENZO2	2.30e-12 exp(-193.00 / t)
BENZO2 + HO2	→	BENZOOH	7.50e-13 exp(700.00 / t)
BENZO2 + NO	→	NO2 + GLYOXAL + 0.5*BIGALD1 + HO2	2.60e-12 exp(365.00 / t)
BENZOOH + OH	→	BENZO2	3.80e-12 exp(200.00 / t)
BZALD + OH	→	ACBZO2	5.90e-12 exp(225.00 / t)
BZOO + HO2	→	BZOOH	7.50e-13 exp(700.00 / t)
BZOOH + OH	→	BZOO	3.80e-12 exp(200.00 / t)
BZOO + NO	→	BZALD + NO2 + HO2	2.60e-12 exp(365.00 / t)
C6H5O2 + HO2	→	C6H5OOH	7.50e-13 exp(700.00 / t)
C6H5O2 + NO	→	PHENO + NO2	2.60e-12 exp(365.00 / t)
C6H5OOH + OH	→	C6H5O2	3.80e-12 exp(200.00 / t)

Table S6: MOZART-TS2 Kinetic Reactions

Reactant		Products	Rate
CRESOL + OH	→	0.2*PHENO2 + 0.73*HO2 + 0.07*PHENO	4.700e-11
DICARBO2 + HO2	→	0.4*OH + 0.07*HO2 + 0.07*CH3COCHO + 0.07*CO + 0.33*CH3O2	4.30e-13 exp(1040.00 / t)
DICARBO2 + NO	→	NO2 + 0.17*HO2 + 0.17*CH3COCHO + 0.17*CO + 0.83*CH3O2	7.50e-12 exp(290.00 / t)
DICARBO2 + NO2 + M	→	M	TROEE(9.70e-29, 5.60, 9.300000e-12, 1.50, 0.60)
MALO2 + HO2	→	0.16*GLYOXAL + 0.16*HO2 + 0.16*CO	4.30e-13 exp(1040.00 / t)
MALO2 + NO	→	0.4*GLYOXAL + 0.4*HO2 + 0.4*CO + NO2	7.50e-12 exp(290.00 / t)
MALO2 + NO2 + M	→	M	TROEE(9.70e-29, 5.60, 9.300000e-12, 1.50, 0.60)
MDIALO2 + HO2	→	0.4*OH + 0.33*HO2 + 0.07*CH3COCHO + 0.14*CO + 0.07*CH3O2 + 0.07*GLYOXAL	4.30e-13 exp(1040.00 / t)
MDIALO2 + NO	→	NO2 + 0.83*HO2 + 0.17*CH3COCHO + 0.35*CO + 0.17*CH3O2 + 0.17*GLYOXAL	7.50e-12 exp(290.00 / t)
MDIALO2 + NO2 + M	→	M	TROEE(9.70e-29, 5.60, 9.300000e-12, 1.50, 0.60)
PHENO2 + HO2	→	PHENOOH	7.50e-13 exp(700.00 / t)
PHENO2 + NO	→	HO2 + 0.7*GLYOXAL + NO2	2.60e-12 exp(365.00 / t)
PHENOL + OH	→	0.14*PHENO2 + 0.8*HO2 + 0.06*PHENO	4.70e-13 exp(1220.00 / t)
PHENO + NO2	→	M	2.100e-12
PHENO + O3	→	C6H5O2	2.800e-13
PHENOOH + OH	→	PHENO2	3.80e-12 exp(200.00 / t)
ACBZO2 + NO2 + M	→	PBZNIT + M	TROEE(9.70e-29, 5.60, 9.300000e-12, 1.50, 0.60)
TOLO2 + HO2	→	TOLOOH	7.50e-13 exp(700.00 / t)
TOLO2 + NO	→	NO2 + 0.6*GLYOXAL + 0.4*CH3COCHO + HO2 + 0.2*BIGALD1 + 0.2*BIGALD2 + 0.2*BIGALD3	2.60e-12 exp(365.00 / t)
TOLOOH + OH	→	TOLO2	3.80e-12 exp(200.00 / t)
TOLUENE + OH	→	0.18*CRESOL + 0.1*TEPOMUC + 0.07*BZOO + 0.65*TOLO2 + 0.28*HO2	1.70e-12 exp(352.00 / t)
PBZNIT + M	→	ACBZO2 + NO2 + M	k(ACBZO2+NO2) * 1.111e28 exp(-14000 / t)
XYLENES + OH	→	0.15*XYLOL + 0.23*TEPOMUC + 0.06*BZOO + 0.56*XYLENO2 + 0.38*HO2	1.700e-11

Table S6: MOZART-TS2 Kinetic Reactions

Reactant		Products	Rate
XYLENO2 + HO2	→	XYLENOOH	7.50e-13 exp(700.00 / t)
XYLENO2 + NO	→	NO2 + HO2 + 0.34*GLYOXAL + 0.54*CH3COCHO + 0.06*BIGALD1 + 0.2*BIGALD2 + 0.15*BIGALD3 + 0.21*BIGALD4	2.60e-12 exp(365.00 / t)
XYLENOOH + OH	→	XYLENO2	3.80e-12 exp(200.00 / t)
XYLOLO2 + HO2	→	XYLOLOOH	7.50e-13 exp(700.00 / t)
XYLOLO2 + NO	→	HO2 + NO2 + 0.17*GLYOXAL + 0.51*CH3COCHO	2.60e-12 exp(365.00 / t)
XYLOL + OH	→	0.3*XYLOLO2 + 0.63*HO2 + 0.07*PHENO	8.400e-11
XYLOLOOH + OH	→	XYLOLO2	3.80e-12 exp(200.00 / t)
C10 Organics			
APIN + NO3	→	**APINNO3**	**1.20e-12 exp(490.00 / t)**
APINNO3 + APINNO3	→	**0.27*TERPNT + 0.09*TERPNS + 1.64*NO2 + 1.64*TERPA**	**5.300e-13**
APINNO3 + CH3CO3	→	**NO2 + TERPA + CH3O2 + CO2**	**2.00e-12 exp(500.00 / t)**
APINNO3 + CH3O2	→	**0.09*TERPNT + 0.09*TERPNS + 0.95*CH2O + 0.05*CH3OH + 0.82*HO2 + 0.82*NO2 + 0.82*TERPA**	**2.000e-12**
APINNO3 + HO2	→	**0.3*TERPNPT + 0.7*TERPA + 0.7*NO2 + 0.7*OH**	**2.71e-13 exp(1300.00 / t)**
APINNO3 + NO	→	**1.86*NO2 + 0.07*TERPFDN + 0.93*TERPA**	**2.70e-12 exp(360.00 / t)**
APINNO3 + NO3	→	**2*NO2 + TERPA**	**2.300e-12**
APINNO3 + TERPA2CO3	→	**NO2 + TERPA + TERPA2O2 + CO2**	**2.00e-12 exp(500.00 / t)**
APINNO3 + TERPA3CO3	→	**NO2 + TERPA + TERPA4O2 + CO2**	**2.00e-12 exp(500.00 / t)**
APINNO3 + TERPACO3	→	**NO2 + TERPA + TERPA1O2 + CO2**	**2.00e-12 exp(500.00 / t)**
APINO2 + CH3CO3	→	**0.39*TERPA + 0.35*TERPA3 + 0.14*TERP1OOH + 0.12*CH3COCH3 + 0.12*TERPF1 + 0.27*CH2O + HO2 + CH3O2 + CO2**	**2.00e-12 exp(500.00 / t)**
APINO2 + CH3O2	→	**0.83*CH2O + 0.14*TERPF1 + 0.42*TERPA + 0.2*TERPA3 + 0.13*TERP1OOH + 0.17*CH3OH + 0.11*TERPK + 0.06*CH3COCH3 + 1.16*HO2**	**2.000e-12**
APINO2 + HO2	→	**0.06*CH3COCH3 + 0.06*TERPF1 + 0.08*CH2O + 0.25*TERP1OOH + 0.48*HO2 + 0.4*TERPOOH + 0.29*TERPA + 0.35*OH**	**2.60e-13 exp(1300.00 / t)**

Table S6: MOZART-TS2 Kinetic Reactions

Reactant		Products	Rate
APINO2 + NO	→	**0.01*TERPHFN + 0.02*TERPNS1 + 0.1*TERPNS + 0.05*TERPNT + 0.05*TERPNT1 + 0.77*NO2 + 0.77*HO2 + 0.3*TERPA + 0.27*TERPA3 + 0.09*CH3COCH3 + 0.09*TERPF1 + 0.21*CH2O + 0.11*TERP1OOH**	**2.70e-12 exp(360.00 / t)**
APINO2 + NO3	→	**NO2 + HO2 + 0.39*TERPA + 0.35*TERPA3 + 0.12*CH3COCH3 + 0.12*TERPF1 + 0.27*CH2O + 0.14*TERP1OOH**	**2.300e-12**
APINO2 + TERPA2CO3	→	**0.39*TERPA + 0.35*TERPA3 + 0.14*TERP1OOH + 0.12*CH3COCH3 + 0.12*TERPF1 + 0.27*CH2O + HO2 + TERPA2O2 + CO2**	**2.00e-12 exp(500.00 / t)**
APINO2 + TERPA3CO3	→	**0.39*TERPA + 0.35*TERPA3 + 0.14*TERP1OOH + 0.12*CH3COCH3 + 0.12*TERPF1 + 0.27*CH2O + HO2 + TERPA4O2 + CO2**	**2.00e-12 exp(500.00 / t)**
APINO2 + TERPACO3	→	**0.39*TERPA + 0.35*TERPA3 + 0.14*TERP1OOH + 0.12*CH3COCH3 + 0.12*TERPF1 + 0.27*CH2O + HO2 + TERPA1O2 + CO2**	**2.00e-12 exp(500.00 / t)**
APIN + O3	→	**0.77*OH + 0.33*TERPA2O2 + 0.22*H2O2 + 0.22*TERPA + 0.01*TERPACID + 0.17*TERPA2 + 0.17*HO2 + 0.17*CO + 0.27*CH2O + 0.27*TERPA2CO3**	**8.05e-16 exp(-640.00 / t)**
APIN + OH	→	**APINO2**	**1.34e-11 exp(410.00 / t)**
BCARY + NO3	→	**BCARYNO3**	1.900e-11
BCARYNO3 + BCARYNO3	→	**0.36*SQTN + 1.64*NO2 + 1.64*TERPF2**	**5.300e-13**
BCARYNO3 + CH3CO3	→	**CH3O2 + CO2 + NO2 + TERPF2**	**2.00e-12 exp(500.00 / t)**
BCARYNO3 + CH3O2	→	**0.18*SQTN + 0.95*CH2O + 0.82*TERPF2 + 0.82*NO2 + 0.82*HO2 + 0.05*CH3OH**	**2.000e-12**
BCARYNO3 + HO2	→	**0.5*SQTN + 0.5*OH + 0.5*NO2 + 0.5*TERPF2**	**2.78e-13 exp(1300.00 / t)**
BCARYNO3 + NO	→	**0.07*SQTN + 1.86*NO2 + 0.93*TERPF2**	**2.70e-12 exp(360.00 / t)**
BCARYNO3 + NO3	→	**2*NO2 + TERPF2**	**2.300e-12**
BCARYNO3 + TERPA2CO3	→	**TERPA2O2 + CO2 + NO2 + TERPF2**	**2.00e-12 exp(500.00 / t)**
BCARYNO3 + TERPA3CO3	→	**TERPA4O2 + CO2 + NO2 + TERPF2**	**2.00e-12 exp(500.00 / t)**

Table S6: MOZART-TS2 Kinetic Reactions

Reactant		Products	Rate
BCARYNO3 + TERPACO3	→	**TERPA1O2 + CO2 + NO2 + TERPF2**	**2.00e-12 exp(500.00 / t)**
BCARYO2 + CH3CO3	→	**TERPF2 + HO2 + CH3O2 + CO2**	**2.00e-12 exp(500.00 / t)**
BCARYO2 + CH3O2	→	**0.25*CH3OH + TERPF2 + 0.75*CH2O + HO2**	**2.000e-12**
BCARYO2 + HO2	→	**0.9*TERP2AOOH + 0.1*OH + 0.1*HO2 + 0.1*TERPF2**	**2.75e-13 exp(1300.00 / t)**
BCARYO2 + NO	→	**0.3*SQTN + 0.7*NO2 + 0.7*HO2 + 0.7*TERPF2**	**2.70e-12 exp(360.00 / t)**
BCARYO2 + NO3	→	**NO2 + HO2 + TERPF2**	**2.300e-12**
BCARYO2 + TERPA2CO3	→	**TERPF2 + HO2 + TERPA2O2 + CO2**	**2.00e-12 exp(500.00 / t)**
BCARYO2 + TERPA3CO3	→	**TERPF2 + HO2 + TERPA4O2 + CO2**	**2.00e-12 exp(500.00 / t)**
BCARYO2 + TERPACO3	→	**TERPF2 + HO2 + TERPA1O2 + CO2**	**2.00e-12 exp(500.00 / t)**
BCARY + O3	→	**0.13*TERPACID + 0.17*H2O2 + 0.08*OH + 0.08*HO2 + 0.08*CH2O + 0.87*TERPF2**	1.200e-14
BCARY + OH	→	**BCARYO2**	2.000e-10
BPIN + NO3	→	**BPINNO3**	**2.500e-12**
BPINNO3 + BPINNO3	→	**0.94*NO2 + 0.92*TERPNS + 0.9*TERPA3 + 0.04*TERPK + 0.04*CH2O + 0.14*TERPNT + 0.94*HO2**	**5.300e-13**
BPINNO3 + CH3CO3	→	**CH3O2 + CO2 + 0.5*NO2 + 0.45*TERPNS + 0.48*TERPA3 + 0.02*TERPK + 0.02*CH2O + 0.05*TERPNT + 0.5*HO2**	**2.00e-12 exp(500.00 / t)**
BPINNO3 + CH3O2	→	**0.56*TERPNS + 0.08*TERPNT + 0.02*TERPK + 0.34*TERPA3 + 0.36*NO2 + 1.1*HO2 + 0.99*CH2O + 0.03*CH3OH**	**2.000e-12**
BPINNO3 + HO2	→	**0.47*OH + 0.45*TERPNPS + 0.22*TERPA3 + 0.02*TERPK + 0.08*TERPNPT + 0.24*NO2 + 0.02*CH2O + 0.23*TERPNS**	**2.71e-13 exp(1300.00 / t)**
BPINNO3 + NO	→	**0.07*TERPFDN + 1.39*NO2 + 0.42*TERPNS + 0.44*TERPA3 + 0.02*TERPK + 0.02*CH2O + 0.05*TERPNT + 0.47*HO2**	**2.70e-12 exp(360.00 / t)**
BPINNO3 + NO3	→	**1.5*NO2 + 0.45*TERPNS + 0.48*TERPA3 + 0.02*TERPK + 0.02*CH2O + 0.05*TERPNT + 0.5*HO2**	**2.300e-12**

Table S6: MOZART-TS2 Kinetic Reactions

Reactant		Products	Rate
BPINNO3 + TERPA2CO3	→	TERPA2O2 + CO2 + 0.5*NO2 + 0.45*TERPNS + 0.48*TERPA3 + 0.02*TERPK + 0.02*CH2O + 0.05*TERPNT + 0.5*HO2	2.00e-12 exp(500.00 / t)
BPINNO3 + TERPA3CO3	→	TERPA4O2 + CO2 + 0.5*NO2 + 0.45*TERPNS + 0.48*TERPA3 + 0.02*TERPK + 0.02*CH2O + 0.05*TERPNT + 0.5*HO2	2.00e-12 exp(500.00 / t)
BPINNO3 + TERPACO3	→	TERPA1O2 + CO2 + 0.5*NO2 + 0.45*TERPNS + 0.48*TERPA3 + 0.02*TERPK + 0.02*CH2O + 0.05*TERPNT + 0.5*HO2	2.00e-12 exp(500.00 / t)
BPINO2 + CH3CO3	→	0.32*TERPK + 0.27*TERPF1 + 0.41*TERPA3 + 0.11*CH3COCH3 + 0.65*CH2O + HO2 + CH3O2 + CO2	2.00e-12 exp(500.00 / t)
BPINO2 + CH3O2	→	1.4*CH2O + 0.37*TERPF1 + 0.32*TERPK + 1.5*HO2 + 0.08*CH3COCH3 + 0.31*TERPA3	2.000e-12
BPINO2 + HO2	→	0.68*TERP1OOH + 0.03*OH + 0.03*TERPK + 0.03*CH2O + 0.03*HO2 + 0.29*TERPOOH	2.60e-13 exp(1300.00 / t)
BPINO2 + NO	→	0.08*CH3COCH3 + 0.49*CH2O + 0.2*TERPF1 + 0.24*TERPK + 0.04*TERPNS1 + 0.02*TERPNS + 0.06*TERPNT + 0.13*TERPNT1 + 0.31*TERPA3 + 0.75*HO2 + 0.75*NO2	2.70e-12 exp(360.00 / t)
BPINO2 + NO3	→	0.11*CH3COCH3 + 0.65*CH2O + 0.27*TERPF1 + 0.32*TERPK + 0.41*TERPA3 + HO2 + NO2	2.300e-12
BPINO2 + TERPA2CO3	→	0.32*TERPK + 0.27*TERPF1 + 0.41*TERPA3 + 0.11*CH3COCH3 + 0.65*CH2O + HO2 + TERPA2O2 + CO2	2.00e-12 exp(500.00 / t)
BPINO2 + TERPA3CO3	→	0.32*TERPK + 0.27*TERPF1 + 0.41*TERPA3 + 0.11*CH3COCH3 + 0.65*CH2O + HO2 + TERPA4O2 + CO2	2.00e-12 exp(500.00 / t)
BPINO2 + TERPACO3	→	0.32*TERPK + 0.27*TERPF1 + 0.41*TERPA3 + 0.11*CH3COCH3 + 0.65*CH2O + HO2 + TERPA1O2 + CO2	2.00e-12 exp(500.00 / t)
BPIN + O3	→	0.51*TERPK + 0.3*OH + 0.3*TERPA2CO3 + 0.32*H2O2 + 0.19*BIGALK + 0.19*CO2 + 0.81*CH2O + 0.11*HMHP + 0.08*HCOOH	1.35e-15 exp(-1270.00 / t)
BPIN + OH	→	BPINO2	1.62e-11 exp(460.00 / t)

Table S6: MOZART-TS2 Kinetic Reactions

Reactant		Products	Rate
LIMON + NO3	→	LIMONNO3	1.200e-11
LIMONNO3 + CH3CO3	→	CH3O2 + CO2 + 0.46*NO2 + 0.46*TERPF1 + 0.19*TERPNT1 + 0.35*TERPNS1 + 0.54*HO2	2.00e-12 exp(500.00 / t)
LIMONNO3 + CH3O2	→	0.27*TERPNT1 + 0.91*CH2O + 0.09*CH3OH + 1.01*HO2 + 0.31*TERPF1 + 0.31*NO2 + 0.42*TERPNS1	2.000e-12
LIMONNO3 + HO2	→	0.18*TERPNPT1 + 0.32*TERPNPS1 + 0.5*OH + 0.23*TERPF1 + 0.23*NO2 + 0.18*TERPNS1 + 0.09*TERPNT1 + 0.27*HO2	2.71e-13 exp(1300.00 / t)
LIMONNO3 + LIMONNO3	→	0.42*TERPNT1 + 0.99*HO2 + 0.86*TERPF1 + 0.86*NO2 + 0.72*TERPNS1	5.300e-13
LIMONNO3 + NO	→	0.07*TERPFDN + 1.36*NO2 + 0.43*TERPF1 + 0.17*TERPNT1 + 0.33*TERPNS1 + 0.5*HO2	2.70e-12 exp(360.00 / t)
LIMONNO3 + NO3	→	1.46*NO2 + 0.46*TERPF1 + 0.19*TERPNT1 + 0.35*TERPNS1 + 0.54*HO2	2.300e-12
LIMONNO3 + TERPA2CO3	→	TERPA2O2 + CO2 + 0.46*NO2 + 0.46*TERPF1 + 0.19*TERPNT1 + 0.35*TERPNS1 + 0.54*HO2	2.00e-12 exp(500.00 / t)
LIMONNO3 + TERPA3CO3	→	TERPA4O2 + CO2 + 0.46*NO2 + 0.46*TERPF1 + 0.19*TERPNT1 + 0.35*TERPNS1 + 0.54*HO2	2.00e-12 exp(500.00 / t)
LIMONNO3 + TERPACO3	→	TERPA1O2 + CO2 + 0.46*NO2 + 0.46*TERPF1 + 0.19*TERPNT1 + 0.35*TERPNS1 + 0.54*HO2	2.00e-12 exp(500.00 / t)
LIMONO2 + CH3CO3	→	TERPF1 + 0.56*CH2O + HO2 + CH3O2 + CO2	2.00e-12 exp(500.00 / t)
LIMONO2 + CH3O2	→	0.25*CH3OH + TERPF1 + 1.03*CH2O + HO2	2.000e-12
LIMONO2 + HO2	→	0.9*TERP1OOH + 0.1*TERPF1 + 0.1*OH + 0.1*HO2 + 0.06*CH2O	2.60e-13 exp(1300.00 / t)
LIMONO2 + NO	→	0.17*TERPNT1 + 0.06*TERPNS1 + 0.77*NO2 + 0.77*TERPF1 + 0.77*HO2 + 0.43*CH2O	2.70e-12 exp(360.00 / t)
LIMONO2 + NO3	→	NO2 + TERPF1 + HO2 + 0.56*CH2O	2.300e-12
LIMONO2 + TERPA2CO3	→	TERPF1 + 0.56*CH2O + HO2 + TERPA2O2 + CO2	2.00e-12 exp(500.00 / t)
LIMONO2 + TERPA3CO3	→	TERPF1 + 0.56*CH2O + HO2 + TERPA4O2 + CO2	2.00e-12 exp(500.00 / t)
LIMONO2 + TERPACO3	→	TERPF1 + 0.56*CH2O + HO2 + TERPA1O2 + CO2	2.00e-12 exp(500.00 / t)

Table S6: MOZART-TS2 Kinetic Reactions

Reactant		Products	Rate
LIMON + O3	→	0.66*OH + 0.66*TERPF1 + 0.33*CH3CO3 + 0.33*CH2O + 0.33*TERPA3CO3 + 0.33*H2O2 + 0.01*TERPACID	2.80e-15 exp(-770.00 / t)
LIMON + OH	→	LIMONO2	3.41e-11 exp(470.00 / t)
MYRC + NO3	→	MYRCNO3	1.100e-11
MYRCNO3 + CH3CO3	→	CH3O2 + CO2 + 0.95*NO2 + 0.95*TERPF2 + 0.04*CH2O + 0.05*TERPNS1 + 0.05*HO2 + 0.91*CH3COCH3	2.00e-12 exp(500.00 / t)
MYRCNO3 + CH3O2	→	0.14*TERPNS1 + 0.98*CH2O + 0.77*TERPF2 + 0.77*NO2 + 0.87*HO2 + 0.74*CH3COCH3 + 0.09*TERPNT1 + 0.05*CH3OH	2.000e-12
MYRCNO3 + HO2	→	0.48*OH + 0.48*TERPF2 + 0.02*CH2O + 0.48*NO2 + 0.46*CH3COCH3 + 0.36*TERPNPS1 + 0.16*TERPNPT1	2.71e-13 exp(1300.00 / t)
MYRCNO3 + MYRCNO3	→	0.19*TERPNS1 + 0.27*TERPNT1 + 1.54*NO2 + 1.54*TERPF2 + 1.48*CH3COCH3 + 0.06*CH2O	5.300e-13
MYRCNO3 + NO	→	0.07*TERPFDN + 1.82*NO2 + 0.89*TERPF2 + 0.04*CH2O + 0.04*TERPNS1 + 0.04*HO2 + 0.85*CH3COCH3	2.70e-12 exp(360.00 / t)
MYRCNO3 + NO3	→	1.95*NO2 + 0.95*TERPF2 + 0.04*CH2O + 0.05*TERPNS1 + 0.05*HO2 + 0.91*CH3COCH3	2.300e-12
MYRCNO3 + TERPA2CO3	→	TERPA2O2 + CO2 + 0.95*NO2 + 0.95*TERPF2 + 0.04*CH2O + 0.05*TERPNS1 + 0.05*HO2 + 0.91*CH3COCH3	2.00e-12 exp(500.00 / t)
MYRCNO3 + TERPA3CO3	→	TERPA4O2 + CO2 + 0.95*NO2 + 0.95*TERPF2 + 0.04*CH2O + 0.05*TERPNS1 + 0.05*HO2 + 0.91*CH3COCH3	2.00e-12 exp(500.00 / t)
MYRCNO3 + TERPACO3	→	TERPA1O2 + CO2 + 0.95*NO2 + 0.95*TERPF2 + 0.04*CH2O + 0.05*TERPNS1 + 0.05*HO2 + 0.91*CH3COCH3	2.00e-12 exp(500.00 / t)
MYRCO2 + CH3CO3	→	TERPF2 + HO2 + 0.46*CH3COCH3 + 0.42*CH2O + CH3O2 + CO2	2.00e-12 exp(500.00 / t)
MYRCO2 + CH3O2	→	0.25*CH3OH + TERPF2 + 0.75*CH2O + HO2	2.000e-12
MYRCO2 + HO2	→	0.9*TERP2AOOH + 0.1*TERPF2 + 0.1*OH + 0.1*HO2 + 0.05*CH3COCH3 + 0.04*CH2O	2.60e-13 exp(1300.00 / t)
MYRCO2 + NO	→	0.1*TERPNS1 + 0.19*TERPNT1 + 0.71*NO2 + 0.71*TERPF2 + 0.33*CH3COCH3 + 0.3*CH2O + 0.71*HO2	2.70e-12 exp(360.00 / t)

Table S6: MOZART-TS2 Kinetic Reactions

Reactant		Products	Rate
MYRCO2 + NO3	→	NO2 + TERPF2 + 0.46*CH3COCH3 + 0.42*CH2O + HO2	2.300e-12
MYRCO2 + TERPA2CO3	→	TERPF2 + HO2 + 0.46*CH3COCH3 + 0.42*CH2O + TERPA2O2 + CO2	2.00e-12 exp(500.00 / t)
MYRCO2 + TERPA3CO3	→	TERPF2 + HO2 + 0.46*CH3COCH3 + 0.42*CH2O + TERPA4O2 + CO2	2.00e-12 exp(500.00 / t)
MYRCO2 + TERPACO3	→	TERPF2 + HO2 + 0.46*CH3COCH3 + 0.42*CH2O + TERPA1O2 + CO2	2.00e-12 exp(500.00 / t)
MYRC + O3	→	TERPF2 + 0.63*OH + 0.63*HO2 + 0.25*CH3COCH3 + 0.39*CH2O + 0.18*HYAC	2.65e-15 exp(-520.00 / t)
MYRC + OH	→	MYRCO2	2.100e-10
TERPA2CO3 + NO2 + M	→	TERPA2PAN + M	TROEE(9.70e-29, 5.60, 9.300000e-12, 1.50, 0.60)
TERPA3CO3 + NO2 + M	→	TERPA3PAN + M	TROEE(9.70e-29, 5.60, 9.300000e-12, 1.50, 0.60)
TERPACO3 + NO2 + M	→	TERPAPAN + M	TROEE(9.70e-29, 5.60, 9.300000e-12, 1.50, 0.60)
TERP1OOHO2 + HO2	→	0.82*TERPDHDP + 0.18*TERPOOHL + 0.18*OH + 0.18*HO2 + 0.08*CH2O	2.71e-13 exp(1300.00 / t)
TERP1OOHO2 + NO	→	0.3*TERPHFN + 0.7*NO2 + 0.7*TERPOOHL + 0.31*CH2O + 0.7*HO2	2.70e-12 exp(360.00 / t)
TERP1OOH + OH	→	TERP1OOHO2	8.900e-11
TERP2AOOH + OH	→	TERP2OOHO2	8.900e-11
TERP2OOHO2 + HO2	→	0.82*TERPDHDP + 0.18*TERP1OOH + 0.18*OH + 0.18*HO2	2.71e-13 exp(1300.00 / t)
TERP2OOHO2 + NO	→	0.3*TERPHFN + 0.7*NO2 + 0.7*TERP1OOH + 0.7*HO2	2.70e-12 exp(360.00 / t)
TERPA1O2 + CH3CO3	→	TERPA2O2 + CH3O2 + CO2	2.00e-12 exp(500.00 / t)
TERPA1O2 + CH3O2	→	0.25*CH3OH + 0.75*CH2O + 0.5*HO2 + 0.5*TERPA2 + 0.5*TERPA2O2	2.000e-12
TERPA1O2 + HO2	→	TERPOOH	2.54e-13 exp(1300.00 / t)
TERPA1O2 + NO	→	0.3*TERPNS + 0.7*NO2 + 0.7*TERPA2O2	2.70e-12 exp(360.00 / t)
TERPA1O2 + NO3	→	NO2 + TERPA2O2	2.300e-12
TERPA1O2 + TERPA2CO3	→	2*TERPA2O2 + CO2	2.00e-12 exp(500.00 / t)

Table S6: MOZART-TS2 Kinetic Reactions

Reactant		Products	Rate
TERPA1O2 + TERPA3CO3	→	TERPA2O2 + TERPA4O2 + CO2	2.00e-12 exp(500.00 / t)
TERPA1O2 + TERPACO3	→	TERPA2O2 + TERPA1O2 + CO2	2.00e-12 exp(500.00 / t)
TERPA2CO3 + CH3CO3	→	2*CO2 + TERPA2O2 + CH3O2	2.90e-12 exp(500.00 / t)
TERPA2CO3 + CH3O2	→	CO2 + TERPA2O2 + CH2O + HO2	2.00e-12 exp(500.00 / t)
TERPA2CO3 + HO2	→	0.15*O3 + 0.51*TERPACID2 + 0.49*OH + 0.49*CO2 + 0.49*TERPA2O2	4.30e-13 exp(1040.00 / t)
TERPA2CO3 + NO	→	NO2 + CO2 + TERPA2O2	8.10e-12 exp(270.00 / t)
TERPA2CO3 + NO3	→	NO2 + CO2 + TERPA2O2	4.000e-12
TERPA2CO3 + TERPA2CO3	→	2*CO2 + 2*TERPA2O2	2.90e-12 exp(500.00 / t)
TERPA2CO3 + TERPACO3	→	2*CO2 + TERPA2O2 + TERPA1O2	2.90e-12 exp(500.00 / t)
TERPA2 + NO3	→	HNO3 + TERPA2CO3	2.000e-14
TERPA2O2 + CH3CO3	→	TERPA3O2 + CH3O2 + CO2	2.00e-12 exp(500.00 / t)
TERPA2O2 + CH3O2	→	TERPA3O2 + CH2O + HO2	2.000e-12
TERPA2O2 + HO2	→	0.62*TERPOOH + 0.38*TERPA3O2 + 0.38*OH	2.62e-13 exp(1300.00 / t)
TERPA2O2 + NO	→	0.17*TERPNT + 0.83*NO2 + 0.83*TERPA3O2	2.70e-12 exp(360.00 / t)
TERPA2O2 + NO3	→	NO2 + TERPA3O2	2.300e-12
TERPA2O2 + TERPA2CO3	→	TERPA3O2 + TERPA2O2 + CO2	2.00e-12 exp(500.00 / t)
TERPA2O2 + TERPA3CO3	→	TERPA3O2 + TERPA4O2 + CO2	2.00e-12 exp(500.00 / t)
TERPA2O2 + TERPACO3	→	TERPA3O2 + TERPA1O2 + CO2	2.00e-12 exp(500.00 / t)
TERPA2 + OH	→	TERPA2CO3	5.20e-12 exp(600.00 / t)
TERPA2PAN + OH	→	CH3COCH3 + 2*CO2 + 2*CH2O + NO2 + 2*CO + HO2	2.520e-11
TERPA3CO3 + CH3CO3	→	2*CO2 + TERPA4O2 + CH3O2	2.90e-12 exp(500.00 / t)
TERPA3CO3 + CH3O2	→	CO2 + TERPA4O2 + CH2O + HO2	2.00e-12 exp(500.00 / t)

Table S6: MOZART-TS2 Kinetic Reactions

Reactant		Products	Rate
TERPA3CO3 + HO2	→	0.15*O3 + 0.51*TERPACID3 + 0.49*OH + 0.49*CO2 + 0.49*TERPA4O2	4.30e-13 exp(1040.00 / t)
TERPA3CO3 + NO	→	NO2 + CO2 + TERPA4O2	8.10e-12 exp(270.00 / t)
TERPA3CO3 + NO3	→	NO2 + CO2 + TERPA4O2	4.000e-12
TERPA3CO3 + TERPA2CO3	→	2*CO2 + TERPA4O2 + TERPA2O2	2.90e-12 exp(500.00 / t)
TERPA3CO3 + TERPA3CO3	→	2*CO2 + 2*TERPA4O2	2.90e-12 exp(500.00 / t)
TERPA3CO3 + TERPACO3	→	2*CO2 + TERPA4O2 + TERPA1O2	2.90e-12 exp(500.00 / t)
TERPA3 + NO3	→	HNO3 + TERPA3CO3	2.000e-14
TERPA3O2 + CH3CO3	→	TERPA4O2 + CH3COCH3 + CH3O2 + CO2	2.00e-12 exp(500.00 / t)
TERPA3O2 + CH3O2	→	TERPA4O2 + CH3COCH3 + CH2O + HO2	2.000e-12
TERPA3O2 + HO2	→	0.85*TERPOOHL + 0.15*TERPA4O2 + 0.15*OH + 0.15*CH3COCH3	2.66e-13 exp(1300.00 / t)
TERPA3O2 + NO	→	0.3*TERPNT + 0.7*NO2 + 0.7*TERPA4O2 + 0.7*CH3COCH3	2.70e-12 exp(360.00 / t)
TERPA3O2 + NO3	→	NO2 + TERPA4O2 + CH3COCH3	2.300e-12
TERPA3O2 + TERPA2CO3	→	TERPA4O2 + CH3COCH3 + TERPA2O2 + CO2	2.00e-12 exp(500.00 / t)
TERPA3O2 + TERPA3CO3	→	2*TERPA4O2 + CH3COCH3 + CO2	2.00e-12 exp(500.00 / t)
TERPA3O2 + TERPACO3	→	TERPA4O2 + CH3COCH3 + TERPA1O2 + CO2	2.00e-12 exp(500.00 / t)
TERPA3 + OH	→	0.75*TERPA3CO3 + 0.25*TERPA4O2	5.20e-12 exp(600.00 / t)
TERPA3PAN + OH	→	CO + NO2 + 3*CO2 + 2*CH3CO3 + CH2O + HO2	1.920e-11
TERPA4O2 + CH3CO3	→	CH3CO3 + HO2 + 2*CH2O + CO + CH3O2 + CO2	2.00e-12 exp(500.00 / t)
TERPA4O2 + CH3O2	→	CH3CO3 + 2*HO2 + 3*CH2O + CO	2.000e-12
TERPA4O2 + HO2	→	0.47*TERPOOHL + 0.53*CH3CO3 + 0.53*HO2 + 1.06*CH2O + 0.53*CO + 0.53*OH	2.51e-13 exp(1300.00 / t)
TERPA4O2 + NO	→	0.09*TERPNS + 0.91*NO2 + 0.91*CH3CO3 + 0.91*HO2 + 1.82*CH2O + 0.91*CO	2.70e-12 exp(360.00 / t)
TERPA4O2 + NO3	→	NO2 + CH3CO3 + HO2 + 2*CH2O + CO	2.300e-12

Table S6: MOZART-TS2 Kinetic Reactions

Reactant		Products	Rate
TERPA4O2 + TERPA2CO3	→	CH3CO3 + HO2 + 2*CH2O + CO + TERPA2O2 + CO2	2.00e-12 exp(500.00 / t)
TERPA4O2 + TERPA3CO3	→	CH3CO3 + HO2 + 2*CH2O + CO + TERPA4O2 + CO2	2.00e-12 exp(500.00 / t)
TERPA4O2 + TERPACO3	→	CH3CO3 + HO2 + 2*CH2O + CO + TERPA1O2 + CO2	2.00e-12 exp(500.00 / t)
TERPACID2 + OH	→	0.71*TERPA2CO3 + 0.29*CO2 + 0.29*TERPA2O2	8.800e-12
TERPACID3 + OH	→	0.71*TERPA3CO3 + 0.29*CO2 + 0.29*TERPA4O2	8.800e-12
TERPACID + OH	→	0.71*TERPACO3 + 0.29*CO2 + 0.29*TERPA1O2	8.800e-12
TERPACO3 + CH3CO3	→	2*CO2 + TERPA1O2 + CH3O2	2.90e-12 exp(500.00 / t)
TERPACO3 + CH3O2	→	CO2 + TERPA1O2 + CH2O + HO2	2.00e-12 exp(500.00 / t)
TERPACO3 + HO2	→	0.15*O3 + 0.51*TERPACID + 0.49*OH + 0.49*CO2 + 0.49*TERPA1O2	4.30e-13 exp(1040.00 / t)
TERPACO3 + NO	→	NO2 + CO2 + TERPA1O2	8.10e-12 exp(270.00 / t)
TERPACO3 + NO3	→	NO2 + CO2 + TERPA1O2	4.000e-12
TERPACO3 + TERPACO3	→	2*CO2 + 2*TERPA1O2	2.90e-12 exp(500.00 / t)
TERPA + NO3	→	HNO3 + TERPACO3	2.000e-14
TERPA + OH	→	0.77*TERPACO3 + 0.23*TERPA2O2	5.20e-12 exp(600.00 / t)
TERPAPAN + OH	→	TERPA2 + NO2 + CO	3.660e-12
TERPDHDP + OH	→	TERPOOH + OH	2.800e-11
TERPF1 + NO3	→	NO2 + 0.44*CH2O + TERPA3	2.600e-13
TERPF1O2 + HO2	→	0.9*TERPOOHL + 0.1*OH + 0.1*HO2 + 0.1*TERPA3 + 0.04*CH2O	2.68e-13 exp(1300.00 / t)
TERPF1O2 + NO	→	0.3*TERPHFN + 0.7*NO2 + 0.7*HO2 + 0.7*TERPA3 + 0.31*CH2O	2.70e-12 exp(360.00 / t)
TERPF1 + O3	→	0.09*OH + TERPA3 + 0.62*CH2O + 0.23*HMHP + 0.02*H2O2 + 0.15*HCOOH	8.300e-18
TERPF1 + OH	→	0.83*TERPF1O2 + 0.17*TERPA3CO3	1.100e-10
TERPF2 + NO3	→	0.5*TERPNS1 + 0.5*HO2 + 0.5*TERPF1 + 0.5*CH2O + 0.5*NO2	2.95e-12 exp(-450.00 / t)
TERPF2O2 + HO2	→	0.9*TERP1OOH + 0.1*OH + 0.1*HO2 + 0.1*TERPF1	2.47e-13 exp(1300.00 / t)

Table S6: MOZART-TS2 Kinetic Reactions

Reactant		Products	Rate
TERPF2O2 + NO	→	**0.18*TERPNT1 + 0.12*TERPNS1 + 0.7*NO2 + 0.7*HO2 + 0.7*TERPF1**	**2.70e-12 exp(360.00 / t)**
TERPF2 + O3	→	**TERPF1 + 0.34*CH2O + 0.4*HMHP + 0.04*H2O2 + 0.26*HCOOH**	**1.100e-16**
TERPF2 + OH	→	**TERPF2O2**	**2.70e-11 exp(390.00 / t)**
TERPFDN + OH	→	**NO2 + TERPNS**	**3.640e-12**
TERPHFN + OH	→	**TERPNS + OH**	**2.800e-11**
TERPK + OH	→	**0.14*TERPA2CO3 + 0.86*TERPA1O2**	**1.700e-11**
TERPNPS1O2 + HO2	→	**0.9*TERPHFN + 0.1*OH + 0.1*TERPNPS + 0.1*HO2**	**2.76e-13 exp(1300.00 / t)**
TERPNPS1O2 + NO	→	**0.3*TERPFDN + 0.7*NO2 + 0.7*TERPNPS + 0.7*HO2**	**2.70e-12 exp(360.00 / t)**
TERPNPS1 + OH	→	**TERPNPS1O2**	**1.100e-10**
TERPNPS + OH	→	**H2O + BPINNO3**	**9.580e-12**
TERPNPT1O2 + HO2	→	**0.9*TERPHFN + 0.1*OH + 0.1*TERPNPT + 0.1*HO2**	**2.76e-13 exp(1300.00 / t)**
TERPNPT1O2 + NO	→	**0.3*TERPFDN + 0.7*NO2 + 0.7*TERPNPT + 0.7*HO2**	**2.70e-12 exp(360.00 / t)**
TERPNPT1 + OH	→	**TERPNPT1O2**	**1.100e-10**
TERPNPT + OH	→	**TERPNT + H2O + OH**	**1.230e-11**
TERPNS1O2 + HO2	→	**0.9*TERPHFN + 0.1*OH + 0.1*TERPNS + 0.1*HO2**	**2.75e-13 exp(1300.00 / t)**
TERPNS1O2 + NO	→	**0.3*TERPFDN + 0.7*NO2 + 0.7*TERPNS + 0.7*HO2**	**2.70e-12 exp(360.00 / t)**
TERPNS1 + OH	→	**TERPNS1O2**	**1.100e-10**
TERPNS + OH	→	**TERPA + NO2**	**3.640e-12**
TERPNT1O2 + HO2	→	**0.9*TERPHFN + 0.1*OH + 0.1*TERPNT + 0.1*HO2**	**2.75e-13 exp(1300.00 / t)**
TERPNT1O2 + NO	→	**0.3*TERPFDN + 0.7*NO2 + 0.7*TERPNT + 0.7*HO2**	**2.70e-12 exp(360.00 / t)**
TERPNT1 + OH	→	**TERPNT1O2**	**1.100e-10**
TERPNT + OH	→	**TERPA + NO2**	**5.500e-12**
TERPOOHL + OH	→	**TERPA3 + OH**	**4.650e-11**
TERPOOH + OH	→	**TERPA + OH**	**2.800e-11**
TERPA2PAN + M	→	**M + TERPA2CO3 + NO2**	
TERPA3PAN + M	→	**TERPA3CO3 + NO2 + M**	
TERPAPAN + M	→	**TERPACO3 + NO2 + M**	
Sulfur Compounds			
OCS + O	→	SO + CO	2.10e-11 exp(-2200.00 / t)
OCS + OH	→	SO2 + CO + H	7.20e-14 exp(-1070.00 / t)
S + O2	→	SO + O	2.300e-12
S + O3	→	SO + O2	1.200e-11
SO + BRO	→	SO2 + BR	5.700e-11

Table S6: MOZART-TS2 Kinetic Reactions

Reactant		**Products**	**Rate**
SO + CLO	→	SO2 + CL	2.800e-11
S + OH	→	SO + H	6.600e-11
SO + NO2	→	SO2 + NO	1.400e-11
SO + O2	→	SO2 + O	1.60e-13 exp(-2280.00 / t)
SO + O3	→	SO2 + O2	3.40e-12 exp(-1100.00 / t)
SO + OCLO	→	SO2 + CLO	1.900e-12
SO + OH	→	SO2 + H	2.70e-11 exp(335.00 / t)
SO2 + OH	→	SO3 + HO2	ko = 3.0e-31 (300 / t)$^{3.3}$, ki = 1.5e-12, f=0.6
SO3 + H2O	→	H2SO4	8.5e-21*[H2O]* exp(6540 / t) * 1.0e-20
Tropospheric Aerosol [b]			
DMS + NO3	→	SO2 + HNO3	1.90e-13 exp(520.00 / t)
DMS + OH	→	SO2	9.60e-12 exp(-234.00 / t)
NH3 + OH	→	H2O	1.70e-12 exp(-710.00 / t)
DMS + OH	→	0.5*SO2 + 0.5*HO2	1.7e-42 exp(7810 / t) * [M] * 0.21 / (1+5.5e-31 exp(7460 / t) * [M] * 0.21)
GLYOXAL	→	SOAG0	γ = 0.0002
HO2	→	0.5*H2O2	γ = 0.2
HONITR	→	HNO3	γ = 0.005
ICHE	→	**M**	γ **= 0.0042**
IEPOX	→	**M**	γ **= 0.0042**
INHEB	→	**HNO3**	γ **= 0.02**
INHED	→	**HNO3**	γ **= 0.02**
ISOPNOOHD	→	**HNO3**	γ **= 0.02**
ISOPFDN	→	**HNO3**	γ **= 0.1**
ISOPFDNC	→	**HNO3**	γ **= 0.1**
ISOPFNC	→	**M**	γ **= 0.1**
ISOPFNP	→	**M**	γ **= 0.1**
ISOPHFP	→	**M**	γ **= 0.1**
ISOPN1D	→	**HNO3**	γ **= 0.02**
ISOPN2B	→	**HNO3**	γ **= 0.02**
ISOPN4D	→	**HNO3**	γ **= 0.02**
N2O5	→	2*HNO3	γ = 0.1

Table S6: MOZART-TS2 Kinetic Reactions

Reactant		Products	Rate
NC4CHO	→	HNO3	γ = 0.005
NH4	→	M	6.340e-8
NO2	→	0.5*OH + 0.5*NO + 0.5*HNO3	γ = 0.0001
NO3	→	HNO3	γ = 0.001
ONITR	→	HNO3	γ = 0.005
SQTN	→	**M**	**γ = 0.1**
TERPDHDP	→	**M**	**γ = 0.1**
TERPFDN	→	**HNO3**	**γ = 0.1**
TERPHFN	→	**M**	**γ = 0.1**
TERPNPT1	→	**HNO3**	**γ = 0.02**
TERPNPT	→	**HNO3**	**γ = 0.02**
TERPNT1	→	**HNO3**	**γ = 0.02**
TERPNT	→	**HNO3**	**γ = 0.02**
Secondary Organic Aerosol [c]			
APIN + NO3	→	**APIN + NO3 + 0.17493*SOAG3 + 0.59019*SOAG4**	**1.20e-12 exp(490.00 / t)**
APIN + O3	→	**APIN + O3 + 0.0508*SOAG0 + 0.1149*SOAG1 + 0.0348*SOAG2 + 0.0554*SOAG3 + 0.1278*SOAG4**	**8.05e-16 exp(-640.00 / t)**
APIN + OH	→	**APIN + OH + 0.0508*SOAG0 + 0.1149*SOAG1 + 0.0348*SOAG2 + 0.0554*SOAG3 + 0.1278*SOAG4**	**1.34e-11 exp(410.00 / t)**
BCARY + NO3	→	BCARY + NO3 + 0.17493*SOAG3 + 0.59019*SOAG4	1.900e-11
BCARY + O3	→	BCARY + O3 + 0.2202*SOAG0 + 0.2067*SOAG1 + 0.0653*SOAG2 + 0.1284*SOAG3 + 0.114*SOAG4	1.200e-14
BCARY + OH	→	BCARY + OH + 0.2202*SOAG0 + 0.2067*SOAG1 + 0.0653*SOAG2 + 0.1284*SOAG3 + 0.114*SOAG4	2.000e-10
BENZENE + OH	→	BENZENE + OH + 0.0023*SOAG0 + 0.0008*SOAG1 + 0.0843*SOAG2 + 0.0443*SOAG3 + 0.1621*SOAG4	2.30e-12 exp(-193.00 / t)
BPIN + NO3	→	**BPIN + NO3 + 0.17493*SOAG3 + 0.59019*SOAG4**	**2.500e-12**
BPIN + O3	→	**BPIN + O3 + 0.0508*SOAG0 + 0.1149*SOAG1 + 0.0348*SOAG2 + 0.0554*SOAG3 + 0.1278*SOAG4**	**1.35e-15 exp(-1270.00 / t)**
BPIN + OH	→	**BPIN + OH + 0.0508*SOAG0 + 0.1149*SOAG1 + 0.0348*SOAG2 + 0.0554*SOAG3 + 0.1278*SOAG4**	**1.62e-11 exp(460.00 / t)**
ISOP + NO3	→	ISOP + NO3 + 0.059024*SOAG3 + 0.025024*SOAG4	3.03e-12 exp(-446.00 / t)
ISOP + O3	→	ISOP + O3 + 0.0033*SOAG3	1.05e-14 exp(-2000.00 / t)
ISOP + OH	→	ISOP + OH + 0.0031*SOAG0 + 0.0035*SOAG1 + 0.0003*SOAG2 + 0.0271*SOAG3 + 0.0474*SOAG4	2.54e-11 exp(410.00 / t)

Table S6: MOZART-TS2 Kinetic Reactions

Reactant		Products	Rate
IVOC + OH	→	OH + 0.2381*SOAG0 + 0.1308*SOAG1 + 0.0348*SOAG2 + 0.0076*SOAG3 + 0.0113*SOAG4	1.340e-11
LIMON + NO3	→	**LIMON + NO3 + 0.17493*SOAG3 + 0.59019*SOAG4**	**1.200e-11**
LIMON + O3	→	**LIMON + O3 + 0.0508*SOAG0 + 0.1149*SOAG1 + 0.0348*SOAG2 + 0.0554*SOAG3 + 0.1278*SOAG4**	**2.80e-15 exp(-770.00 / t)**
LIMON + OH	→	**LIMON + OH + 0.0508*SOAG0 + 0.1149*SOAG1 + 0.0348*SOAG2 + 0.0554*SOAG3 + 0.1278*SOAG4**	**3.41e-11 exp(470.00 / t)**
MYRC + NO3	→	**MYRC + NO3 + 0.17493*SOAG3 + 0.59019*SOAG4**	**1.100e-11**
MYRC + O3	→	**MYRC + O3 + 0.0508*SOAG0 + 0.1149*SOAG1 + 0.0348*SOAG2 + 0.0554*SOAG3 + 0.1278*SOAG4**	**2.65e-15 exp(-520.00 / t)**
MYRC + OH	→	**MYRC + OH + 0.0508*SOAG0 + 0.1149*SOAG1 + 0.0348*SOAG2 + 0.0554*SOAG3 + 0.1278*SOAG4**	**2.100e-10**
SVOC + OH	→	OH + 0.5931*SOAG0 + 0.1534*SOAG1 + 0.0459*SOAG2 + 0.0085*SOAG3 + 0.0128*SOAG4	1.340e-11
TOLUENE + OH	→	TOLUENE + OH + 0.1364*SOAG0 + 0.0101*SOAG1 + 0.0763*SOAG2 + 0.2157*SOAG3 + 0.0232*SOAG4	1.70e-12 exp(352.00 / t)
XYLENES + OH	→	XYLENES + OH + 0.1677*SOAG0 + 0.0174*SOAG1 + 0.086*SOAG2 + 0.0512*SOAG3 + 0.1598*SOAG4	1.700e-11
Stratospheric Heterogeneous Uptake Reactions			
Sulfate aerosol reactions			
N2O5 + H2O(l)	→	2*HNO3	γ = f(wt%)
CLONO2 + H2O(l)	→	HOCL + HNO3	γ = f(T,P,HCl,H2O,r)
BRONO2 + H2O(l)	→	HOBR + HNO3	γ = f(T,P,H2O,r)
CLONO2 + HCL(l)	→	CL2 + HNO3	γ = f(T,P,HCl,H2O,r)
HOCL + HCL(l)	→	CL2 + H2O	γ = f(T,P,HCl,HOCl,H2O,r)
HOBR + HCL(l)	→	BRCL + H2O	γ = f(T,P,HCl,HOBr,H2O,r)
Nitric Acid Tri-hydrate Reactions			
N2O5 + H2O(s)	→	2*HNO3	γ = 4e-4
CLONO2 + H2O(s)	→	HOCL + HNO3	γ = 4e-3
CLONO2 + HCL(s)	→	CL2 + HNO3	γ = 0.2
HOCL + HCL(s)	→	CL2 + H2O	γ = 0.1
BRONO2 + H2O(s)	→	HOBR + HNO3	γ = 0.006
Water-Ice Aerosol Reactions			
N2O5 + H2O(s)	→	2*HNO3	γ = 0.02
CLONO2 + H2O(s)	→	HOCL + HNO3	γ = 0.3

Table S6: MOZART-TS2 Kinetic Reactions

Reactant		**Products**	**Rate**
BRONO2 + H2O(s)	$\rightarrow$	HOBR + HNO3	γ = 0.3
CLONO2 + HCL(s)	$\rightarrow$	CL2 + HNO3	γ = 0.3
HOCL + HCL(s)	$\rightarrow$	CL2 + H2O	γ = 0.2
HOBR + HCL(s)	$\rightarrow$	BRCL + H2O	γ = 0.3
Synthetic Tracers			
AOA_NH	$\rightarrow$	AOA_NH	1.000e+0
E90	$\rightarrow$	sink	1.290e-7
NH_50	$\rightarrow$	M	2.310e-7
NH_5	$\rightarrow$	M	2.310e-6
ST80_25	$\rightarrow$	M	4.630e-7

• [a] For all isoprene peroxy radicals, the RO_2 + NO general reaction rate constant (2.7e-12 exp(360/T)) from MCM v3.3.1 is used with the pressure and temperature dependent organic nitrate yield recommended by Wennberg et al. (2018), which is based on Arey et al. (2001). The organic nitrate yield (α) at T = 293 K and M = 2.45e19 molecules cm^{-3} and the number of heavy atoms excluding the peroxy group (n) are reported above. α and n are used in the following equation to calculate the temperature and pressure dependent organic nitrate branching ratio (α_RONO2):

α_RONO2 = $\frac{A(T,M,n)}{A(T,M,n)+A_0(n)*\frac{1-\alpha(n)}{\alpha(n)}}$, where $A_0(n) = A(T = 293K, M = 2.45e19, n)$,

γ = 2e-22 cm^3 molecule^{-1}, T = temperature (K), [M] is the number density of air in molecules cm^{-3},

and $A(T,M,n)$ = $\frac{\gamma e^n[M]}{1+\frac{\gamma e^n[M]}{0.43(T(K)/298)^{-8}}} * 0.41^{(1+[log(\gamma e^n[M]/0.43(T(K)/298)^{-8})]^2)^{-1}}$

• [b] For new gas-phase species undergoing aerosol uptake, the aerosol uptake coefficient (γ) value is reported.

• [c] Secondary organic aerosol reactions in bold were added only to treat the new tracers (APIN, BPIN, LIMON, and. MYRC) separately. No changes are made to the yields of the SOA gas-phase tracers.

Table S7: MOZART-TS2 Kinetic Reactions Changed For Box-Model Sensitivity Tests

Reactant		Products	Rate
Caltech assumptions for PAN and C_4 dihydroperoxy carbonyls			
Removed the following reactions:			
PAN + hν	→	**0.6*CH3CO3 + 0.6*NO2 + 0.4*CH3O2 + 0.4*NO3 + 0.4*CO2**	**jpan**
CH3CO3 + CH3CO3	→	**2*CH3O2 + 2*CO2**	**2.90e-12 exp(500.00 / t)**
Changed the following reactions:			
PAN + OH	→	**CH2O + CO + NO2**	**3.000e-14**
CH3CO3 + NO2	→	**PAN**	**TROE_I(2.591E-28,0.,-6.87,1.125E-11,0.,-1.105,0.3)**
PAN	→	**CH3CO3 + NO2**	**TROE_I(3.871E-3,-12100.,0.,5.4E16,-13830.,0.,0.3)**
ISOPZD1O2	→	0.15*HPALDB1C + 0.25*HPALD1 + 0.4*HO2 + **1.5*OH + 0.3*CH3COCHO + 0.3*CH2O + 0.3*HCOCH2OOH + 0.3*CH3CO3** + 0.6*CO	5.05e15 exp(-12200.00 / t) exp(1e8 / t^3)
ISOPZD4O2	→	0.15*HPALDB4C + 0.25*HPALD4 + 0.4*HO2 + **1.5*OH + 0.3*CH3COCHO + 0.3*CH2O + 0.3*HYPERACET + 0.9*CO**	2.22e9 exp(-7160.00 / t) exp(1e8 / t^3)
Caltech assumptions for PAN, C_4 dihydroperoxy carbonyls, and carbonyl nitrates			
Removed the following reactions:			
PAN + hν	→	**0.6*CH3CO3 + 0.6*NO2 + 0.4*CH3O2 + 0.4*NO3 + 0.4*CO2**	**jpan**
CH3CO3 + CH3CO3	→	**2*CH3O2 + 2*CO2**	**2.90e-12 exp(500.00 / t)**
Changed the following reactions:			
PAN + OH	→	**CH2O + CO + NO2**	**3.000e-14**
CH3CO3 + NO2	→	**PAN**	**TROE_I(2.591E-28,0.,-6.87,1.125E-11,0.,-1.105,0.3)**
PAN	→	**CH3CO3 + NO2**	**TROE_I(3.871E-3,-12100.,0.,5.4E16,-13830.,0.,0.3)**
ISOPZD1O2	→	0.15*HPALDB1C + 0.25*HPALD1 + 0.4*HO2 + **1.5*OH + 0.3*CH3COCHO + 0.3*CH2O + 0.3*HCOCH2OOH + 0.3*CH3CO3** + 0.6*CO	5.05e15 exp(-12200.00 / t) exp(1e8 / t^3)
ISOPZD4O2	→	0.15*HPALDB4C + 0.25*HPALD4 + 0.4*HO2 + **1.5*OH + 0.3*CH3COCHO + 0.3*CH2O + 0.3*HYPERACET + 0.9*CO**	2.22e9 exp(-7160.00 / t) exp(1e8 / t^3)

Table S7: MOZART-TS2 Kinetic Reactions Changed For Box-Model Sensitivity Tests

Reactant		Products	Rate
ISOPFDNC + hν	→	2*NO2 + 0.5*CH3COCHO + 0.5*GLYALD + 0.5*HYAC + 0.5*GLYOXAL	**0.86***jch2o_a
ISOPFNC + hν	→	OH + NO2 + 0.5*GLYALD + 0.5*CH3COCHO + 0.5*HYAC + 0.5*GLYOXAL	**0.89***jch2o_a
MACRN + hν	→	0.75*CO + 0.75*NO2 + 0.5*HYAC + 1.25*HO2 + 0.25*CH3COCHO + 0.25*CH2O + 0.25*NOA	**0.70***jch2o_a
MVKN + hν	→	0.75*NO2 + 0.25*NO3CH2CHO + 0.75*CH3CO3 + 0.5*GLYALD + 0.5*HO2 + 0.25*CH2O + 0.25*CH3COCHO	**1.15***jch2o_a
NC4CHO + hν	→	NO2 + HO2 + HYDRALD	**4.86***jch2o_a
NO3CH2CHO + hν	→	NO2 + CH2O + CO + HO2	**1.39***jch2o_a
NOA + hν	→	NO2 + CH2O + CH3CO3	**0.18***jch2o_a
MCM v3.3.1 assumptions for pinonaldehyde nitrate yield			
Changed the following reactions:			
TERPA1O2 + NO	→	**0.16***TERPNS + **0.84***NO2 + **0.84***TERPA2O2	2.70e-12 exp(360.00 / t)
TERPA2O2 + NO	→	**0.03***TERPNT + **0.97***NO2 + **0.97***TERPA3O2	2.70e-12 exp(360.00 / t)
TERPA3O2 + NO	→	**0.12***TERPNT + **0.88***NO2 + **0.88***TERPA4O2 + **0.88***CH3COCH3	2.70e-12 exp(360.00 / t)
TERPA4O2 + NO	→	**0.05***TERPNS + **0.95***NO2 + **0.95***CH3CO3 + **0.95***HO2 + **1.9***CH2O + **0.95***CO	2.70e-12 exp(360.00 / t)
MCM v3.3.1 assumptions for pinonaldehyde and limonaldehyde/limaketone nitrate yield			
Changed the following reactions:			
TERPA1O2 + NO	→	**0.16***TERPNS + **0.84***NO2 + **0.84***TERPA2O2	2.70e-12 exp(360.00 / t)
TERPA2O2 + NO	→	**0.03***TERPNT + **0.97***NO2 + **0.97***TERPA3O2	2.70e-12 exp(360.00 / t)
TERPA3O2 + NO	→	**0.12***TERPNT + **0.88***NO2 + **0.88***TERPA4O2 + **0.88***CH3COCH3	2.70e-12 exp(360.00 / t)
TERPA4O2 + NO	→	**0.05***TERPNS + **0.95***NO2 + **0.95***CH3CO3 + **0.95***HO2 + **1.9***CH2O + **0.95***CO	2.70e-12 exp(360.00 / t)
TERPF1O2 + NO	→	**0.15***TERPHFN + **0.85***NO2 + **0.85***HO2 + **0.85***TERPA3 + 0.31*CH2O	2.70e-12 exp(360.00 / t)
MCM pinonaldehyde and limonaldehyde/limaketone nitrate yield and oxidation of unsaturated hydroxy nitrates			
Changed the following reactions:			
TERPA1O2 + NO	→	**0.16***TERPNS + **0.84***NO2 + **0.84***TERPA2O2	2.70e-12 exp(360.00 / t)
TERPA2O2 + NO	→	**0.03***TERPNT + **0.97***NO2 + **0.97***TERPA3O2	2.70e-12 exp(360.00 / t)

Table S7: MOZART-TS2 Kinetic Reactions Changed For Box-Model Sensitivity Tests

Reactant		**Products**	**Rate**
TERPA3O2 + NO	→	**0.12***TERPNT + **0.88***NO2 + **0.88***TERPA4O2 + **0.88***CH3COCH3	2.70e-12 exp(360.00 / t)
TERPA4O2 + NO	→	**0.05***TERPNS + **0.95***NO2 + **0.95***CH3CO3 + **0.95***HO2 + **1.9***CH2O + **0.95***CO	2.70e-12 exp(360.00 / t)
TERPF1O2 + NO	→	**0.15***TERPHFN + **0.85***NO2 + **0.85***HO2 + **0.85***TERPA3 + 0.31*CH2O	2.70e-12 exp(360.00 / t)
TERPNS1 + OH	→	**TERPF1+NO2**	1.100e-10
TERPNT1 + OH	→	**TERPF1+NO2**	1.100e-10

Table S8: MOZART-TS2 Kinetic Reactions Changed For CESM/CAM-Chem Sensitivity Tests

Reactant		Products	Rate
I_TEST1 Sensitivity Test			
Updated the following reactions:			
ISOPB1O2 + NO	→	NO2 + MVK + CH2O + HO2	In code, α **= 0.09**, n = 6
ISOPB1O2 + NO	→	ISOPN2B	In code, α **= 0.09**, n = 6
ISOPB4O2 + NO	→	NO2 + MACR + CH2O + HO2	In code, α **= 0.13**, n = 6
ISOPB4O2 + NO	→	ISOPN3B	In code, α **= 0.09**, n = 6
ISOPED1O2 + NO	→	NO2 + 0.45*HYDRALD + 0.45*HO2 + 0.55*MVKOOH + 0.55*CO + 0.55*OH	In code, α **= 0.09**, n = 6
ISOPED1O2 + NO	→	ISOPN4D	In code, α **= 0.09**, n = 6
ISOPED4O2 + NO	→	NO2 + 0.45*HYDRALD + 0.45*HO2 + 0.55*MACROOH + 0.55*CO + 0.55*OH	In code, α **= 0.09**, n = 6
ISOPED4O2 + NO	→	ISOPN1D	In code, α **= 0.09**, n = 6
ISOPZD1O2 + NO	→	NO2 + 0.45*HYDRALD + 0.45*HO2 + 0.55*MVKOOH + 0.55*CO + 0.55*OH	In code, α **= 0.09**, n = 6
ISOPZD1O2 + NO	→	ISOPN4D	In code, α **= 0.09**, n = 6
ISOPZD4O2 + NO	→	NO2 + 0.45*HYDRALD + 0.45*HO2 + 0.55*MACROOH + 0.55*CO + 0.55*OH	In code, α **= 0.09**, n = 6
ISOPZD4O2 + NO	→	ISOPN1D	In code, α **= 0.09**, n = 6
I_TEST2 Sensitivity Test			
Updated the following reactions:			
ISOPN1DO2 + NO	→	NO2 + HO2 + 0.94*NOA + 0.94*GLYALD + 0.06*MACRN + 0.06*CH2O	In code, α **= 0.3**, n = 11
ISOPN1DO2 + NO	→	ISOPFDN	In code, α **= 0.3**, n = 11
ISOPN2BO2 + NO	→	1.73*NO2 + 0.27*MACRN + 0.27*CH2O + 0.27*HO2 + 0.73*HYAC + 0.73*GLYALD	In code, α **= 0.3**, n = 11
ISOPN2BO2 + NO	→	ISOPFDN	In code, α **= 0.3**, n = 11
ISOPN3BO2 + NO	→	NO2 + MVKN + CH2O + HO2	In code, α **= 0.3**, n = 11
ISOPN3BO2 + NO	→	ISOPFDN	In code, α **= 0.3**, n = 11
ISOPN4DO2 + NO	→	NO2 + HO2 + 0.13*MVKN + 0.13*CH2O + 0.87*HYAC + 0.87*NO3CH2CHO	In code, α **= 0.3**, n = 11
ISOPN4DO2 + NO	→	ISOPFDN	In code, α **= 0.3**, n = 11
ISOPNBNO3O2 + NO	→	NO2 + HO2 + 0.21*MACRN + 0.12*MVKN + 0.33*CH2O + 0.34*NOA + 0.34*GLYALD + 0.33*HYAC + 0.33*NO3CH2CHO	In code, α **= 0.3**, n = 11
ISOPNBNO3O2 + NO	→	ISOPFDN	In code, α **= 0.3**, n = 11

Table S8: MOZART-TS2 Kinetic Reactions Changed For CESM/CAM-Chem Sensitivity Tests

Reactant		**Products**	**Rate**
ISOPNOOHBO2 + NO	→	NO2 + 0.53*CH2O + 0.53*HO2 + 0.49*MACRN + 0.04*MVKN + 0.4*NOA + 0.4*GLYALD + 0.07*HYAC + 0.07*NO3CH2CHO + 0.47*OH	In code, α **= 0.3**, n = 12
ISOPNOOHBO2 + NO	→	ISOPFDN	In code, α **= 0.3**, n = 12
ISOPNOOHDO2 + NO	→	NO2 + 0.04*CH2O + 0.04*OH + 0.02*MACRN + 0.02*MVKN + 0.81*NOA + 0.81*HCOCH2OOH + 0.15*HYPERACET + 0.15*NO3CH2CHO + 0.96*HO2	In code, α **= 0.3**, n = 12
ISOPNOOHDO2 + NO	→	ISOPFDN	In code, α **= 0.3**, n = 12
NC4CHOO2 + NO	→	NO2 + HO2 + 0.13*NOA + 0.13*GLYOXAL + 0.12*CH3COCHO + 0.12*NO3CH2CHO + 0.39*MACRN + 0.36*MVKN + 0.75*CO	In code, α **= 0.3**, n = 11
NC4CHOO2 + NO	→	ISOPFDNC	In code, α **= 0.3**, n = 11
I_TEST3 Sensitivity Test			
Removed the following reactions:			
ISOPN1DO2	→	**ISOPFNP + HO2**	**1.26e+13 exp(-10000.00 / t)**
ISOPN2BO2	→	**ISOPFNC + HO2**	**1.88e+13 exp(-10000.00 / t)**
ISOPN3BO2	→	**ISOPFNC + HO2**	**1.88e+13 exp(-10000.00 / t)**
ISOPN4DO2	→	**ISOPFNP + HO2**	**5.09e+12 exp(-10000.00 / t)**
ISOPNOOHBO2	→	**OH + ISOPFNP**	**8.72e+12 exp(-10000.00 / t)**
ISOPNOOHDO2	→	**OH + ISOPFNP**	**6.55e+12 exp(-10000.00 / t)**
T_TEST1 Sensitivity Test			
Updated the following reactions:			
APINO2 + NO	→	0.01*TERPHFN + **0.04***TERPNS1 + **0.13***TERPNS + **0.06***TERPNT + **0.06***TERPNT1 + **0.7*NO2** + **0.7***HO2 + **0.26***TERPA + **0.24***TERPA3 + 0.09*CH3COCH3 + 0.09*TERPF1 + 0.21*CH2O + 0.11*TERP1OOH	2.70e-12 exp(360.00 / t)
BPINO2 + NO	→	0.08*CH3COCH3 + 0.49*CH2O + 0.2*TERPF1 + 0.24*TERPK + **0.05***TERPNS1 + 0.02*TERPNS + **0.07***TERPNT + **0.16***TERPNT1 + **0.26***TERPA3 + **0.7***HO2 + **0.7***NO2	2.70e-12 exp(360.00 / t)
LIMONO2 + NO	→	**0.22***TERPNT1 + **0.08***TERPNS1 + **0.7***NO2 + **0.7***TERPF1 + **0.7***HO2 + 0.43*CH2O	2.70e-12 exp(360.00 / t)
MYRCO2 + NO	→	0.1*TERPNS1 + **0.2***TERPNT1 + **0.7***NO2 + **0.7***TERPF2 + 0.33*CH3COCH3 + 0.3*CH2O + **0.7***HO2	2.70e-12 exp(360.00 / t)
T_TEST2 Sensitivity Test			

Table S8: MOZART-TS2 Kinetic Reactions Changed For CESM/CAM-Chem Sensitivity Tests

Reactant		Products	Rate
Updated the following reactions:			
APINO2 + NO	→	0.01*TERPHFN + 0.02*TERPNS1 + **0.06***TERPNS + **0.03***TERPNT + **0.03***TERPNT1 + **0.85***NO2 + **0.85***HO2 + **0.34***TERPA + **0.31***TERPA3 + 0.09*CH3COCH3 + 0.09*TERPF1 + 0.21*CH2O + 0.11*TERP1OOH	2.70e-12 exp(360.00 / t)
BCARYO2 + NO	→	**0.15***SQTN + **0.85***NO2 + **0.85***HO2 + **0.85***TERPF2	2.70e-12 exp(360.00 / t)
BPINO2 + NO	→	0.08*CH3COCH3 + 0.49*CH2O + 0.2*TERPF1 + 0.24*TERPK + **0.02***TERPNS1 + **0.01***TERPNS + **0.04***TERPNT + **0.08***TERPNT1 + **0.41***TERPA3 + **0.85***HO2 + **0.85***NO2	2.70e-12 exp(360.00 / t)
LIMONO2 + NO	→	**0.11***TERPNT1 + **0.04***TERPNS1 + **0.85***NO2 + **0.85***TERPF1 + **0.85***HO2 + 0.43*CH2O	2.70e-12 exp(360.00 / t)
MYRCO2 + NO	→	**0.05***TERPNS1 + **0.1***TERPNT1 + **0.85***NO2 + **0.85***TERPF2 + 0.33*CH3COCH3 + 0.3*CH2O + **0.85***HO2	2.70e-12 exp(360.00 / t)
T_TEST3 Sensitivity Test			
Updated the following reactions:			
APINO2 + CH3CO3	→	**0.1***TERPF1 + **0.32***TERPA + **0.36***TERPA3 + **0.22***TERP1OOH + HO2 + CH3O2 + CO2	2e-12 exp (500.00 / t)
APINO2 + CH3O2	→	**0.87***CH2O + **0.13***CH3OH + **1.49***HO2 + **0.1***TERPF1 + **0.15***TERPK + **0.17***TERPA + **0.36***TERPA3 + **0.22***TERP1OOH	2e-12
APINO2 + HO2	→	**0.32***TERP1OOH + **0.43***TERPOOH + **0.03***TERPA + **0.22*TERPA3** + **0.26***OH + **0.26***HO2	2.6e-13 exp(1300.00 / t)
APINO2 + NO	→	**0.04***TERPNS + 0.05*TERPNT + **0.015***TERPNS1 + **0.015***TERPNT1 + **0.88***NO2 + **0.88***HO2 + **0.08***TERPF1 + 0.3*TERPA + **0.31***TERPA3 + **0.19***TERP1OOH	2.7e-12 exp(360.00 / t)
APINO2 + NO3	→	NO2 + HO2 + **0.1***TERPF1 + **0.32***TERPA + **0.36***TERPA3 + **0.22***TERP1OOH	2.3e-12
APINO2 + TERPA2CO3	→	**0.1***TERPF1 + **0.32***TERPA + **0.36***TERPA3 + **0.22***TERP1OOH + HO2 + TERPA2O2 + CO2	2e-12 exp(500 / t)
APINO2 + TERPA3CO3	→	**0.1***TERPF1 + **0.32***TERPA + **0.36***TERPA3 + **0.22***TERP1OOH + HO2 + TERPA4O2 + CO2	2e-12 exp(500 / t)
APINO2 + TERPACO3	→	**0.1***TERPF1 + **0.32***TERPA + **0.36***TERPA3 + **0.22***TERP1OOH + HO2 + TERPA1O2 + CO2	2e-12 exp(500 / t)
APIN + OH	→	**0.06*TERP1OOH** + **0.06*HO2** + **0.94***APINO2	1.34e-11 exp(410 / t)

Table S8: MOZART-TS2 Kinetic Reactions Changed For CESM/CAM-Chem Sensitivity Tests

Reactant		**Products**	**Rate**
BPINO2 + CH3CO3	→	**0.1***TERPF1 + **0.35***TERPK + **0.35***CH2O + **0.28***TERPA3 + **0.19*TERPA3CO3** + **0.08*TERP1OOH** + **0.81***HO2 + CH3O2 + CO2	2e-12 exp(500 / t)
BPINO2 + CH3O2	→	**1.26***CH2O + **0.06*CH3OH** + **0.1***TERPF1 + 0.32*TERPK + 0.31*TERPA3 + **0.19*TERPA3CO3** + **0.08*TERP1OOH** + **1.57***HO2	2e-12
BPINO2 + HO2	→	**0.18***TERP1OOH + **0.65***TERPOOH + 0.03*TERPK + 0.03*CH2O + **0.03*TERPA3** + **0.11*TERPA3CO3** + **0.18***OH + **0.07***HO2	2.6e-13 exp(1300 / t)
BPINO2 + NO	→	**0.03***TERPNS + **0.09***TERPNT + **0.01***TERPNS1 + **0.87***NO2 + **0.72***HO2 + **0.08***TERPF1 + **0.31***TERPK + **0.31***CH2O + **0.26***TERPA3 + **0.15*TERPA3CO3** + **0.07*TERP1OOH**	2.7e-12 exp(360 / t)
BPINO2 + NO3	→	**0.1***TERPF1 + **0.35***TERPK + **0.35***CH2O + **0.28***TERPA3 + **0.19*TERPA3CO3** + **0.08*TERP1OOH** + **0.81***HO2 + NO2	2.3e-12
BPINO2 + TERPA2CO3	→	**0.1***TERPF1 + **0.35***TERPK + **0.35***CH2O + **0.28***TERPA3 + **0.19*TERPA3CO3** + **0.08*TERP1OOH** + **0.81***HO2 + TERPA2O2 + CO2	2e-12 exp(500 / t)
BPINO2 + TERPA3CO3	→	**0.1***TERPF1 + **0.35***TERPK + **0.35***CH2O + **0.28***TERPA3 + **0.19*TERPA3CO3** + **0.08*TERP1OOH** + **0.81***HO2 + TERPA4O2 + CO2	2e-12 exp(500 / t)
BPINO2 + TERPACO3	→	**0.1***TERPF1 + **0.35***TERPK + **0.35***CH2O + **0.28***TERPA3 + **0.19*TERPA3CO3** + **0.08*TERP1OOH** + **0.81***HO2 + TERPA1O2 + CO2	2e-12 exp(500 / t)
T_TEST4 Sensitivity Test			
Updated the following reactions:			
TERPA1O2 + NO	→	**0.16***TERPNS + **0.84***NO2 + **0.84***TERPA2O2	2.70e-12 exp(360.00 / t)
TERPA2O2 + NO	→	**0.03***TERPNT + **0.97***NO2 + **0.97***TERPA3O2	2.70e-12 exp(360.00 / t)
TERPA3O2 + NO	→	**0.12***TERPNT + **0.88***NO2 + **0.88***TERPA4O2 + **0.88***CH3COCH3	2.70e-12 exp(360.00 / t)
TERPA4O2 + NO	→	**0.05***TERPNS + **0.95***NO2 + **0.95***CH3CO3 + **0.95***HO2 + **1.9***CH2O + **0.95***CO	2.70e-12 exp(360.00 / t)
TERPF1O2 + NO	→	**0.15***TERPHFN + **0.85***NO2 + **0.85***HO2 + **0.85***TERPA3 + 0.31*CH2O	2.70e-12 exp(360.00 / t)

Table S8: MOZART-TS2 Kinetic Reactions Changed For CESM/CAM-Chem Sensitivity Tests

Reactant		Products	Rate
A_TEST1 Sensitivity Test			
Removed the following reactions:			
HONITR	→	**HNO3**	**In code**
INHEB	→	**HNO3**	**In code, γ = 0.02**
INHED	→	**HNO3**	**In code, γ = 0.02**
ISOPNOOHD	→	**HNO3**	**In code, γ = 0.02**
ISOPFDN	→	**HNO3**	**In code, γ = 0.1**
ISOPFDNC	→	**HNO3**	**In code, γ = 0.1**
ISOPFNC	→	**M**	**In code, γ = 0.1**
ISOPFNP	→	**M**	**In code, γ = 0.1**
ISOPN1D	→	**HNO3**	**In code, γ = 0.02**
ISOPN2B	→	**HNO3**	**In code, γ = 0.02**
ISOPN4D	→	**HNO3**	**In code, γ = 0.02**
NC4CHO	→	**HNO3**	**In code**
ONITR	→	**HNO3**	**In code**
SQTN	→	**M**	**In code, γ = 0.1**
TERPFDN	→	**HNO3**	**In code, γ = 0.1**
TERPHFN	→	**M**	**In code, γ = 0.1**
TERPNPT1	→	**HNO3**	**In code, γ = 0.02**
TERPNPT	→	**HNO3**	**In code, γ = 0.02**
TERPNT1	→	**HNO3**	**In code, γ = 0.02**
TERPNT	→	**HNO3**	**In code, γ = 0.02**
A_TEST2 Sensitivity Test			
Removed the following reactions:			
INHEB	→	**HNO3**	**In code, γ = 0.02**
INHED	→	**HNO3**	**In code, γ = 0.02**
ISOPNOOHD	→	**HNO3**	**In code, γ = 0.02**
Added the following reactions:			
ISOPN3B	→	**HNO3**	**In code, γ = 0.005**
ISOPNBNO3	→	**HNO3**	**In code, γ = 0.005**
MVKN	→	**HNO3**	**In code, γ = 0.005**
MACRN	→	**HNO3**	**In code, γ = 0.005**
TERPNPS1	→	**HNO3**	**In code, γ = 0.01**
TERPNPS	→	**HNO3**	**In code, γ = 0.01**
TERPNS	→	**HNO3**	**In code, γ = 0.01**

Table S8: MOZART-TS2 Kinetic Reactions Changed For CESM/CAM-Chem Sensitivity Tests

Reactant		**Products**	**Rate**
TERPNS1	→	**HNO3**	**In code, γ = 0.01**
Updated the following reactions:			
NC4CHO	→	HNO3	**In code, γ = 0.005**
ISOPFDN	→	HNO3	**In code, γ = 0.005**
ISOPFNP	→	M	**In code, γ = 0.005**
ISOPN1D	→	HNO3	**In code, γ = 0.005**
ISOPN2B	→	HNO3	**In code, γ = 0.005**
ISOPN4D	→	HNO3	**In code, γ = 0.005**
ISOPFNC	→	M	**In code, γ = 0.005**
ISOPFDNC	→	HNO3	**In code, γ = 0.005**
TERPNT1	→	HNO3	**In code, γ = 0.01**
TERPNT	→	HNO3	**In code, γ = 0.01**
TERPNPT1	→	HNO3	**In code, γ = 0.01**
TERPNPT	→	HNO3	**In code, γ = 0.01**
TERPFDN	→	HNO3	**In code, γ = 0.01**
SQTN	→	M	**In code, γ = 0.01**
TERPHFN	→	M	**In code, γ = 0.01**
A_TEST3 Sensitivity Test			
Added the following reactions:			
ISOPNOOHB	→	**HNO3**	**In code, γ = 0.02**
ISOPN3B	→	**HNO3**	**In code, γ = 0.02**
ISOPNBNO3	→	**HNO3**	**In code, γ = 0.02**
MVKN	→	**HNO3**	**In code, γ = 0.02**
MACRN	→	**HNO3**	**In code, γ = 0.02**
TERPNPS1	→	**HNO3**	**In code, γ = 0.02**
TERPNPS	→	**HNO3**	**In code, γ = 0.02**
TERPNS	→	**HNO3**	**In code, γ = 0.02**
TERPNS1	→	**HNO3**	**In code, γ = 0.02**

References

Allou, L., Maimouni, L. E., and Le Calve, S.: Henry's law constant measurements for formaldehyde and benzaldehyde as a function of temperature and water composition, Atmos. Environ., 45, 2991–2998, https://doi.org/10.1016/j.atmosenv.2010.05.044, 2011.

Arey, J., Aschmann, S. M., Kwok, E. S. C., and Atkinson, R.: Alkyl nitrate, hydroxyalkyl nitrate, and hydroxycarbonyl formation from the NO_x-air photooxidations of C_5-C_8 n-alkanes, J. Phys. Chem. A., 105, 1020–1027, https://doi.org/10.1021/jp003292z, 2001.

Atkinson, R., Baulch, D. L., Cox, R. A., Crowley, J. N., Hampson, R. F., Hynes, R. G., Jenkin, M. E., Rossi, M. J., Troe, J., and Subcommittee, I.: Evaluated kinetic and photochemical data for atmospheric chemistry: Volume II – gas phase reactions of organic species, Atmos. Chem. Phys., 6, 3625–4055, https://doi.org/10.5194/acp-6-3625-2006, 2006.

Burkholder, J. B., Sander, S. P., Abbatt, J., Barker, J. R., Huie, R. E., Kolb, C. E., Kurylo, M. J., Orkin, V. L., Wilmouth, D. M., and Wine, P. H.: Chemical Kinetics and Photochemical Data for Use in Atmospheric Studies, Evaluation No. 18, Tech. Rep. JPL Publication 15-10, Jet Propulsion Laboratory, Pasadena, CA, http://jpldataeval.jpl.nasa.gov, 2015.

Chameides, W. L.: The Photochemistry of a Remote Marine Stratiform Cloud, J. Geophys. Res. Atmos., 89, 4739–4755, https://doi.org/10.1029/JD089iD03p04739, 1984.

Chan, M. N., Surratt, J. D., Claeys, M., Edgerton, E. S., Tanner, R. L., Shaw, S. L., Zheng, M., Knipping, E. M., Eddingsaas, N. C., Wennberg, P. O., and Seinfeld, J. H.: Characterization and quantification of isoprene-derived epoxydiols in ambient aerosol in the Southeastern United States, Environ. Sci. Technol., 44, 4590–4596, https://doi.org/10.1021/es100596b, 2010.

Copolovici, L. O. and Niinemets, U.: Temperature dependencies of Henry's law constants and octanol/water partition coefficients for key plant volatile monoterpenoids, Chemosphere, 61, 1390–1400, https://doi.org/10.1016/j.chemosphere.2005.05.003, 2005.

Dohnal, V. and Fenclova, D.: Air-water partitioning and aqueous solubility of phenols, J. Chem. Eng. Data, 40, 478–483, https://doi.org/10.1021/je00018a027, 1995.

Emmons, L. K., Orlando, J. J., Tyndall, G., Schwantes, R. H., Kinnison, D., Lamarque, J.-F., Marsh, D., Mills, M., Tilmes, S., Buchholz, R., Gettelman, A., Garcia, R., Simpson, I., Blake, D., and Petron, G.: The chemistry mechanism in the Community Earth System Model version 2 (CESM2) [In Review], JAMES, http://www.cesm.ucar.edu/publications/, 2020.

Fried, A., Henry, B. E., Calvert, J. G., and Mozurkewich, M.: The reaction probability of N_2O_5 with sulfuric acid aerosols at stratospheric temperatures and compositions, J. Geophys. Res. Atmos., 99, 3517–3532, https://doi.org/10.1029/93JD01907, 1994.

Goldstein, S. and Czapski, G.: Reactivity of peroxynitric acid (O_2NOOH): A pulse radiolysis study, Inorg. Chem., 36, 4156–4162, https://doi.org/10.1021/ic961186z, 1997.

Guo, X. X. and Brimblecombe, P.: Henry's law constants of phenol and mononitrophenols in water and aqueous sulfuric acid, Chemosphere, 68, 436–444, https://doi.org/10.1016/j.chemosphere.2007.01.011, 2007.

Hiatt, M. H.: Determination of Henry's law constants using internal standards with benchmark values, J. Chem. Eng. Data, 58, 902–908, https://doi.org/10.1021/je3010535, 2013.

Jenkin, M. E., Boyd, A. A., and Lesclaux, R.: Peroxy radical kinetics resulting from the OH-initiated oxidation of 1,3-butadiene, 2,3-dimethyl-1,3-butadiene and isoprene, J. Atmos. Chem., 29, 267–298, https://doi.org/10.1023/A:1005940332441, 1998.

Jenkin, M. E., Young, J. C., and Rickard, A. R.: The MCM v3.3.1 degradation scheme for isoprene, Atmos. Chem. Phys., 15, 11 433–11 459, https://doi.org/10.5194/acp-15-11433-2015, 2015.

Kames, J. and Schurath, U.: Henry's law and hydrolysis-rate constants for peroxyacyl nitrates (PANs) using a homogeneous gas-phase source, J. Atmos. Chem., 21, 151–164, https://doi.org/10.1007/BF00696578, 1995.

Leng, C., Kish, J. D., Kelley, J., Mach, M., Hiltner, J., Zhang, Y., and Liu, Y.: Temperature-dependent henry's law constants of atmospheric organics of biogenic origin, J. Phys. Chem. A, 117, 10 359–10 367, https://doi.org/10.1021/jp403603z, 2013.

Leu, M.-T. and Zhang, R.: Solubilities of $CH_3C(O)O_2NO_2$ and HO_2NO_2 in water and liquid H_2SO_4, Geophys. Res. Lett., 26, 1129–1132, https://doi.org/10.1029/1999GL900158, 1999.

McNeill, V. F., Woo, J. L., Kim, D. D., Schwier, A. N., Wannell, N. J., Sumner, A. J., and Barakat, J. M.: Aqueous-phase secondary organic aerosol and organosulfate formation in atmospheric aerosols: A modeling study, Environ. Sci. Technol., 46, 8075–8081, https://doi.org/10.1021/es3002986, 2012.

Raventos-Duran, T., Camredon, M., Valorso, R., Mouchel-Vallon, C., and Aumont, B.: Structure-activity relationships to estimate the effective Henry's law constants of organics of atmospheric interest, Atmos. Chem. Phys., 10, 7643–7654, https://doi.org/10.5194/acp-10-7643-2010, 2010.

Reichl, A.: Messung und Korrelierung von Gaslöslichkeiten halogenierter Kohlenwasserstoffe, Ph.D. thesis, Technische Universitat Berlin, Germany, 1995.

Sander, R.: Compilation of Henry's law constants (version 4.0) for water as solvent, Atmos. Chem. Phys., 15, 4399–4981, https://doi.org/10.5194/acp-15-4399-2015, 2015.

Schwartz, S. E. and White, W. H.: Solubility equilibria of the nitrogen oxides and oxyacids in dilute aqueous solution, in: Advances in Environmental Science and Engineering, edited by Pfafflin, J. R. and Ziegler, E. N., vol. 4, p. 1–45, Gordon and Breach Science Publisher, NY, 1981.

Sieg, K., Starokozhev, E., Schmidt, M. U., and Puttmann, W.: Inverse temperature dependence of Henry's law coefficients for volatile organic compounds in supercooled water, Chemosphere, 77, 8–14, https://doi.org/10.1016/j.chemosphere.2009.06.028, 2009.

Smith, R. M. and Martell, A. E.: Critical stability constants, Vol 4: Inorganic complexes, Plenum Press, New York, 1976.

Staudinger, J. and Roberts, P. V.: A critical compilation of Henry's law constant temperature dependence relations for organic compounds in dilute aqueous solutions, Chemosphere, 44, 561–576, https://doi.org/10.1016/S0045-6535(00)00505-1, 2001.

Travis, K. R., Jacob, D. J., Fisher, J. A., Kim, P. S., Marais, E. A., Zhu, L., Yu, K., Miller, C. C., Yantosca, R. M., Sulprizio, M. P., Thompson, A. M., Wennberg, P. O., Crounse, J. D., St. Clair, J. M., Cohen, R. C., Laughner, J. L., Dibb, J. E., Hall, S. R., Ullmann, K., Wolfe, G. M., Pollack, I. B., Peischl, J., Neuman, J. A., and Zhou, X.: Why do models overestimate surface ozone in the Southeast United States?, Atmos. Chem. Phys., 16, 13 561–13 577, https://doi.org/10.5194/acp-16-13561-2016, 2016.

van Roon, A., Parsons, J. R., Kloeze, A.-M. T., and Govers, H. A. J.: Fate and transport of monoterpenes through soils. Part I. Prediction of temperature dependent soil fate model input-parameters, Chemosphere, 61, 599–609, https://doi.org/10.1016/j.chemosphere.2005.02.081, 2005.

Wennberg, P., Bates, K. H., Crounse, J. D., Dodson, L. G., McVay, R. C., Mertens, L. A., Nguyen, T. B., Praske, E., Schwantes, R. H., Smarte, M. D., St Clair, J. M., Teng, A. P., Zhang, X., and Seinfeld, J. H.: Gas-Phase Reactions of Isoprene and Its Major Oxidation Products, Chem. Rev., 118, 3337–3390, https://doi.org/10.1021/acs.chemrev.7b00439, 2018.